Guide to Remote Sensing Applications for Aquatic Environment Monitoring

Qredo

Aquatic Remote Sensing in Higher Education

Toma Dabulevičienė Diana Vaičiūtė Edvinas Tiškus

Jonas Gintauskas Rasa Idzelytė Martynas Bučas

2023

Bibliografinė informacija pateikiama Lietuvos integralios bibliotekų informacinės sistemos (LIBIS) portale ibiblioteka.lt

Klaipeda University
Marine Research Institute

This publication (manual) is the product of a collaborative effort of the Qredo project team, that included researchers from Klaipeda University Marine Research Institute.

Acknowledgement

This publication has been developed within the framework of the Project "Aquatic Remote Sensing in Higher Education (Qredo)" (No. 4000135270/21/NL/SC) financed by the European Space Agency (ESA).

Contributors:

Toma Dabulevičienė, Diana Vaičiūtė, Edvinas Tiškus, Jonas Gintauskas, Rasa Idzelytė, Martynas Bučas

The manual should be cited as: Dabulevičienė T., Vaičiūtė D., Tiškus E., Gintauskas J., Idzelytė R., and Bučas M., *Guide to Remote Sensing Applications for Aquatic Environment Monitoring*, 2023. Klaipėdos universiteto leidykla, ISBN 978-609-481-199-9

ISBN 978-609-481-199-9

Preface

Technological progress and globalisation offer tremendous opportunities for innovation, job creation, and growth. In turn, remote sensing is one of the rapidly growing areas of technological advancements, that can be defined as the technology of obtaining information about different objects, land surface, aquatic environment, various phenomena, or processes without making physical contact with them. This may include data collection from satellites, aerial images, unmanned aerial vehicles and others. Remote sensing is a crucial source of data for Earth Observation (EO), enabling gathering information on the physical, chemical, biological, and any other related data about the planet, that is necessary to monitor land, aquatic (seas, rivers, lakes) environment, and atmosphere.

With its wide variety of areas of application, remote sensing has an increasing impact on different groups of society – from scientific communities to industry, public institutions, and day-to-day users. However, the lack of understanding of the technical characteristics of remotely sensed data and their suitability for analysis limits the capacity of EO. Therefore, driving and supporting the advancement requires people to obtain new skills in remote sensing and Geographical Information Systems (GIS). The synergistic use of EO and GIS techniques allows one to transform data into information, therefore, it could be one of the areas in environmental education that are of high interest to future employers and stakeholders.

The project Aquatic Remote Sensing in Higher Education (Qredo) was aiming to address the gap in the preparation of remote sensing experts capable of using the advancements offered by EO. An essential aspect of Qredo was the identification of the need for aquatic remote sensing applications considering the requirements of potential employers in Lithuania. Further, an advanced course to improve the knowledge and skills in EO data application was organised, and, as a final achievement of the project, the practical sessions' manual on the Remote Sensing and GIS applications for the aquatic environment assessment was prepared.

Aimed at supporting and contributing to the advancement of labour market-oriented skills in remote sensing and GIS, this manual covers in-depth knowledge about Earth Observation and its practical applications for the studies of the aquatic environment. The manual has been designed in a way to help students, graduates, and other interested parties reach a more extensive and deeper understanding of the synergist use of remote sensing and GIS and to gain more practical skills. This work represents one of the most relevant deliverables of the Qredo project and it is expected to support filling the gap between the supply of and demand for space/geospatial education and training, focusing on marine satellite data products from past and current EO missions.

The manual is organized as follows: the chapter on the basics of remote sensing introduces the user to the different sensors for gathering remote sensing data on aquatic environment. An introductory chapter on ESA SNAP software includes basic information on how to navigate the software, providing the main steps for satellite data analysis. QGIS for remote sensing data analysis and visualisation chapter is dedicated to QGIS – the open-source GIS software, that can be used to process, analyse, and visualize data gathered from remote sensing and UAVs. The chapter will explain how to import different types of data from different remote sensing and GIS data sources, and how to apply various GIS tools and functions to process remote sensing data. The thematic chapters on water temperature, ice, flood detection, chlorophyll-a (chl-a) mapping, bathymetry, water transparency, and ship detection cover different fields of remote sensing applications for the assessment of the aquatic environment and consist of a short theoretical part, data acquisition, and practical cases studies.

Qredo Project Team

Contents

Glossary

Backscattering – process, when the energy is reflected directly back at an active sensor after hitting a target.

Coordinate reference system (CRS) – A coordinate-based local, regional, or global system used to locate geographical entities.

Electromagnetic Spectrum – continuum of all electromagnetic waves arranged according to frequency and wavelength, encompassing phenomena such as radio waves, microwaves, infrared radiation, visible light, ultraviolet radiation, X-rays, and gamma rays.

Earth Observation – collection of data about Earth's physical, chemical, and biological systems through remote sensing technologies, often involving satellites or aircrafts.

Georeference – to link spatial data to its correct location.

HELCOM – The Baltic Marine Environment Protection Commission – also known as the Helsinki Commission.

In situ - the observation and / or measurement of events in its original place. In remote sensing commonly referring to data collected on the ground to validate data collected from airborne or spaceborne sensors.

LiDAR - Light Detection and Ranging — is a remote sensing method used to examine the surface of the Earth.

MERIS – The Medium Resolution Imaging Spectrometer (MERIS) was an instrument onboard the European Space Agency's Envisat satellite, aimed at monitoring ocean color, surface temperature, and atmospheric parameters.

MODIS – Moderate Resolution Imaging Spectroradiometer (MODIS) is a key instrument aboard NASA's Terra and Aqua satellites, designed to collect data in 36 spectral bands and provide comprehensive imaging across the Earth's surface for various environmental monitoring applications.

NOAA - National Oceanic and Atmospheric Administration.

Pixel – smallest unit of a digital image that can be displayed and represented on a digital display device. Pixel represents a square area on an image an is a measure of the sensor's ability to resolve (see) objects of different sizes.

Swath – The area imaged on Earth’s surface by one pass of an aircraft or satellite.

USGS – The United States Geological Survey.

I. Basics of Remote Sensing

Remote sensing is the technique of obtaining information about objects or areas from a distance, often by using satellites or flying aircrafts. There are primarily two types of remote sensing sensors: passive and active (Figure I-1). **Passive sensors** rely on natural radiation, usually sunlight, to illuminate the target. Examples include optical cameras and infrared sensors. These sensors measure the reflected or emitted radiation from the target area and convert these measurements into useful data. **Active sensors**, on the other hand, generate their own energy to illuminate the target, as is the case with radar and LiDAR systems. These systems emit a pulse of energy and measure the time it takes for the pulse to return after hitting the target, thereby determining characteristics like distance, speed, and shape.

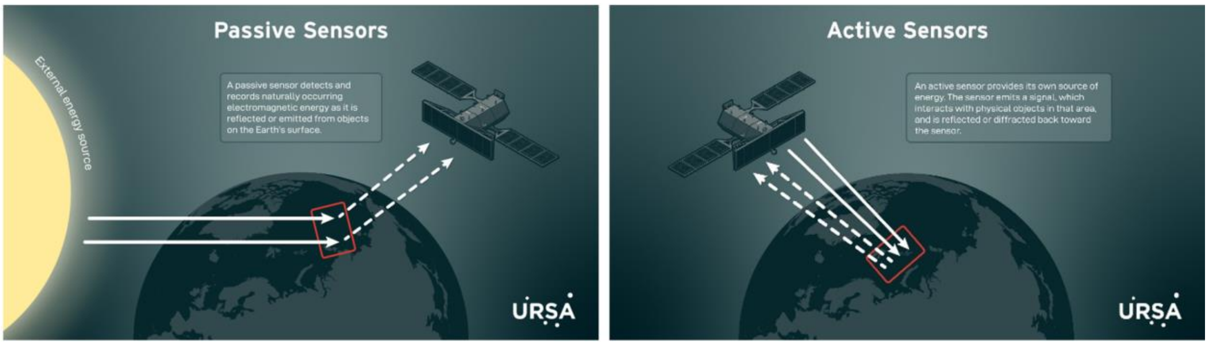

Figure I-1. *Passive sensors detecting energy when the naturally occurring energy is available, and Active sensors provide their own energy source for illumination (Credit: URSA Space).*

Satellite data is often made available from a variety of sources, such as governmental space agencies like NASA, ESA, and commercial providers. The data can be acquired from different types of orbits, including geostationary, sun-synchronous, and polar orbits, each offering unique vantage points and revisiting times.

Some of the most common **databases** for open-source remote sensing data include:

- USGS Earth Explorer: Provides access to an extensive archive of satellite and aerial imagery, including Landsat and Sentinel data.
- NASA Earthdata: Offers a wide range of NASA's Earth observation data, including MODIS, ASTER, and airborne datasets.
- Copernicus Open Access Hub: Source for Sentinel-1, Sentinel-2, and Sentinel-3 data, focusing primarily on environmental monitoring.
- Copernicus Data Space Ecosystem: A new service to better access and exploit the EU's Copernicus satellites data, including Sentinel-1, Sentinel-2, and Sentinel-3.
- NOAA CLASS: The Comprehensive Large Array-data Stewardship System provides data from NOAA's operational and research satellites.
- JAXA Global ALOS Portal: Offers PALSAR and optical data from the Advanced Land Observing Satellite (ALOS) missions of the Japan Aerospace Exploration Agency.

- GloVis: The Global Visualization Viewer is another USGS service, providing a simplified way to search for remote sensing data.
- Australian Geoscience Data Cube: Focuses on providing satellite data specific to the Australian continent, including Landsat and other data types.
- INPE Image Catalog: The Brazilian National Institute for Space Research offers datasets primarily focused on South America.
- EUMETSAT Data Centre: Provides meteorological data from European geostationary satellites, like the Meteosat series.
- Alaska Satellite Facility: Specializes in radar and SAR data, including data from missions like RADARSAT and UAVSAR.

These databases offer various types of remote sensing data, with different spatial, spectral, and temporal resolutions, catering to a wide range of scientific research and applications.

Key attributes of satellite data include spatial, temporal spectral, and radiometric resolutions. **Spatial resolution** refers to the size of a single pixel in ground units and can range from centimetres in high-resolution imaging systems to hundreds of meters in moderate to low-resolution systems.

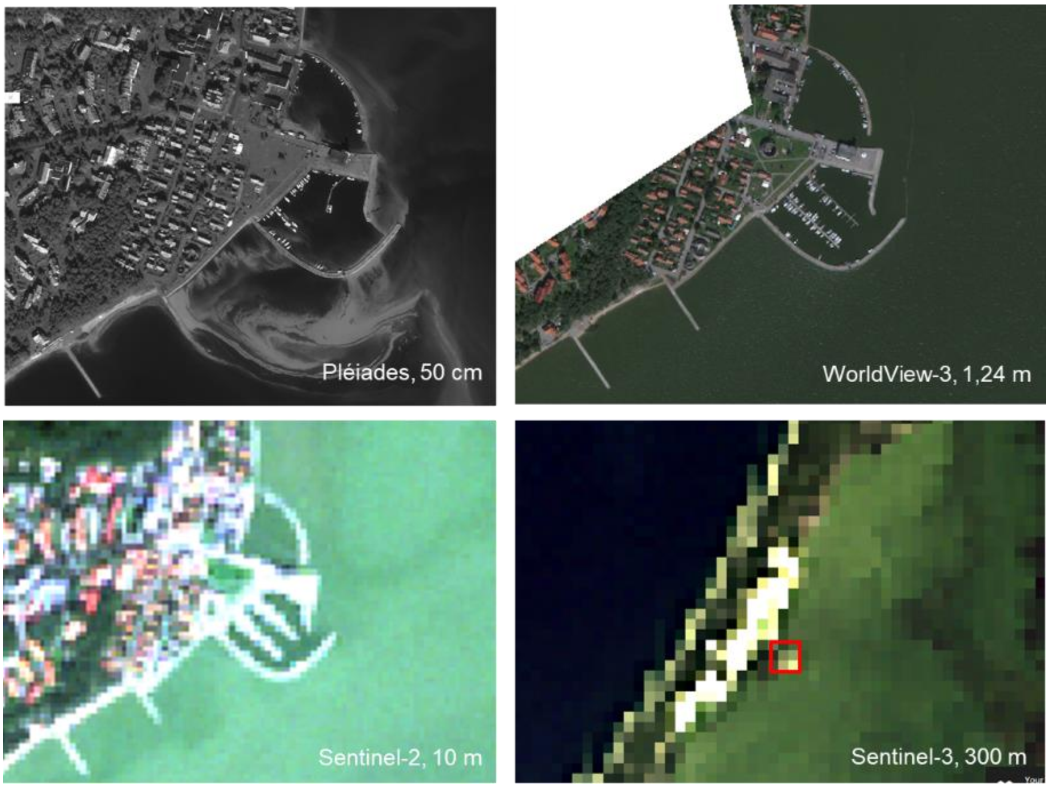

Figure I-2. *High-resolution satellite images (Pléiades and WorldView-3), and moderate resolution satellite images (Sentinel-2 and Sentinel-3). Example of Nida village and harbour in the Curonian Spit (Lithuania).*

Temporal resolution indicates how frequently a sensor revisits the same location, which can be from multiple times a day to once in several days, depending on the satellite's orbit. However, because of some degree of overlap in the imaging swaths of adjacent orbits for most satellites (e.g., Aqua and Terra) and the increase in this overlap with increasing latitude, some areas of the Earth tend to be re-imaged more frequently. **Spectral resolution** pertains to the number and width of specific wavelength bands that a sensor can record. For example, multi-spectral sensors capture data in a few wide bands, whereas hyperspectral sensors capture data in many narrow bands, offering more detailed information about the target. Radiometric characteristics describe the actual information content in an image. Every time an image is acquired by a sensor, its sensitivity to the magnitude of the electromagnetic energy determines the radiometric resolution. **The radiometric resolution** of an imaging system describes its ability to discriminate very slight differences in energy. The finer the radiometric resolution of a sensor, the more sensitive it is to detecting small differences in reflected or emitted energy. Imagery data are represented by positive digital numbers which vary from 0 to (one less than) a selected power of 2. This range corresponds to the number of bits used for coding numbers in binary format. Each bit records an exponent of power 2 (e.g., 1 bit = 2^1=2). The maximum number of brightness levels available depends on the number of bits used in representing the energy recorded. Thus, if a sensor used 8 bits to record the data, there would be 2^8=256 digital values available, ranging from 0 to 255. However, if only 4 bits were used, then only 2^4=16 values ranging from 0 to 15 would be available. The radiometric resolution would be much less.

All sensors employed on satellites use electromagnetic radiation to view the Earth. The capability of particular sensors to measure certain properties and how well they can view through the atmosphere or penetrate clouds depends critically on which part of the electromagnetic spectrum they use. Figure I-3 shows regions of the electromagnetic spectrum that are of relevance to remote sensing and in particular the bands occupied by the four broad classes of satellite sensors used for viewing the Earth. Figure I-3 also shows how transmittance of the atmosphere varies with electromagnetic wavelength, which accounts for why sensors are only found in certain wavebands. For much of the electromagnetic spectrum the atmosphere is opaque and, therefore, unusable for remote sensing of the ocean. However, there are a number of **atmosphere "window"** regions where most of the radiation gets through, although it may be attenuated to some extent. One of these windows extends from the visible part of the spectrum (between 400nm and 700 nm, used by the human eye) into the near-infrared (IR). This is used by radiometers that observe sunlight reflected from the ground and the ocean. Between wavelengths of about 3.5 mm and 13 mm are found a number of narrow windows exploited by IR radiometers. This is called the thermal IR part of the spectrum because much of the radiation has been emitted by surfaces according to their temperature. At much longer wavelengths, greater than a few millimetres, the atmosphere becomes almost completely transparent. This is referred to as the microwave part of the spectrum, normally differentiated spectrally in terms of frequency rather than wavelength. Because it is widely exploited for many technological aspects of modern civilization, including radio and TV broadcasts, telecommunications, mobile telephony, certain parts have to be specially reserved for remote sensing and are allocated by international regulation. They are found as discrete narrow frequency bands within the broad regions for microwave radiometry and radars. Microwave radiometers are passive sensors, simply measuring the naturally ambient radiation that is emitted by the ocean, atmosphere, and land surfaces. Radars are active microwave devices which emit pulses and measure echoes from the sea surface, in order to gain information about some aspect of the surface.

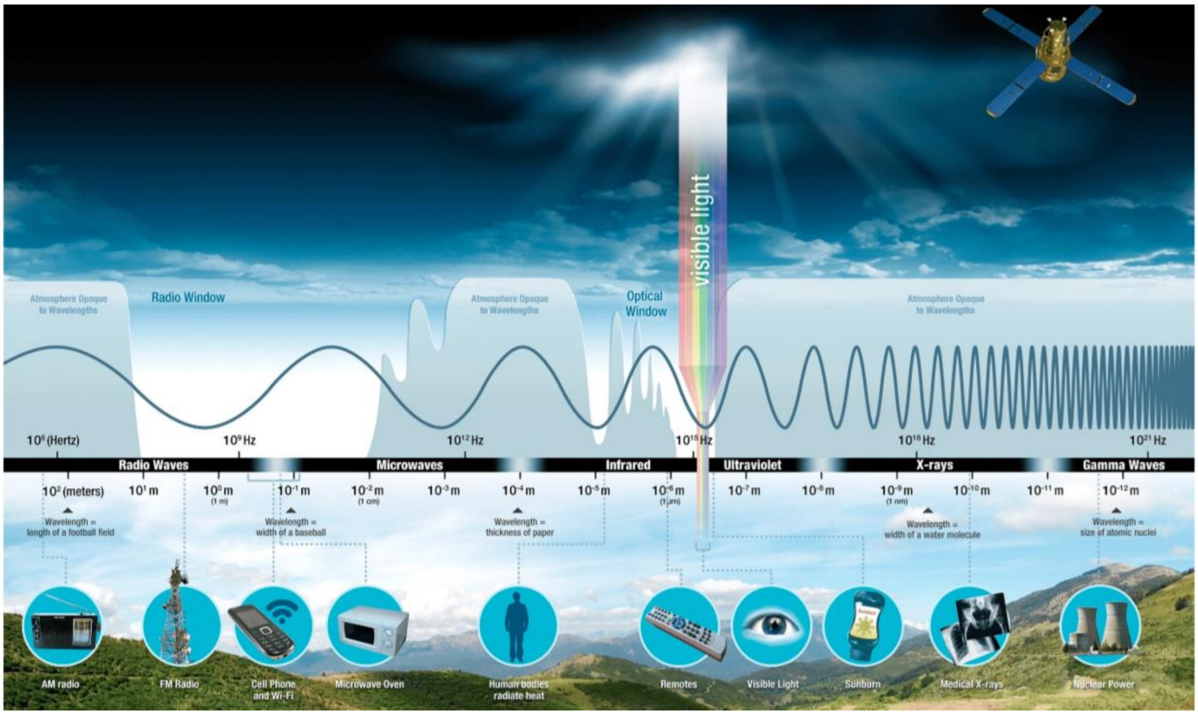

Figure I-3. *Diagram of the electromagnetic spectrum and the regions of atmosphere "windows" exploited by typical remote sensing instruments. (Credit: NASA Science)*

Levels of satellite data generally refer to the stages of processing the raw data goes through before it is ready for analysis (Figure I-4). **Level 0** data are the raw signals, **Level 1** involves radiometric and geometric corrections, **Level 2** data are derived geophysical variables, and **Level 3** and **4** represent processed, gridded, and sometimes model-integrated datasets. These levels help standardize data for research and operational applications.

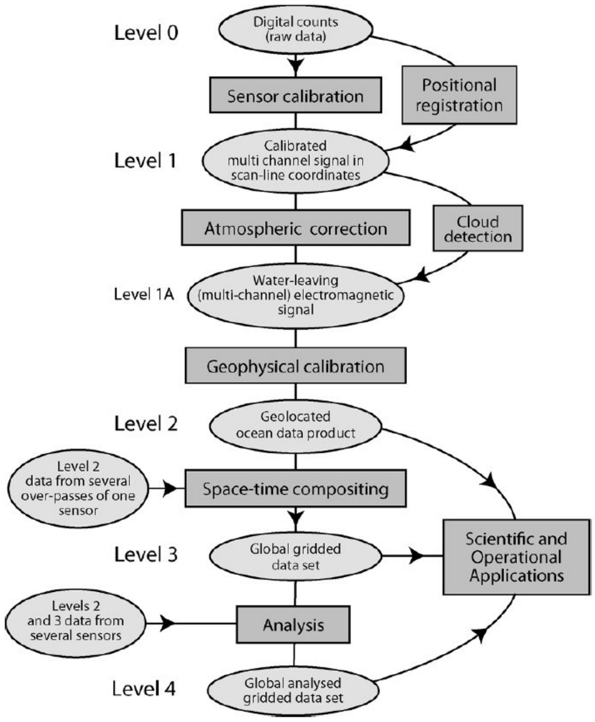

Figure I-4. *Outline of data-processing tasks to convert raw satellite data into environmental variables (after Robinson, 2010).*

Optical data.

The optical satellite sensors are passive. They take imagery in the visible or near-visible portion of the electromagnetic spectrum, using the sun's radiation as it reflects off of our planet and atmosphere (Figure I-5).

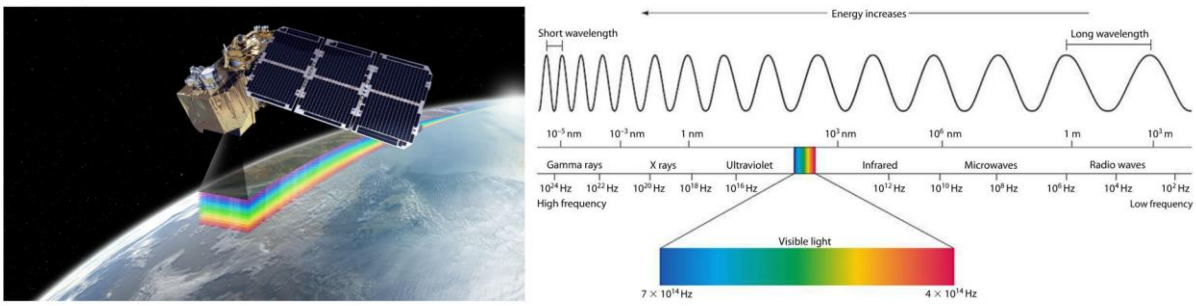

Figure I-5. *Sentinel-2 acquiring the data and the electromagnetic spectrum (Credit: Mini Physics 2006).*

The basic principle of optical remote sensing is straightforward. The light measured by an optical sensor pointing towards the Earth surface comes originally from the Sun. Some photons of light emitted by the Sun, with energies that place them in the visible part of the spectrum, enter the surface where they are either absorbed or scattered, depending on the objects. Those of the scattered photons are quantified by a satellite optical sensor, which measures the amounts of different wavelengths of light reaching it. In practice, it is the spectral radiance at the top of the atmosphere that is measured from a satellite. This consists of light reflected by the atmosphere and the land or water surface. The retrieval of useful quantities from top-of atmosphere measurements is a challenging task, requiring careful separation of atmospheric scattering and surface reflection.

In aquatic environment, direct Sun light and scattered sky light, that penetrate the water surface, may be absorbed or scattered by the water molecules, or by the various suspended and dissolved materials present in the water (Figure I-6). In shallow, clear waters, a significant part of the light from the sun may reach the bottom and be reflected from it. Some of the scattered and reflected photons eventually find their way to the remote sensor. Remote sensing involves analyses of the variations in magnitude and spectral quality of the water-leaving radiation to derive quantitative information on the type of substances present in the water and their concentrations. Clearly, this has to be based on a sound understanding of the optical properties of the medium, and of the optical processes in the medium.

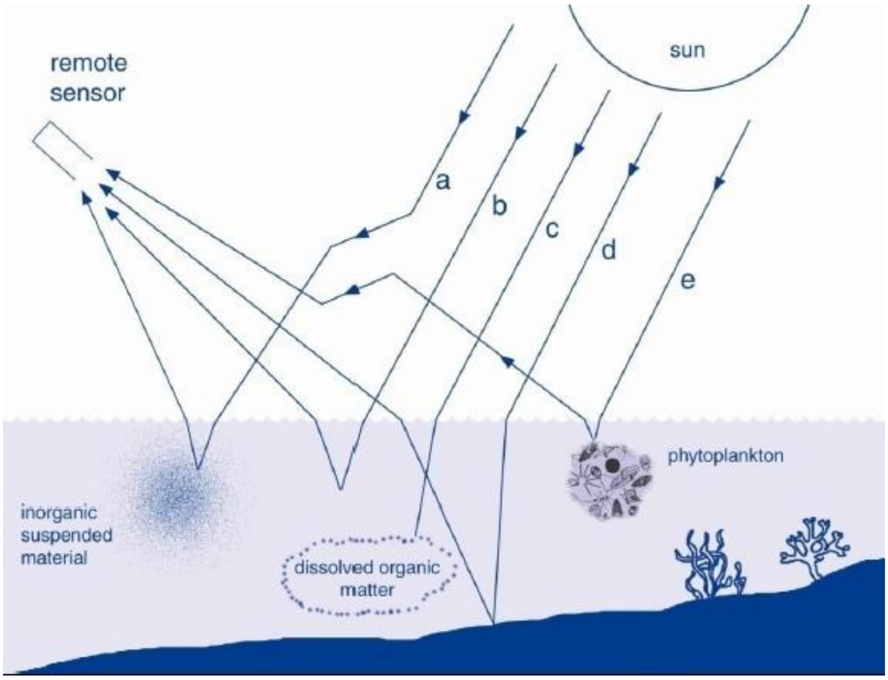

Figure I-6. *Factors that influence upwelling light leaving the sea surface. (a) upward scattering by inorganic suspended material; (b) upward scattering from water molecules; (c) absorption by the yellow-substances component; (d) reflection off the bottom; and (e) upward scattering from the phytoplankton component. Note that absorption by any of these components or by the bottom will serve to decrease the water-leaving signal. Light from the sun may be scattered by atmospheric constituents before it reaches the sea surface. Similarly, light leaving the water may be scattered away from, or towards the remote sensor by the atmosphere (Credits: IOCCG, 2000).*

A serious disadvantage of remote sensing from Earth observation satellites is the atmosphere. The greater part of the measurement of visible wavelengths of light made looking down from a satellite orbit comes from light scattered by the atmosphere into the field of view of the sensor, which may contribute more than 90% of total measured radiance. The atmosphere is opaque to electromagnetic radiation at many wavelengths, and there are only certain wavelength windows through which radiation may be fully or partially transmitted. Atmospheric gas molecules themselves may absorb or scatter radiation, and, in addition, water vapour, aerosols, and suspended particles of dust will do the same. If water droplets are present in the form of clouds, they may completely change the transmission properties of the atmosphere. A major task for the analysis of satellite data is to take into account the effect of the atmosphere and perform the **atmospheric correction**. Otherwise, it involves estimation of the effect that the atmosphere has had on measured electromagnetic radiation, between leaving the Earth and reaching the sensor.

Environmental optical satellite missions are designed to acquire information on the biogeochemical status of Earth's ecosystems. No instruments currently exist that can directly measure biogeochemical variables from space. Because remote sensing devices record physical electromagnetic emanations from some combination of organic and/or inorganic matter, comprising the biosphere, these electromagnetic data must be converted through appropriate multidisciplinary modelling activities into inferred estimates of the environmental variables (Figure I-7). Therefore, development of biophysical **models and algorithms** is essential to remote sensing. Most satellite data models and algorithms require knowledge of the optical properties of the organic and inorganic biospheric matter admixture indigenous to the local environmental target or scene. Invariably, such admixtures are temporally and spatially variable. Consequently, the development of general or universal environmental parameter-extraction algorithms for remotely sensed data on a global scale is highly unlikely. Extraction algorithms, therefore, are constrained to be local in application (particularly, if such algorithms are based on regressions between ground-measured environmental variables and satellite-recorded values of radiation at some wavelength or group of mathematically entwined radiations from several wavelengths). It is possible to generate theoretical models that possess degrees of acceptable rigor and robustness. However, application of these models invariably requires precise numerical values of the optical properties of the indigenous ecosystem membership and/or the rates of photobiological and photochemical productivity as a function of wavelength (action spectra) pertinent to the ecosystem under study. Calibration and validation of existing and developing models and algorithms remain a crucial step for the retrieval of accurate information from the optical satellite data.

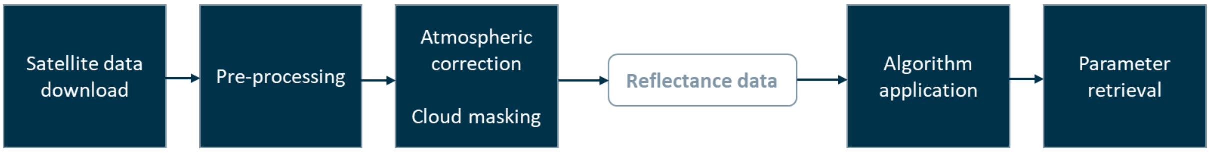

Figure I-7*. Generic optical satellite image processing chain. Pre-processing is the correction of satellite image data containing the distortion due to the properties of the imaging system and imaging conditions. This type of distortion is corrected in this step and mainly include radiometric correction, geometric correction, geo-referencing and resampling. The atmospheric correction and cloud masking is referred to removal of any distortions that are caused by atmosphere, could or cloud shadows.*

In general, the models and algorithms can be categorised as:

- Image Classification and Segmentation Algorithms:
    - Supervised Classification: Algorithms that use training data to classify pixels or regions into predefined classes (e.g., land cover types).

- Unsupervised Classification: Clustering algorithms that group pixels based on similarity without predefined classes.
    - Semantic Segmentation: Algorithms that assign semantic labels to each pixel to distinguish different object categories within the image.
    - Instance Segmentation: Identifying and delineating individual objects or instances within a scene.
- Radiometric indices - quantitative measures of features that are obtained by combining several spectral bands, features that are not otherwise obvious if using only one band:
    - Normalized Difference Vegetation Index (NDVI): Calculates vegetation health and density by comparing the reflectance in the near-infrared and red bands.
    - Leaf Area Index (LAI) Estimation: Estimates the amount of foliage in a vegetated area.
    - Vegetation Indices: Various indices (e.g., EVI, SAVI) for assessing vegetation characteristics and health.
    - Water Indices: Calculating water indices like the Normalized Difference Water Index (NDWI) to identify water bodies.
- Semi-analytical algorithms are a class of algorithms used in remote sensing, particularly in the field of water quality and aquatic ecosystem monitoring. These algorithms are designed to estimate various water quality parameters, such as concentrations of chlorophyll-a, suspended sediments, and other optically active substances in water bodies, based on the analysis of spectral reflectance or radiance data obtained from optical remote sensing sensors, such as those on satellite or airborne platforms. The term "semi-analytical" is used because these algorithms incorporate both analytical and empirical components in their modelling approach.
- Machine Learning and Deep Learning Algorithms: various machine learning and deep learning techniques, including neural networks (NNs) - a full spectrum version using a set of neural networks which are trained on simulated top-of-atmosphere reflectance, convolutional neural networks (CNNs), are used for tasks such as image classification, object detection, and semantic segmentation.

The decision on the most appropriate algorithm or model for remote sensing of aquatic environment, in order to prevent the failure and inaccurate results, relies on the initial step, determining the type of water masses. Water masses are commonly classified into one of two types: Case 1 or Case 2. A bipartite classification scheme was introduced by Morel and Prieur (1977) and refined later by Gordon and Morel (1983). By definition, Case 1 waters are those waters in which phytoplankton (with their accompanying and co-varying retinue of material of biological origin) are the principal agents responsible for variations in optical properties of the water. On the other hand, Case 2 waters are influenced not just by phytoplankton and related particles, but also by other substances, that vary independently of phytoplankton, notably inorganic particles in suspension and yellow substances.

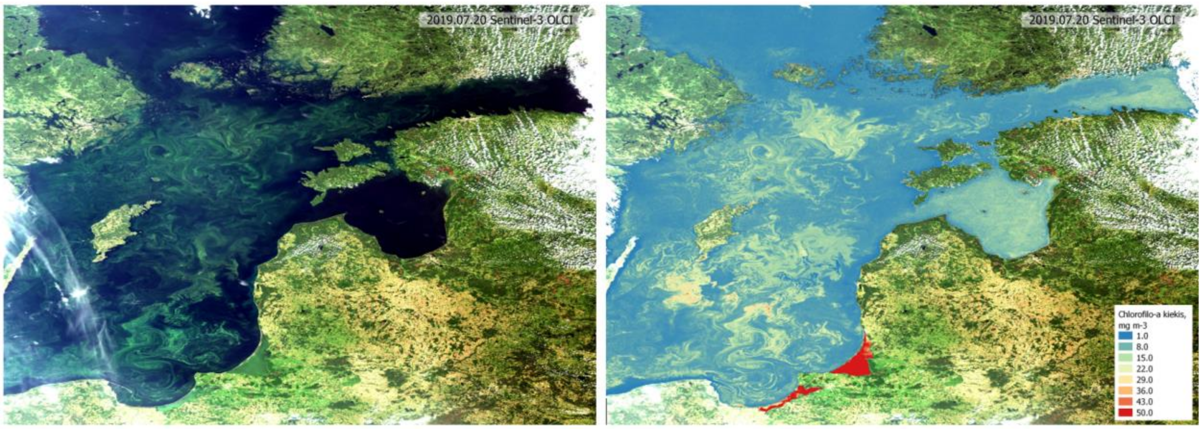

Figure I-8. *Cyanobacteria bloom in the Baltic Sea. True colour Sentinel-3 image and spatial distribution of chlorophyll-a concentration after the application of retrieval algorithm.*

Applications: Optical satellite images, which are captured using sensors that detect visible light, are valuable for a wide range of applications across various fields. Each application itself has specific demands, for spectral resolution, spatial resolution, and temporal resolution. Optical satellite imagery is a versatile tool that continues to evolve with advances in technology, enabling a wide range of applications for environmental monitoring, disaster management, resource management. **Key applications of optical satellite imagery are:**

- Environmental Monitoring:
  - Water Quality Assessment: Identifying changes in water bodies such as rivers, lakes, and oceans, including pollution and algal blooms, suspended sediments, coloured dissolved organic matter, water transparency and photic zone, aquatic vegetation (Figure I-9).
  - Land Cover and Land Use Analysis: Optical satellite images help track changes in land cover and land use, including deforestation, urban expansion, and agricultural trends.
  - Vegetation Health Assessment: Monitoring vegetation health and detecting issues like forest fires, pest infestations, and drought stress.
- Agriculture:
  - Crop Monitoring: Assessing crop health, growth, and yield estimation.
  - Precision Farming: Optimizing resource allocation, including irrigation and fertilization, for efficient agricultural practices.
  - Crop Disease Detection: Identifying diseases and pests affecting crops.
- Disaster Management:
  - Natural Disaster Assessment: Rapidly assessing the extent of damage caused by events like hurricanes, earthquakes, floods, and wildfires.
  - Search and Rescue: Aiding in the search for missing persons in disaster-stricken areas.
- Urban Planning and Development:
  - Urban Growth Analysis: Monitoring urban expansion and infrastructure development.

    - Traffic and Transportation Planning: Analyzing traffic patterns and optimizing transportation systems.
- Forestry and Natural Resource Management:
    - Forest Inventory: Estimating timber volumes and monitoring illegal logging.
    - Wildlife Conservation: Studying wildlife habitats and migration patterns.
- Geology and Mining:
    - Geological Mapping: Identifying geological features and potential mineral resources.
    - Mine Monitoring: Monitoring mining operations and environmental impacts.
- Climate Change Studies:
    - Glacier and Ice Cap Monitoring: Tracking changes in ice cover and sea-level rise.
    - Snow Cover Analysis: Assessing snowpack levels and snowmelt patterns.
- Natural Resource Management:
    - Wetland and Coastal Zone Mapping: Monitoring changes in wetlands and coastal areas.
    - Water Resource Management: Assessing water levels, quality, and usage.
- Weather Forecasting:
    - Cloud Cover Analysis: Monitoring cloud patterns for weather prediction.
    - Hurricane and Cyclone Tracking: Tracking the movement and intensity of storms.

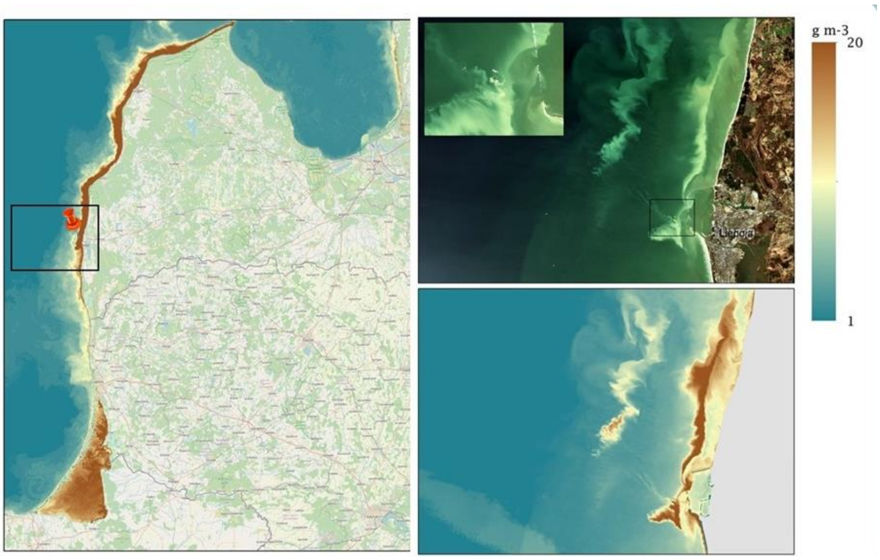

Figure I-9. *Suspended matter distribution in the coastal waters of the Baltic Sea retrieved from OLCI Sentinel-3 and MSI Sentinel-2 data. The increase of suspended matter is caused by the intensive renovation of Liepaja port in Latvia during February 2018.*

Thermal Infrared Remote Sensing data

All bodies having temperatures higher than the absolute zero (-273.15 °C) emit thermal radiation, the strength of which depends on the body's surface temperature. The higher is the temperature, the greater the radiant energy of the body. Therefore, the determination of the SST from space is based on measuring the thermal radiation energy coming from the sea surface. The instruments, called radiometers, determine the radiant energy flux within distinct intervals of the electromagnetic spectrum.

Clear sky conditions are required for the derivation of SST from IR measurements as the IR radiation does not propagate unhindered through clouds, and, even in cloud-free conditions, the constituents of the atmosphere such as CO_2, H_2O, CH_4, NO_2 and aerosols absorb some of the radiation emitted by the sea before it reaches the detector in space, and at the same time they re-emit radiation (Minnett et al., 2019). To overcome the issue of atmospheric absorption, the spectral intervals (wavelengths), therefore, are chosen at the locations where the sea emits a measurable amount of radiant energy, and where the atmosphere is sufficiently transparent to allow the energy to propagate to the spacecraft (Minnett, 2001). This is the so-called atmospheric window – a wavelength of energy that is most easily transmitted to Earth. For this reason, IR radiometry of the sea surface is restricted to two spectral windows in the approximate ranges 3.5–4.1 µm and 10.0–12.5 µm that are used for IR sensing of the ocean; the microwave measurements are made at frequencies of 6–12 GHz. However, one must note, that none of the atmospheric windows is completely transparent, therefore, atmospheric corrections for cloud-free pixels are still required. In addition, the effect of reflected sunlight shall also be considered, as it has a different effect for different spectral windows. Though the 3.5–4.1 µm channel is more sensitive to SST changes, it is primarily used only for night-time measurements as the reflected sunlight can create strong errors; while 10-12.5 µm channel can be used both, day, and night.

Passive Microwave Remote Sensing of SST

As was discussed in the previous chapter, infrared radiometers are mainly used for the sea surface temperature estimates from space, however, it is only possible under cloud-free conditions. Thermal radiation at microwave frequencies, however, is much less likely to be blocked by clouds. Therefore, spaceborne passive microwave (PMW) imagers can use this radiation for SST estimates under a much wider range of atmospheric conditions than infrared radiometers can (Langille, Buckley, 2002) and can be a good alternative to acquire satellite SST data. Nevertheless, a lower signal strength of the radiation curve in the microwave region makes the accuracy and resolution of passive microwave SST poorer as compared to IR SST. Another difference between IR and PMW SST is measurement depth, i.e., at the wavelengths where PMW operates the penetration depth is 1-3mm (SSTsubskin) while IR SST measurements represent only approximately 10-20 m µm within the ocean skin layer (more information on SST in chapter IV).

Passive microwave SST measurements are primarily made at channels near 6-7 GHz and/or 11 GHz with a water vapour correction enabled by observations at 21 GHz. But even though radiation at longer wavelengths is unaffected by clouds, wind-generated roughness at the ocean surface and precipitation influences passive microwave signal return. Land (also ice marginal zone) contamination is also an issue with microwave measurements, as within 50-100 km of land microwave measurements are affected by emissions from land, therefore, microwave SST observations are typically not produced within 50-100 km of land (Cummings, 2011). Due to the aforementioned limitations (mainly land contamination and coarse resolution) of PMW, SST measurements from IR radiometers are more suitable for the monitoring of landlocked water bodies that are smaller in size (e.g., the Baltic Sea and its coastal lagoons). Nevertheless, PMW SST is a valuable source for the global ocean coverage to be observed at daily frequencies (Figure I-10).

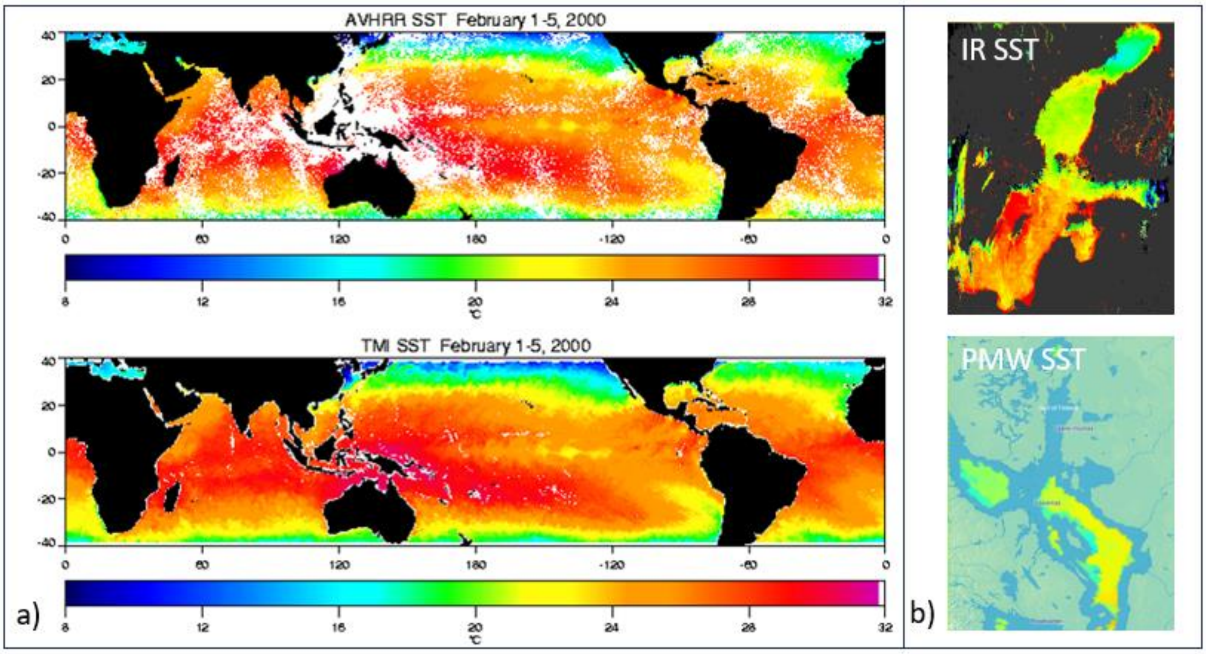

Figure I-10. *a) SST of the Global Ocean derived from IR measurements (top image) and a microwave-derived SST (bottom image) ©NASA JPL/PO.DAAC; b) SST of the Baltic Sea: derived from MODIS IR measurements (top image) and from microwave AMSR-2 measurements (bottom) ©*

Passive microwave instruments used for deriving SST include Advanced Microwave Scanning Radiometer – Earth Observing System (AMSR-E) and Advanced Microwave Radiometer 2 (AMSR2) on the NASA EOS Aqua satellite, Tropical Rainfall Measuring Mission (TRMM) Microwave Imager (TMI) and others. Currently, a new radiometer of ESA for the Copernicus Expansion program of the European Union, the Copernicus Imaging Microwave Radiometer (CIMR), is in the preparatory phase, with an estimated launch date in the 2025+ time frame. It is designed to observe the ocean and sea ice and more particularly the Arctic environment. Amongst other parameters, such as the Sea-Surface Salinity (SSS) and Sea Ice Concentration (SIC), CIMR will also be used for deriving Sea Surface Temperature data (more information at eoportal.org).

Synthetic Aperture Radar

Synthetic Aperture Radar (SAR) represents a paradigm shift in remote sensing technology by employing active data collection, where the sensor generates its own energy and measures the energy reflected back after interacting with the Earth. Unlike interpreting optical imagery, which is analogous to analysing a photograph, SAR data interpretation requires a nuanced approach as the signal responds to surface characteristics like structure and moisture.

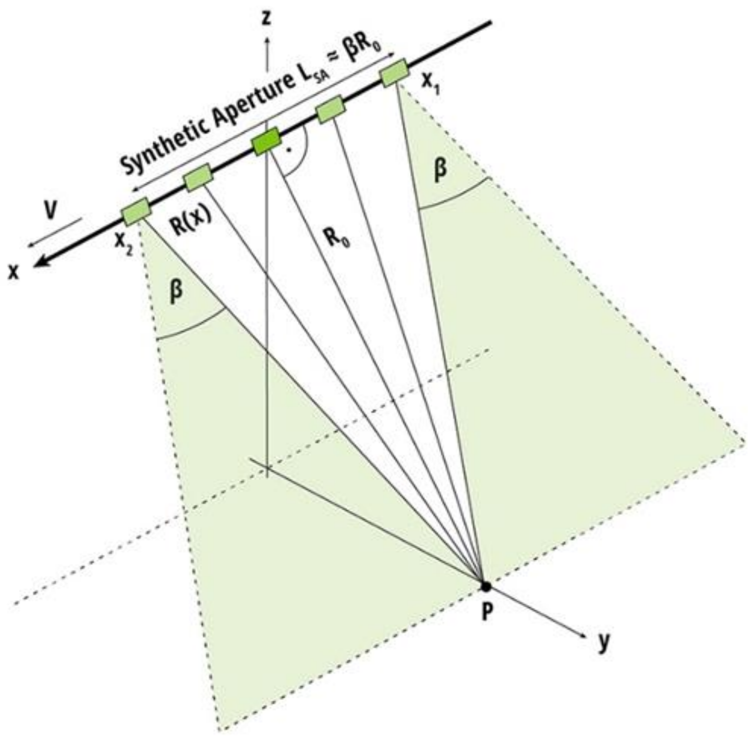

Figure I-11. *Geometry of observations used to form the synthetic aperture for target P at along-track position x=0 (Credit: NASA SAR Handbook).*

SAR Platforms: The availability of consistent SAR datasets became more widespread with the launch and open data policy of ESA's Sentinel-1a in 2014. Other prominent SAR platforms contributing to the availability of varied datasets include ERS-1 and 2, ENVISAT, ALOS PALSAR, TerraSAR-X, COSMO-SkyMed, and RADARSAT-2. Main SAR data providers are: European Space Agency (ESA), National Aeronautics and Space Administration (NASA) Canadian Space Agency (CSA), Deutsches Zentrum für Luft- und Raumfahrt e.V. (DLR).

Different Wavelengths: Wavelength is a pivotal feature in SAR technology, dictating how the radar signal interacts with the surface and the depth of signal penetration into a medium. The different wavelengths, often referred to as bands like X, C, L, and P, have distinct applications ranging from high-resolution urban monitoring to airport surveillance. For instance, the X band, with a frequency of 8–12 GHz and wavelength of 3.8–2.4 cm, is utilized for high-resolution SAR applications, such as urban monitoring (Table I-1).

Table I-1. Different wavelengths / bands of SAR and their applications.

Band	Frequency	Wavelength	Application
Ka	27–40 GHz	1.1–0.8 cm	Rarely used for SAR (airport surveillance)
K	18–27 GHz	1.7–1.1 cm	rarely used (H2O absorption)
Ku	12–18 GHz	2.4–1.7 cm	rarely used for SAR (satellite altimetry)
X	8–12 GHz	3.8–2.4 cm	High resolution SAR (urban monitoring, ice and snow, little penetration into vegetation cover; fast coherence decay in vegetated areas)
C	4–8 GHz	7.5–3.8 cm	SAR Workhorse (global mapping; change detection; monitoring of areas with low to moderate penetration; higher coherence); ice, ocean maritime navigation
S	2–4 GHz	15–7.5 cm	Little but increasing use for SAR-based Earth observation; agriculture monitoring (NISAR will carry an S-band channel; expends C-band applications to higher vegetation density)
L	1–2 GHz	30–15 cm	Medium resolution SAR (geophysical monitoring; biomass and vegetation mapping; high penetration, InSAR)
P	0.3–1 GHz	100–30 cm	Biomass. First p-band spaceborne SAR will be launched ~2024; vegetation mapping and assessment. Experimental SAR.

SAR's ability to penetrate clouds gives it a distinct advantage over optical data, expanding its application in diverse fields. The uses for SAR data are extensive and include airport surveillance, aiding in maritime navigation, monitoring agriculture, mapping biomass and vegetation, determining sea surface temperature, and analyzing wave patterns. The versatility of SAR data makes it an invaluable tool in various scientific, environmental, and security applications. More information on SAR can be also found in Chapter V.

Unmanned Aerial Vehicles (UAVs)

UAVs play a pivotal role across a spectrum of remote sensing applications. They are instrumental in acquiring detailed local measurements, crucial for microclimate studies and soil analysis, and offer invaluable insights into forest production, aiding in sustainable management and conservation efforts. Additionally, UAVs are indispensable for monitoring the health of ecosystems, crops, and urban areas, facilitating early detection of diseases, pest infestations, and environmental stress. They are also employed for species identification, contributing to biodiversity studies and ecological conservation. Beyond natural environments, UAVs are extensively used for infrastructure inspection and disaster assessment, ensuring structural integrity of buildings, and providing rapid evaluations of areas affected by natural calamities.

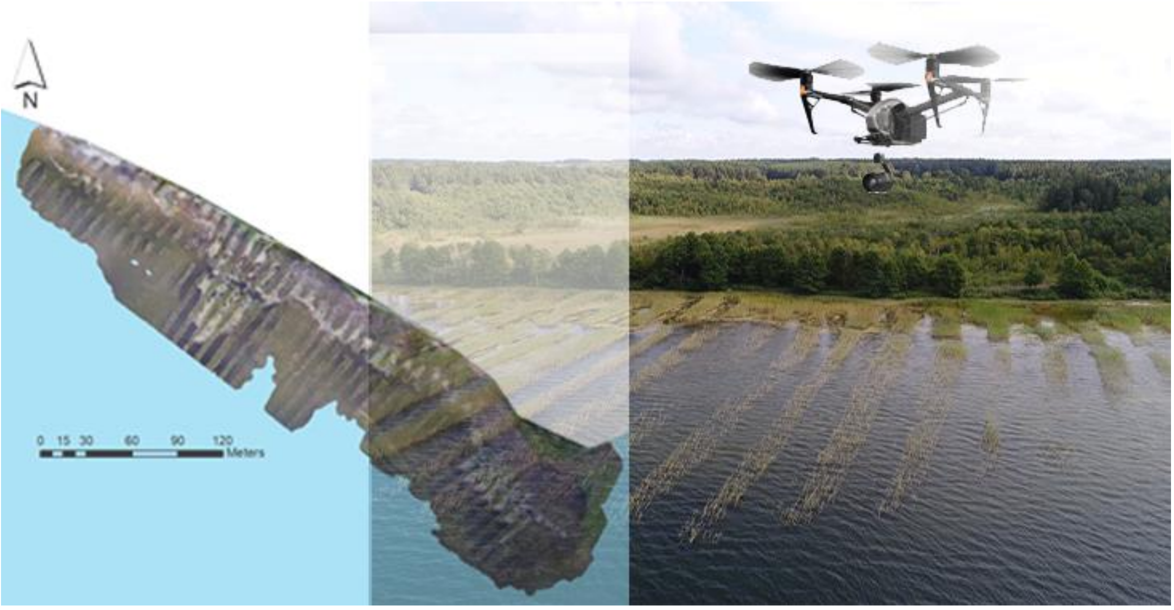

Figure I-12. *A single drone-captured image on the right with a detailed, cohesive map formed by mosaicking multiple images on the left, illustrating how UAVs enhance spatial coverage and detail in remote sensing applications.*

Equipment: Both piloted and unmanned aircraft equipped with advanced sensors such as optical cameras, multispectral imagers, thermal cameras, and LiDAR sensors are employed in remote sensing. This diverse array of equipment allows UAVs to capture multifaceted data, catering to the specific requirements of various applications.

Point Clouds and 3D Structures: Utilizing sensors such as LiDAR, UAVs can generate detailed point clouds—sets of data points in space representing the external surface of objects. These point clouds are instrumental in creating accurate 3D models of structures, landscapes, and vegetation, offering a comprehensive spatial representation of the surveyed area.

Software and Data Acquisition: Data gathered by UAVs is processed using specialized software that uses Structure From Motion (SFM) algorithms to mosaic images into maps, allowing users to analyse, visualize, and interpret the collected data. Some examples of the software would be Pix4D or DroneDeploy. Practical acquisition of data involves careful planning, ensuring optimal flight paths, and adhering to legal and safety regulations.

II. Introduction to ESA SNAP

ESA's Sentinel Application Platform (SNAP) is an open-source and free to use set of toolboxes ideal for the exploitation of Earth Observation data. In this manual, only the basic information on how to navigate ESA SNAP software will be provided with some useful steps and tips for satellite data analysis.

Downloading SNAP: You can download SNAP from ESA's Science Toolbox Exploitation Platform: https://step.esa.int/main/download/snap-download/

There are three different installers to choose (Windows 64-Bit, Mac OS X and Unix ,4-Bit), select one according to your system: **Sentinel Toolboxes > *Installer you have chosen > Main Download** (Figure II-1).

	Windows 64-Bit	Mac OS X	Unix 64-bit
Sentinel Toolboxes	These installers contain the **Sentinel-1**, **Sentinel-2**, **Sentinel-3** Toolboxes, download size is close to 900MB.		
	Main Download Mirror Download	Main Download Mirror Download	Main Download Mirror Download
SMOS Toolbox	These installers contain only the **SMOS Toolbox**, download size is close to 500MB. Download also the Format Conversion Tool (Earth Explorer to NetCDF) and the user manual.		
	Main Download Mirror Download	Main Download Mirror Download	Main Download Mirror Download
All Toolboxes	These installers contain the **Sentinel-1**, **Sentinel-2**, **Sentinel-3** Toolboxes, **SMOS** and **PROBA-V** Toolbox, download size is close to 1GB.		
	Main Download Mirror Download	Main Download Mirror Download	Main Download Mirror Download

Figure II-1. *SNAP installation window (from SNAP Download – STEP (esa.int))*

Then follow the steps of ESA SNAP installation wizard to complete the installation.

SNAP interface: ESA SNAP interface (Figure II-2) is user friendly, enabling one to process and analysis the Earth observation data in a simple steps.

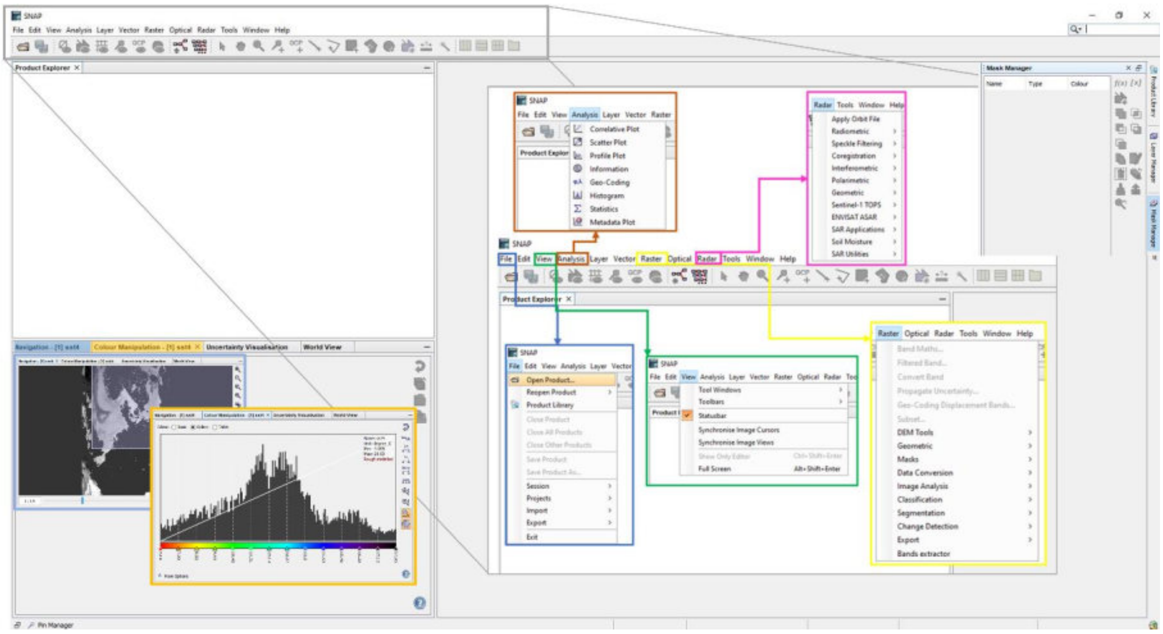

Figure II-2. *SNAP interface.*

General tools and steps of satellite data processing

Importing data: There are many input data formats that SNAP supports, therefore, here only few examples of loading data will be demonstrated. To load the data into SNAP one may choose from several options, e.g., **File > Import > *file type of your choice*** or **File > Open Product...** (Figure II-3).

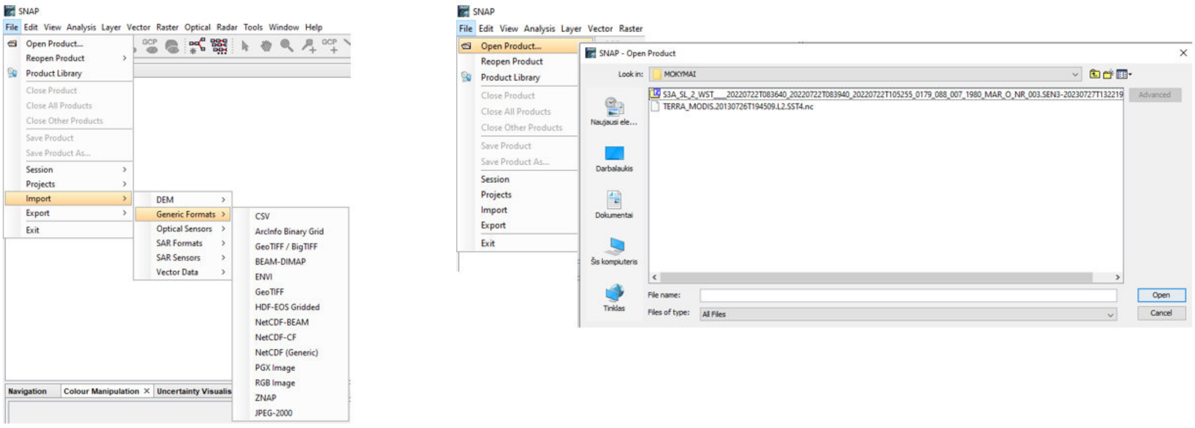

Figure II-3. *Example of loading data into SNAP.*

This allows user to import satellite data or other formats of data to be processed via SNAP software.

After importing satellite data (e.g., **File > Import > Generic Formats > NetCDF**) the band of interest must be selected (Figure II-4), then colour scale (Figure II-5 and Figure II-6), reprojection (Figure II-7) and/or other modifications can be applied.

Selecting bands: In the **Product Explorer** window click on the box ⊞ to expand selections and choose the band to work with. In the provided example, sea_surface_temperature (SST) band is chosen.

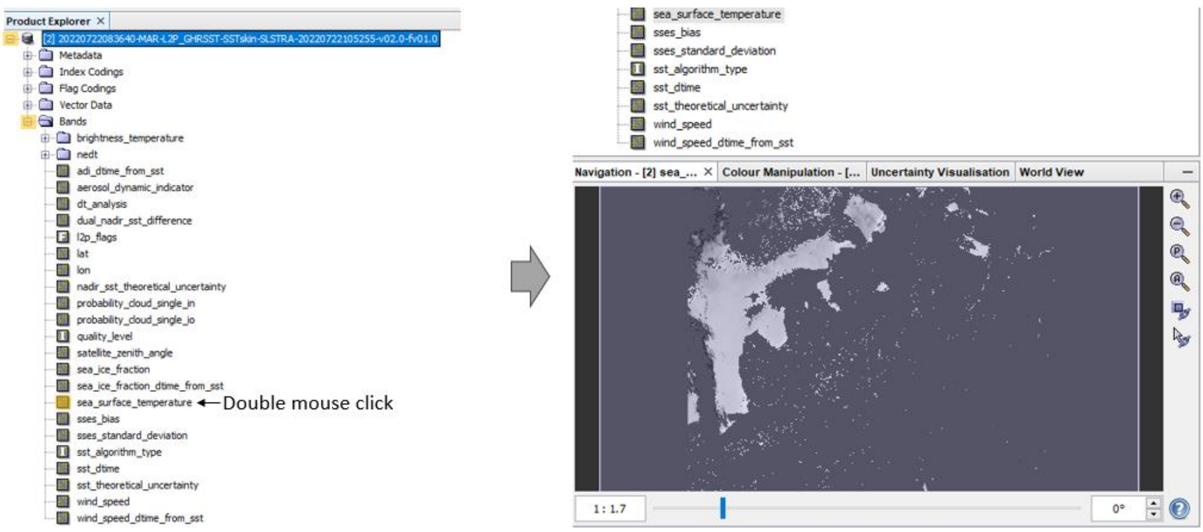

Figure II-4. *Selecting band to be displayed in SNAP.*

Adding colour scale: In the **Colour Manipulation** window press on the **Import colour palette from text file** icon and choose the preferred colour palette (Figure II-5).

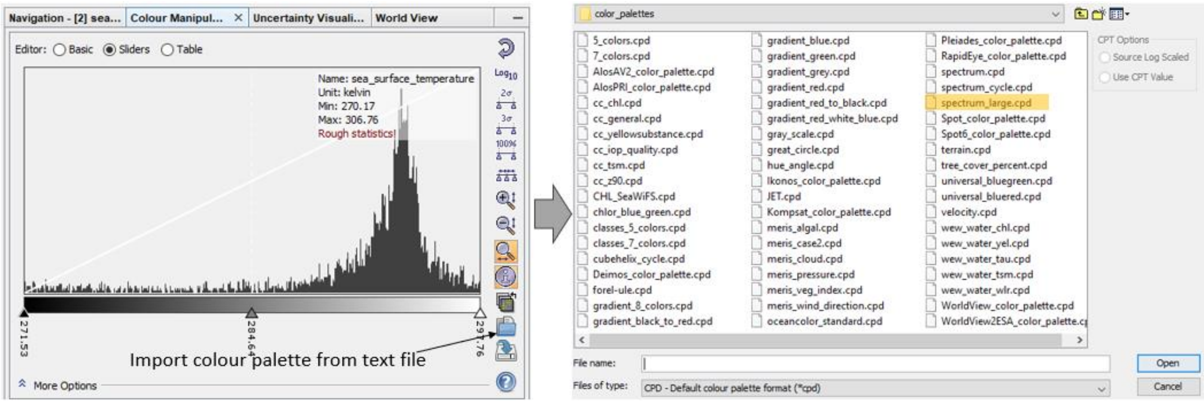

Figure II-5. Importing colour palette.

In the provided example **spectrum_large.cpd** was chosen to best reflect the SST values. After importing the colour palette, the spectrum range can be modified using **Basic**, **Sliders** or **Table** editor options.

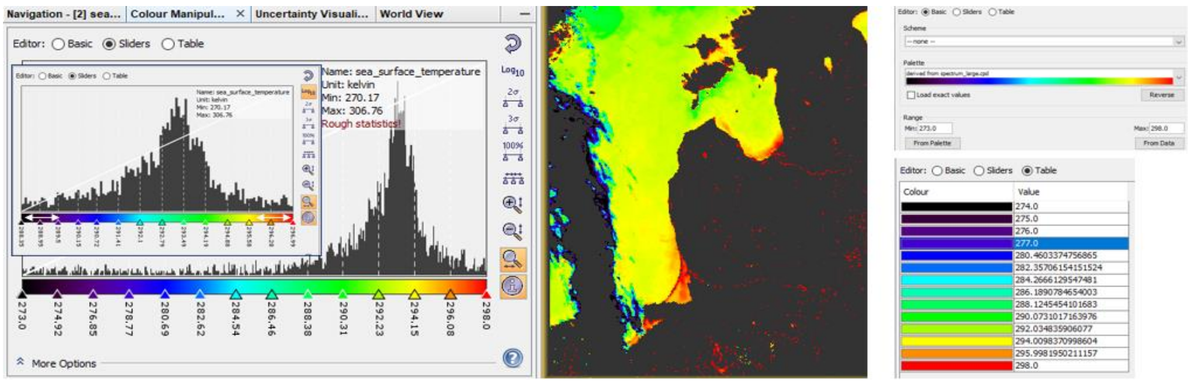

Figure II-6. Adjusting colours of the displayed image.

Using **Sliders** editor one can manually adjust the range of the histogram; using **Basic** option the Min and Max values of the range can be modified; using **Table** option a distinct value can be assigned to each colour.

Reprojecting the image: Reprojecting – i.e., transforming an image from one coordinate system to another is sometimes necessary to align different images or data sets that have been acquired with different sensors or platforms, also it is used to adjust for geometric distortions or to change the resolution or the projection of an image. The steps are the following: **Raster > Geometric > Reprojection > *the coordinate system of your preferences***

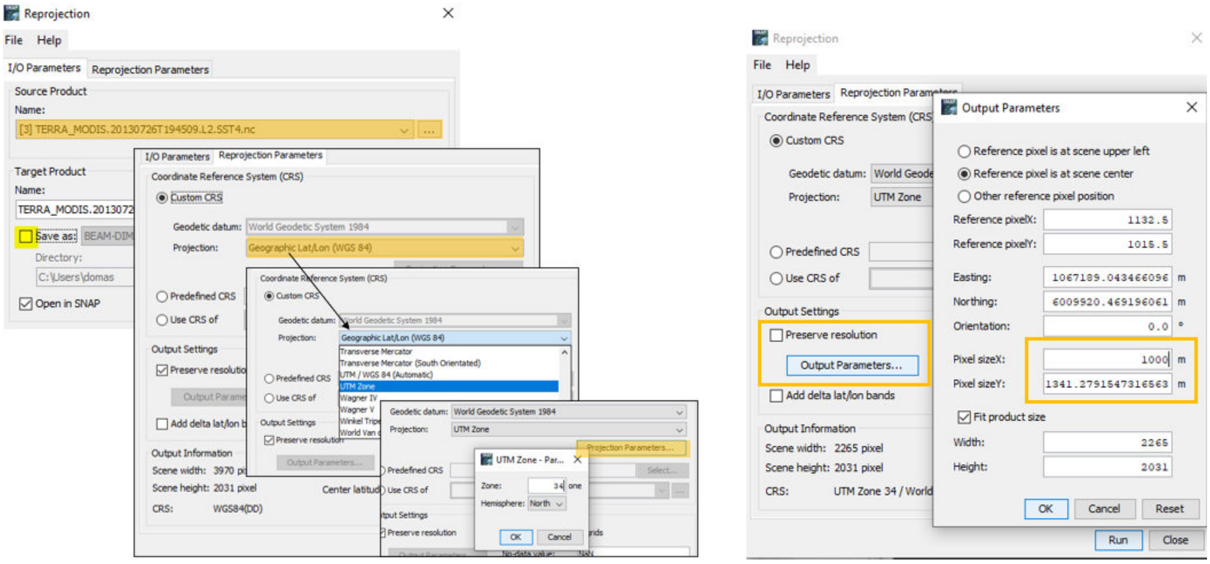

Figure II-7. *Steps of reprojecting the image.*

Before reprojecting, check if the **Source Product** name is the one you want to work with. Deselecting **Save as: BEAM-DIMAP** (or other file formats) is recommended as it makes the tool run faster. Unless you want the file to be physically saved to the file system in a specific format, keep it selected. In the **Reprojection Parameters** section one can choose the **Coordinate Reference System (CRS)** (from "Custom CRS" – creating yourself; "Predefined CRS" – selecting one; or - "Use CRS of file" – using coordinate system from the file). In the example of Figure II-8, a WGS 84 / UTM zone 34N was chosen as the area of interest – Lithuanian Baltic Sea, is attributed to this zone.

In the **Output Settings** section one can deselect **Preserve resolution** and manually set the parameters, such as Pixel size and others. After successful reprojection of the data, a new file in the **Product Explorer** will appear, which will have the same file name as the original file, only with an ending "_reprojected".

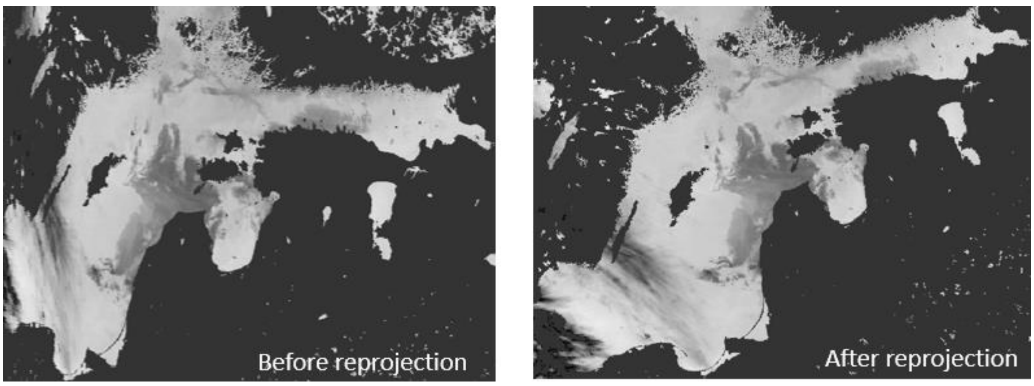

Figure II-8. An example of image before and after reprojecting.

Importing vector data: Once the raster data is imported, user can import additional data, e.g., vector data can be inserted, following steps: **File > Import > Vector data > *format of your preference*.** Imported vector data can be used for the further analysis of the data. One can import profile lines, polygons, points with coordinates etc., in the format of ESRI Shapefiles (*in the same coordinate reference system as the raster product), CSV files and others. Vectors can also be used as masks in the Mask manager and for lots of other purposes.

In the **Analysis** tools there are many useful options, such as making **correlative, histogram, profile, scatter, spectrum** plots or calculating **statistics** of the selected bands. Correlative plots **Analysis > Correlative Plot** might be useful, e.g., for investigating how the satellite data and in situ data match. Profile plots enable to display profile plots for selected band. An example in Figure II-9 demonstrates a profile plot generated from an imported shapefile (**File > Import > Vector data > ESRI Shapefile > *name of your file***) and one of the possible ways to analyse the data (**Analysis > Profile Plot**).

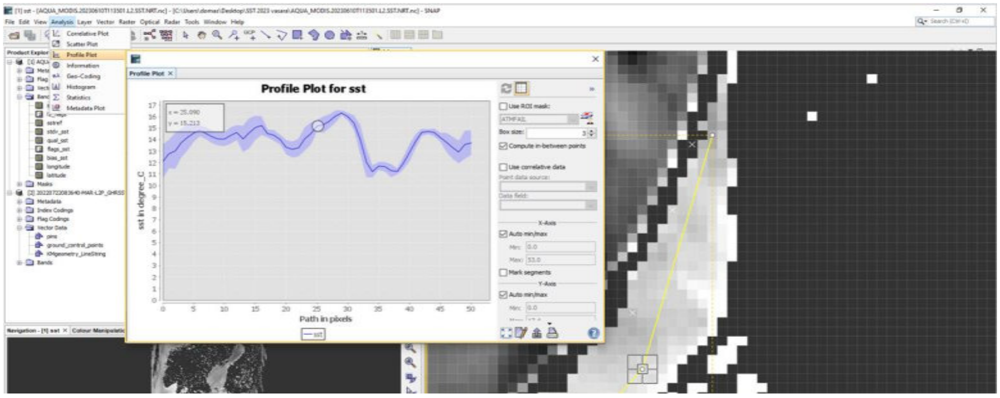

Figure II-9. *Generating a profile plot.*

The profile plot can also be edited (name of the axis, title, colours etc.) using **Edit chart properties** tool and then it can be saved as an image (Figure II-10)

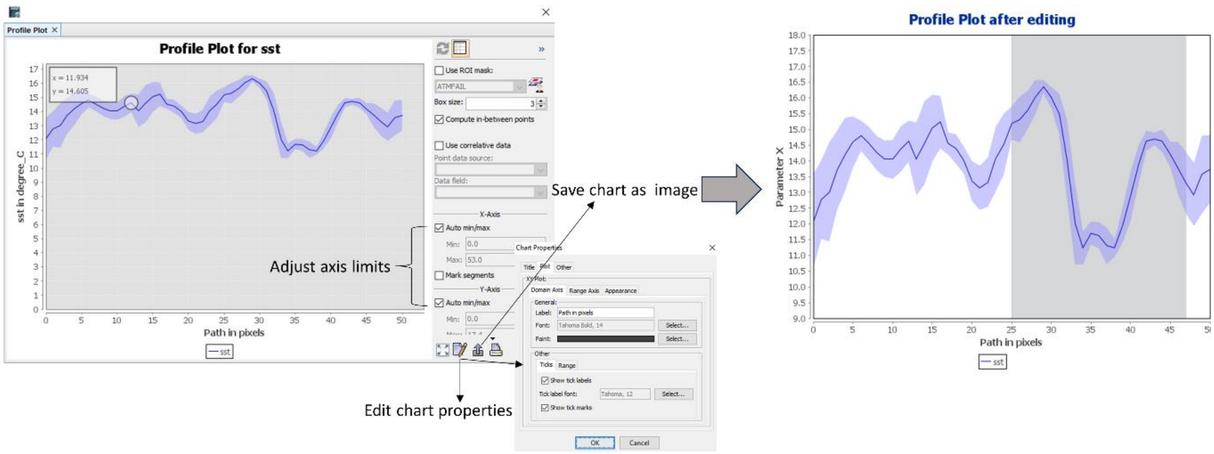

Figure II-10*. Editing/saving a profile plot.*

Before importing CSV file, make sure that it has a header line with column names (e.g., "lat" or "latitude" – for latitude, "DateTime", in situ values, etc.). When the file can be imported following the steps: **File > Import > Vector data > Vector from CSV > *name of your file* > Use target CRS > Leave imported data unchanged.**

Selecting the box Use ROI mask(s) lets one choose the file to be displayed. In figure 10 an example of statistics, calculated for Sea Surface Temperature (SST) pixels at the given coordinates (CSV file "coord") is presented. As can be seen, pixel A is located at the land, therefore, statistics for SST values are only available for pixels at the locations B and C (Figure II-11). The statistics can be displayed on screen or can be exported as CSV file via selecting this icon .

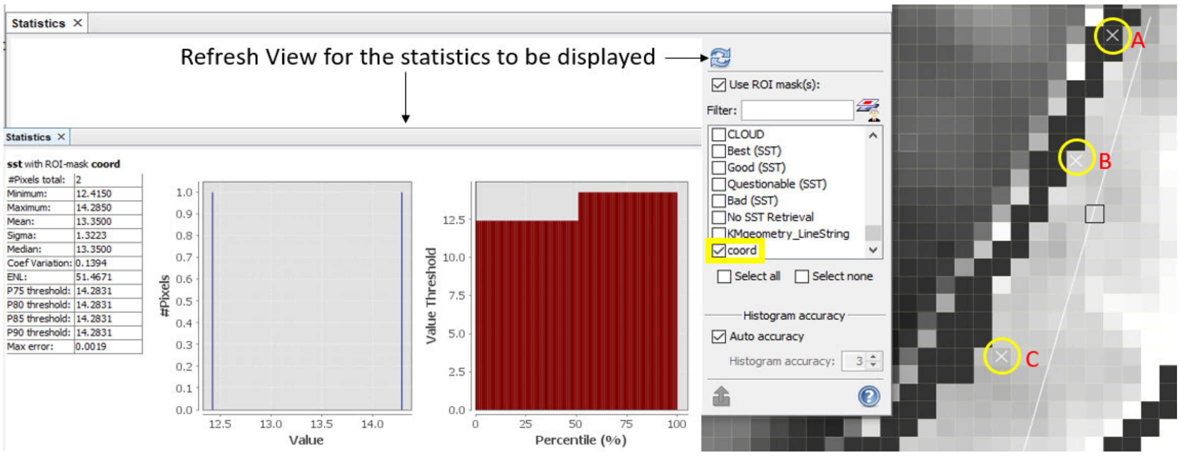

Figure II-11. An example of analysis for imported CSV files.

Masks: Masks can be useful for masking certain image pixels for the display or for image analysis. They can be generated from geometries (e.g., line, polygon), flags, and band math expression; also, different combinations of masks are available. Masks can be applied **View > Tool Windows > Mask Manager** or choosing this icon. When new masks can be created, or existing ones applied (Figure II-12). Via pressing this icon masks can also be transferred to other products.

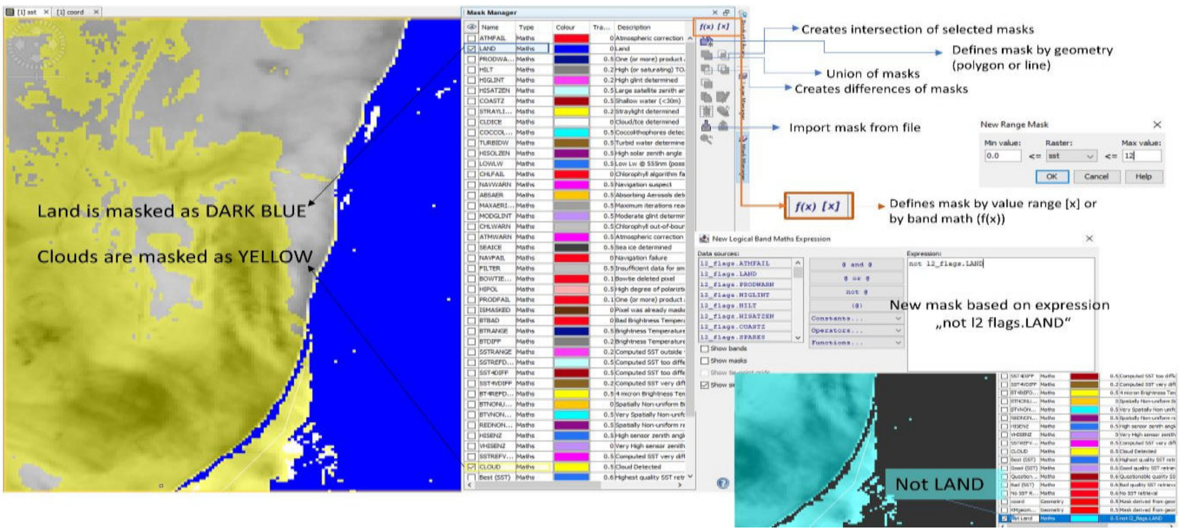

Figure II-12. An example of applying masks.

Exporting data: The steps of exporting data are similar to the steps of importing data. **Note:** prior exporting, the data file, from which data is going to be exported, needs to be selected (highlighted).

Steps for exporting the data: **File > Export > *file type of your choice*.** The Figure II-13 demonstrates the option to export **View** and **Colour Legend as image**.

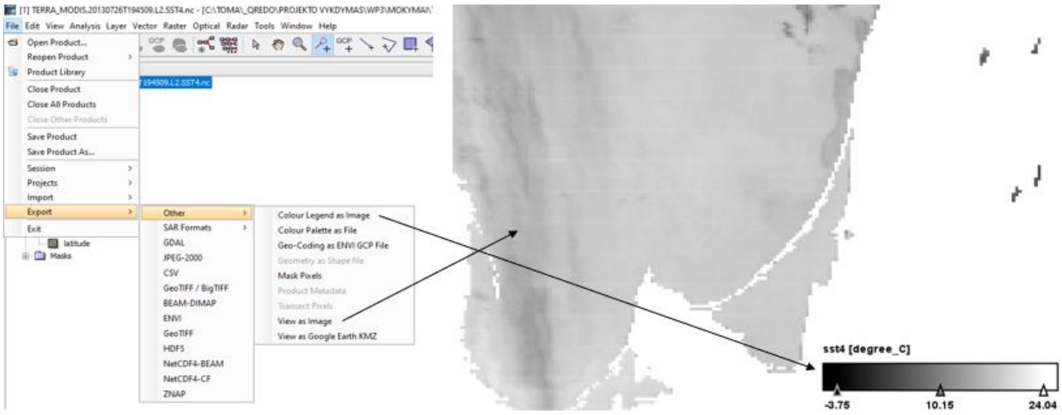

Figure II-13. An example of exporting image and colour legend.

Choosing option **File > Export > GeoTIFF > Export Product** lets one export product as it is, however, sometimes satellite data files can be quite large, also not all bands are needed for further analysis, in that case one may choose to modify the **Subset** he wants to export. **Spatial Subsets** enables modifying the scene, **Band Subset** lets one choose the bands to be exported. As Figure II-14 demonstrates, choosing only sst4, longitude and latitude bands instead of all available bands reduced the **Estimated raw storage size** from 60.3M to 26.3M.

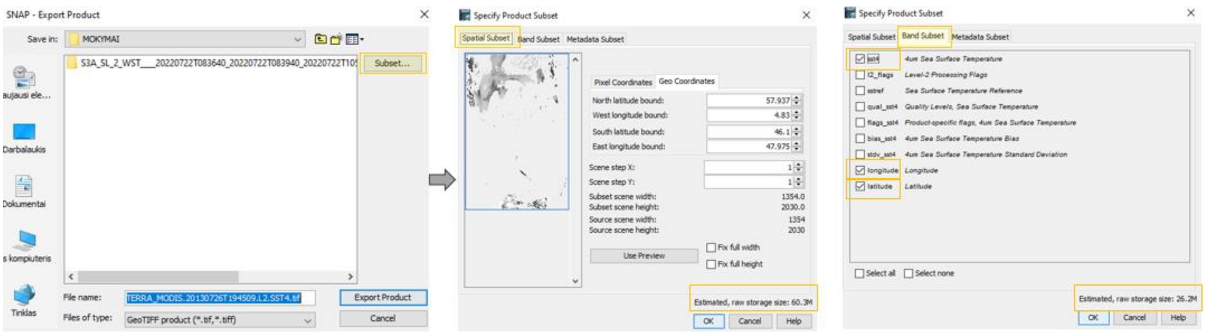

Figure II-14. Exporting Product Subset.

Masks can be exported by pressing a right mouse click on the image and choosing **Export Mask Pixels > *mask to be exported* > Copy to Clipboard / Write to File** or **File > Export > Other > Export Mask Pixels** (Figure II-15).

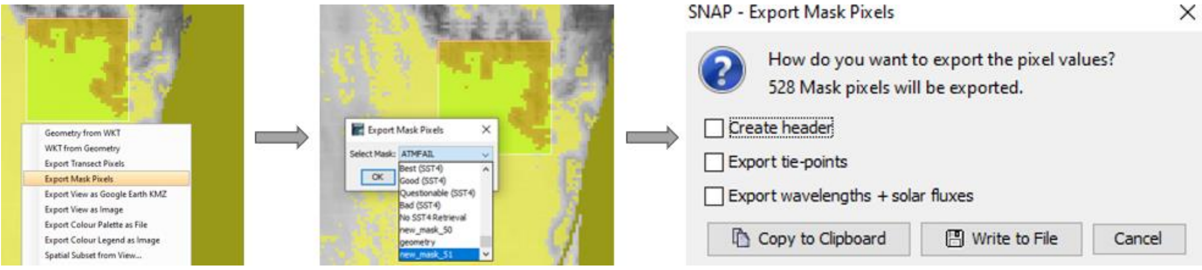

Figure II-15*. Exporting Masks.*

Band Maths: The Band Maths Expression Editor provides a convenient way to construct maths expressions from various data sources, such as bands, tie-point grids and flag values. E.g., one can calculate a difference between the same band in two different products (note: to use the Band Maths they must be compatible, i.e., have the same width and height), create new bands, etc. The example in Figure II-16 demonstrates how one can create a new band containing sea surface temperature information in degrees Celsius, instead of Kelvin degrees (as was in the original satellite image), following the steps: **Raster > Band Maths > Edit Expression.** Then from the sea_surface_temperature band (in Kelvins), 273.15 are subtracted, converting it to degrees Celsius. A new band will appear in the product bands.

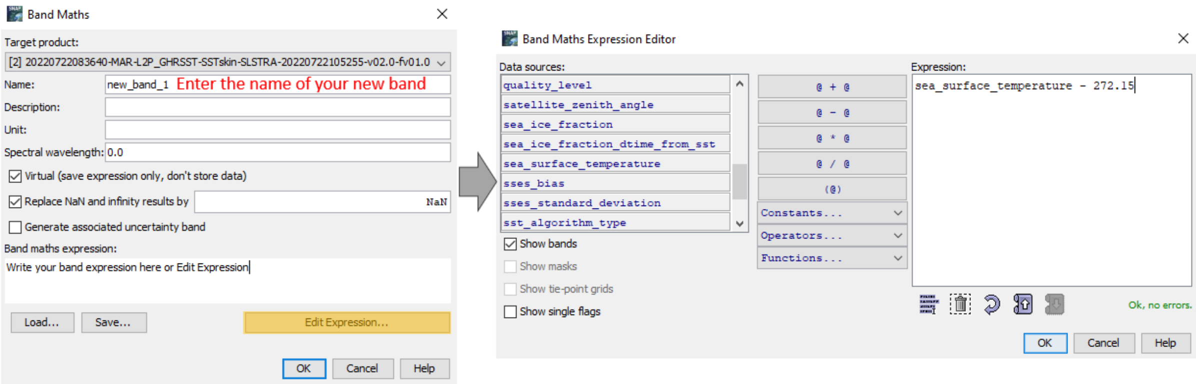

Figure II-16*. An example of creating Band Maths.*

Pin Tools: A pin is a marker for a certain geographical position within a geo-referenced image. You can find them in the toolbar section  - Pin Placing Tool;  - Pin Manager, or in **View > Tool Windows.** Pins can be useful for displaying the values of a pixel at the location the pin is placed. After placing pins, use **Pin Manager** to display the values. To select the band values to be displayed, select **Filter pixel data to be displayed in table** icon  and then check the necessary boxes (Figure II-17). Pins can also be imported/exported from/to XML or text files and can be transferred to other products.

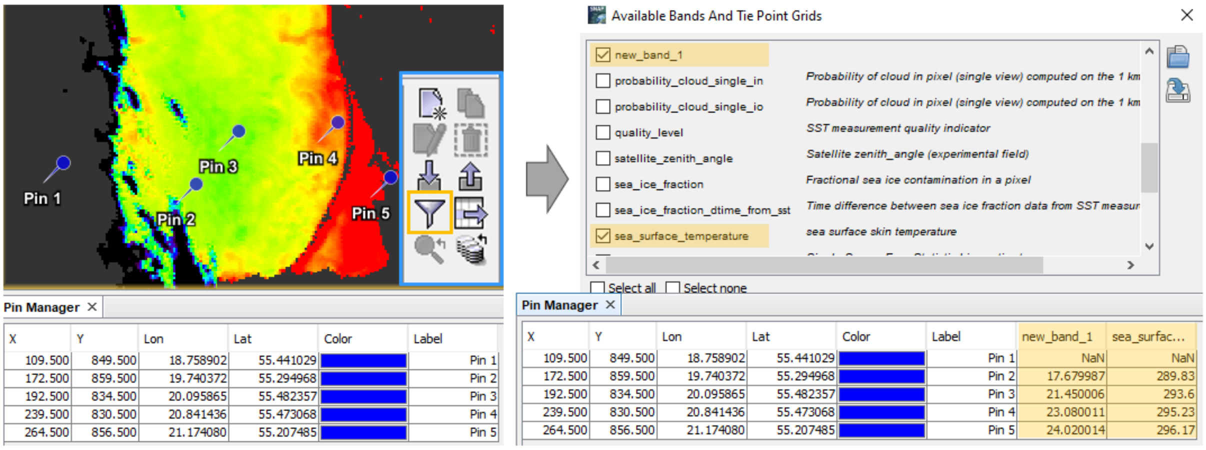

Figure II-17. *Working with Pins.*

SAR image processing workflow

> **NOTE:** Data providers process and provide data at different levels. This workflow is focused on Level 1 Ground Range Detected (GRD) data acquired from Sentinel-1 satellite.

Image Sub-setting/cropping: Satellite data files are very large; thus, their processing requires a lot of computing power. All subsequent SAR image processing steps will be time-consuming or potentially unsuccessful if sufficient resources are unavailable. To overcome this limitation one possible solution would be to first crop the image and focus solely on the desired location. To achieve this:

1. Open one band of the chosen satellite image by pressing a “+” sign next to your uploaded file in the **Product Explorer window**. Then extend the **Bands** folder (“+”) and with the left mouse button double-click one band of your choice. An image should appear on the right side of the SNAP interface.
2. Zoom in to the targeted area and clip the image (Figure II-18):
   2.1. Press the right mouse click on the image and choose **Spatial subset from view**.
   2.2. Clarify the bounding box (by moving the bounding box edges in the preview or by entering the starting and ending coordinates) and clip by pressing **OK** in the dialogue window.

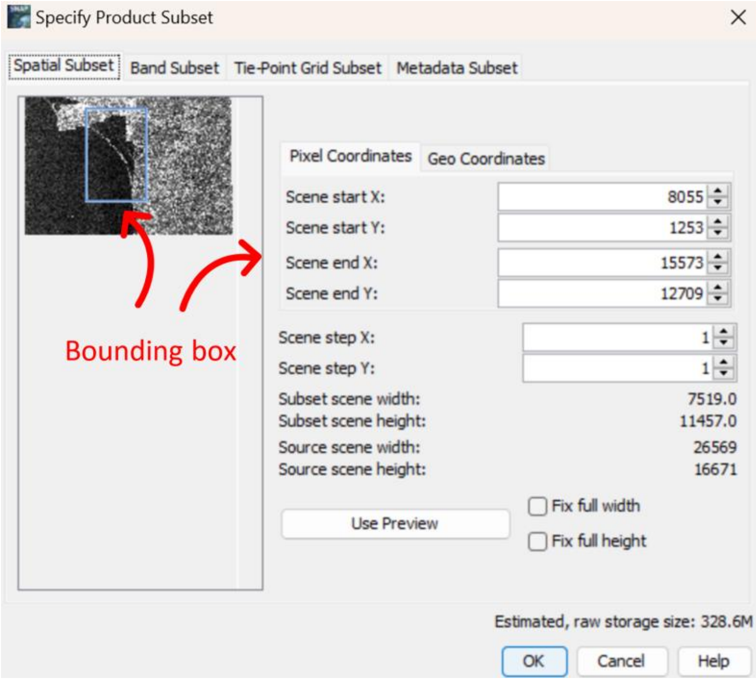

***Figure II-18**. Specifying product subset.*

Now you can close the large SAR image by right-clicking it and choosing **Close Product**. If a window pops up asking if you want to save this file, then choose **No**.

Application of Orbit File: Next, we will use the orbit update function, which is a process that automatically updates and corrects information about the satellite's position and speed. This is important because small variations in the satellite's orbit can introduce errors in the radar images it captures. By regularly collecting tracking data and incorporating it into the processing pipeline, we ensure that the radar images are accurately aligned with geographical coordinates. This helps to produce high-quality images that can be used for precise mapping and other applications that rely on accurate location information.

SAR product metadata initially contains inaccurate orbit state vectors. It takes several days to determine the precise orbit of the satellite, and this information becomes available days to weeks after the product generation. The orbit update function in SNAP software automatically downloads and updates the orbit state vectors for each SAR scene, providing accurate satellite position and velocity information. To do this, in the upper menu bar choose **Radar > Apply orbit file**. In the popped-up window, you will see two tabs of settings (Figure II-19), make sure that in: (1) **I/O Parameters** tab: the source file is selected using your subset file, also, select the location where to save the intermediate files; (2) **Processing Parameters** tab: if you are using Sentinel-1 image, leave the setting as it is, otherwise chose the appropriate parameter from the **Orbit State Vectors** drop-down list. In case you are processing a very recent image, the **Orbit State Vectors** might not be yet available, thus check-mark the box that does not allow this tool to fail in case the orbit file is not found.

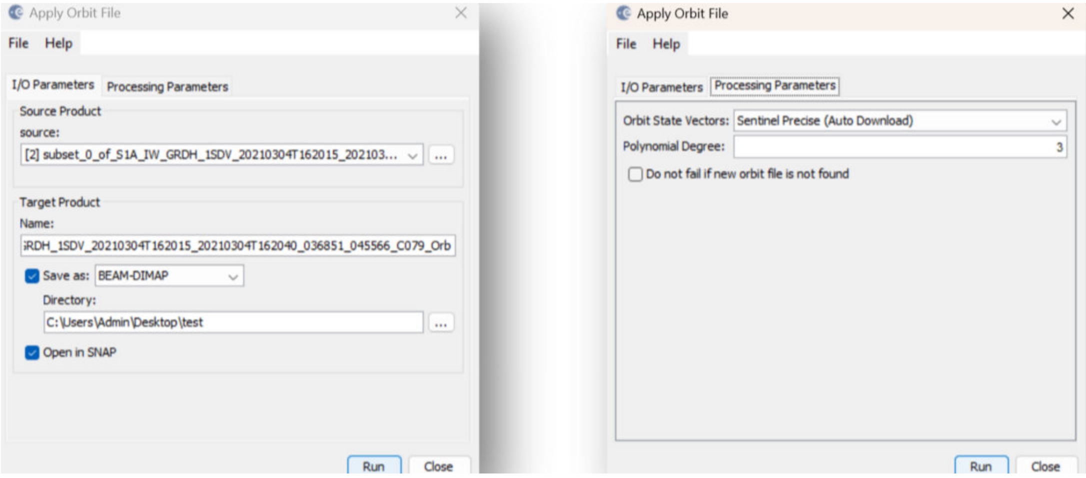

Figure II-19. *Application of Orbit file.*

After this step, you will find a new layer in the **Product Explorer** window.

Calibration: Next, we need to undergo a calibration procedure in which the digital pixel values are transformed into radiometrically calibrated radar backscatter values. Radiometric calibration is necessary to compare SAR images obtained with different sensors or obtained from the same sensor at different times, in different modes, or processed by different algorithms. Without radiometric calibration, the radar signal variations can lead to differences in brightness and contrast in the SAR images, making accurate comparison and interpretation challenging. To calibrate your SAR image:

1. In the upper menu bar choose **Radar**, then select **Radiometric** and then the **Calibrate** function (Figure II-20).

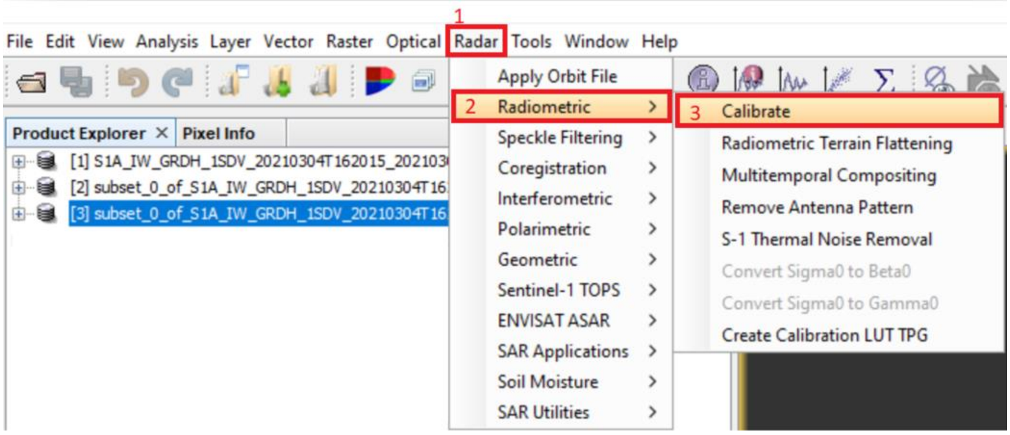

Figure II-20. *Image calibration steps.*

2. In the pop-up window you will again see two tabs:
   2.1. **I/O Parameters**: as before, make sure that your orbit-applied subset layer and desired saving locations are specified.
   2.2. **Processing Parameters**: make sure that the **sigma0** (backscatter coefficient) band is selected for the output. Click **Run** to execute.

After running this tool, in the **Product Explorer** section on the left of your screen, you will find a new layer (Figure II-21), which has your new calibrated bands of radar backscatter.

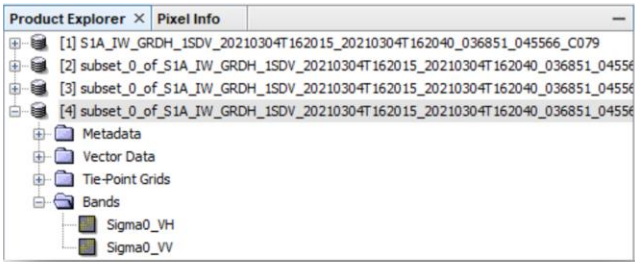

***Figure II-21**. New layer.*

Speckle filtering (optional step): A speckle is a form of granular noise caused by the coherent nature of SAR imaging. It manifests as random variations in brightness and texture, creating a grainy appearance in the images. Speckle filtering is a technique used in SAR image processing to reduce this unwanted noise while preserving the important details and structures, i.e., the image's overall quality. Various speckle filtering methods exist, each with its own strengths and weaknesses. The choice of speckle filtering method depends on factors such as the desired level of noise reduction, preservation of image details, and computational efficiency. It's important to strike a balance between reducing the speckle noise and retaining the essential information in the SAR image to ensure accurate interpretation and analysis of the data.

If you choose to apply the speckle filtering in the SAR image processing workflow, it is important to apply it before the other steps of image processing so that it does not transfer to them. The comparison of different filtering methods available on SNAP can be found in Jagtap and Shafiyoddin (2021) paper. To perform this step in SNAP software:

1. In the upper menu bar choose **Radar > Speckle filtering > Single Product Speckle Filter** function (Figure II-22).

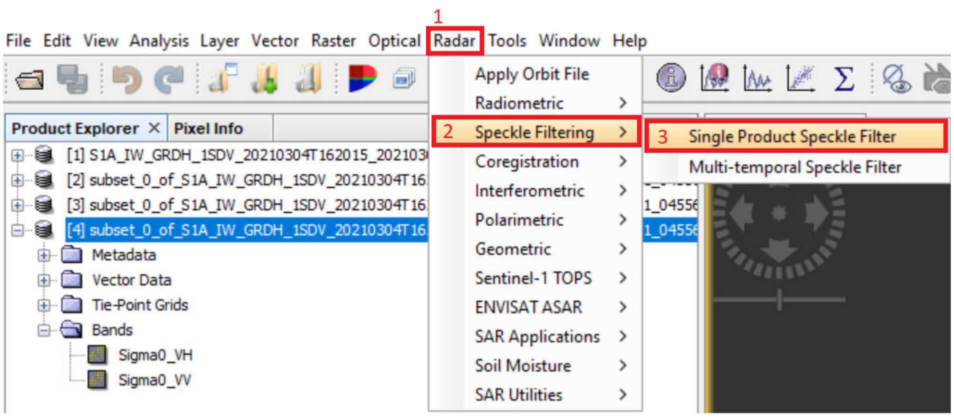

Figure II-22. Steps of Speckle filtering.

2. In the popped-up window you will see two tabs of settings, make sure that in:

2.3. **I/O Parameters** tab: the source file is selected using your calibrated subset file, also select the location where to save the intermediate files

2.4. **Processing Parameters** tab: set the appropriate parameters to fit your needs of detail and hit **Run** (Figure II-23).

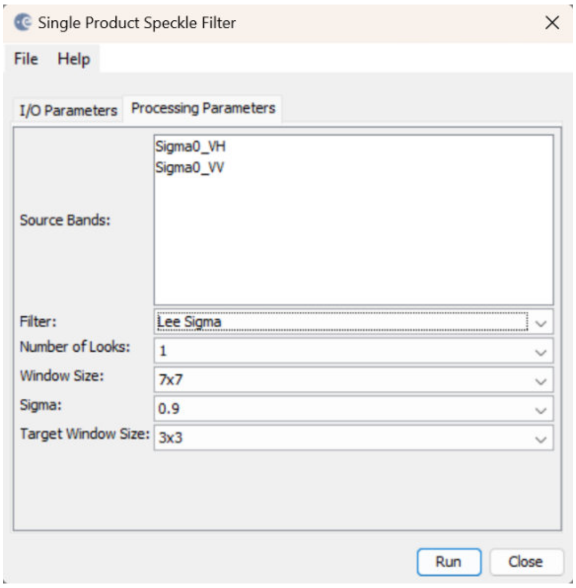

Figure II-23. *Example of setting the processing parameters.*

Range-Doppler Terrain correction: Radar images are acquired through the observation of Earth's surface from different vantage points, resulting in potential distortions based on the satellite's observation direction and orbit (whether ascending or descending). Sometimes, depending on the satellite orbit trajectory, the image of the area of your interest that you see in your display can appear upside-down and/or flipped (Figure II-24).

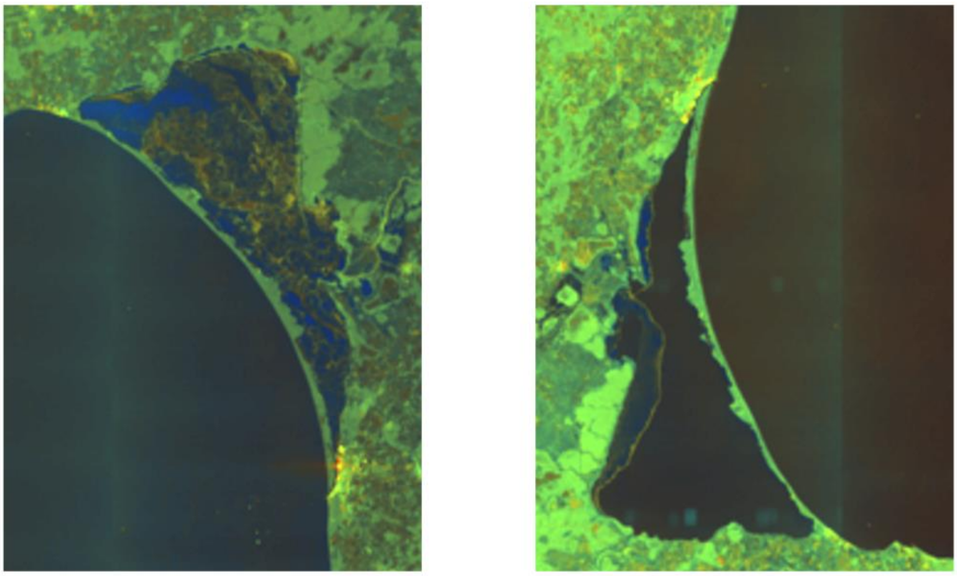

Ascending Descending

Figure II-24. *Examples of image display based on the satellite's observation direction.*

These distortions must be rectified to ensure that the obtained image accurately represents the actual surface. To achieve this:

1. In the upper menu bar choose **Radar > Geometric > Range-Doppler Terrain correction**.
2. In the pop-up window you will again see two tabs:
   2.1. **I/O Parameters**: as before, make sure that your last image processing layer and desired saving locations are specified.
   2.2. **Processing Parameters**: make sure to remove the check mark next to **Mark out areas without elevation** if you want to work not only with land area. Click **Run** to execute.

After running this tool, in the **Product Explorer** section on the left of your screen, you will find a new layer, which now has your study in the correct place on the map, without distortions. You can look at the image by double-clicking on the data in the **Bands** subfolder (Figure II-25).

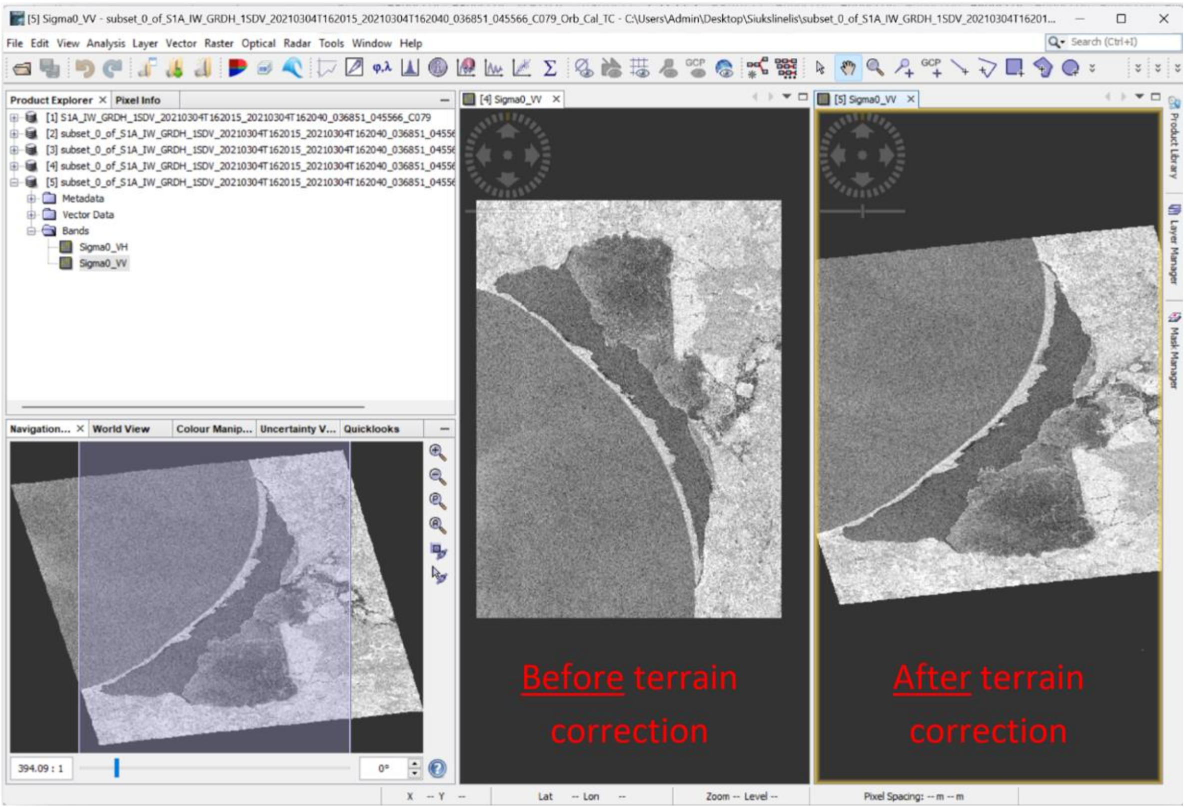

Figure II-25. *Image display in SNAP.*

Backscatter conversion to decibels (dB): When we talk about backscatter in SAR, we're referring to the strength of the radar signal that bounces back from the Earth's surface to the satellite. This signal can range from very weak to very strong, depending on the properties of the surface being observed. To make it easier to understand and work with, scientists convert the backscatter values to decibels (dB), which is a way of measuring the strength of a signal. Converting SAR backscatter to decibels, which employ a logarithmic scale, enhances data interpretation, visualization, and analysis by compressing a wide range of values into a more manageable scale. To achieve this:

I. Right-click on one of the bands of your terrain-corrected layer and select **Linear to/from dB** (Figure II-26). This will create a virtual band in your layer.

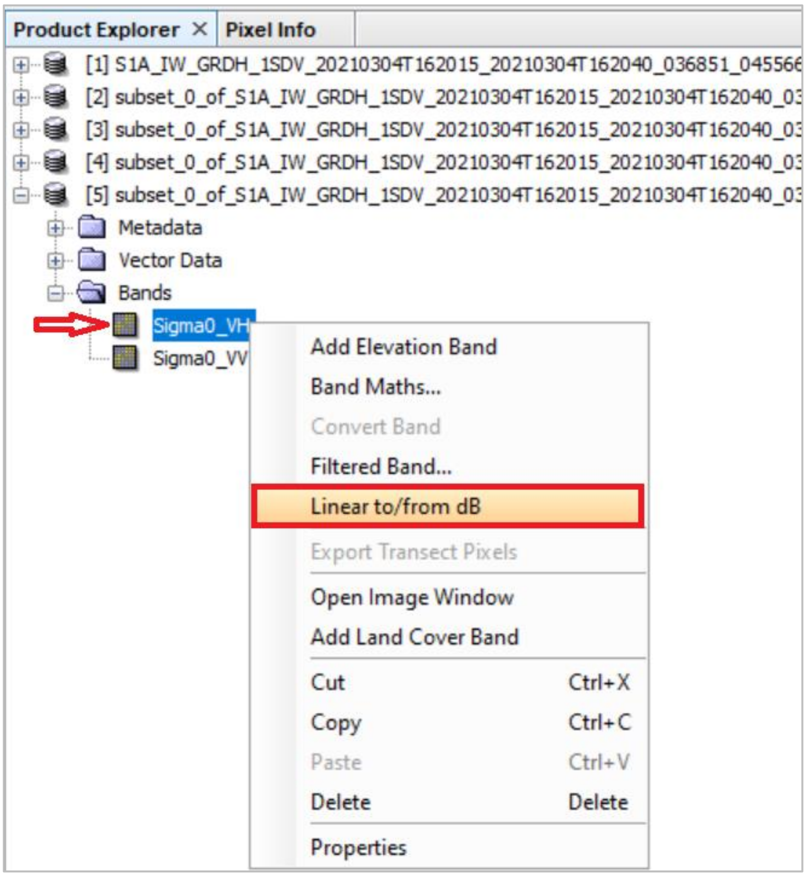

Figure II-26. *Pre-processing steps.*

With this step, you have finished pre-processing the SAR image and now are ready to use it for other applications, i.e., retrieving ship locations, identifying oil spills, monitoring changes in sea ice, etc.

III. QGIS for Remote Sensing Data Analysis and Visualisation

Martynas Bučas

A geographic information system (GIS) is a computer system for capturing, storing, checking, and displaying data related to positions on Earth's surface. Although SNAP includes these functionalities, it lacks tools of spatial data (especially vector) manipulations and visualisation. Quantum GIS (QGIS) is an open-source software that allows spatial data collection/creation, conversion, data storage, manipulation, analysis, and visualisation. QGIS provides a continuously growing number of capabilities provided by core functions and plugins (additionally developed tools) therefore it is at par with proprietary softwares such as Environmental Systems Research Institute (ESRI) ArcGIS desktop in general-purpose GIS functionalities (Kumar et al., 2018). QGIS supports data in vector formats (PostGIS, Shapefiles and all OGR formats) and raster formats (DEM, ArcGrid, ERDAS, SDTS, GeoTIFF, etc.). QGIS is a preferred visualisation environment providing a modern user interface and map element symbology editor. The growing number of plugins is being created by developer communities using libraries provided or using C++ or Python. In this manual, we provide basic steps to import, analyse EO data in spatial and time context and to create a final map. For more description of QGIS tools and functions look for the training manual in https://www.qgis.org/en/docs/index.html.

The QGIS desktop is available on Windows, macOS, Linux, Android and iOS, which can be downloaded from https://www.qgis.org/en/site/forusers/alldownloads.html (Figure III-1).

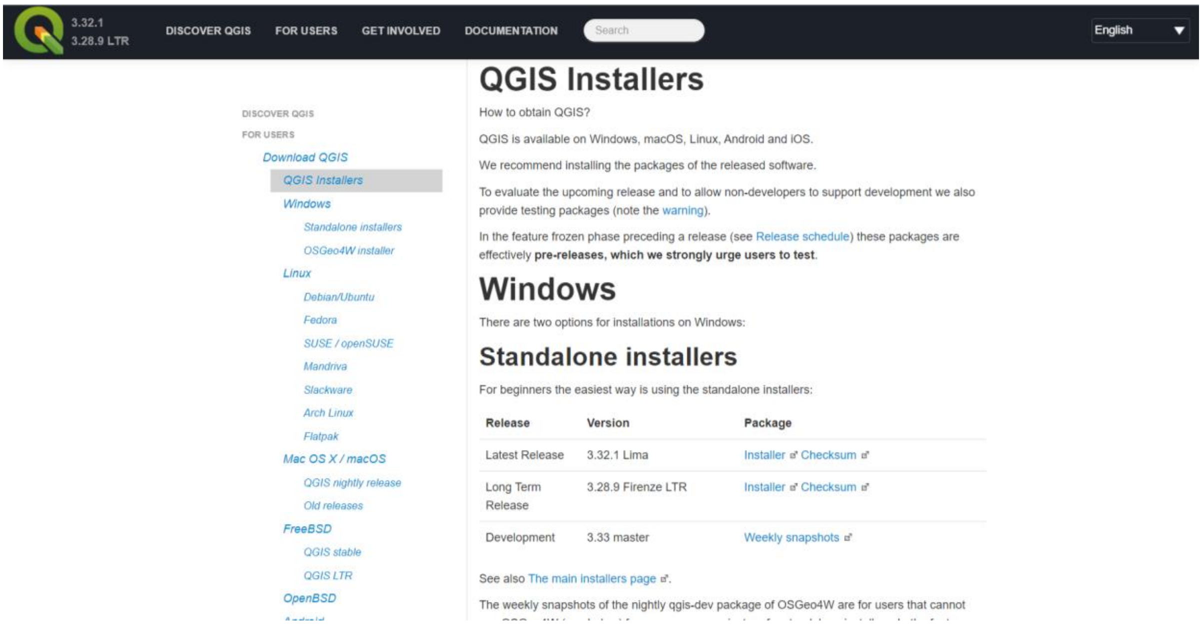

Figure III-1. *Installing QGIS. The long-term release is suggested for a more stable run.*

After installation of QGIS, it includes other GIS software such as GRASS and SAGA; we open it using the QGIS Desktop. The interface of QGIS consists of several panels (Figure III-2): a Menu bar (with standard functions of importing, editing, saving, exporting, settings, plugin installing, etc.), Toolbars (as a Menu bar + additional GIS data editing and analysis), a Browser (for GIS data search and selection), Layers (GIS data management), a Map canvas(for visualisation of GIS layers) and a Status bar (for control of map display).

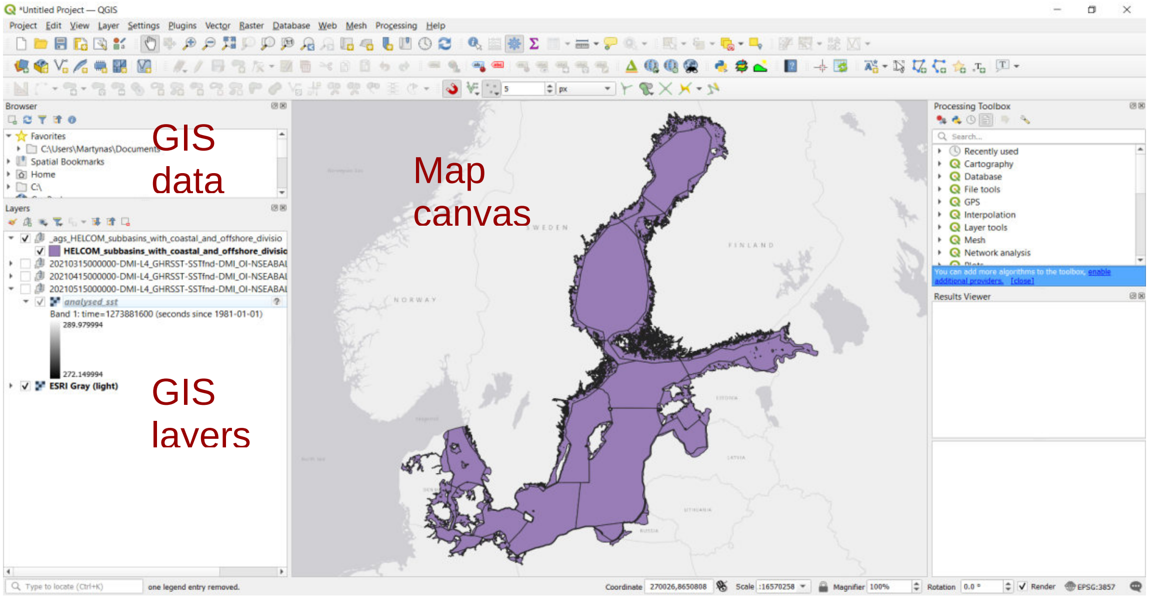

Figure III-2. *The QGIS desktop interface with imported GIS layers of SST and HELCOM sub-basins and further division into coastal and off-shore areas of the Baltic Sea.*

There are several plugins created for satellite data download, visualisation and analysis (e.g., https://www.geodose.com/2021/05/how-to-download-visualize-sentine-qgis.html), which can be found in a Menu bar: **Plugins > Manage and Install Plugins...** In the new window (Figure III-3), select **Not installed** and in the search panel type “satellite” and plugins for satellite data will be provided, then you may select which one you need and install it by pressing **Install Plugin**…

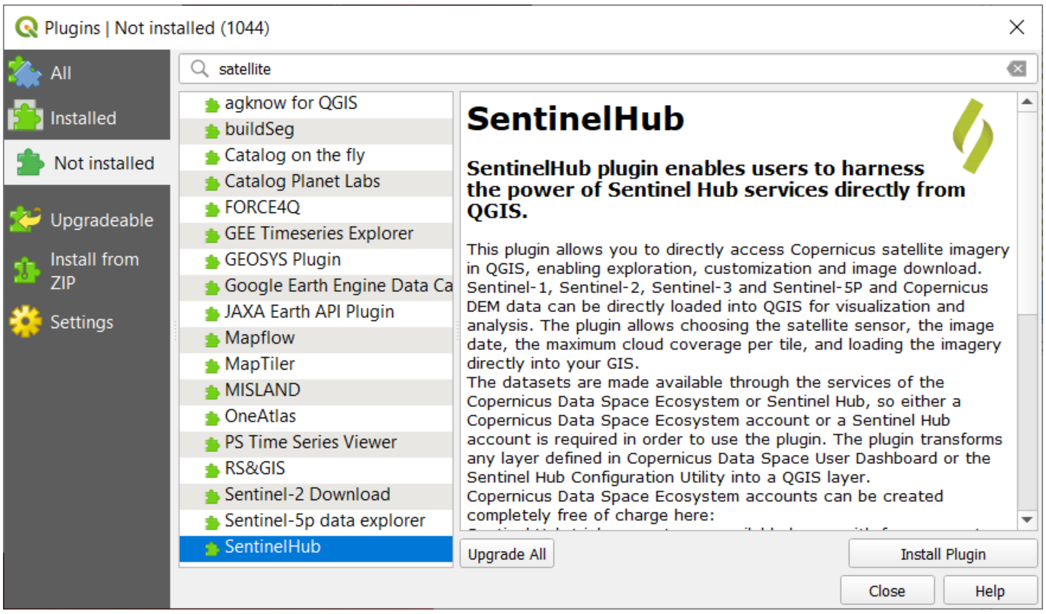

Figure III-3. *The search of plugins for satellite data.*

Data import

For the training, the sea surface temperature (SST) data ("Baltic Sea- Sea Surface Temperature Reprocessed") of the Baltic Sea will be used, which was obtained from the reprocessed EO products by the Copernicus Marine Service: https://marine.copernicus.eu/about/producers/sst-tac. The data format is the Network Common Data Format (NCDF); the Coordinate Reference System (CRS) is WGS84 projection (EPSG: 4326). For example, three data set of SST were downloaded from the year 2021: 15 March, 15 April and 15 May.

For the training, additionally the vector data (polygons) containing the sub-basins and further division into coastal and off-shore areas of the Baltic Sea ("HELCOM subbasins with coastal and offshore division 2022 (level 3)") was downloaded from the HELCOM GIS database: https://metadata.helcom.fi/geonetwork/srv/eng/catalog.search#/metadata/e5a59af9-c244-4069-9752-be3acc5dabed. The data format is ESRI Shapefile; the CRS is WGS84 / Pseudo-Mercator projection (EPSG: 3857).

The GIS data can be loaded in several ways, here it is done via **Browser.** In the Browser panel, navigate to each downloaded GIS file, and then simply drag it to the panel of Layer and the layer will appear in the Map canvas (Figure III-4). The base map was selected from a Menu bar: **Web > QuickMapServices > ESRI > ESRI Gray (light)**, which was obtained from the **QuickMapServices Settings** under the **More services** (see more how to add a base map from the *QuickMapServices* plugin: https://docs.qgis.org/3.28/en/docs/training_manual/qgis_plugins/plugin_examples.html).

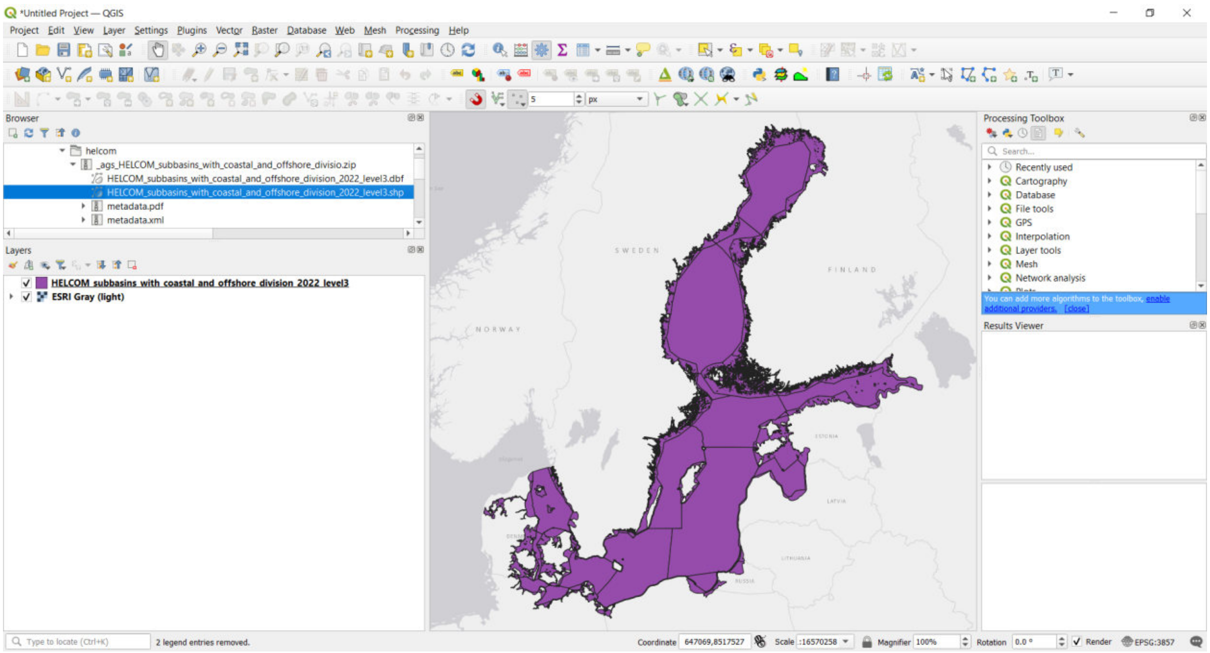

Figure III-4. *Importing vector (shape) data.*

The window will appear for the NCDF, where select the "analysed_sst" layer and press **Add Layers** (Figure III-5).

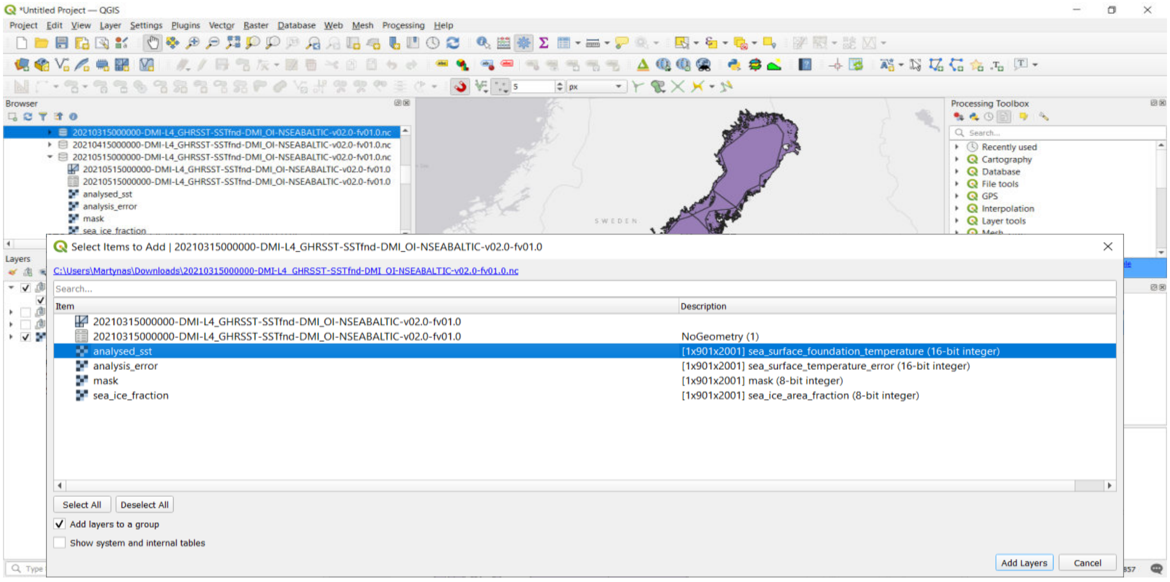

***Figure III-5**. Importing raster data.*

Note, that after importing the raster layers of SST (NCDF), they did not show up over the imported vector layer. The question mark on the right side of the layer indicates that the CRS is not indicated for the raster. If GIS data is obtained from a trusted source, the information on CRS and other important information (date, resources, methods, resolution, name of creators, accuracy, etc.) should be indicated in the metadata or described on the website. Check the metadata of the SST raster: select the raster layer in the panel of Layer and press the right mouse button, then select **Properties…**

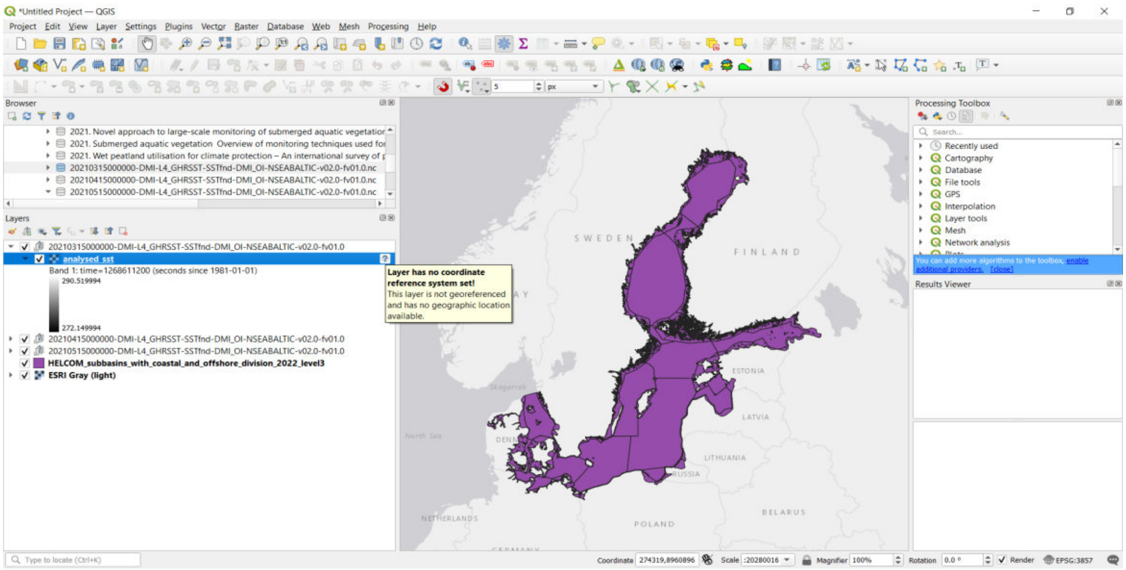

***Figure III-6.** The imported raster layer does not appear over the Baltic Sea since there is no indicated CRS.*

In the new window, select **Information**, where you may find metadata provided for this layer (Figure III-7): extent, width, height, data type, etc. Under the section of

Band 1, you may see that the source of SST is ESA CCI and C3S L2P satellite product, where the units are Kelvins. Under the section of **More information**, you may find that CRS used for this raster was geographical coordinates (WGS84 projection).

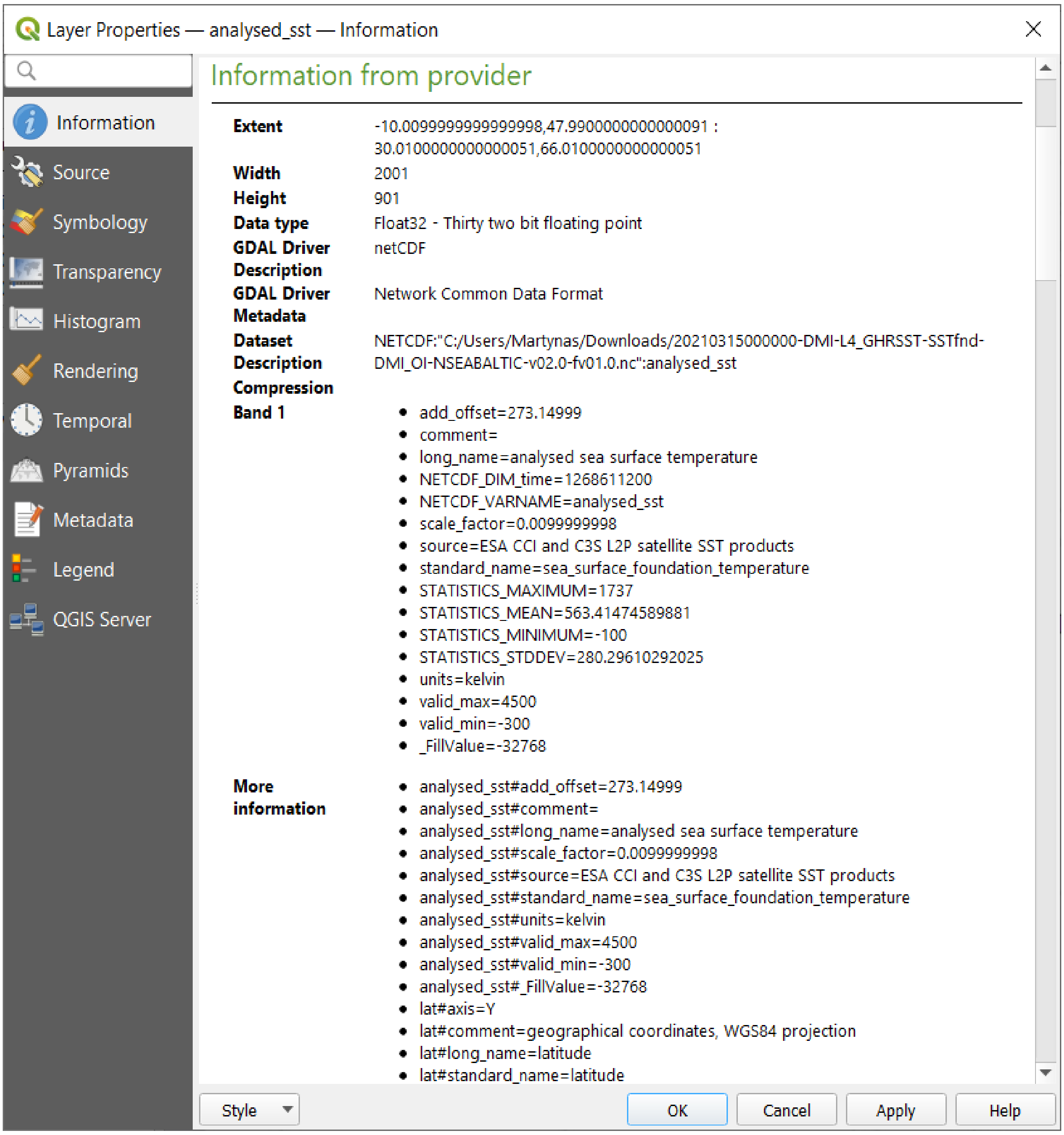

Figure III-7. *The properties of the raster layer.*

As we know the CRS of the rasters, it can be indicated by selecting each file and after pressing a mouse right button, select **Layer CRS > Set Layer CRS ...** In the new window, write EPSG code of needed CRS (in this case - 4326, which is for the WGS84 projection) and press **OK** (Figure III-8). Now the raster layer is over the Baltic Sea (Figure III-9).

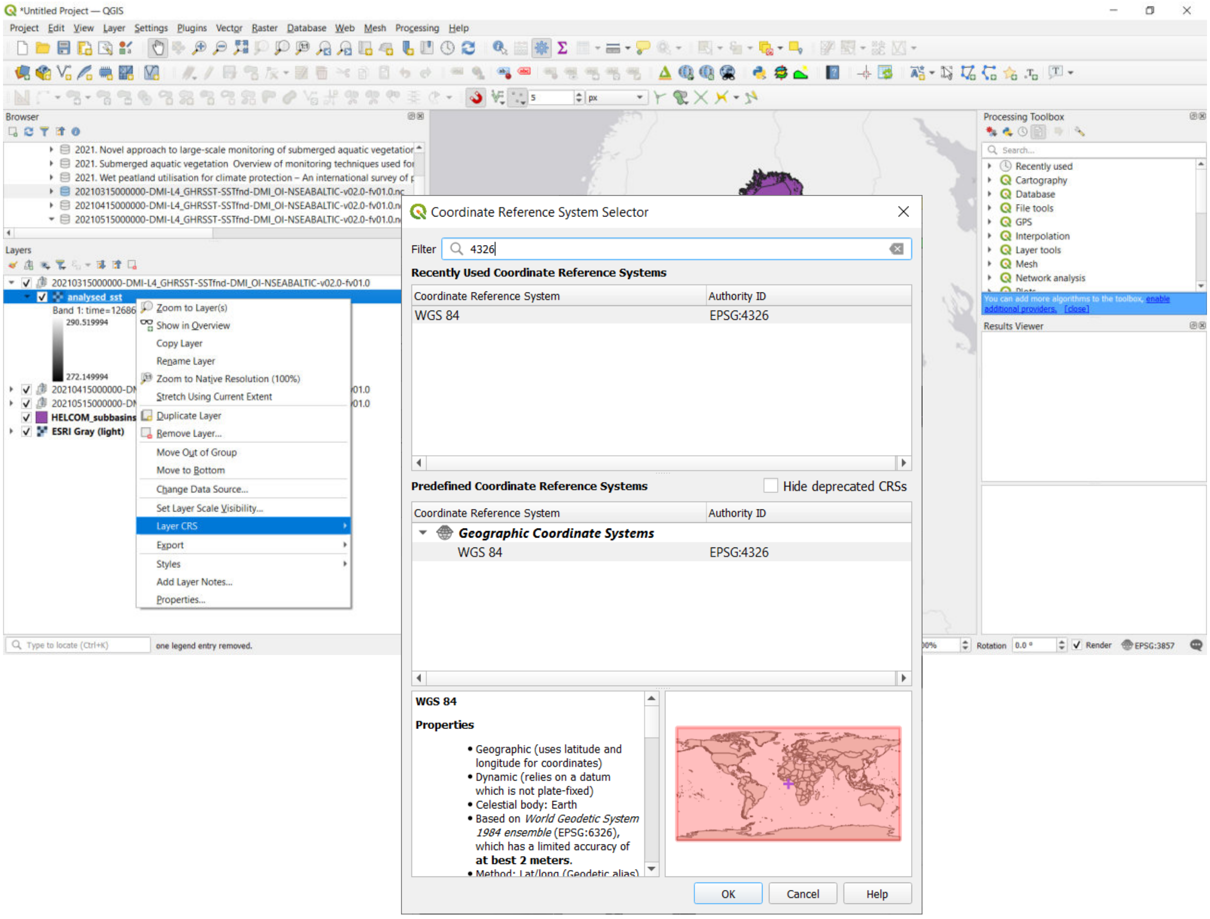

Figure III-8. *How to set the CRS (i.e., WGS84) for the layer.*

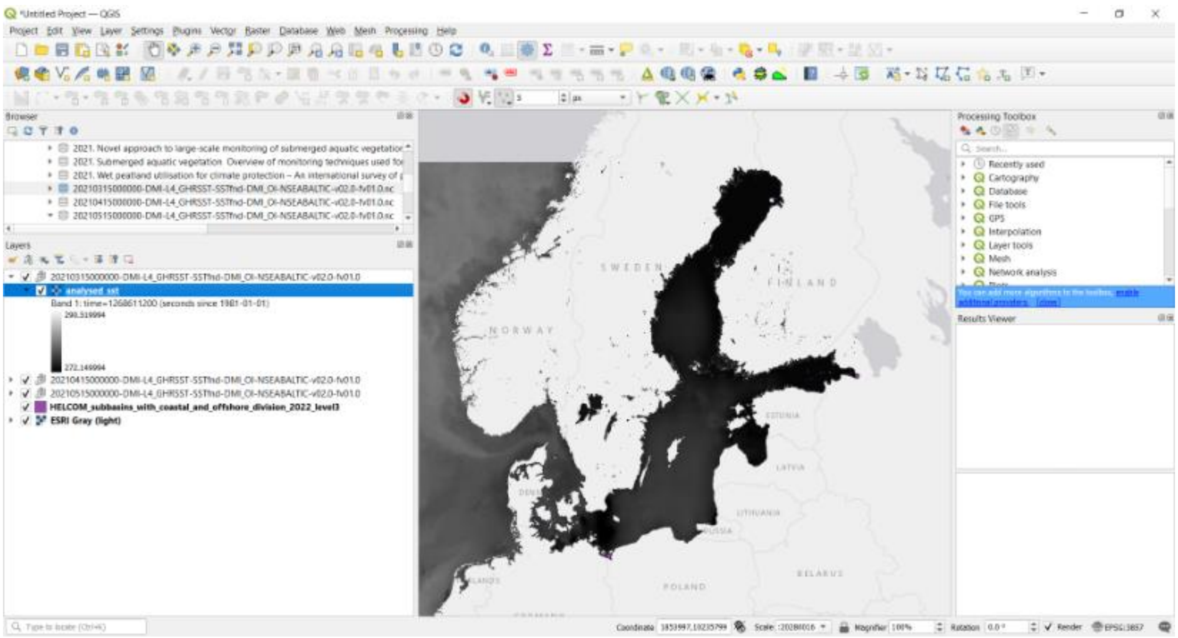

Figure III-9. *The imported raster layer is projected and placed over the Baltic Sea.*

When all data is imported, the first step is to unify their CRS, in this case, EPSG: 3857 will be used according to the shape file as it was the first imported layer. The CRS of the Map canvas is set by the CRS of the first imported layer, although it can be changed by clicking with a mouse on the rightest side of the status bar (EPSG: 3857). The transformation of CRS of raster layers can be changed by selecting each file and after pressing a mouse right button, select **Export > Save As...** In the new window, navigate where to save the new raster (select as GeoTIFF under the **Format** panel); rename it (e.g., “march”) under the **File name** panel, select relevant CRS (in this case, EPSG: 3857) under the panel of **CRS** and press **OK** (Figure III-10).

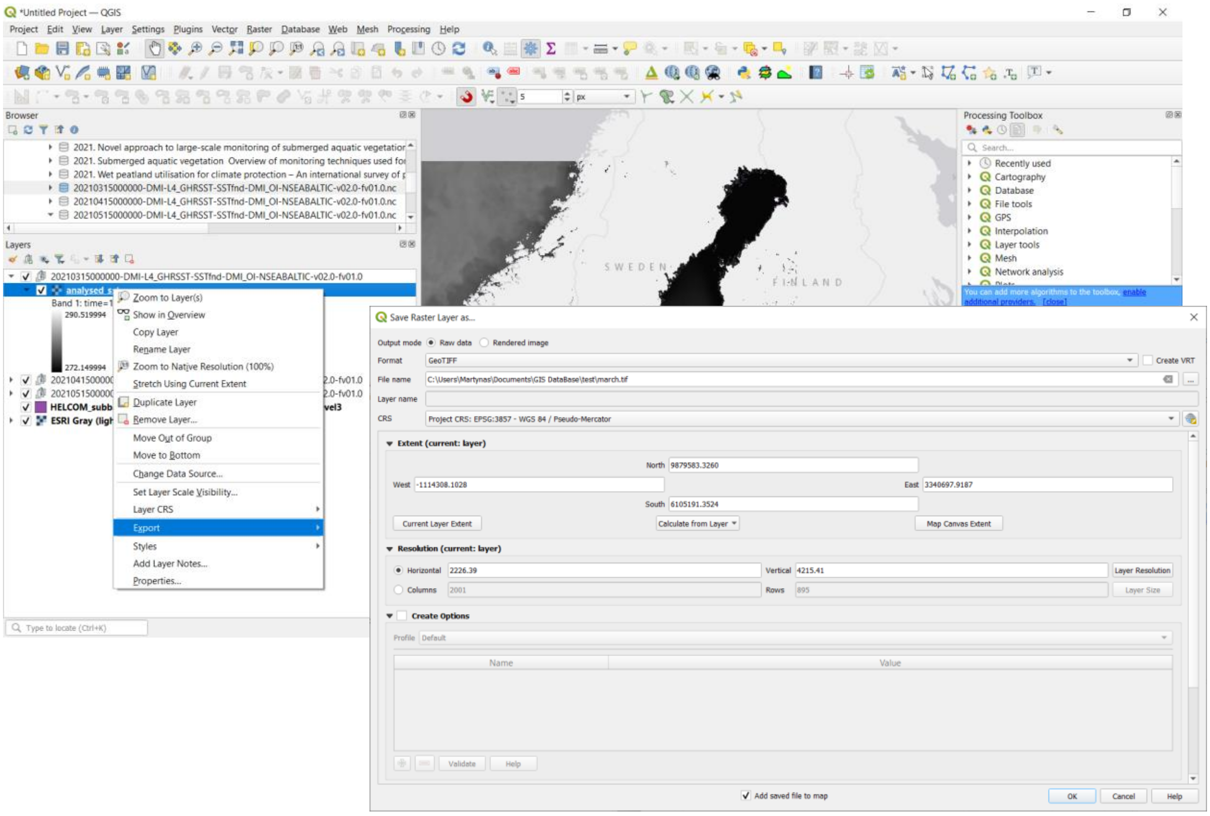

Figure III-10. *The raster layer is exported as a new layer with new CRS (EPSG: 3857).*

The new raster layer will be added to the Layer panel, while the old one can be removed by selecting it and pressing **Remove Layer and groups** (or Ctrl+D) and **OK** (Figure III-11).

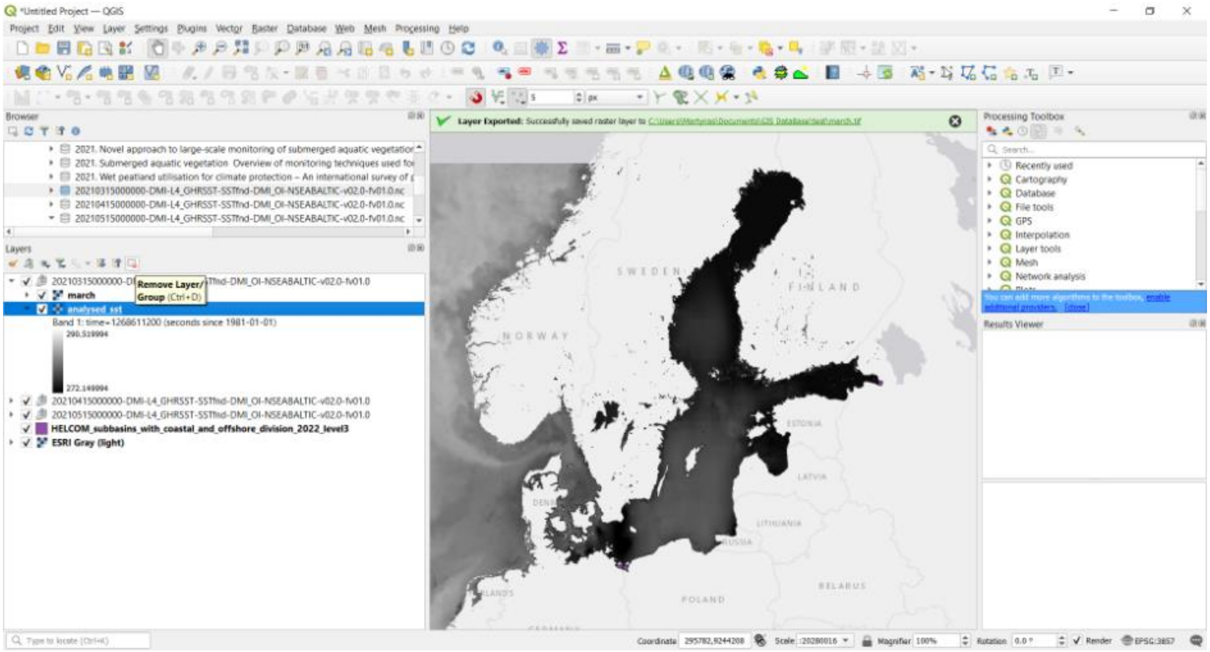

Figure III-11. The new raster layer is added, and the old one can be removed.

After the CRS transformation and saving of all rasters, and removing old ones, 4 layers should be left in order to keep only necessary data for further analysis (Figure III-12). Otherwise, it is common to make a mistake by selecting the right layer when performing different GIS functions. Now the layers are ready for analysis.

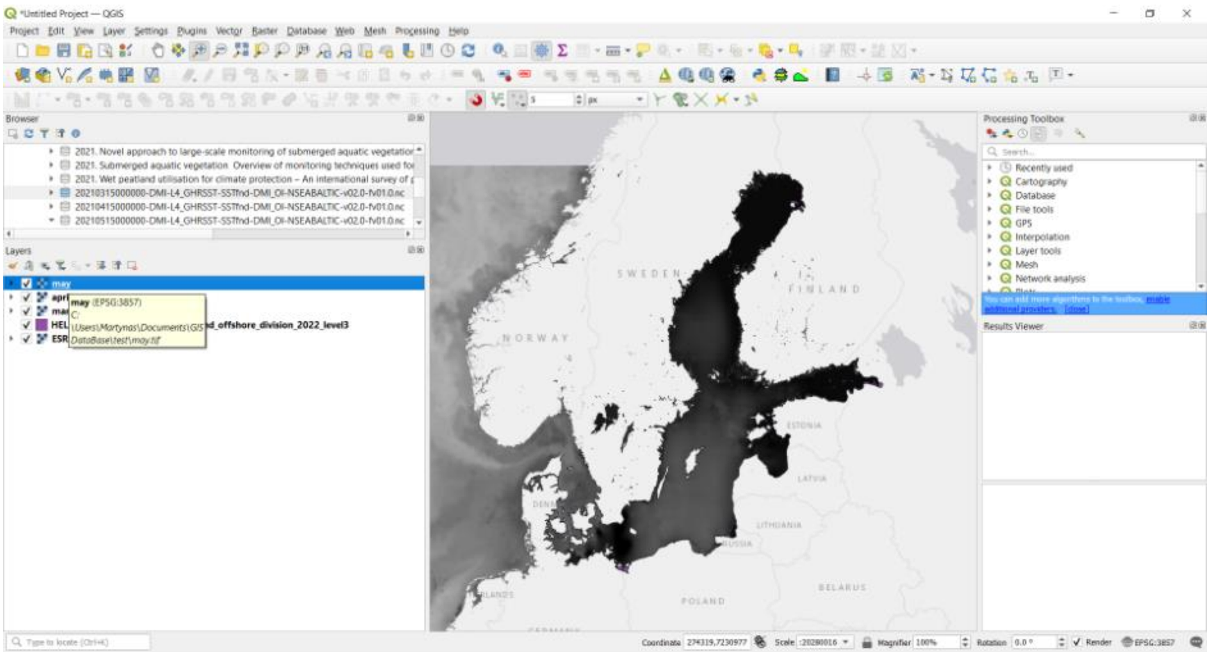

Figure III-12. The new saved raster layers with the same CRS (EPSG: 3857).

48

Transform raster values (cell analysis)

Often values in cells of a raster need to be transformed in order to convert units, to meet the Normal distribution, etc. Current units of SST rasters are in Kelvins (**Figure III-13**), while temperature on the Celsius scale is clearer and therefore such maps are usually provided. The formula to convert a temperature in Kelvins (K) to Celsius (°C) is: Celsius (°C) = Kelvin - 273.15.

The units of SST can be converted under a Menu bar: **Raster > Raster Calculator…** In the new window (Figure III-13), navigate where to save a new layer and name it (e.g., “may_C”) under the **Output layer**, select GeoTIFF format under the **Output format**. Double click on the raster layer (e.g., “may@1”) so it will appear in the **Raster Calculator Expression** pane, then using **Operators** (mathematical and logic functions) and numbers write the conversion formula. You can also change the **Spatial Extent** of a layer by changing the coordinates of raster corners (X and Y), the **Resolution** by changing the number of Columns and Rows and **CRS**. Then, press **OK** and a new map will appear in the panel of Layers. Remove all SST rasters with Kelvin units, leaving 3 converted layers (Figure III-14).

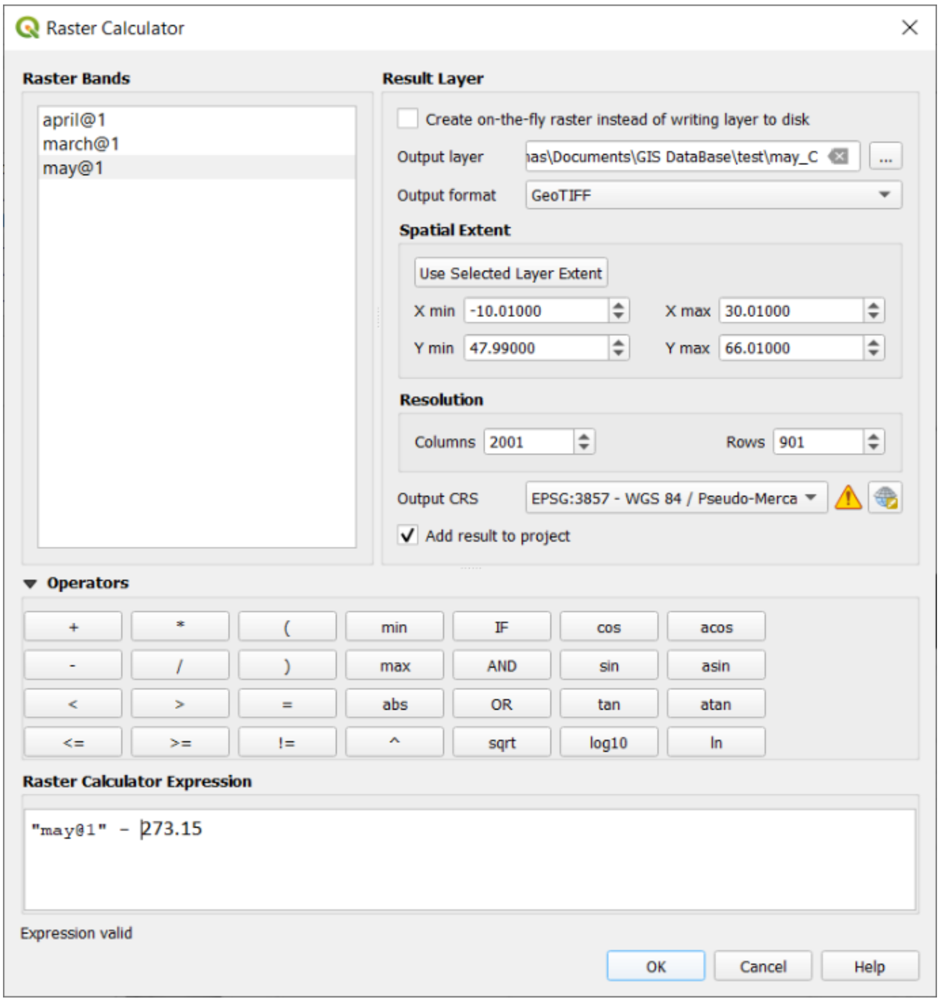

Figure III-13*. Raster Calculator to convert the SST values in Kelvins (K) to Celsius (°C).*

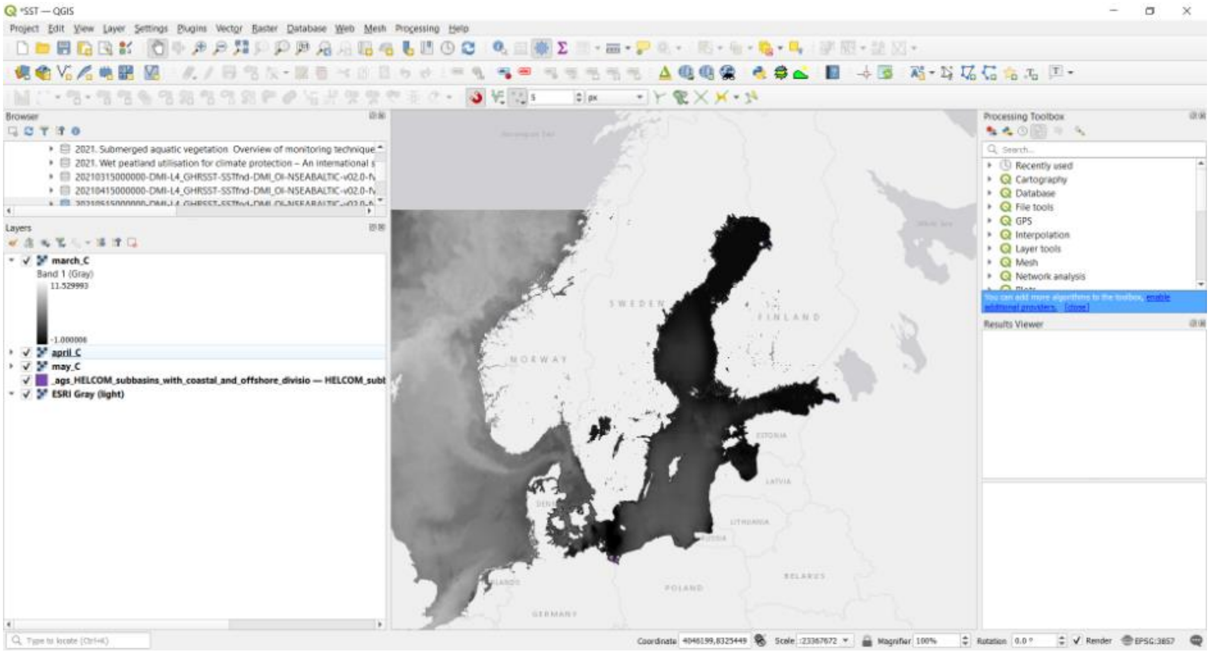

Figure III-14*. Converted three SST layers on the Celsius scale. To see the scale and range of other raster values - press with a mouse on the grey arrow (pointing towards the right direction) on the left side of a layer; the raster information will expand, and the grey arrow will be pointing downwards (as for the "march_C" raster).*

Spatial statistics

Working with GIS data often requires a summary of data over some spatial units, e. g. average of SST in the coastal and offshore areas. SST values can be extracted by polygons of HELCOM subbasins, wherein the SST statistics can be calculated. The polygons can be selected directly on the Map canvas using the feature selection button or feature selection from the attribute table (auxiliary data about spatial features such as names, date, area, etc.) on the Toolbar.

For the training, select the open sea area of the Eastern Gotland Basin using the first selection tool and the second tool can be used to select the coastal waters of Lithuania since it is a relatively narrow and small area. The first selection tool allows you to select features (in this case - polygons) by a mouse click (**Select Feature(s)**), by drawing a polygon (**Select Features by Polygon or Freehand**) or radius (**Select Features by Radius**). A certain polygon (e. g. the Eastern Gotland Basin) can be located on the Map canvas by adding names of the open sea features stored in the attribute table: select the vector layer of the HELCOM subbasins and press a mouse right button and select **Properties…** In the new window (Figure III-15), select **Labels** and in the upper panel with "No Labels" change to the "Single Labels" and select "open_sea" under **Value**, then press **OK**. The names of open subbasins will appear on the Map canvas (Figure III-16). Now you can select the Eastern Gotland Basin using the first option: click by mouse on this polygon, where the selected area will be indicated by yellow colour.

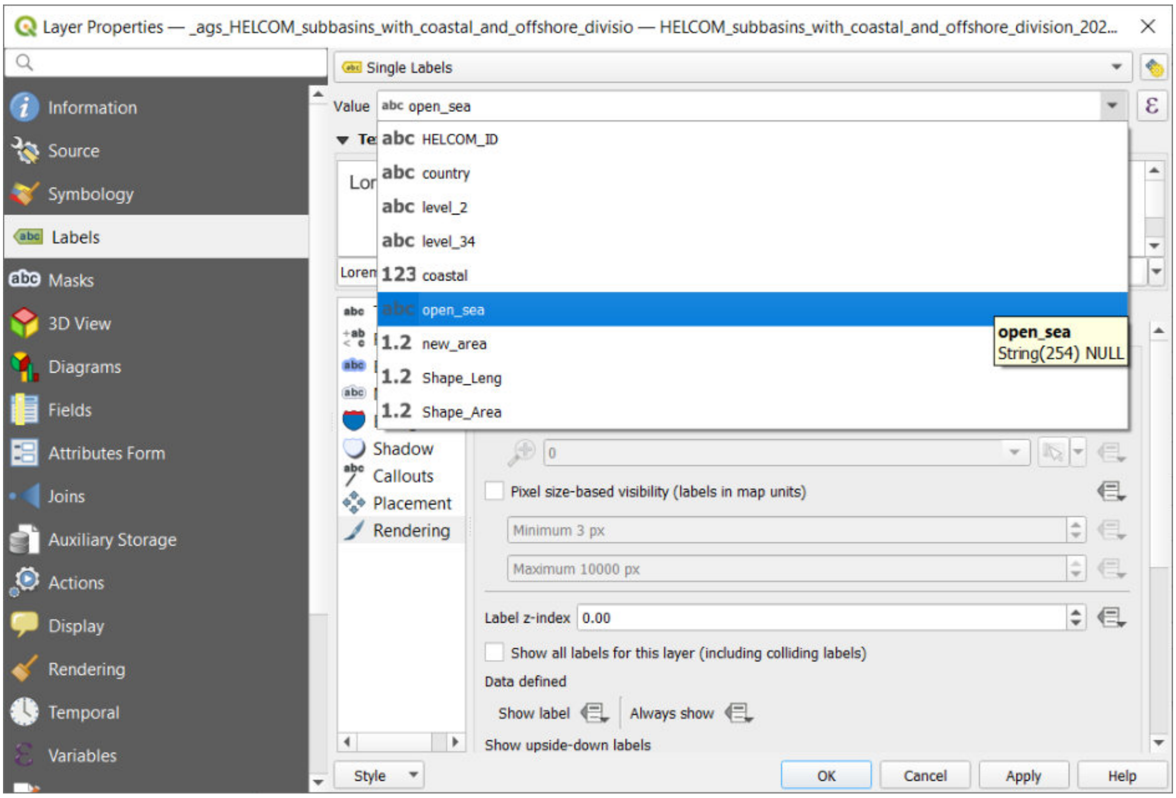

Figure III-15*. Add labels of open sea features from the attribute table.*

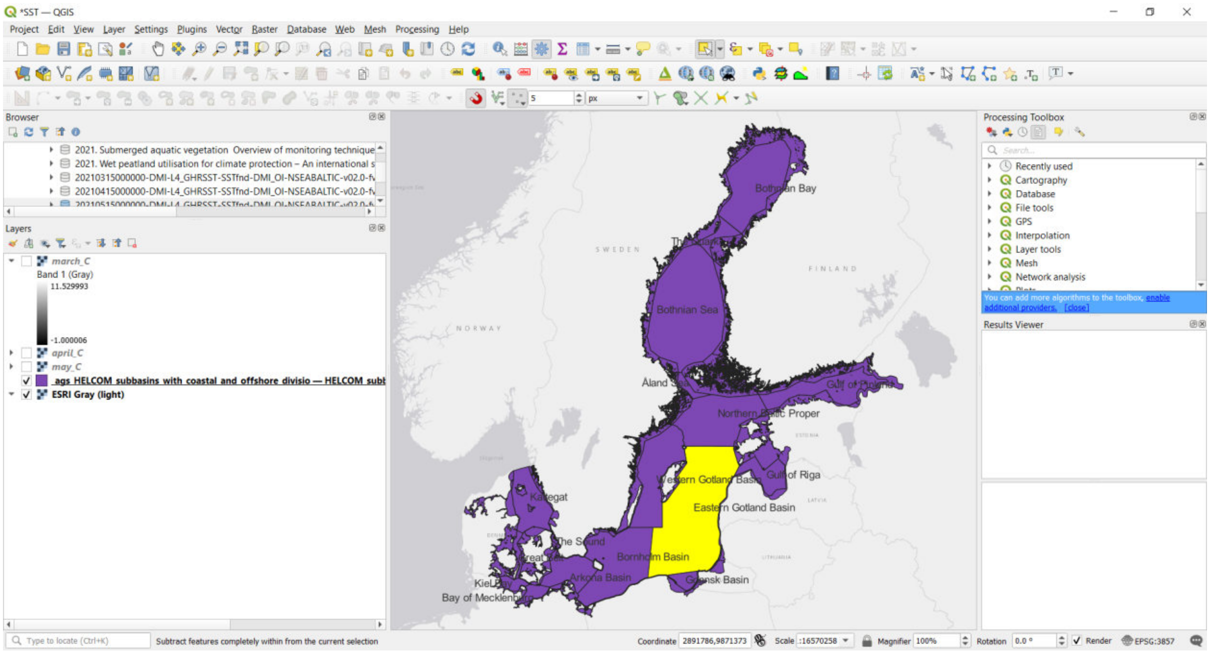

Figure III-16*. Labels of open sea features from the vector layer of the HELCOM subbasins and the selected Eastern Gotland Basin (indicated by yellow colour).*

The second feature selection option allows select features in several ways: by value, expression, all and invert selection. You may choose the selection by value and the new window will appear (Figure III-17). Under the **country** panel, type “Lithuania” and on the right side select **Equal to (=)**, choose **Add to Current Selection** under the **Select Features** drop bar since you have already selected one polygon (the Eastern Gotland Basin). Then close the window and you can see on the Map canvas both areas of interest (open sea of the Eastern Gotland Basin and the coastal waters of Lithuania) are indicated in yellow (Figure III-18).

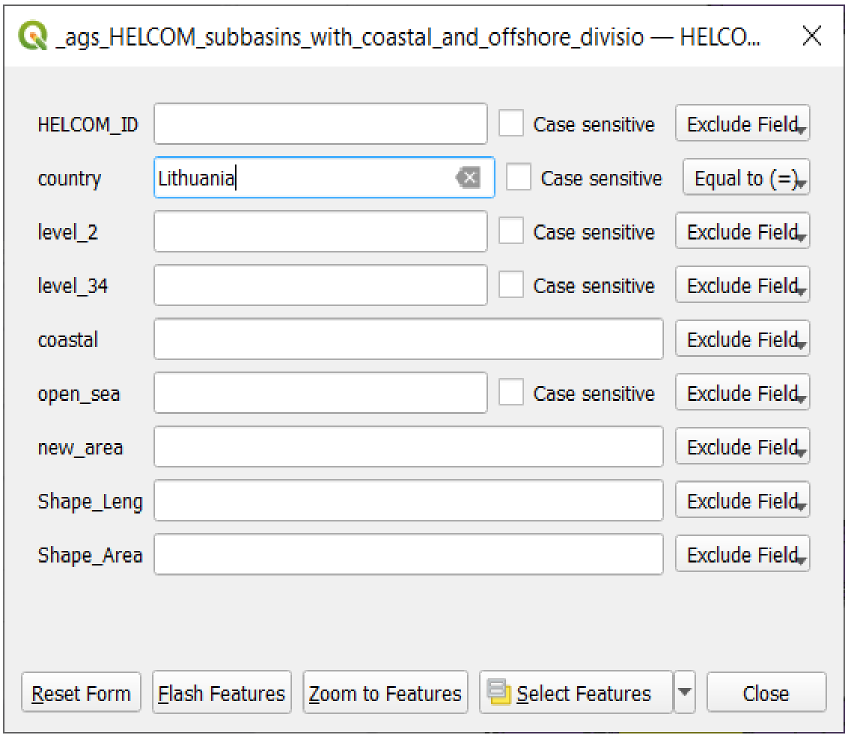

Figure III-17. *Select features by value from the vector layer of the HELCOM subbasins.*

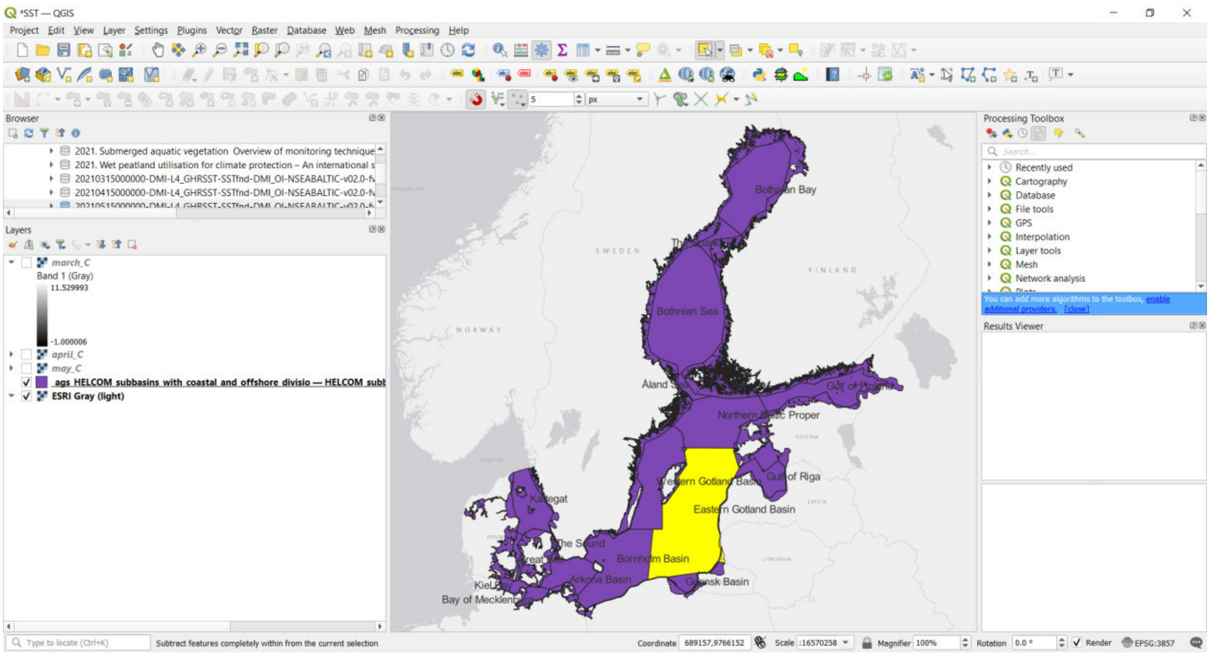

Figure III-18. *Selected (indicated by yellow colour) areas of interest: the open sea of the Eastern Gotland Basin and the coastal waters of Lithuania.*

Zonal statistics tool can be used to extract the SST values over selected polygons of HELCOM subbasins and to calculate the SST statistics (e.g., mean). Under the search panel of the **Processing Toolbox**, type the "zonal" and it should narrow down the GIS tools, where you may find the **Zonal statistics** tool (Figure III-19). In the new window, select vector layer of HELCOM subbasins under the **Input layer**, click on **Selected features only** (otherwise analysis will be performed for all polygons of the vector layer), select one of SST raster (e.g., "may_C"), select **Mean** (or other statistics) under **Statistics to calculate** and press **OK**, and choose how you want to save a new vector layer under the **Zonal Statistics** panel (in this case **Create Temporary Layer** will be used). Then press **Run** and **Close**.

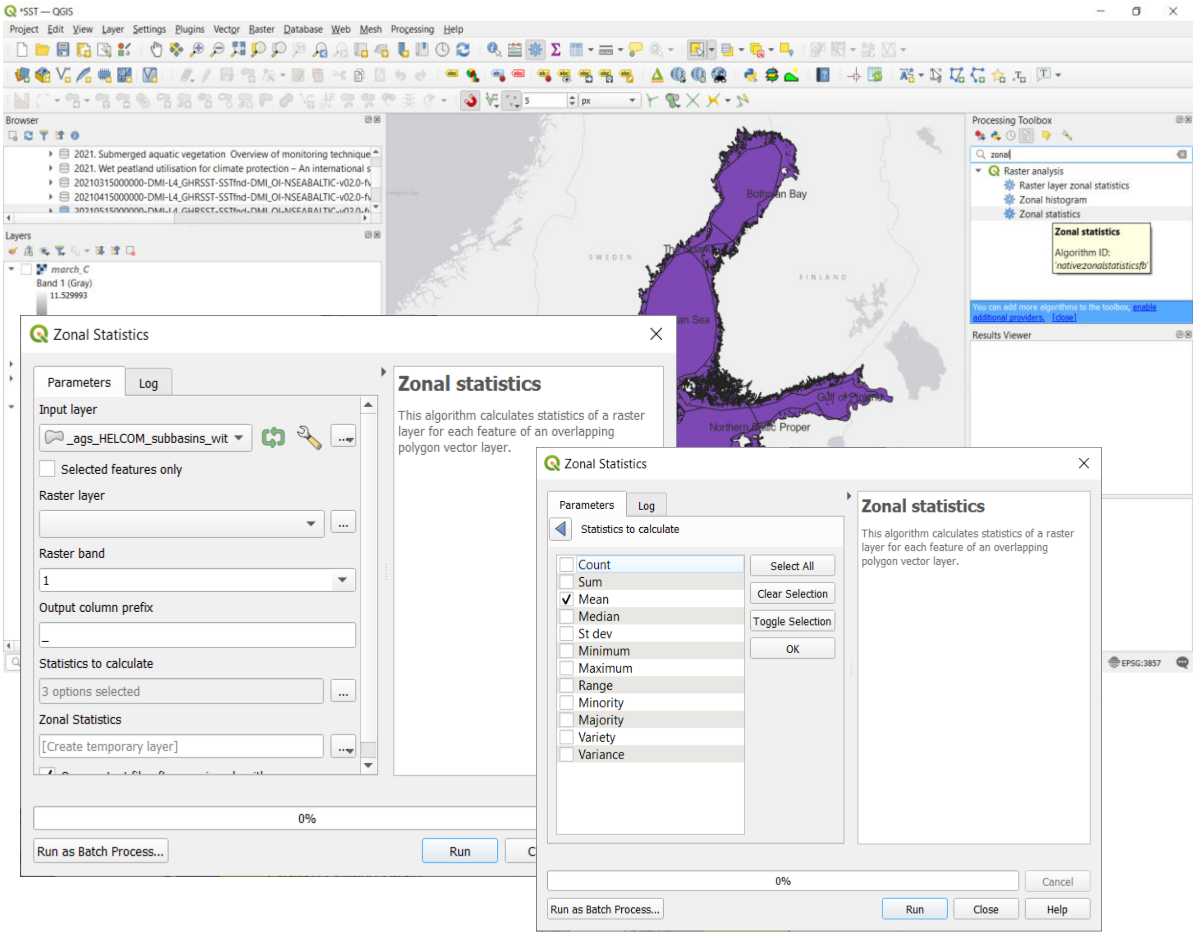

Figure III-19. *The Zonal statistics tool in the Processing Toolbox.*

A new temporary vector layer "Zonal Statistics" will appear in the panel of **Layers** (Figure III-20). The results of statistical analysis (i.e., means) can be found in the attribute table, after the selection of this layer and press of a mouse right button and selection of the **Open Attribute Table**. Under the column "_mean", you can see that mean SST is higher in the coastal waters (9.8 °C) than in the open sea (7.4 °C) on 15 May 2021.

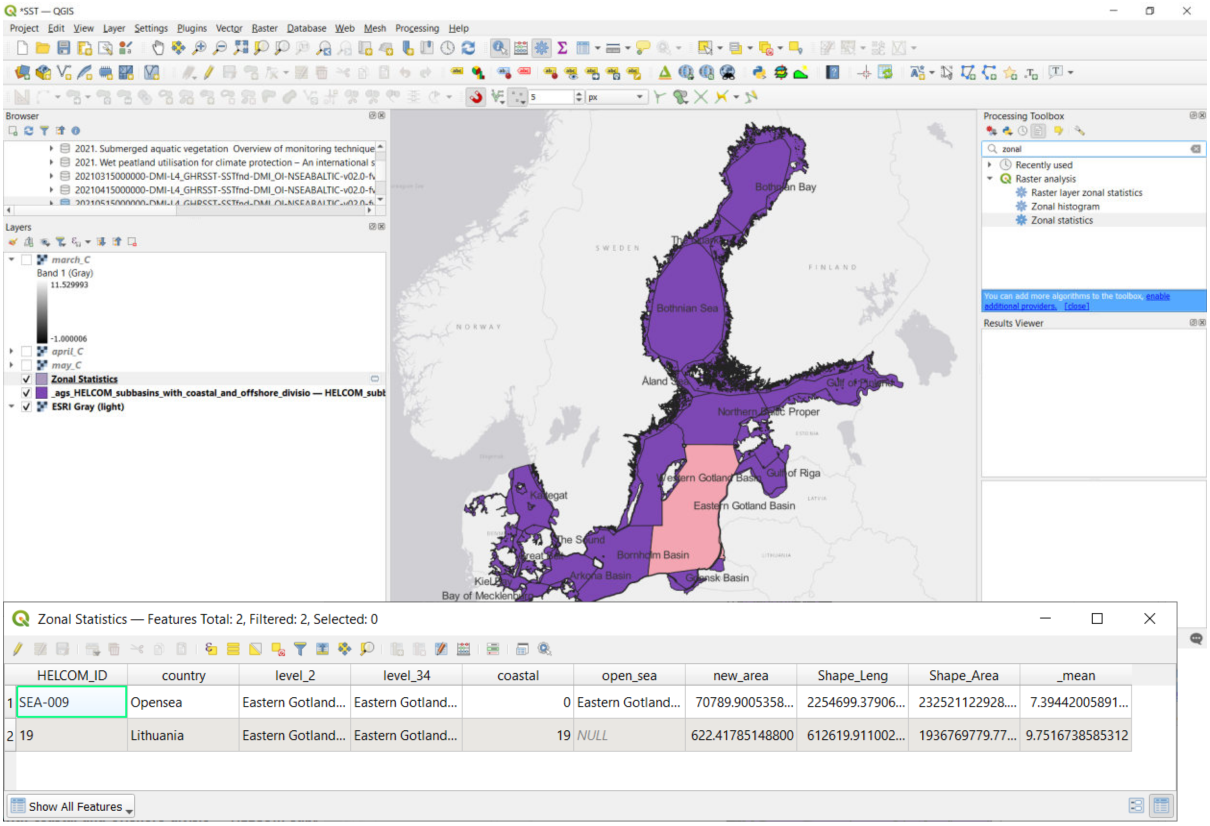

Figure III-20. *The results (under the column "_mean") of the zonal statistics tool in the attribute table of the new vector layer.*

If you do not want to lose data by averaging, the actual SST values can be extracted by points from the raster cells. This can be done by a layer of points imported by you (i.e., x and y coordinates of interest sites) or created using the vector tools (under a Menu bar: **Vector > Research Tools**) such as **Regular points...**, **Random Points in Lines...**, **Random Points in Polygons...** (https://freegistutorial.com/how-to-create-random-points-inside-polygon-on-qgis/). For the training, the first approach will be used in order to get the same SST values. Copy provided coordinates (Table III-1) to any text format file such as a Comma Separated Values (.csv) or standard Text document (.txt). The later format was selected to save it in the notepad (Figure III-21).

Table III-1. *The coordinates (with CRS of EPSG: 3857) of sites in the Eastern Gotland Basin.*

Site nr.	x	y
1	2258546.421	8009988.772
2	2240903.966	7866063.481
3	2218618.760	7726780.942
4	2195405.003	7576355.799
5	2175905.448	7430573.407

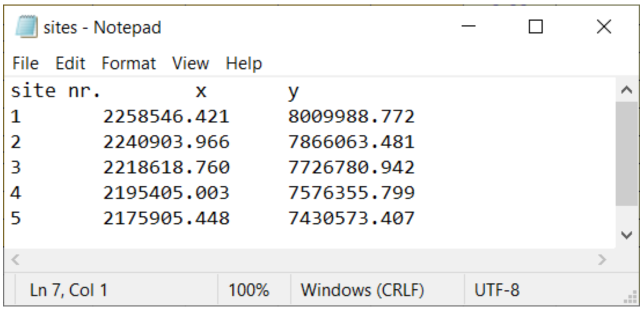

Figure III-21. The notepad (i.e., sites.txt) with copied coordinates of sites.

The text file with the coordinates (.txt or .csv) can be opened in QGIS from a Menu bar (or Ctrl+shift+t). In the new window (Figure III-22), navigate to the text file under the **File name**, indicate file type and column delimiters (in this case - Tab) under the **File Format**, change the **CRS** to EPSG: 3857 and inspect the data structure under the **Sample Data**. If you can recognize the columns and values, press **Add** and **Close**.

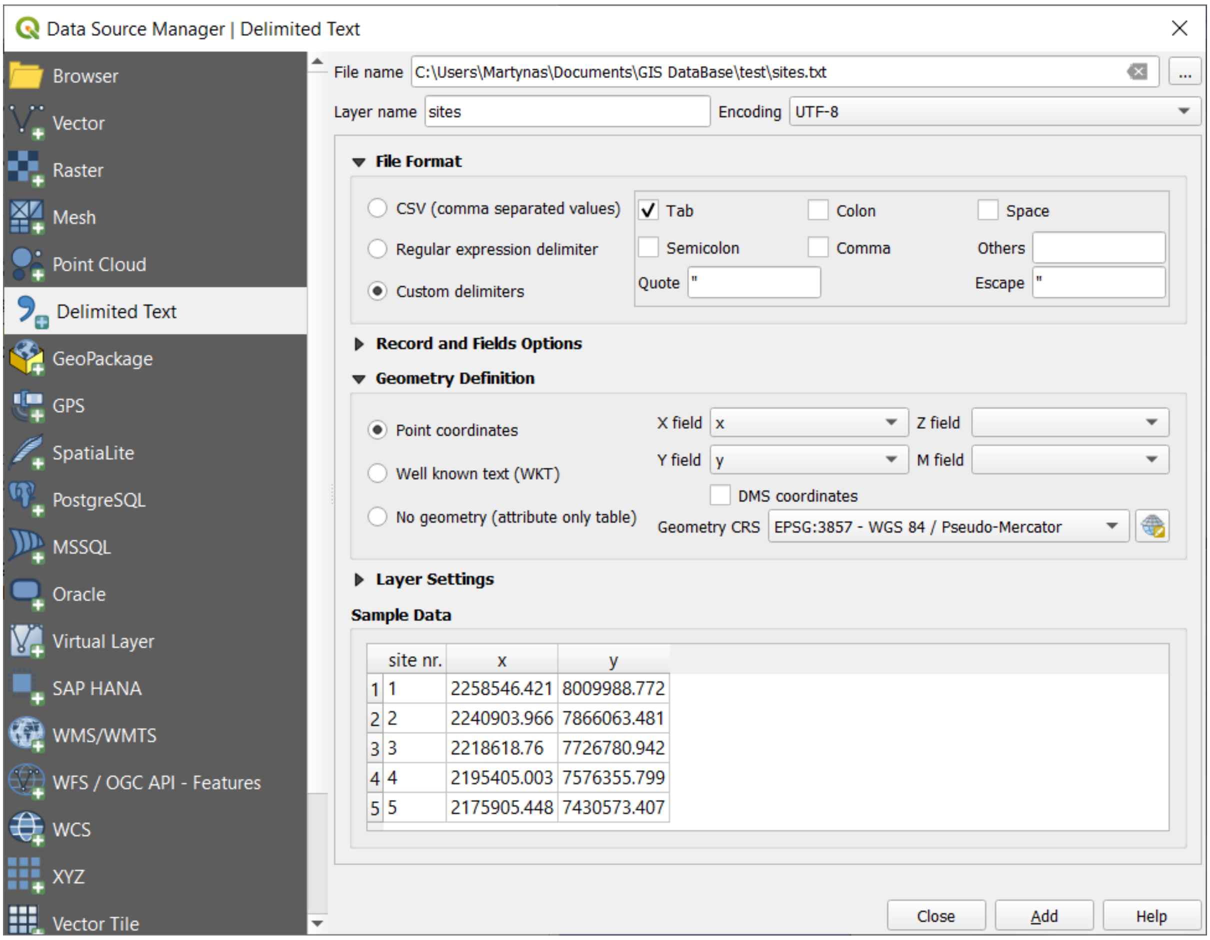

Figure III-22. Import of sites.txt (points of sites of interest).

The imported sites will appear in the Map display, where the mean SST raster was removed in order to keep only necessary layers (Figure III-23).

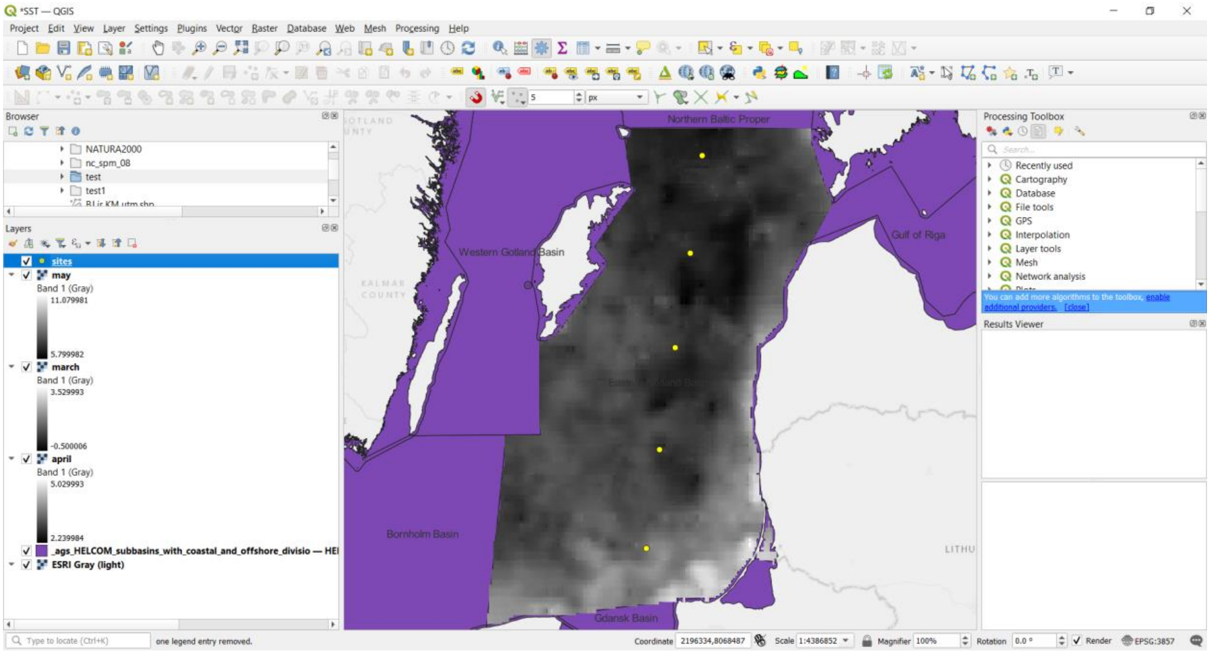

Figure III-23. *The imported sites of interest.*

For the extraction of SST values from the rasters to the imported points, you will need an additional tool which can be added from a Menu bar: **Plugins > Manage and Install Plugins...** In the new window (Figure III-24), select **Not installed** and in the search panel type "point sampling" and the *Point sampling tool* will be provided, then press **Install Plugin**. The icon of this plugin will appear on the toolbar.

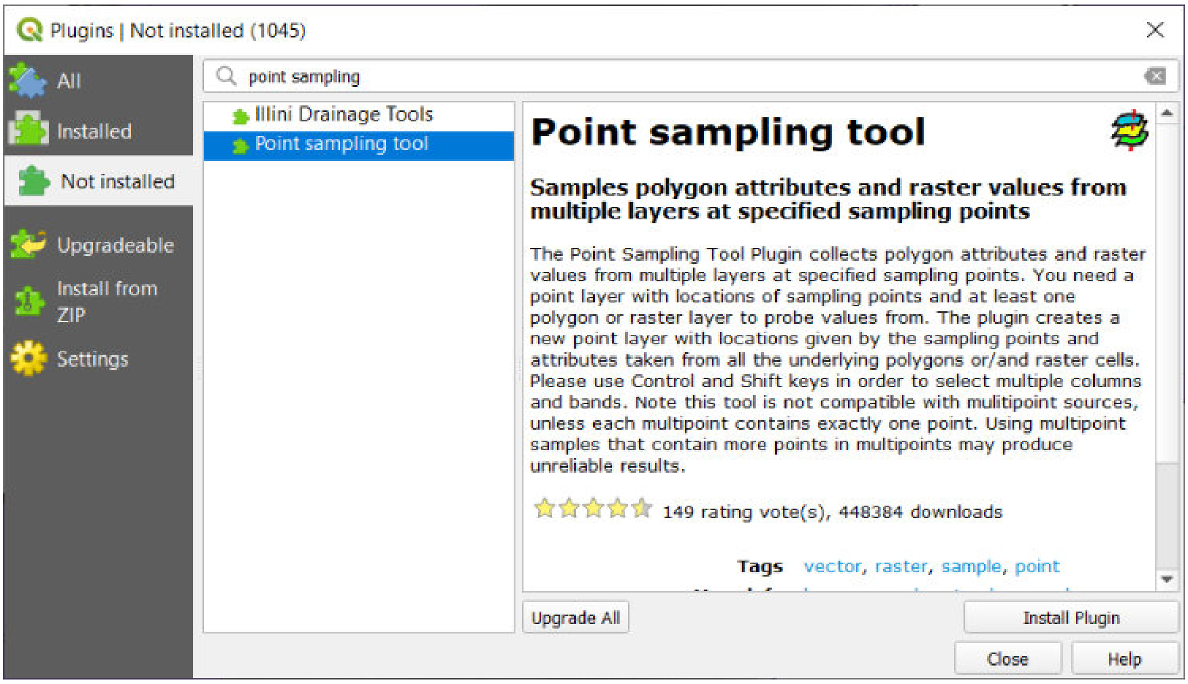

Figure III-24. *The Point sampling tool added from the plugins.*

Press the icon of installed plugin (*Point sampling tool*) and in the new window (**Figure III-25**) select **General**, where select point layer ("sites") under the **Layer containing sampling points:**, then select attributes to include in the new vector layer (points) such as the site number, the values of SST from three rasters under the **Layers with fields/bands to get values from:**, and navigate where to save the new vector (e.g., "site_extr") and in which format (in this case shape file - .shp) under the **Output point vector layer**. Then press **OK**.

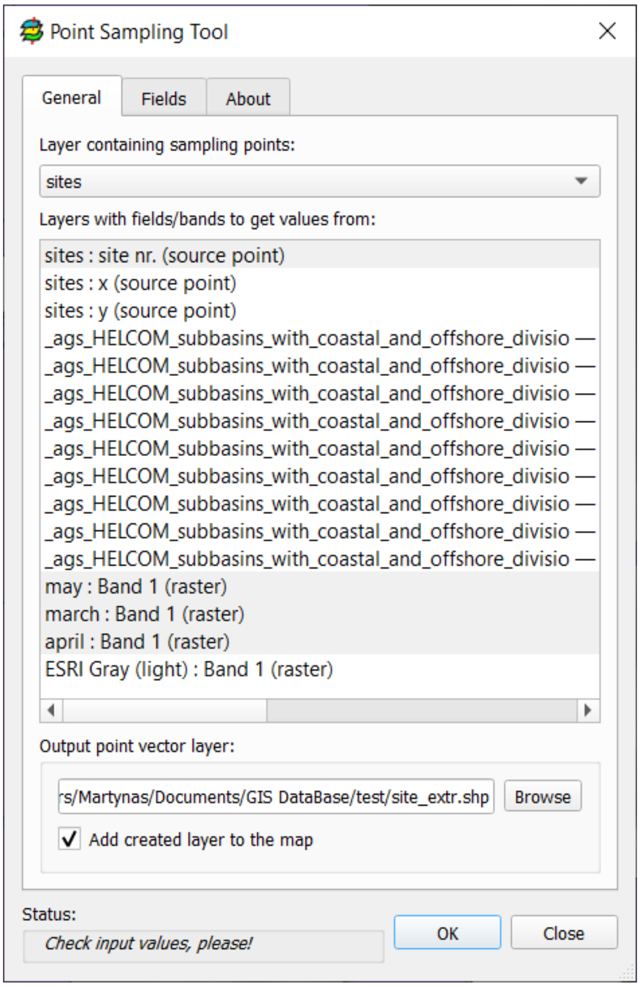

Figure III-25. *Selection of raster layers to extract to the point vector using the Point sampling tool.*

The extracted raster values from 3 layers (March-May 2021) to the 5 sites of point vector ("site_extr") can be found in the attribute table (Figure III-26). The table can be selected and copied to other documents using the icon on the attribute table (or Ctrl+C).

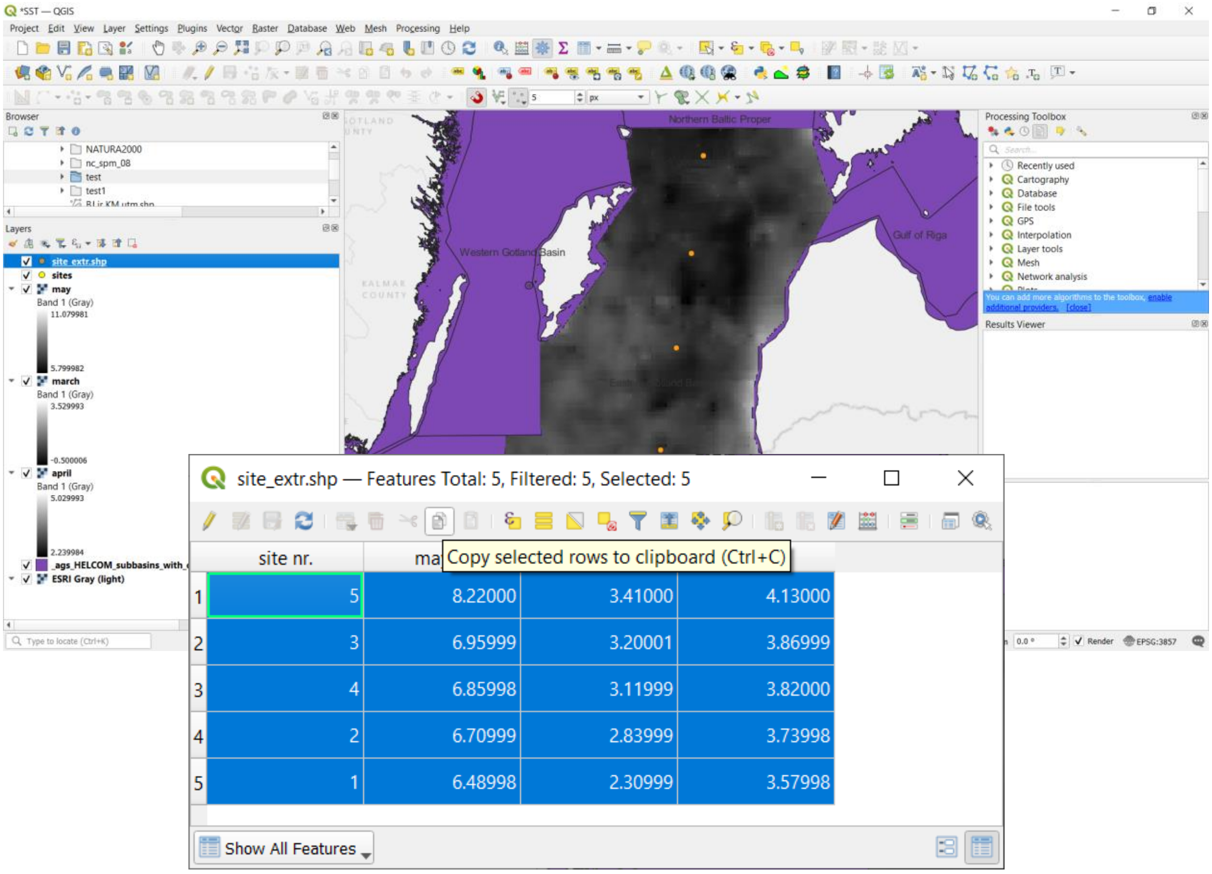

Figure III-26. *Extracted raster values from 3 layers (March-May 2021) to the point vector ("site_extr") and its attribute table with extracted SST values for 5 sites.*

Time statistics.

The satellite products can provide a long time series of data; therefore, it can be necessary to summarise data not only spatially but also temporarily. For the training, you may assess the mean SST during March-May 2021 in the open sea of the Eastern Gotland Basin and the coastal waters of Lithuania. The raster layer of SST covers the North Sea and Atlantic Ocean, which is outside of our interest, therefore it is recommended to clip rasters before analysis, which will reduce processing time, especially having high resolution data and long-time series.

The raster clipping can be performed in a Menu bar (Figure III-27): **Raster > Extraction > Clip Raster byMask Layer...** In the new window, select the raster of SST (e.g., "march_C") under the **Input layer** and clipping polygon under the **Mask layer** (i.e., "Zonal Statistics"). You may indicate Source and Target **CRS** if needed and other options (in this case we use the default). The name of the new raster can be provided ("march") under **Clipped (mask)** and then press **Run**. Repeat the same for all rasters and then remove the unclipped rasters from a panel of Layers to keep the Map canvas clean (Figure III-27).

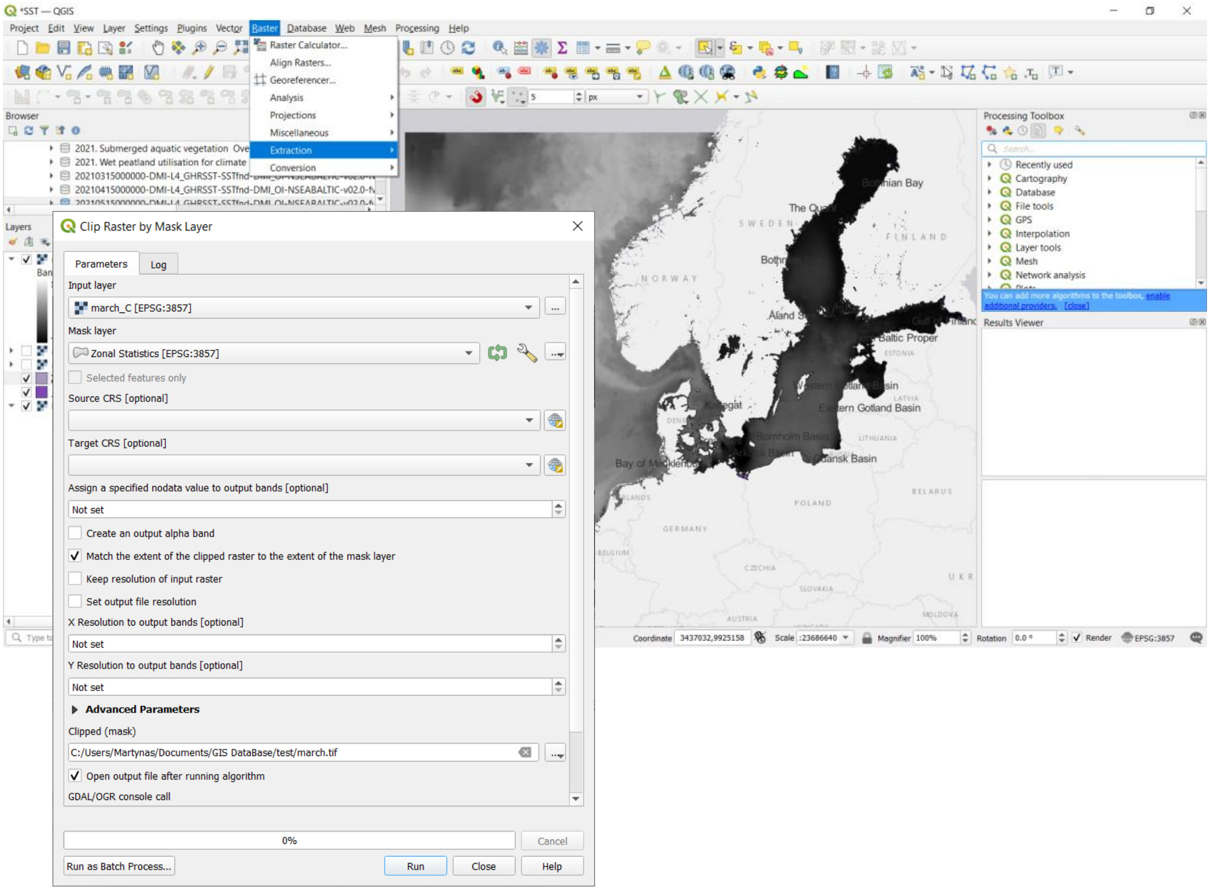

Figure III-27. The clipping of SST raster by mask (polygon of the open sea of the Eastern Gotland Basin and the coastal waters of Lithuania).

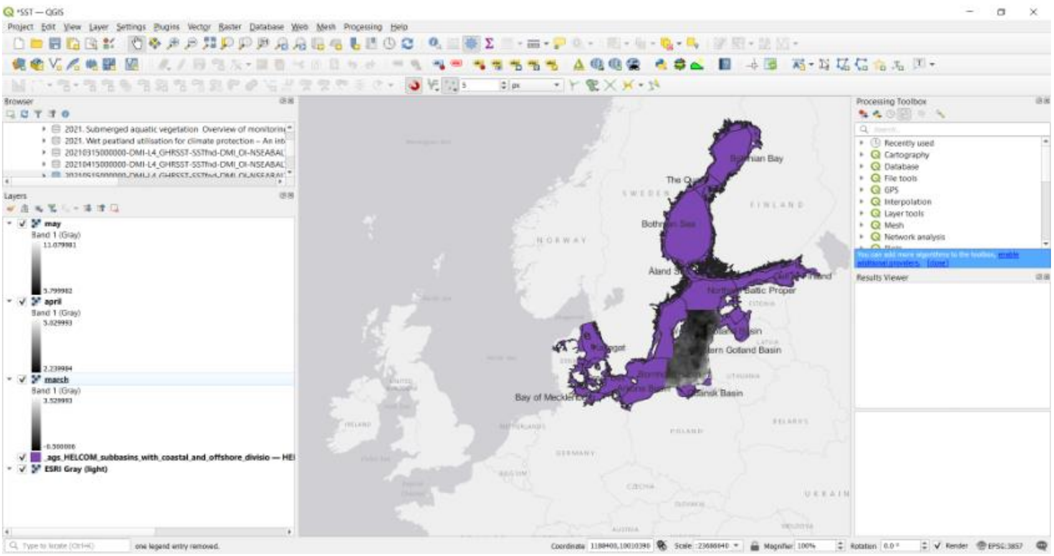

Figure III-28*. The clipped rasters of SST by mask.*

Now, the mean SST for the time series can be calculated by the *Raster calculator* (Under a Menu bar: **Raster > Raster Calculator...**) as it was used for the transformation of raster cell values (Figure III-13). In the new window (Figure III-29), navigate where to save a new layer and name it (e.g., “mean”) under the **Output layer**, select GeoTIFF format under the **Output format**. In the **Raster Calculator Expression** pane, type the formula to calculate mean SST using the raster layers from the **Raster Bands** pane, and mathematical functions using the **Operators** and numbers. You can also change the **Spatial Extent** of a layer by changing the coordinates of raster corners (**X** and **Y**), the **Resolution** by changing the number of Columns and Rows and **CRS**. Then, press **OK** and a new clipped raster will appear in the panel of Layers (Figure III-30).

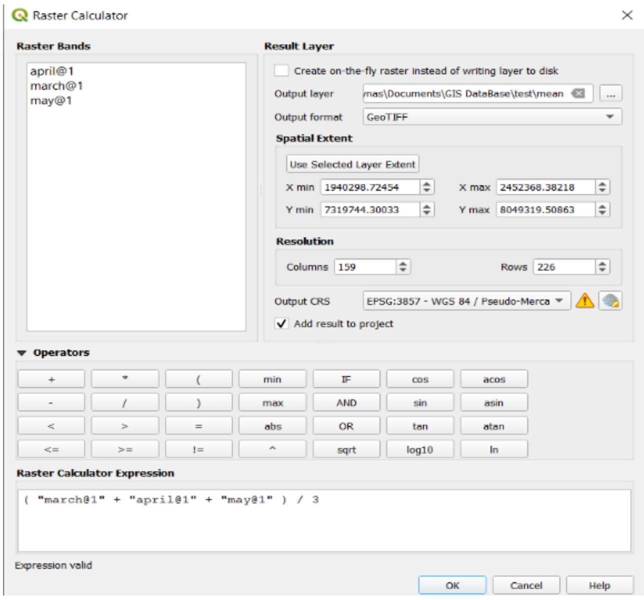

Figure III-29. *Raster Calculator to calculate the mean SST values for each cell from March-May 2021.*

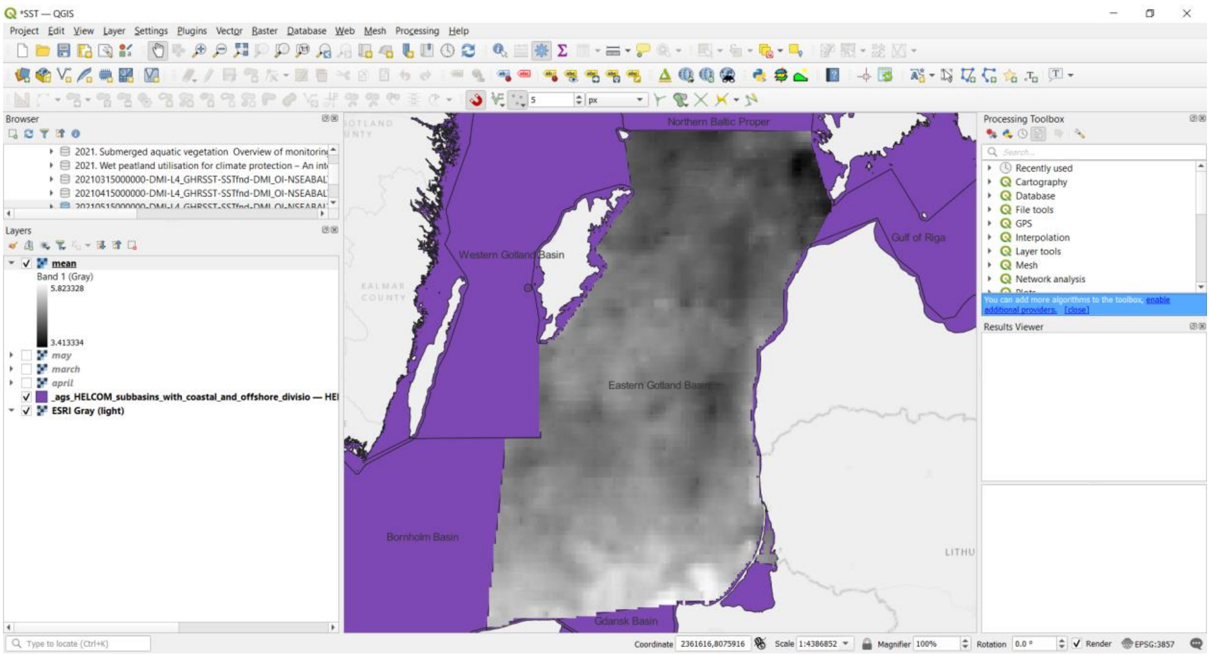

Figure III-30. *The mean SST values for each cell from March-May 2021 in the Eastern Gotland Basin and the coastal waters of Lithuania.*

Reclassify raster

Often raster values are summarized by classifying them to certain groups in order to show spatial patterns: temperature anomalies, upwelling events, etc. You can classify the mean SST raster to several groups. The number of groups can be decided after inspecting the histogram of SST (Figure III-31), which can be obtained by selecting the layer and after pressing a right mouse button, selecting **Properties...** and **Histogram**.

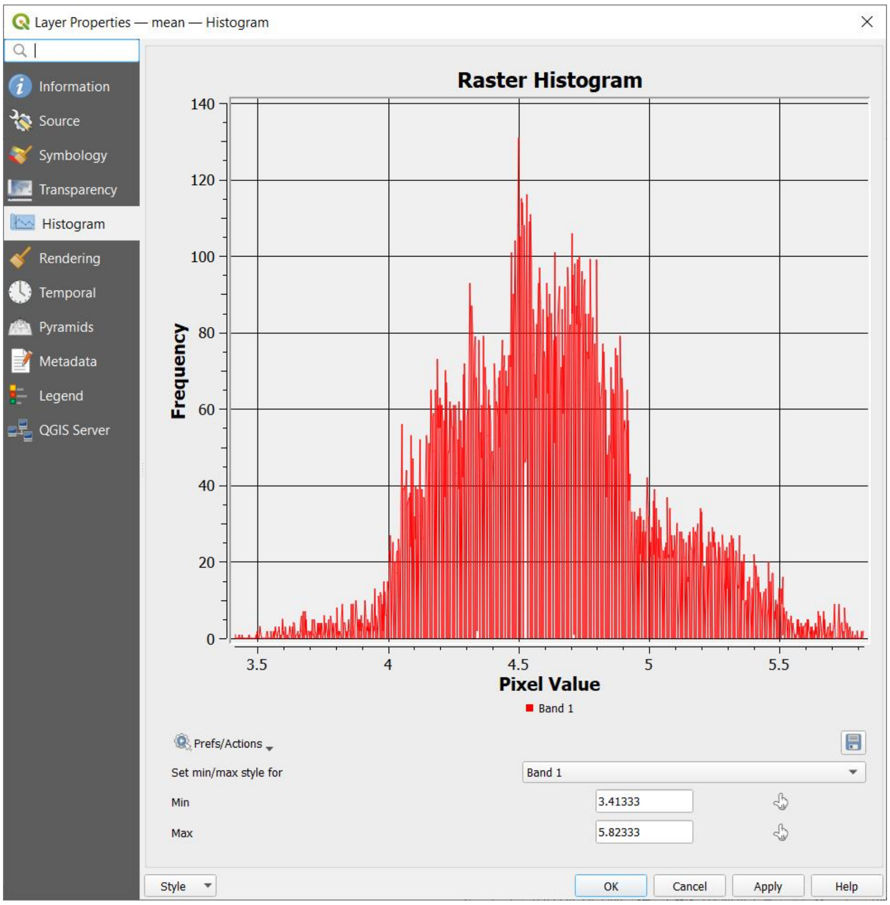

Figure III-31. *The histogram of mean SST raster.*

From the histogram of SST (Figure III-31), we decided to classify raster values into 3 groups: < 4 °C, 4-5 °C and > 5 °C. This can be done using the *Raster Calculator* tool, which was introduced in the chapter of cell analysis. After selection of **Raster > Raster Calculator...** under a Menu bar, in the new window (Figure III-13), navigate where to save a new layer and name it (e.g., "mean_class") under the **Output layer**, select GeoTIFF format under the **Output format**. In the **Raster Calculator Expression** pane, by double clicking on the raster layer ("mean@1") and using **Operators** (mathematical and logic functions) and numbers write the conversion formula. You can also change the **Spatial Extent** of a layer by changing the coordinates of raster corners (X and Y), the **Resolution** by changing the number of Columns and Rows and **CRS**. Then, press **OK** and a new map will appear in the panel of Layers.

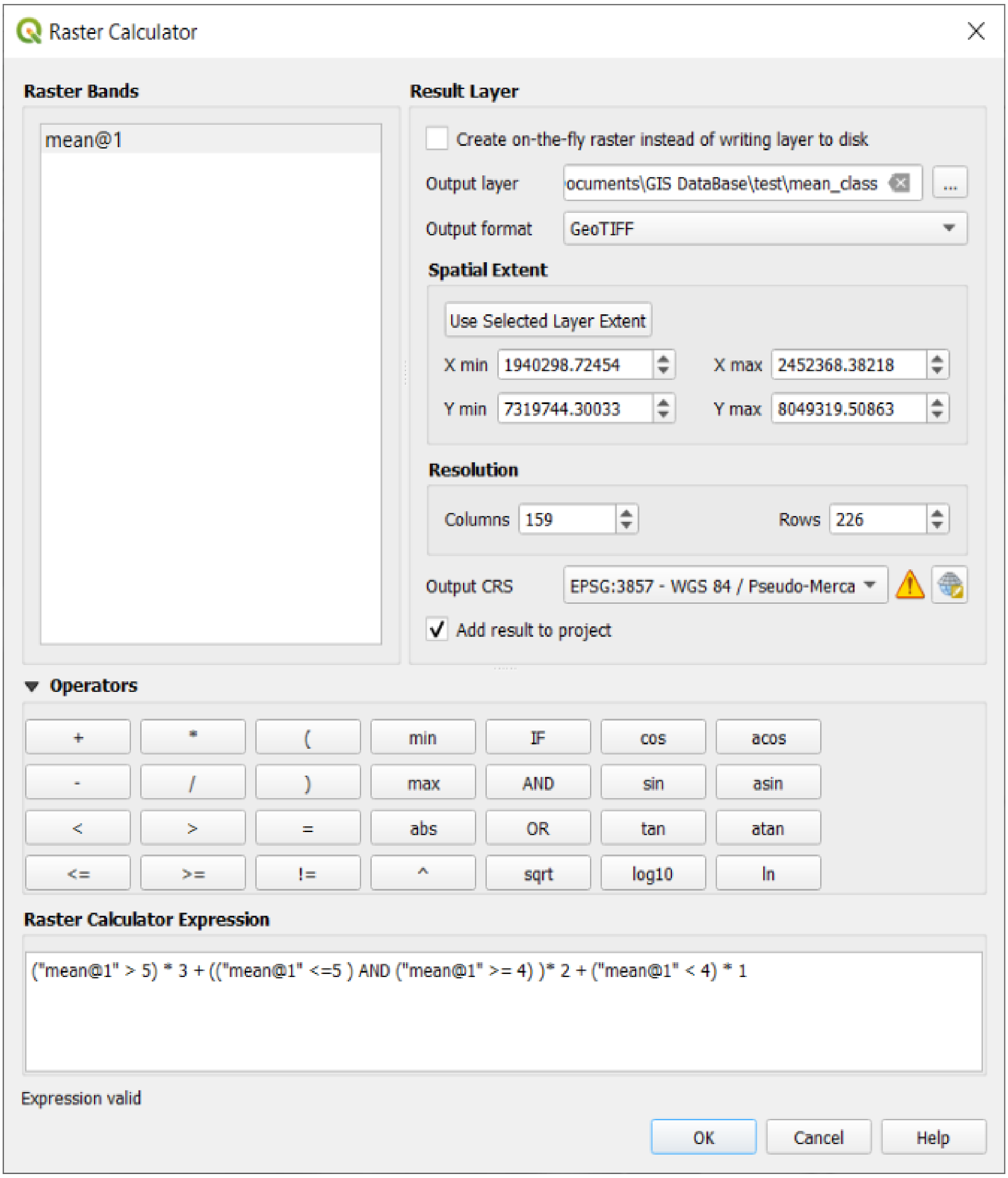

Figure III-32. *Raster Calculator tool to classify SST values into 3 groups: 1 (< 4 °C), 2 (4-5 °C) and 3 (> 5 °C).*

The grey scale of classified raster is not very useful for inspecting spatial patterns of SST, therefore, you may change the colour of scale. Select the layer and after pressing a right mouse button, select **Properties...** and **Symbology** (Figure III-33). Then, select **Singleband pseudocolor** under the **Render type** pane, **Discrete** under the **Interpolation** pane, **Reds** colour scale the **Color ramp** pane, **Equal interval** under the **Mode** pane, **3** groups under the **Classes** pane, you may change value precision under the **Label precision** pane or their labels under **Label** pane, and press **OK**.

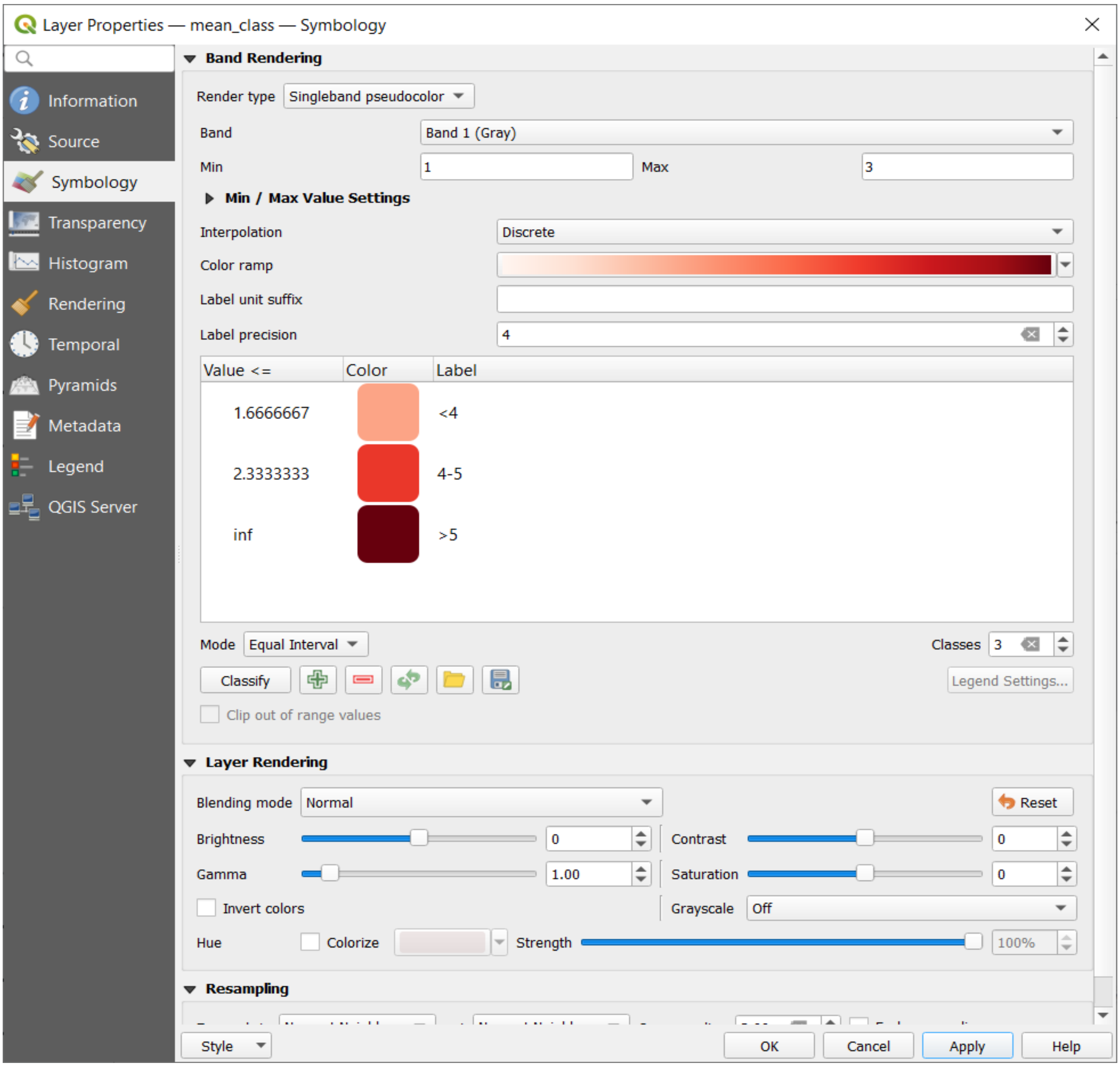

Figure III-33. *Change of classified SST grey scale into 3 colours.*

From the classified SST raster several SST patterns can be found. The warmest area was in the southern part of the Baltic Sea and in the coastal sections of Klaipeda-Sventoji and Liepoja, where the riverine waters enter the coastal waters (Figure III-34). The lowest SST was located in the northern part and near the Gulf of Riga.

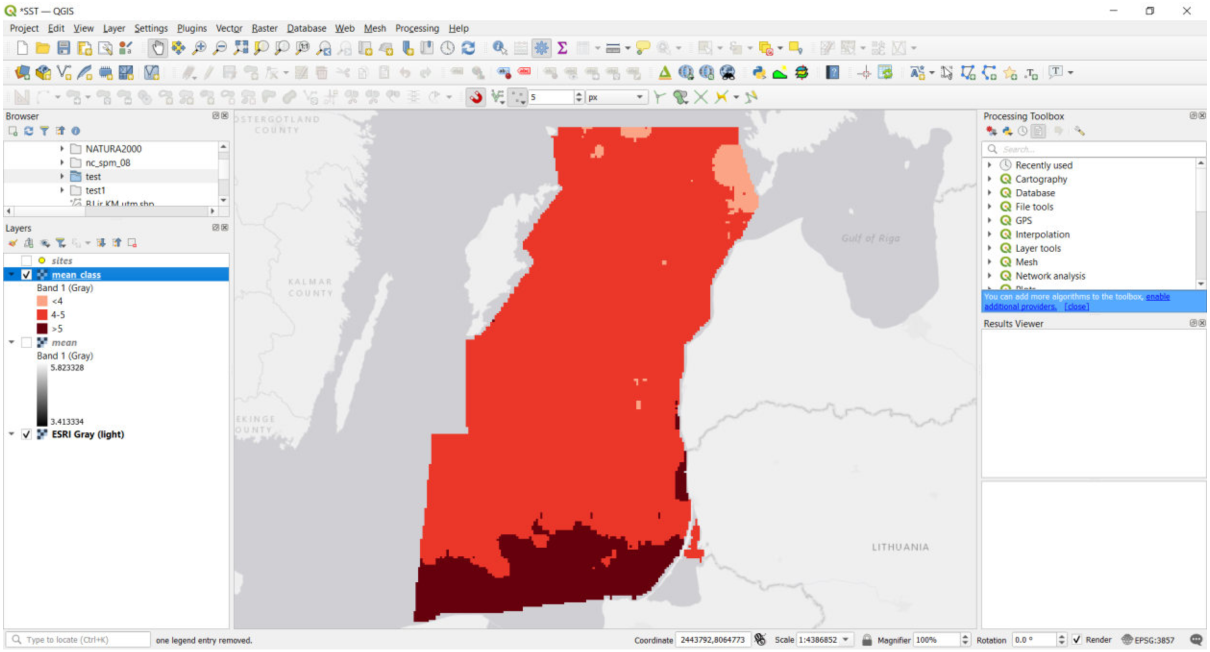

Figure III-34. *The classified the mean SST raster from March-May 2021 in the Eastern Gotland Basin and the coastal waters of Lithuania.*

Creating a map

Creating maps is usually the final step of EO data analysis. In QGIS, maps can be 2D, 3D type or plotted along a profile line (https://docs.qgis.org/3.28/en/docs/user_manual/map_views/index.html).

The 2D maps can be created mainly by two approaches: decorating a Map canvas or using a Print layout (https://docs.qgis.org/3.28/en/docs/user_manual/print_composer/overview_composer.html#sample-session-for-beginners). The second approach has more tools and functions for map making, where you can size, group, align, position, and rotate each element and adjust their properties to create your layout. The layout can be printed or exported to image formats, PostScript, PDF or to SVG. You can save a layout as a template and load it again in another session. Finally, generating several maps based on a template can be done through the atlas generator (https://docs.qgis.org/3.28/en/docs/training_manual/forestry/forest_maps.html).

Thus, the Print layout approach was selected for the training, to create a map with the mean SST (March-May 2021) with overlaid 5 sampling sites in the Eastern Gotland Basin and the coastal waters of Lithuania. Before creating the map, the layers should be understandable on a Map canvas. Firstly, you may want to add labels of the site numbers (this information is stored in the attribute table). You can do this by selecting this layer and pressing a right mouse button and selecting **Properties…**, select **Single Labels** under the **Labels** pane and the "site nr." under the **Value** panel (Figure III-35). You may also change font, style, size, colour and opacity and press **OK**.

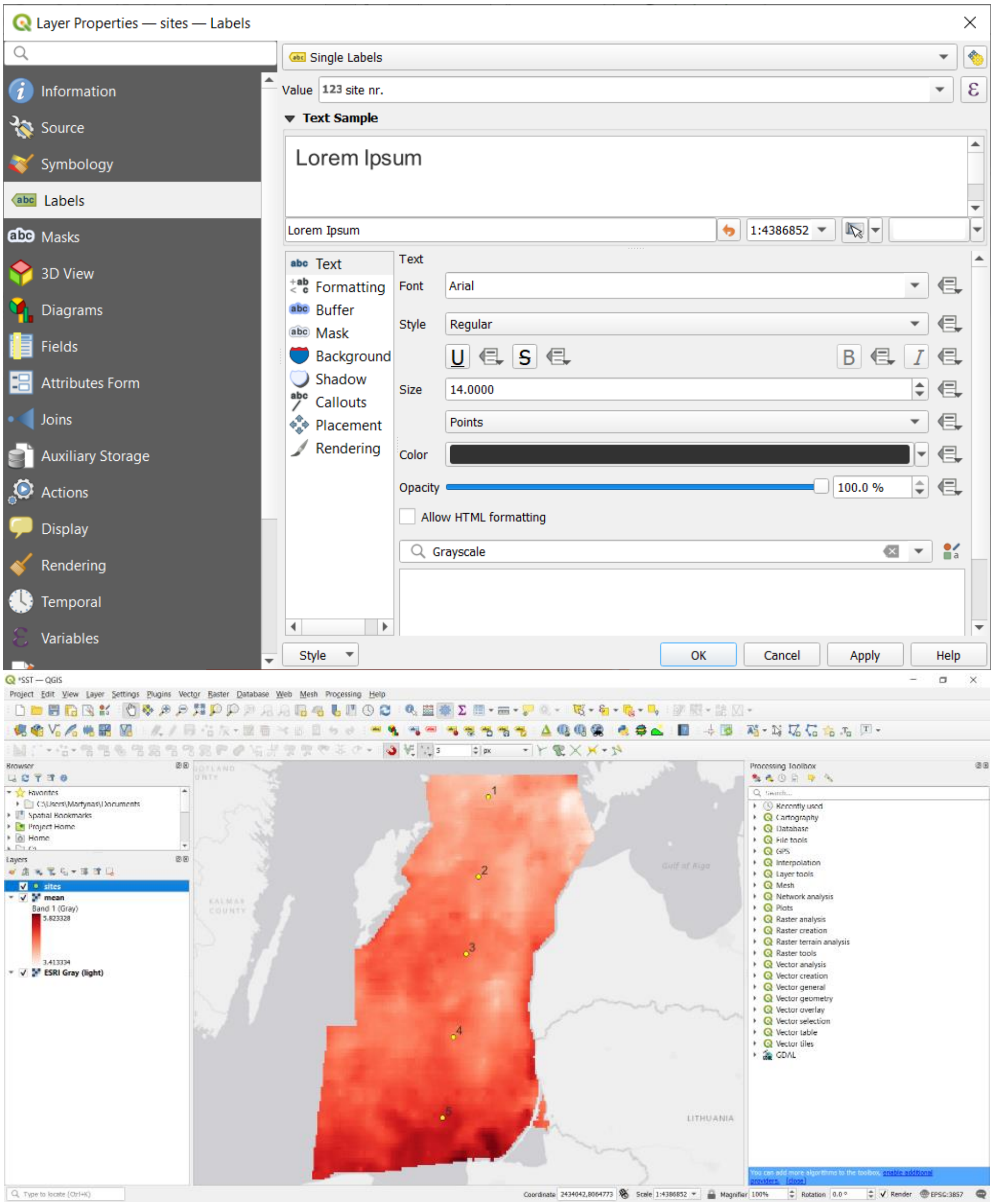

__Figure III-35.__ Adding the labels of study site numbers to a map canvas.

Although you may use the classified mean SST layer, for the final map actual mean SST values could be used in order to make it more realistic. The actual mean SST map has a grey scale; therefore, it is recommended to change it into colourful ramp. For this, elect the layer and after pressing a right mouse button, select **Properties…** and **Symbology** (Figure III-36). Then, select **Singleband pseudocolor** under the **Render type** pane, 3.4 and 5.8 respectively under **Min** and **Max**, **Linear** under the **Interpolation** pane, **Reds** colour scale the **Color ramp** pane, **Continuous** under the **Mode** pane, you may change value precision under the **Label precision** pane or their labels under **Label** pane, and press **OK**.

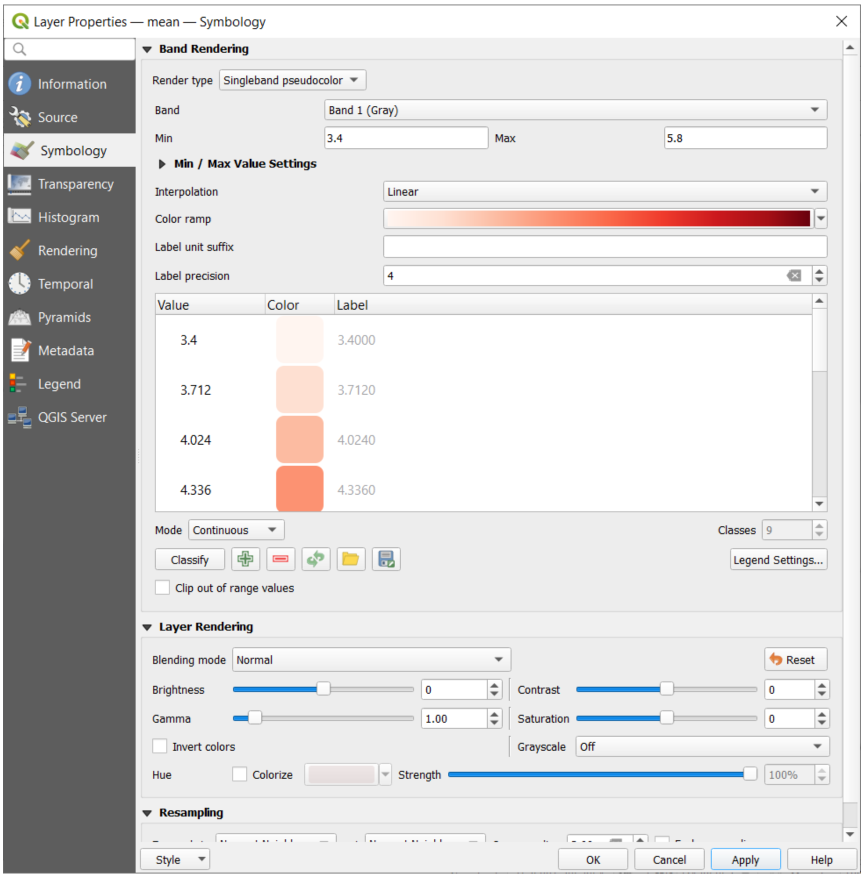

Figure III-36. The change of the mean SST grey scale into colour ramp.

The layer of the sampling points and the mean SST with changed colour ramp (Figure III-37) are ready to be included in the final map.

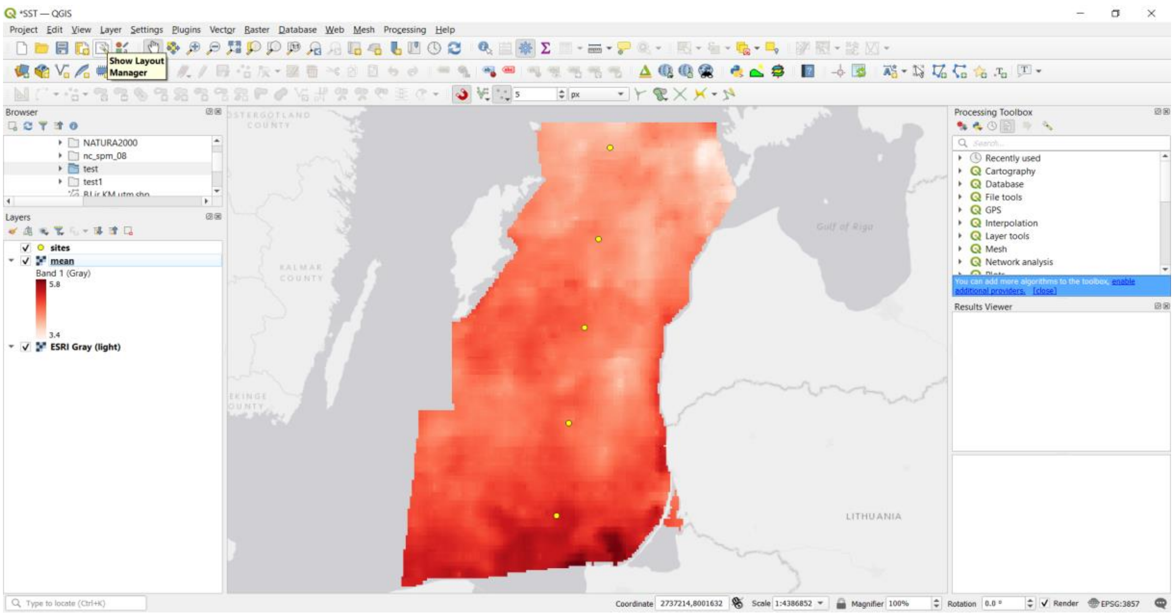

Figure III-37. *Ready layers of the sampling sites and the mean SST with the changed colour ramp.*

In a Toolbar, select *New Print Layout* (Ctrl+p), which allows to create maps, atlases, and print them or save them as image, PDF or SVG files. In the new window, you will be prompted to choose a title for the new layout (Figure III-38).

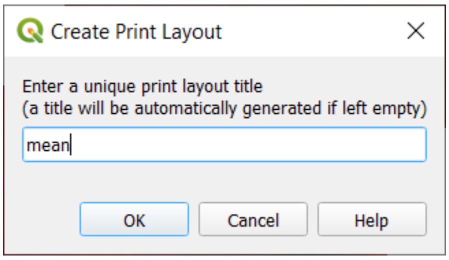

Figure III-38. Create a new Print Layout.

The print layout provides a blank canvas that represents the paper surface when using the print option in a new window (Figure III-39). On the left side of a canvas, there are tools to add print layout items: the current QGIS map canvas, text labels, images, legends, scale bars, basic shapes, arrows, attribute tables and HTML frames. In this toolbar you also find buttons to navigate, zoom in on an area and pan the view on the layout a well as buttons to select any layout item and to move the contents of the map item.

For the training, you may add the layers from the Map canvas using *Add Map* tool (Figure III-39). After selecting this tool drag a mouse to on the blank canvas to mark an area where the map should be displayed (in this case – over the whole canvas).

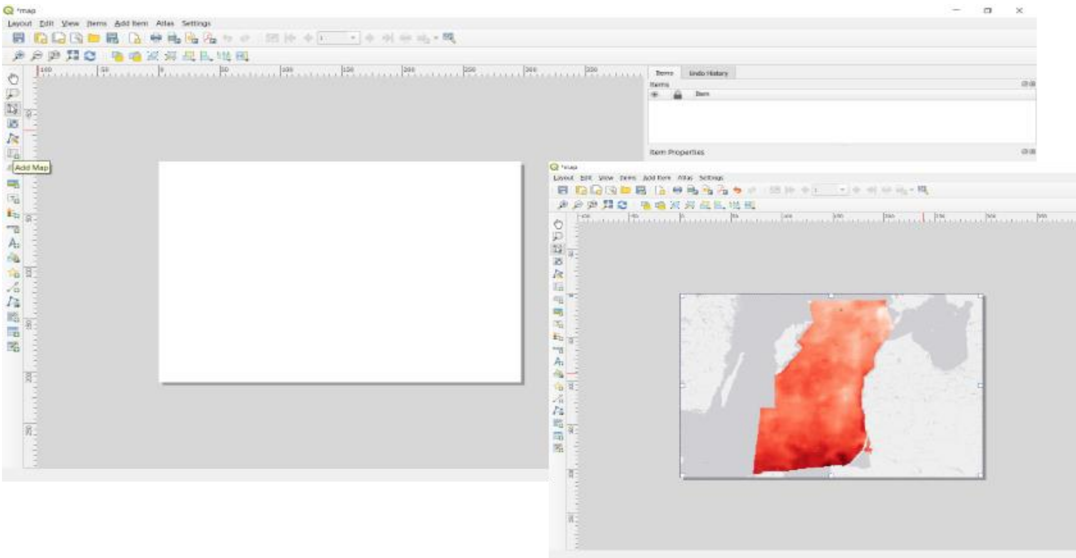

Figure III-39. *Initial view of the print layout (left) and adding the layers from the Map canvas using Add Map tool (right).*

The next important feature of a map is a legend that explains the meanings of the symbols used. A legend item can be added selecting the *Add Legend* tool (Figure III-40) and manipulate it the same way as *Add Map* tool. The layer symbols from the Map canvas will appear in the selected area.

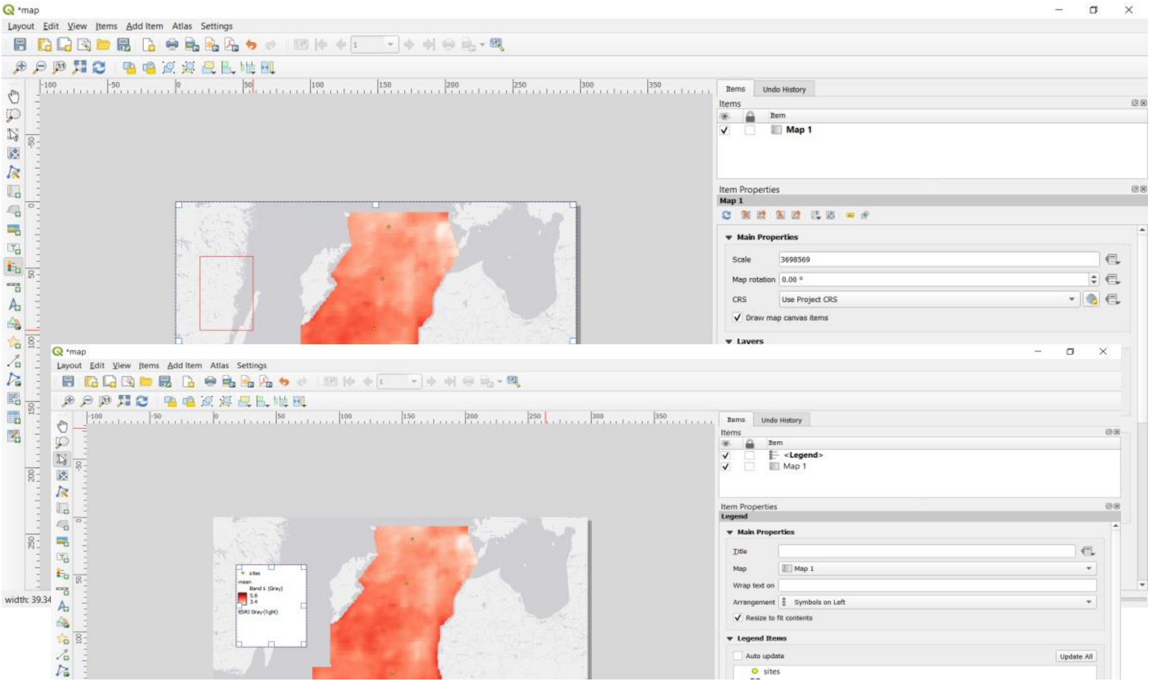

Figure III-40. *Selection of area where a legend will be displayed (upper) and inserted legend with the layer symbols from the Map canvas (below).*

All layer names and symbols displayed on the Map canvas will be provided on the legend area, therefore to remove unnecessary layers (e.g., a base map) you can select them (after selecting the legend plot) using **Ctrl** in the **Item Properties** under the **Legend Items** panel (also unselect **Auto update**) and remove them by pressing **Remove selected item(s) from legend** (Figure III-41).

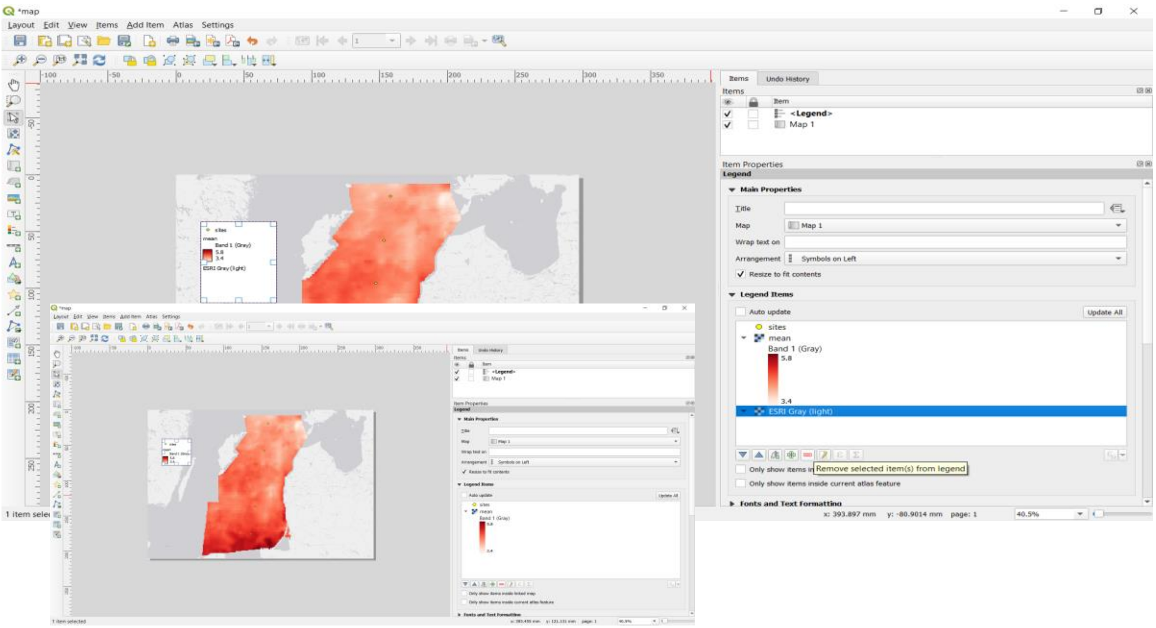

Figure III-41. *Removing of unnecessary layer from the legend (above) and the view after the remove (below).*

Then you have a final set of layers, you may want to change their names in a legend plot, as usually they are not clear or miss some information. For instance, the imported layer name of study sites you may want to change it to “study site” (Figure III-42). This can be done by selecting the layer name under the **Legend Items** panel in the **Item Properties** and press **Edit selected item properties** and you may change it under the new pane of **Label**.

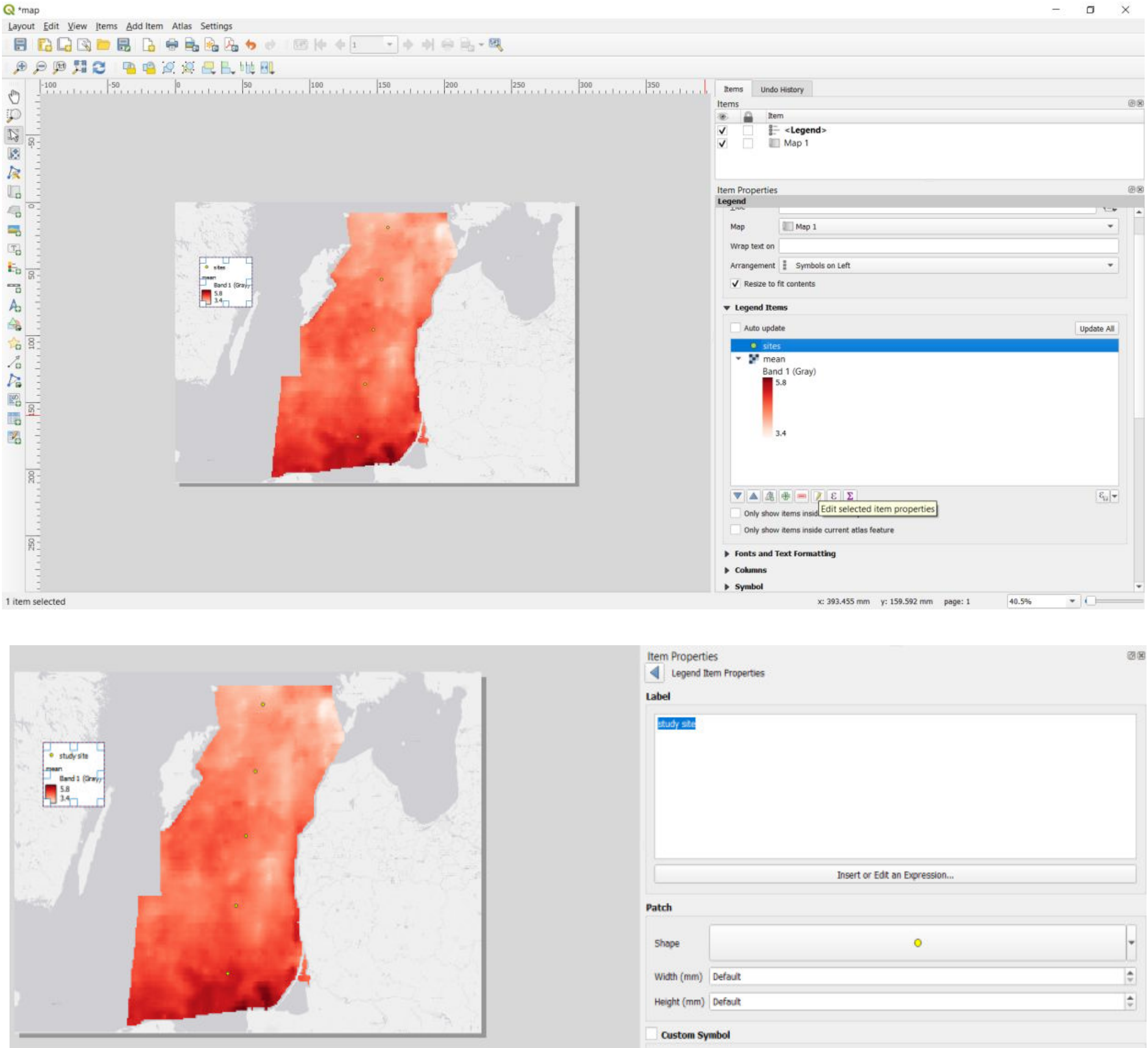

Figure III-42. *Changing then names of layers in the legend plot (above) and the view after the change (below).*

Using the same approach, the name of the mean SST layer can also be changed as in the Figure III-43.

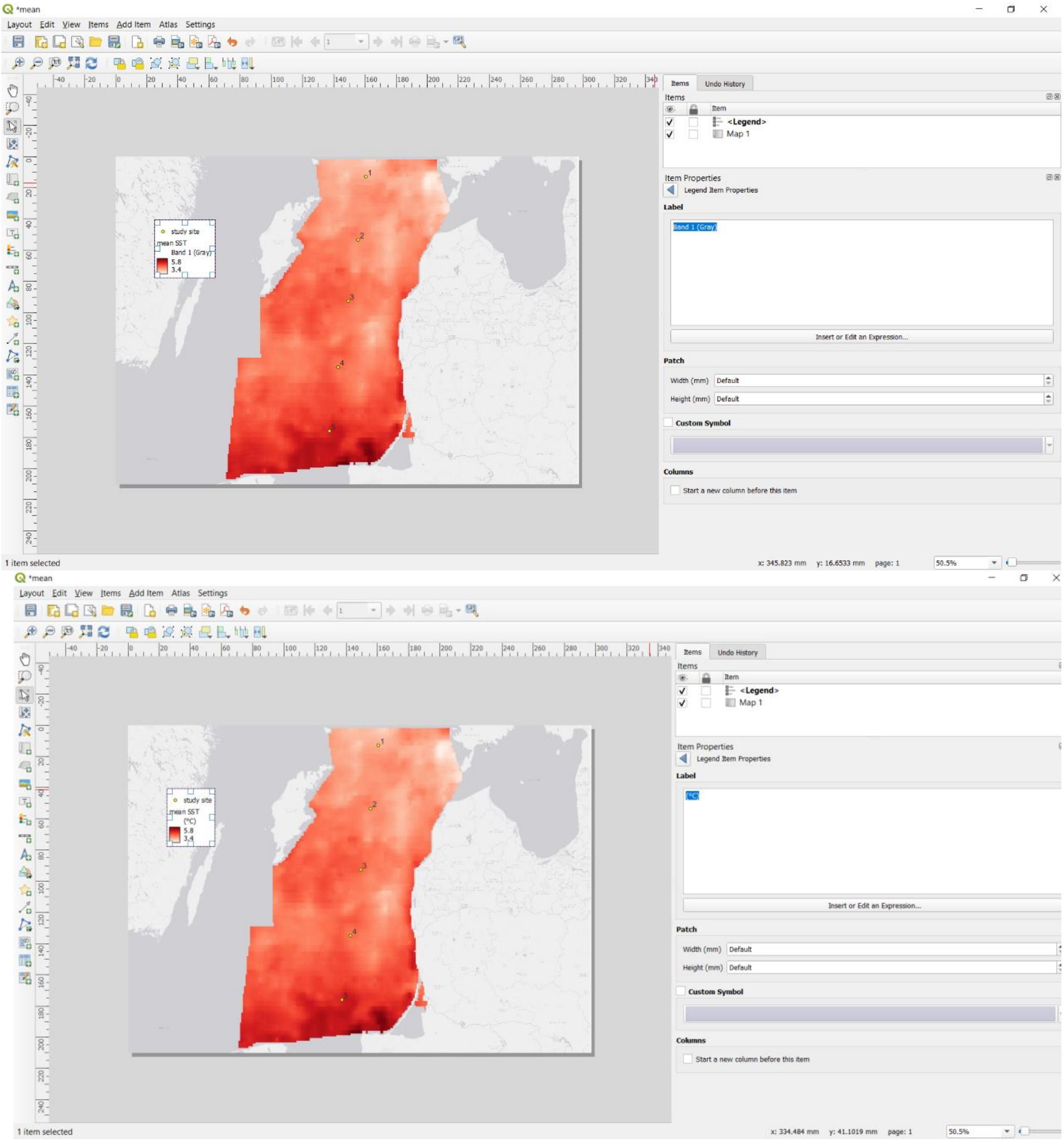

Figure III-43. *Changing then names of the mean SST layer in the legend plot (above) and the view after the change (below).*

Another attribute of a map is a scale bar, which can be added using the **Add scalebar** button from the left side toolbar (Figure III-44). A scale bar can be moved (e.g., bottom left side), its style and size can be also changed according to needs. In this case, the **Line Ticks Up** style was selected under the **Style** pane in the **Main Properties** panel, and 1 mm height was set under the **Height** and **Subdivisions height** panes in the **Segments panel.**

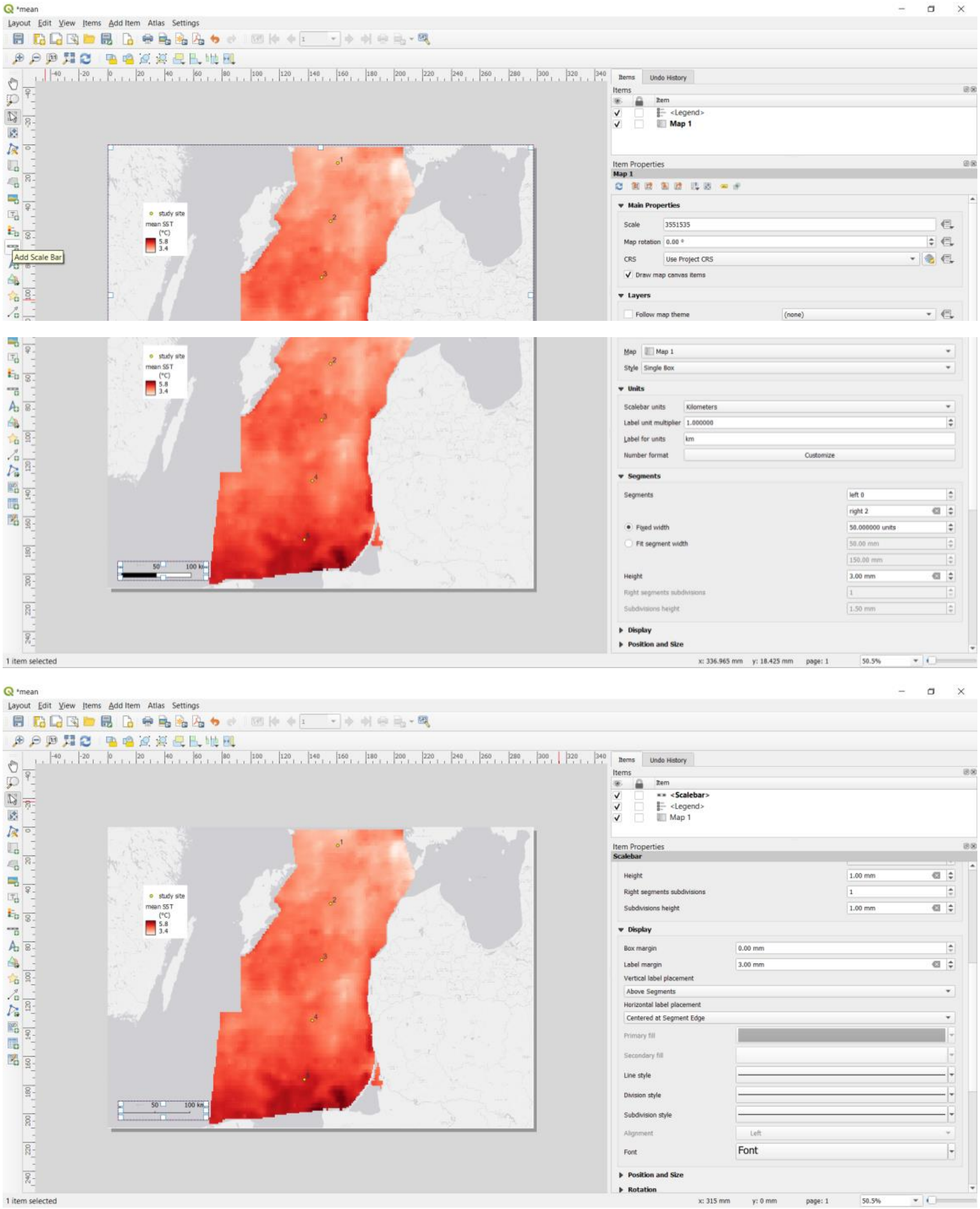

Figure III-44. *Selecting a scale bar (above), adding it to a map (middle) and changing its appearance (below).*

The North arrow is often used attribute of a map, which can be added using the **Add North Arrow** button from the left side toolbar (Figure III-45). The North arrow can be moved, its style and size can be also changed according to needs. In this case, the arrow with “N” symbol was selected from **SVG Images** pane after selecting the folder of **arrows** under the **SVG groups** pane in the **SVG browser** panel and placed on the top right side of the map.

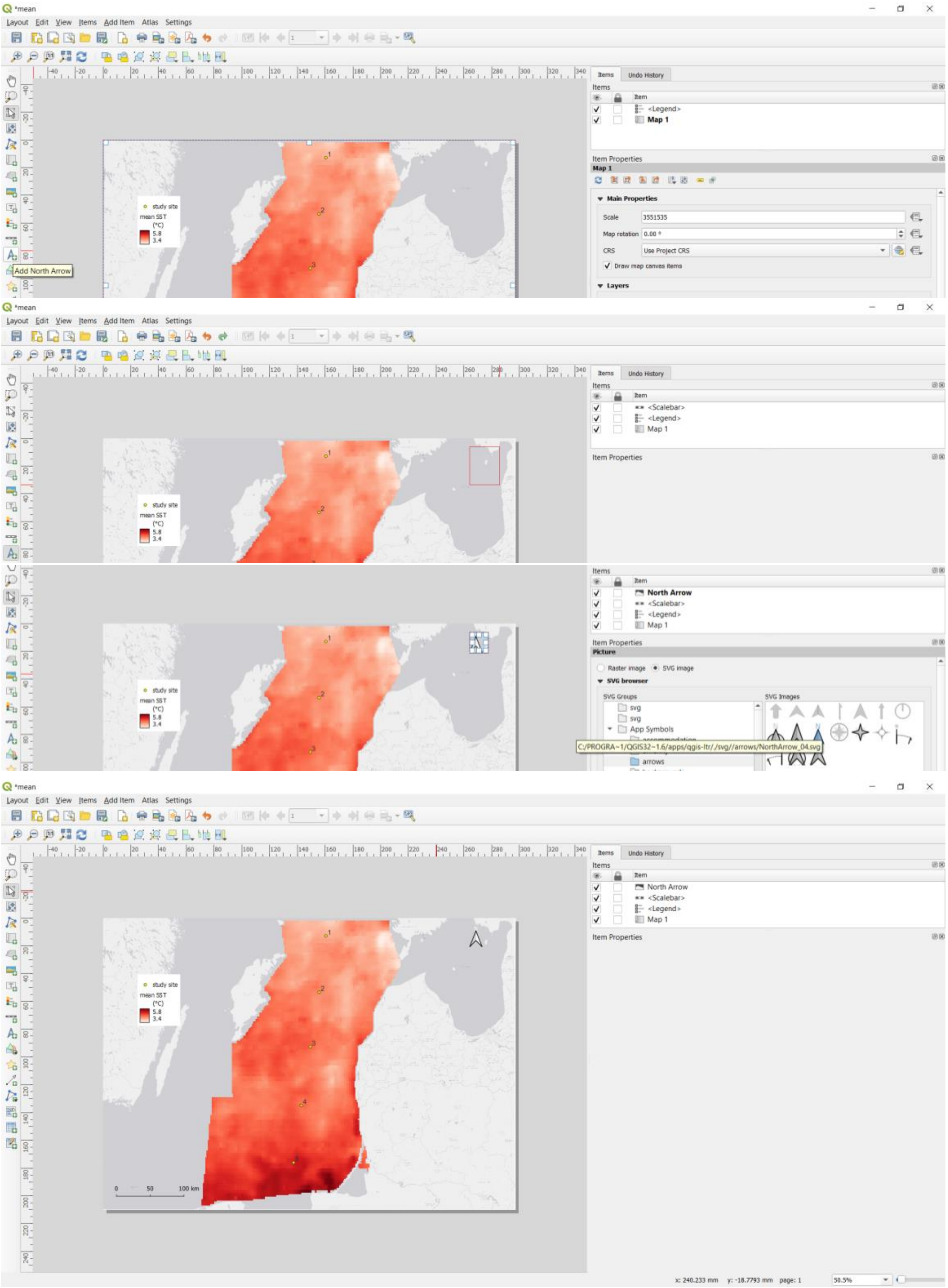

Figure III-45. *Selecting a North arrow (above), adding it and changing its size and style (middle), and a final view after adjustments (below).*

You are almost done with a map. It is recommended to also add a grid of coordinates in order someone could georeference a map or its objects if only image is provided (e.g., in a report or article). You may add a grid of coordinates after selecting the

Select/Move item button from the left side toolbar (Figure III-46) and add a grid by clicking the **Add a new grid** button under the **Grids** pane in the **Item Properties** panel. An appearance of a grid of coordinates can be modified after pressing the **Modify Grid...** button. Under the **Appearance** panel, mark the **Enable grid** pane, which will allow you to select **Cross** under the **Grid type** pane and type 100000 for **X** and **Y** coordinate intervals under the **Interval** panes, and also change colour of a grid (e.g., white) under the **Line style** pane.

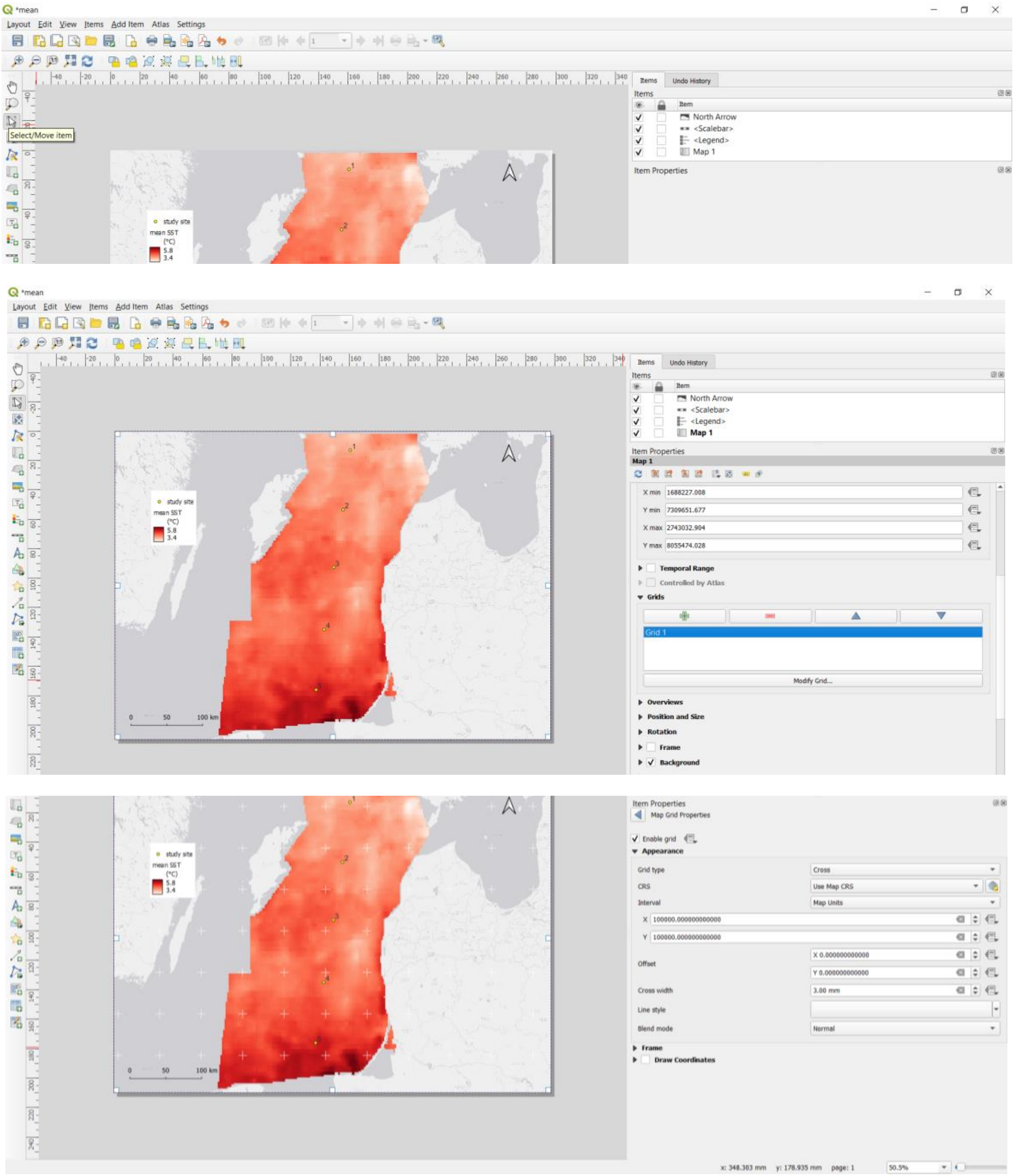

Figure III-46. *Selecting a map canvas in the print layout (upper) and adding a grid of coordinates (middle), and changing its properties (below).*

The added grid is without coordinates, which can be labelled by adding a frame of ticks for coordinates under the **Frame** panel in the **Appearance** panel. Select **Interior Ticks** under the **Frame style** pane and change colour (e.g., white), select **Latitude/Y Only** under the **Left divisions** panes and **Right divisions** panes, and **Longitude/X Only** under the **Top divisions** panes and **Bottom divisions** panes (Figure III-47). The labels of coordinates can be added by selecting the Draw Coordinates under the **Appearance** panel, where you may modify appearance and position of labels.

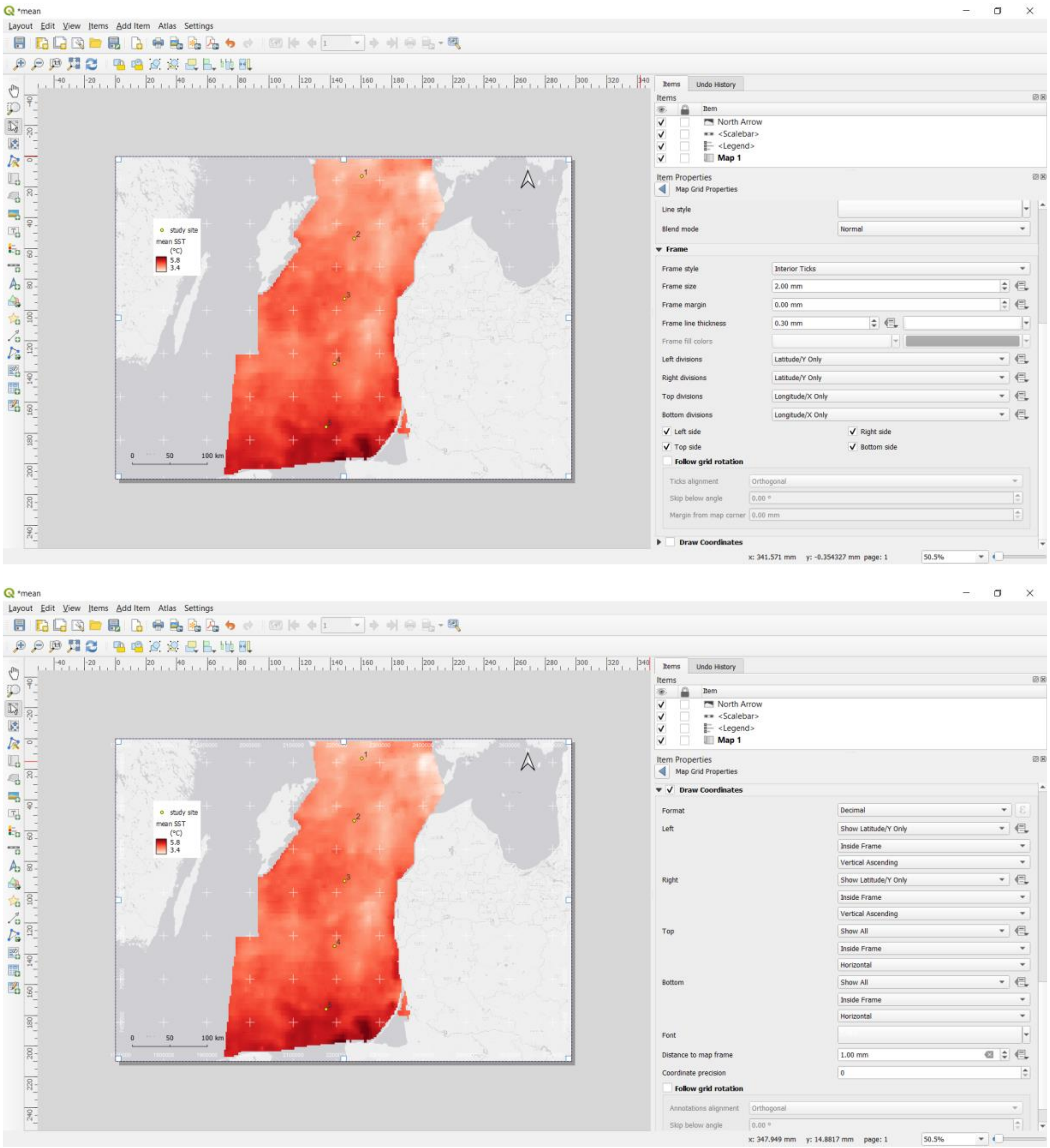

Figure III-47. Adding a frame of ticks for coordinates (upper) and labels of coordinates (bellow).

For the final makeup of a map, you may add title or other labels of objects on a map (e.g., “Baltic Sea”). This can be done by selecting the **Add Label** button from the left side toolbar (Figure III-48). You may also modify font, size, colour and alignment of a label under the **Appearance** panel.

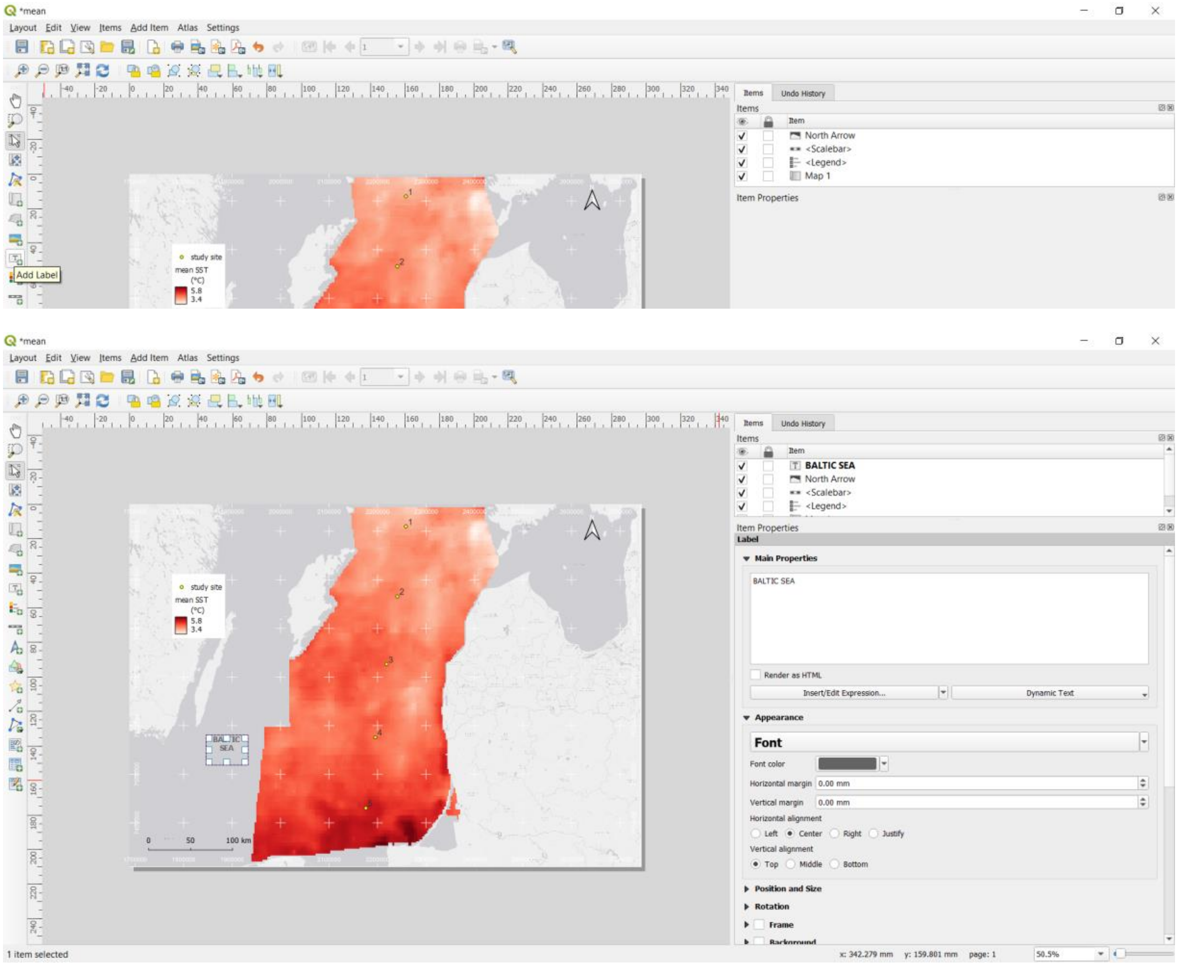

Figure III-48. *Adding the label “BALTIC SEA” on the map.*

Finally, the print layout project can be saved using **Ctrl+s** and the map can be exported as image under the Menu bar: **Layout > Export as Image…** (Figure III-49). If a warning window with the note of “Some WMS servers (e.g., UMN map server) have a limit for the WIDTH and HEIGHT parameter. Printing layers from such servers may exceed this limit. If this is the case, the WMS layer will not be printed” will pop up - press **Close**. Then, navigate where to save the map and press **Save**. A new window with properties of image will appear, where you may modify resolution and size of page, and press **Save**.

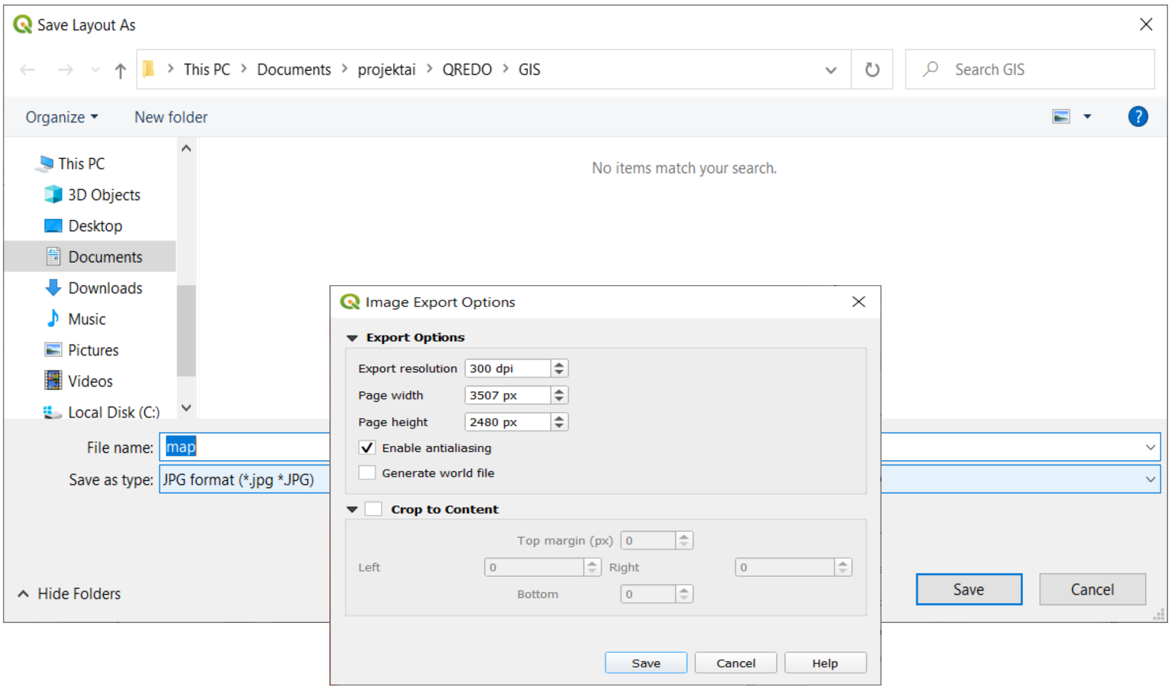

Figure III-49. *Saving a map as image (.jpg).*

The image of final map can be viewed in the Figure III-50.

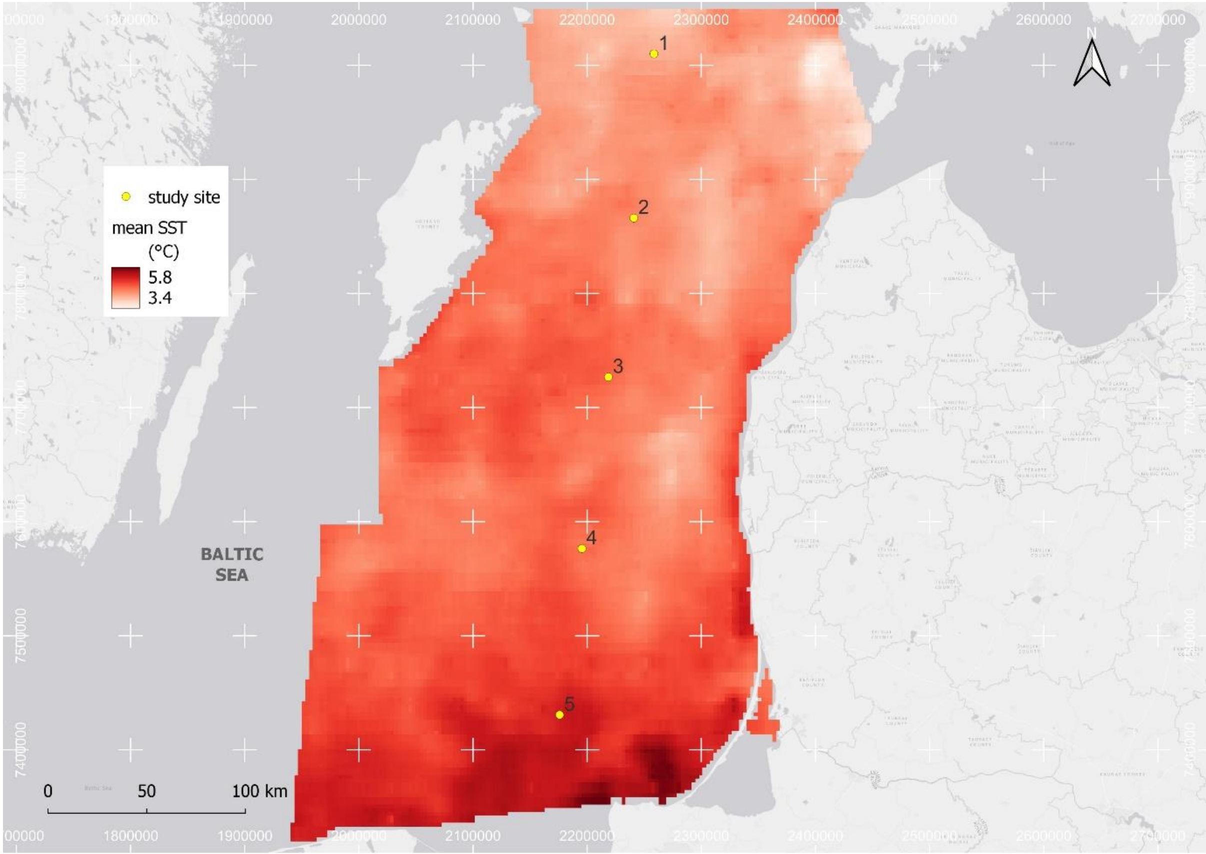

Figure III-50*. A final saved map as image.*

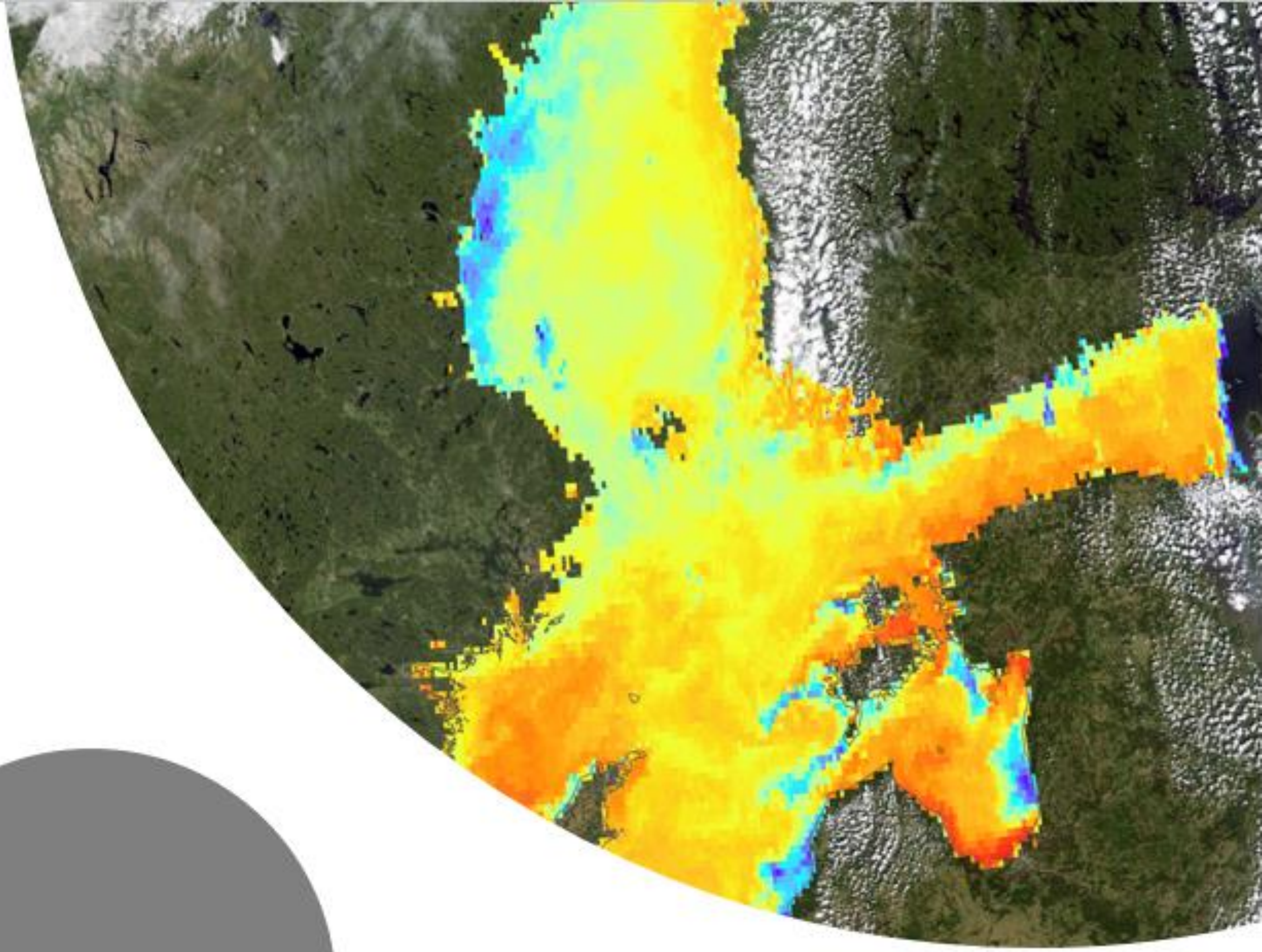

IV. Sea Surface Temperature Retrievals from Remote Sensing

Toma Dabulevičienė

Sea Surface Temperature (SST) is one of the key physical properties of the ocean, a knowledge of which is essential for understanding the rate of the ongoing climate change, as the variability of SST has a significant local and remote influence on the global climate changes through the distribution and transport of heat and moisture (Ruela et al., 2020). SST is also fundamental for understanding, quantifying, and predicting complex interactions between the ocean and the atmosphere, e.g., for understanding how the heat from the sun is redistributed across the global oceans and how it directly impacts large- and small-scale weather and climate patterns (O'Carroll et al., 2019). SST variations influence ocean circulation and primary production and can impact species abundance, distribution, and behaviour (Biguino et al., 2023). It is also an important indicator of productivity, thermal pollution, upwelling areas and might be used as an indicator of stress to ocean ecosystems (Fingas, 2019). Local variations of SST are important for regional climate and, through the influence on meteorological conditions, SST might have various impacts on socio-economic activities in the coastal regions, affecting maritime safety, military operations, ecosystem assessment, fisheries and tourism, transport and energy, human health, food security and environmental policy (O'Carroll et al., 2019). In turn, all of this makes monitoring changes in SST an important aspect for understanding and mitigating the impacts of climate change, in weather predictions and various model simulations.

SST, in general, is a difficult parameter to define precisely, as the upper ocean (~10 m) has a complex and variable vertical temperature structure related to the turbulent regime and air-sea fluxes of heat, moisture and momentum in this layer (Garcon et al., 2014). So, in order to understand how satellites are measuring sea surface temperature, one needs to understand, what the sea surface temperature is, as it depends on how and where is measured (Figure IV-1; Table IV-1).

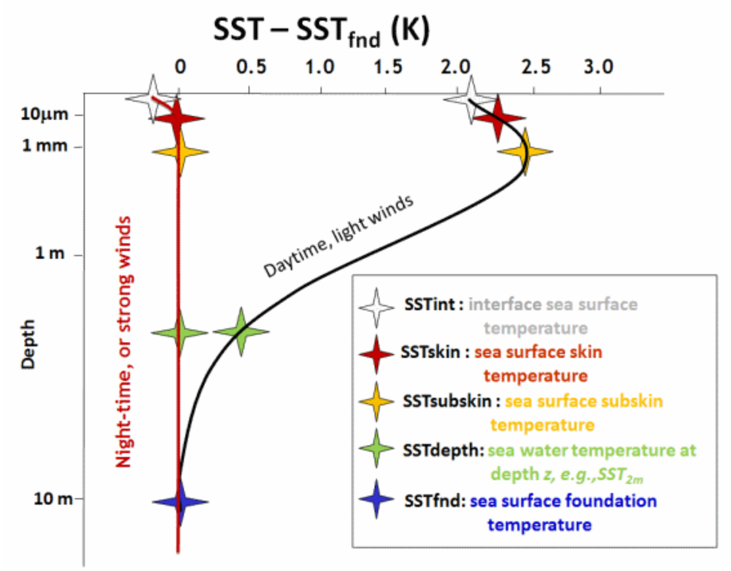

***Figure IV-1**. The schematic diagram summarizing the definition of SST in the upper 10 m of the ocean in strong wind conditions / night time (red) and low wind speeds during the day (black) proposed by GHRSST. © GHRSST – The Group of High Resolution Sea Surface Temperature.*

Table IV-1. *More detailed explanation of vertical structure of SST (according to Donlon et al., 2012).*

SSTint	A **hypothetical** temperature at the exact air-sea interface. Cannot be measured using current technology.
SSTskin	A temperature measured by a radiometer at depth within a thin layer (~500 μm) at the water side of the air–sea interface. In this manual **SSTskin** will be reffered as the temperature of the sea surface measured by an **infrared radiometeter** typically operating at wavelenghts 3.7–12 μm, representing the temperature of the sublayer of water at a **depth of 10–20 μm**
SSTsubskin	Represents the SST at the bottom of the SSTskin temperature gradient (layer) where molecular and viscous heat transfer processes begin to dominate. **STTsubskin** may be approximated by measurements made by a low-frequency (6–10 GHz) **microwave radiometer**. In this region of the electromagnetic spectrum, the penetration depth in seawater is much greater, resulting in measurements **depths of greater than 1 mm**.
Bulk SST (depth)	**SSTdepth** is measured using **conventional methods**, e.g., traditional temperature sensors mounted on buoys, profilers, and ships at any depth beneath SSTsubskin. It may be significantly influenced by local solar heating and has a timescale of hours and typically varies with depth.
SSTfnd	The temperature free of diurnal temperature variability; can only be **measured in situ**.

SST Data Acquisition: Satellite SST data can be retrieved from infrared sensors like Sentinel-3 SLSTR of ESA, MODIS of NASA and AVHRR of NOAA and others. In this manual, applications of SST from Sentinel-3 SLSTR and MODIS Aqua/Terra will be mainly presented as due to their spatial and temporal resolution and relatively long data record they are widely used in different studies and, therefore, are a valuable source for the analysis of SST changes in the Baltic Sea and its coastal lagoons.

SLSTR: Sea surface temperature from Sentinel-3.

ESA's SLSTR (the Sea and Land Surface Temperature Radiometer) is a multi-channel imaging radiometer responsible for taking sea (and land) surface temperature measurements on Sentinel-3A and B. The instrument provides global sea surface temperature measurements with zero bias and uncertainties of ± 0.3 K. SLSTR has a spatial resolution of 1 km, with less than half a day revisit time (with Sentinel-3 A and B) and a swath of 1400 km. Data is available since May 2016.

More information:

- https://sentinel.esa.int/web/sentinel/missions/sentinel-3
- https://docs.sentinel-hub.com/api/latest/data/sentinel-3-slstr-l1b/

Sentinel-3 SLSTR Level-2 water surface temperature (WST) data acquisition:

- Level-2 WST data products are freely available to the public.
- Data is available to registered users.
- Registered users can obtain Sentinel-3 SLSTR Level-2 WST data by searching: EUMETSAT Data Store.

- Data Store can be accessed through the **Earth Observation Portal** (Figure IV-2 a) or directly via **https://data.eumetsat.int** (Figure IV-2 b). To get the most out of the service, new users will require a user registration, and the EUMETSAT data policy applies. More information: https://www.eumetsat.int/eumetsat-data-store
- When entering the browser, define **Time range**, additional **Filters**, select **Area of Interest (AOI)** via entering the coordinates or by drawing polygon on the map by using toolbars at the righthand side of the map. Data can be downloaded directly from the browser by selecting the file to download or, if more data are needed, the **results can be added to the cart** and an order can be placed. A notification email will be sent with a link for downloading the data.

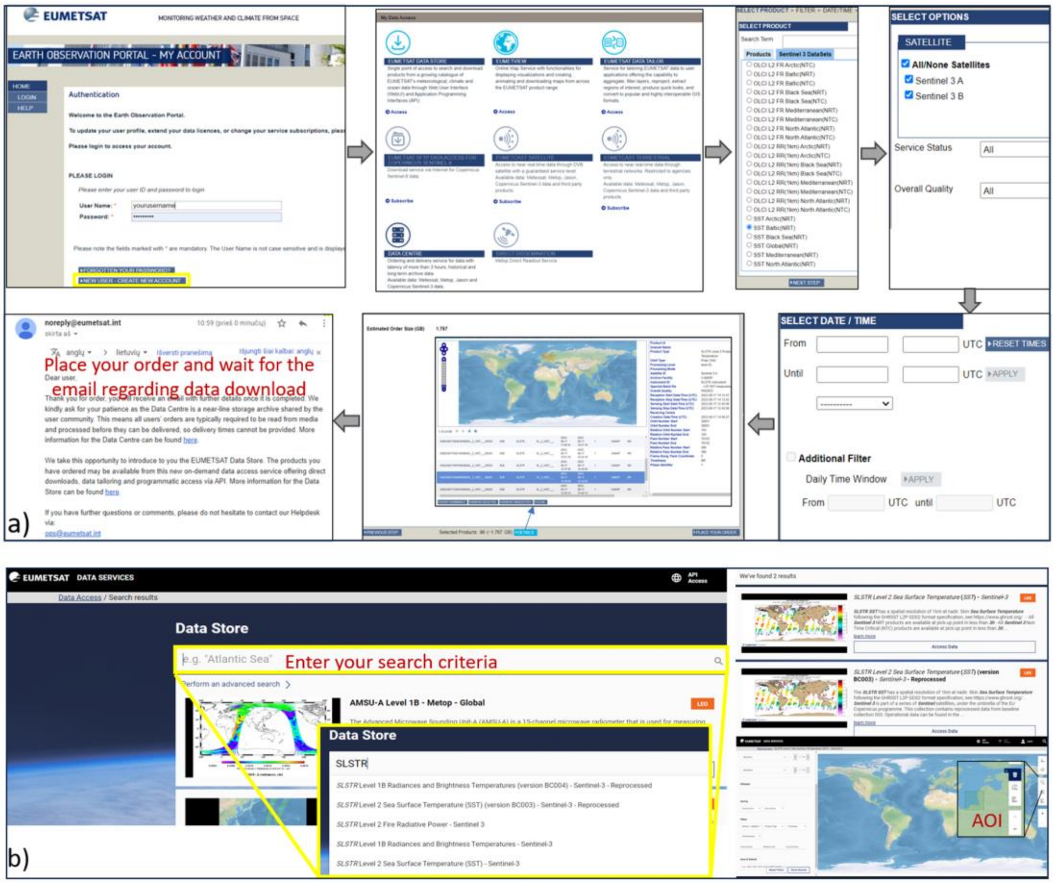

Figure IV-2. Data Store access through the (a) Earth Observation Portal and (b) direct access from EUMETSAT.

NOTE: Sentinel-3 satellite images downloaded from the archive are zipped and should be unzipped prior to use. Some images might also be relatively big in size (e.g., the noncompressed size is 2.2GB for the marine Level-2 stripe, more information at sentinel.esa.int).

NASA MODIS (or Moderate Resolution Imaging Spectroradiometer) is a key instrument aboard the Terra and Aqua satellites. The first MODIS instrument was launched aboard Terra in 1999; the second MODIS instrument was launched aboard the Aqua platform in 2002, therefore, it has a long data record of the SST spanning from year 2000 to this day. MODIS SST data products have a spatial resolution of 1 km.

More information:

https://modis.gsfc.nasa.gov/about/

https://ladsweb.modaps.eosdis.nasa.gov/missions-and-measurements/modis/

MODIS Terra/Aqua Sea surface temperature (SST) data acquisition:

- SST data products are freely available to the public.
- Registered users can obtain MODIS SST data by searching MODIS SST data product catalogue and submitting an order for selected archived products at oceancolor.gsfc.nasa.gov (Figure IV-3).
- After entering the **Level 1 & 2 Browser**, (1) define the Data you want to download; (2) define selection criteria; (3) view results (click on **Find swaths**) & (4) select data to order / download, as demonstrated in Figure IV-3.

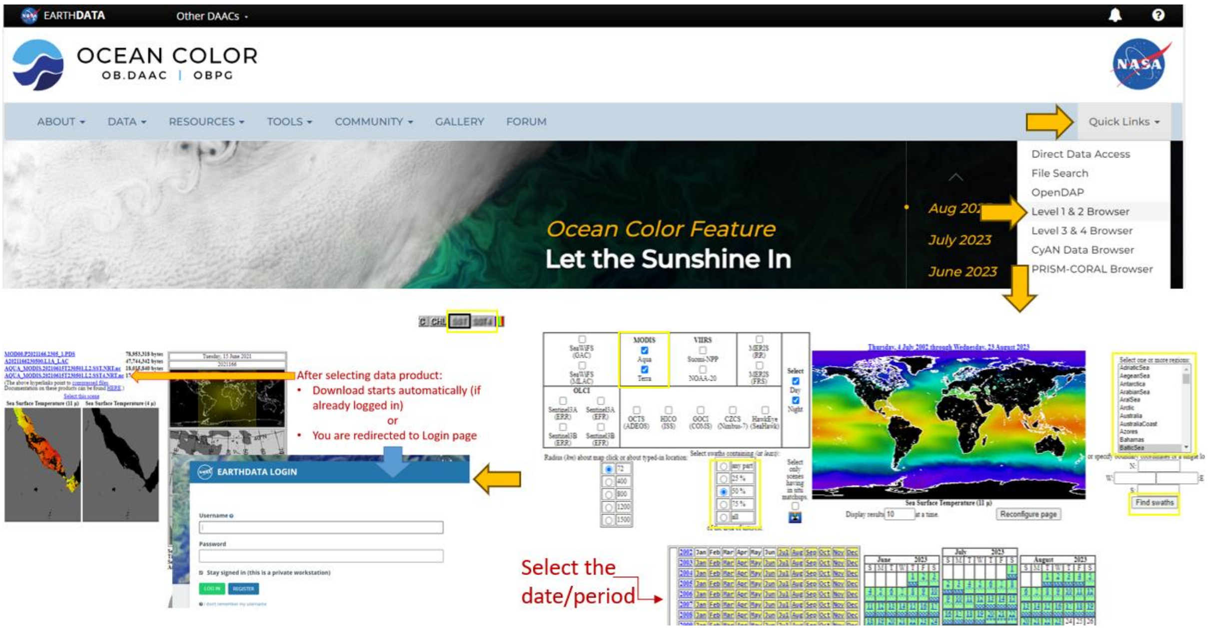

Figure IV-3. *MODIS Terra/Aqua data acquisition.*

Case study: SST analysis: Sentinel-3 and MODIS observations of sea (water) surface temperature are widely used for the coastal upwelling[1] analysis. Because of its frequent nature and spatial extent, coastal upwelling may be considered as one of the main factors, affecting the circulation of the Baltic Sea, and thus, its ecosystem

[1] The term "Coastal upwelling" describes the vertical flux of water moving upwards at the coast, which, in the case of a thermally stratified water column, brings cooler, nutrient-rich subsurface waters to the surface (Leppäranta and Myrberg, 2009).

functioning. Comprehensive upwelling studies are important assessing regional variability of water and energy exchange, salinity dynamics and response of marine ecosystems to extreme events. In this exercise an example of upwelling event that took place on 10th of June 2023, at the SE coast of the Baltic Sea, will be demonstrated.

Data used:

Sentinel-3B Level 2 SST image acquired on 10 June 2023, 19:12 UTC (S3B_SL_2_WST____20230610T191225_20230610T205325_20230612T051645_6059_080_241______MAR_O_NT_003.SEN3)

and

MODIS Aqua Level 2 SST image acquired on 10 June 2023, 02:00 UTC (AQUA_MODIS.20230610T020001.L2.SST4.NRT.nc)

For the characterization of upwelling parameters ESA SNAP software will be used.

First, load the satellite data into SNAP. Note, that the NTC product contains data of the full orbital track, and it will be displayed as a long stripe covering a full orbit (Figure IV-4 a) or you might select an individual tile (NRT product) (Figure IV-4 b) to download.

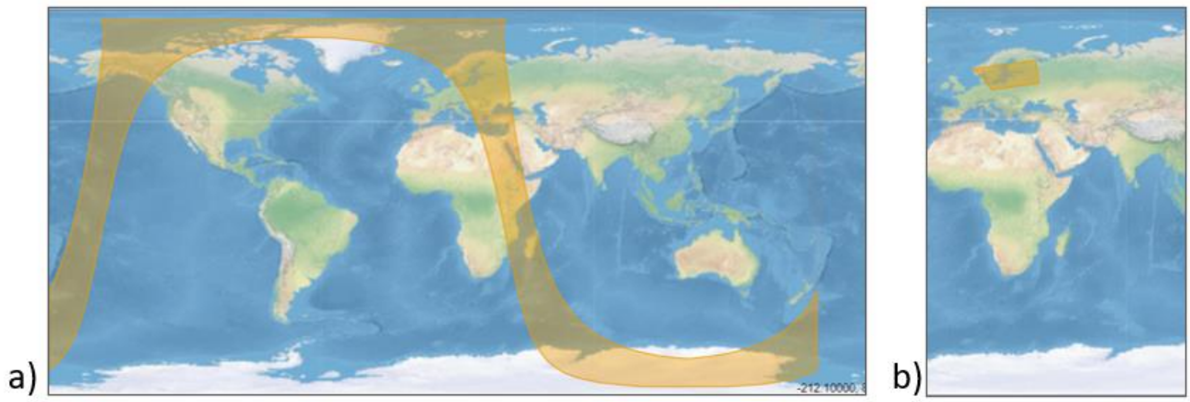

Figure IV-4. *An example of (a) full orbital track from NTC product and (b) a single tile from NRT product.*

In this excercise, an example of full orbital track is presented (Figure IV-4 a). After loading Sentinel-3 SLSTR data product into SNAP, select **Bands > Sea Surface Temperature**. After identifying the location of your area of interest (AOI) (b) zoom the image until it meets your AOI requirements (Figure IV-5 c-d) and then create a **Spatial Subset from View**. In this exercise for both, Sentinel-3 and MODIS SST data products the Spatial subset was created using Geo Coordinates (North latitude bound 56.18, West latitude bound 19.09, South latitude bound 54.87 and East latitude bound 22.97) and **Band subset (sea_surface_temperature, lat, lon bands** were selected).

As one may notice, the image still need **reprojection** (Figure IV-5) so it would be properly oriented. In this excercise, UTM zone N34 was used and the resolution (**Pixel sizeX** and **PixelsizeY**) was 1000×1000 m for both satellite images.

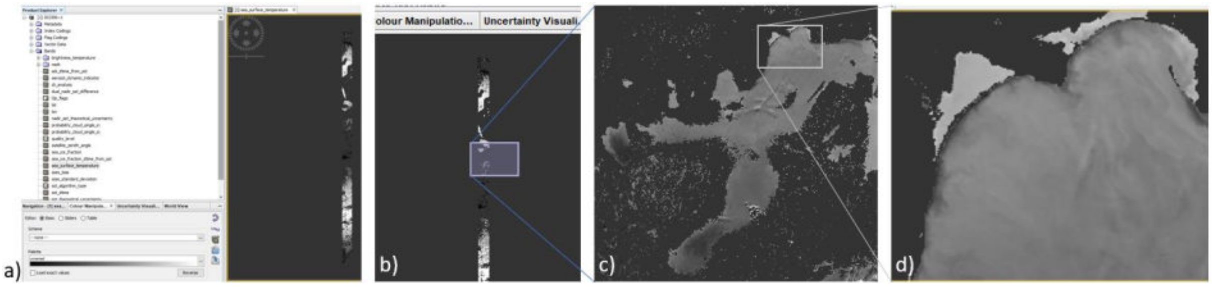

Figure IV-5. Example of selecting area of interest before reprojection.

> **NOTE:** Sea surface temperature in SLSTR product is in degrees Kelvin, therefore using **Band Maths**, recalculate it to degrees Celsius (read chapter II (SNAP) for more details on Band Maths).

Now, let's analyse SST patterns in horizontal transect during coastal upwelling using **Profile Plot** tools. To compare the SST changes in two satellite SST images (one taken at night, one in the evening), one may draw a transect on the map and then Export transect as Shape file (Figure IV-6 a), so it could be imported (Figure IV-6 b) and used at the same location for the analysis of the second satellite image.

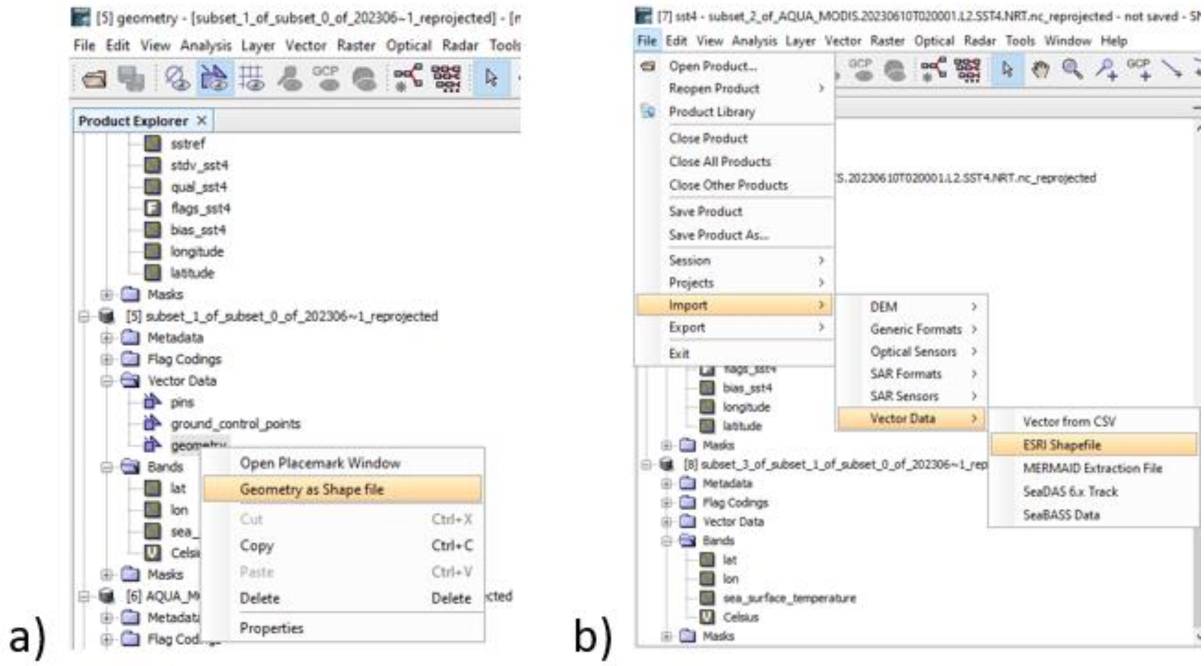

***Figure IV-6.** (a) exporting/(b) importing a Shape file.*

Then, using **Analysis > Profile Plots** tool one can analyse SST data at both profiles and asses e.g., the width of coastal upwelling, compare SST in the upwelling zone and in the ambient waters and other. The **Chart** can be saved **as Image** (Figure IV-7

a) or **Export Mask Pixels** of both transects option is available, enabling to compare/analyse them, e.g., in Excel (Figure IV-7 b) or other software.

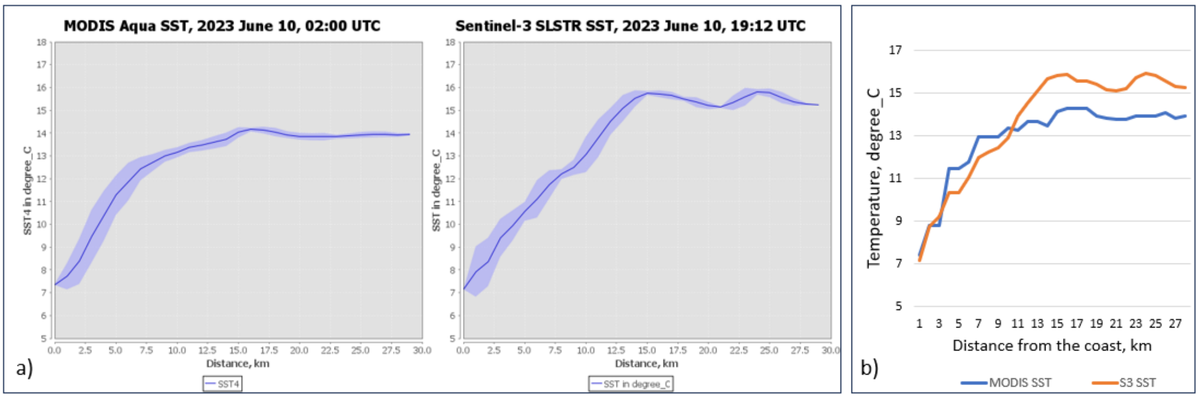

Figure IV-7. *Examples of exporting data.*

Using **Pin placing tool** in S-3 SLTSR satellite image and then **transferring pins to** MODIS SST map, we will compare SST at the same locations in both satellite images (Figure IV-8).

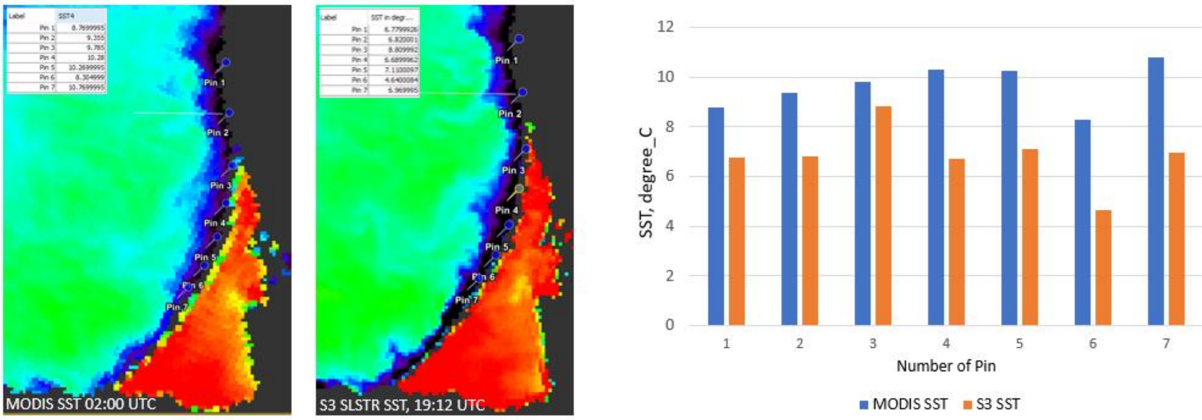

Figure IV-8*. Example of analysis using Pin placing tool data extraction option.*

One can see that the more developed coastal upwelling in the SE Baltic Sea coast is, the lower are the SST values, i.e., lower SSTs are recorded in the S3 SLSTR satellite SST image.

Create an SST map using SNAP: Adding map elements to the map is possible via **Layer > Layer manager**. After opening Layer manager click on the + icon and select **Mapping Tools > Next** where you can add North arrow, scale, or logo. Selecting **ESRI Shapefile** enables one to add shapefiles, e.g., to demonstrate, where the analysed transect was located, as was in demonstrated case. The legend can be added manually after **Exporting View as Image** and **Exporting Colour Legend as Image**. In Figure IV-9 a map created using SNAP tools is presented.

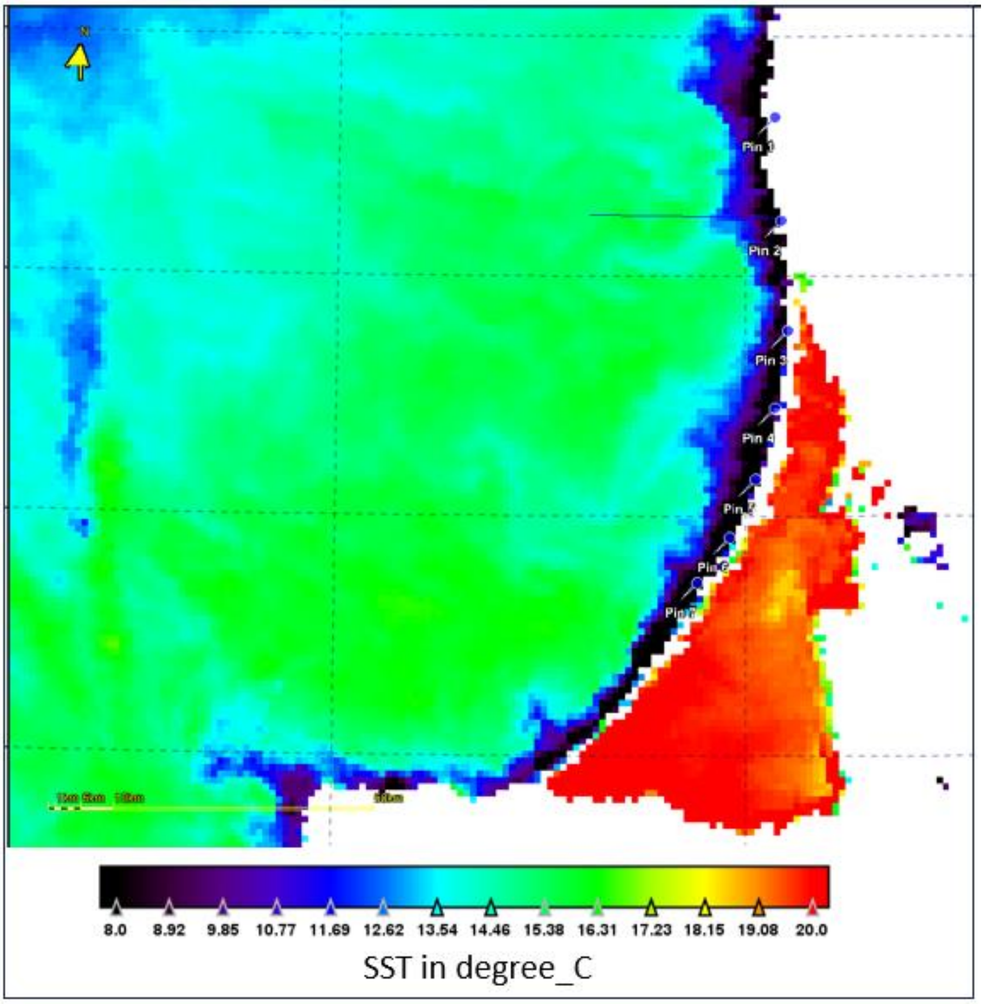

Figure IV-9. *Example of a map created via SNAP.*

NOTE: GIS functionalities are not well elaborated in SNAP as it is not a GIS software, therefore, it is recommended to use other software, such as QGIS for creation of more professional maps. More information can be found in Chapter III.

V. Ice Cover Detection from Satellite Images

Rasa Idzelytė

In recent years, the monitoring and analysis of ice cover in lagoons and lakes have become increasingly important due to the significant influence of ice dynamics on the environment and human activities. Satellite remote sensing offers a powerful tool for detecting and studying ice cover on a large scale, providing valuable insights into the spatial and temporal variations of ice formation, growth, and melt (Figure V-1).

This section explores the application of satellite imagery in detecting and analysing ice cover in lagoons and lakes. It delves into the techniques, methodologies, and challenges involved in utilising satellite data to monitor ice extent, thickness, and phenology. By leveraging satellite observations, researchers and stakeholders can enhance their understanding of ice cover dynamics, contribute to climate studies, and support decision-making processes related to winter resource management, navigation safety, and ecological conservation.

Ice cover observations: Ice cover in aquatic environments is a dynamic and critical component of Earth's climate system, influencing ecological processes, hydrology, and human activities.

Observing ice cover using traditional methods poses challenges due to inaccessibility, limited spatial coverage, and time-consuming fieldwork. Additionally, the rapid seasonal variability of ice conditions further complicates accurate observations.

Remote sensing plays a crucial role in overcoming these challenges. With its ability to provide large-scale coverage, timely and repeated observations, and enhanced safety for researchers, remote sensing offers a comprehensive view of ice cover dynamics.

Integrating data from various sensors and sources enables assessing environmental changes, understanding ecosystem responses, and making informed decisions for sustainable management of aquatic resources.

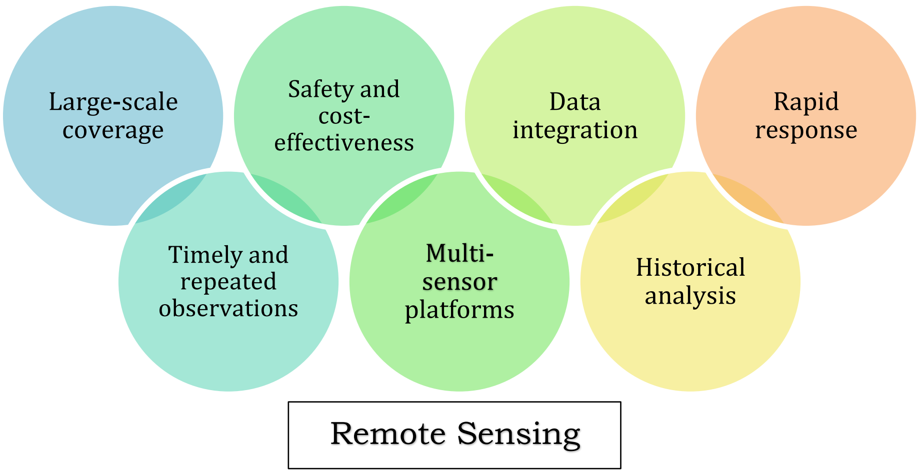

***Figure V-1**. Advantages of Remote Sensing.*

Remote sensing's cost-effectiveness, rapid response capability, and integration with other environmental data make it a valuable tool for monitoring ice cover in aquatic environments. By leveraging remote sensing capabilities, researchers and decision-makers can efficiently monitor ice cover, study its variations, and gain valuable insights into the impacts of climate change and other environmental factors on ice-covered regions.

Additionally, remote sensing data can support the development of ice prediction models, assist in navigation planning, and aid in mitigating potential hazards associated with changing ice conditions.

Ice types: Satellite observations play a crucial role in studying the dynamics, extent, and variations of different types of sea ice, providing valuable data for climate research, navigation, and environmental monitoring.

Different ice types (Figure V-2) may not always be easily detectable or distinguishable in satellite imagery. This is particularly true for the initial ice forms (i.e., frazil, grease ice, etc.), which may be too small to be detected from space.

However, when these initial ice forms consolidate, cover a large area of the water body, and change its surface patterns, then it can be detected in the satellite images.

In situ measurements, field campaigns, and numerical modelling efforts are often employed to complement and validate satellite observations, particularly for studying these early stages of ice formation and the dynamics of smaller ice types.

***Figure V-2**. Example of different ice types.*

wordpress.com

Frazil ice - small, needle-like ice crystals that form in turbulent or supercooled water. It often appears as a slushy mixture of floating ice particles.

Grease ice - a thin, soupy layer of floating ice that forms on the water surface when frazil ice crystals accumulate and freeze together. It often appears as a greasy or slushy layer.

noaa.gov

livescience.com

Pancake ice - circular or rounded pieces of ice, having raised edges and a depressed center. It forms when the frazil ice or grease ice crystals collide, freeze together, and accumulate into circular discs.

Ice types determined by satellite: Satellite sensors generally have a limited spatial resolution because they are designed to cover larger-scale areas. As mentioned before, this means that they may not be able to capture fine-scale details of small ice features. Instead, their primary focus is on capturing larger-scale ice formations and patterns. Some of the types of ice features that satellite sensors are particularly well-suited to capture (Figure V-3) include:

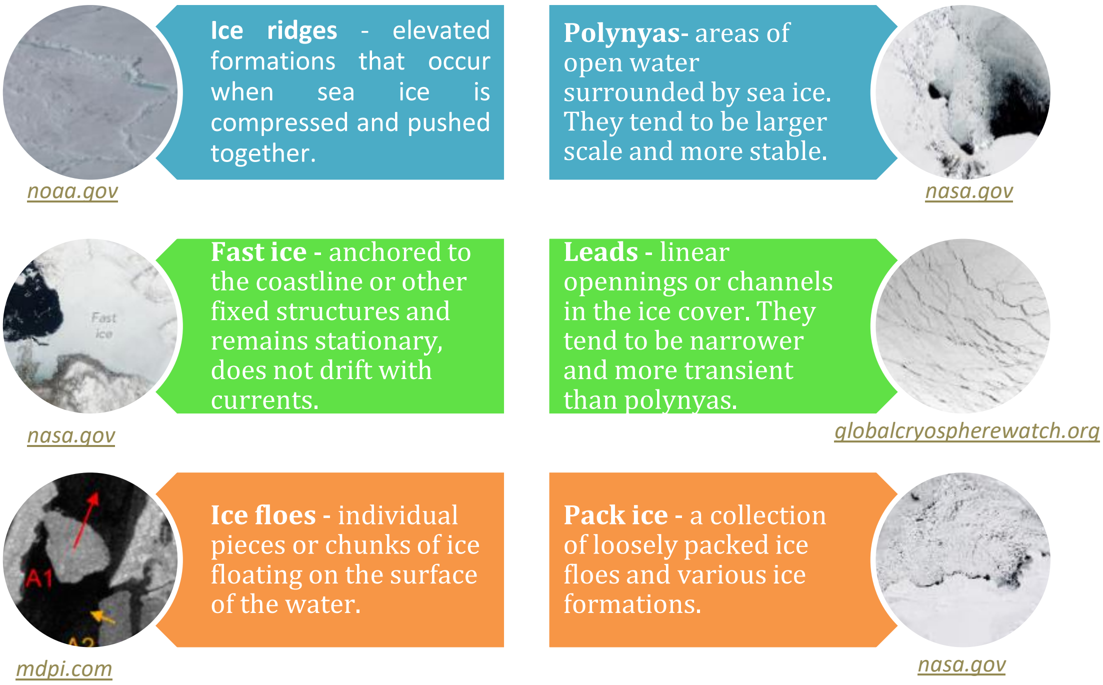

Figure V-3. *Types of ice features.*

Ice thickness: In the decade when radar altimeters were introduced, they became useful devices for measuring the height of the ice above the water. It sends pulses toward the ice surface, and the time taken for the signal to return provides the height of the ice above the water level.

By subtracting this ice cover height from the measured water surface level, one can estimate the thickness of the ice above the water level. However, this calculated thickness only reflects the part of the ice above the water - the part of the ice submerged under the water is not estimated. Estimating the thickness of the submerged ice is challenging (Figure V-4).

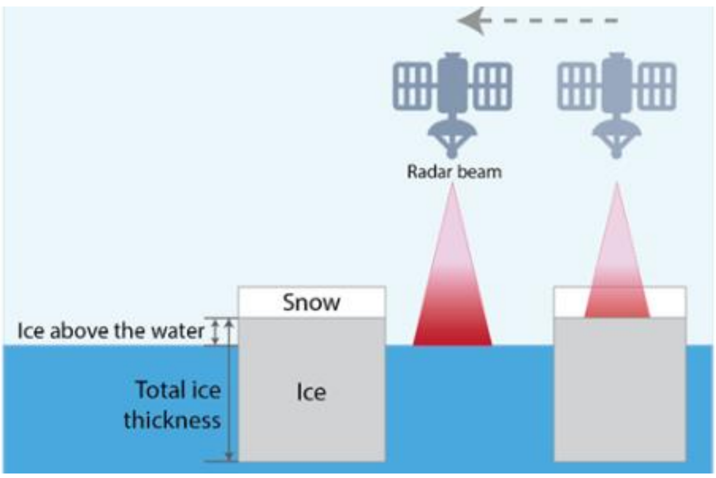

Figure V-4. *An example of the submerged ice detection challenges.*

The submerged part is typically not measured directly by satellite sensors or altimeters. Instead, it is often inferred or modelled using ice thermodynamic models that consider factors like ice density, temperature, and buoyancy. However, this introduces some uncertainties in the final estimation.

Snow cover on the ice surface can also introduce errors in ice thickness estimation. More snow weight means more ice will be submerged. These errors are significant because only a portion of the ice is assumed to have emerged above the water.

Ice thickness estimation is more complex and often requires additional data beyond satellite imagery. For example, by combining data from satellite measurements with thermodynamic models and additional field measurements of the ice cover, it is possible to calculate the growth of ice thickness quite efficiently.

Understanding ice through a variety of sensors: Ice cover monitoring from space relies on various sensors operating in different parts of the electromagnetic spectrum (Figure V-5). These sensors include those operating in the visible part of the spectrum, passive microwave sensors, and radars. Each sensor type has distinct specifications and characteristics influencing its suitability for ice monitoring.

High resolution is crucial to assess the monitored surface and accurately analyse small areas. Sensors with higher spatial resolution can provide detailed information about ice dynamics and capture fine-scale variations. Additionally, given that ice primarily forms during the winter season, when clouds are abundant during the day, it becomes imperative for sensors to be capable of penetrating through cloud cover for effective ice cover assessment.

Radars, specifically **SAR**s, emerge as a favourable option due to their high spatial resolution, cloud independence, and ability to observe the Earth's surface day and night, making them an ideal remote sensing instrument for comprehensive ice monitoring from space.

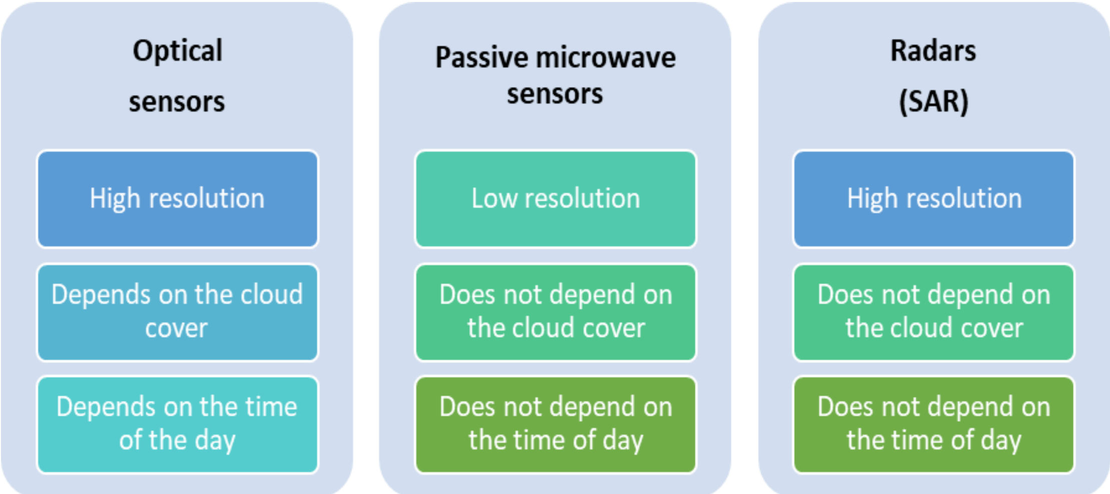

Figure V-5. *Example of different types of sensors for ice cover monitoring.*

Radar backscatter

Radars emit a certain amount of energy towards the surface of the earth, and it reflects this energy, but only a part of the energy is scattered back and red by the radar antenna sensor. The strength of the reflected signal depends on the objects on the Earth's surface. Generally speaking, radar measures the roughness of a surface, the rougher it is, the greater the backscattered signal.

The satellite image of the ice cover depends on its roughness, age, thickness, amount of air bubbles, and many other factors. When the surface of the ice cover is smooth or the ice is covered with water, then such a surface acts as a specular reflector, when the surface is rough (consisting of broken, deformed ice), the signal can be reflected in all directions (Figure V-6).

The backscattering of ice depends on its types and stages of formation. Newly formed ice (e.g. ice sheets) has a smooth surface and is dominated by specular reflection, so it will appear dark on radar images.

However, the presence of small, rough ice surface features such as ridges can significantly increase the intensity of backscattering.

Backscatter values are also highly dependent on topographic features, deformations such as ice ridges, or big wave-beaten ice floes.

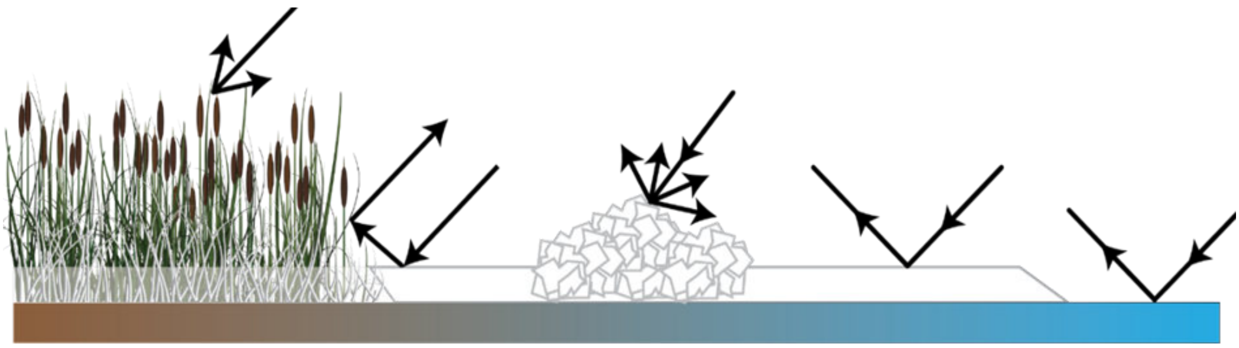

Figure V-6. *Example of backscatter.*

Polarisation

One important aspect of SAR is polarisation. Polarisation refers to the orientation of the electric field in the radar wave as it propagates.

The backscattered signal contains information about the surface's response to all polarizations.

However, SAR systems are designed with specific antennas that have fixed polarizations, and they can only measure the component of the backscattered signal that matches their own polarisation orientation.

__Figure V-7.__ Three main types of polarizations used in SAR.

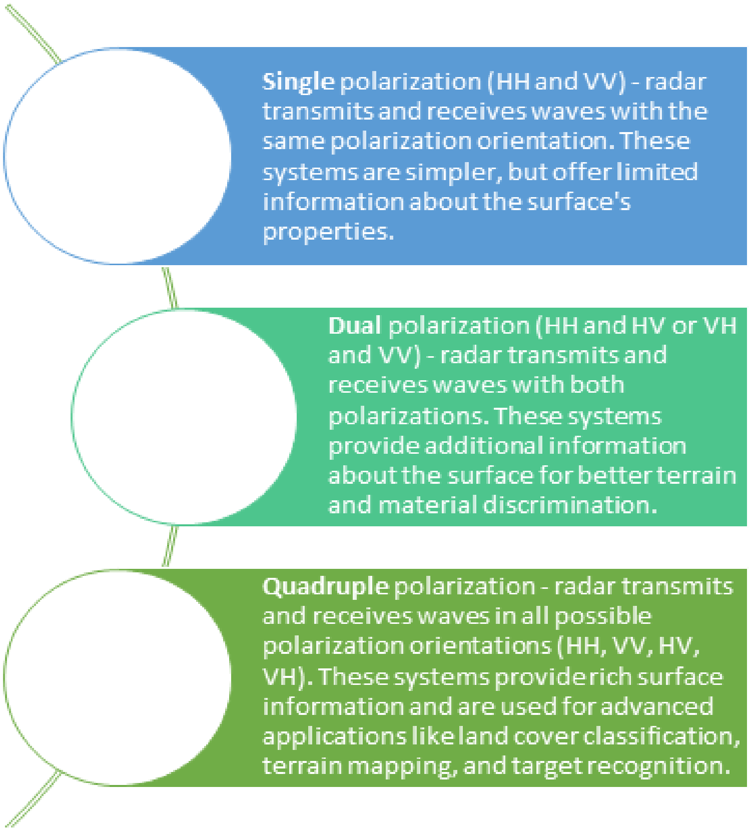

For instance, if a SAR sensor has an HH polarisation (horizontal transmit and receive), it can only measure the portion of the backscattered signal that corresponds to the horizontal polarisation. If the surface reflects the radar wave in a different polarisation (e.g., VV), the sensor won't be able to measure that part of the backscatter.

Polarisation and ice: By changing the polarisation of the emitted and received signal, we can obtain different images that can provide different and complementary surface information. The interaction of the transmitted signal with the observed surface determines how bright it will be in the radar image in a specific polarisation.

Below you can see examples of ice in different polarizations (Figure V-8). On the left, it is clear that the ice is much brighter in the same vertical polarisation (VV) image than in the VH polarizations.

However, on the right, the difference between the HH and HV polarizations (when the horizontal polarisation signal is sent to the ground) is not so obvious, the contours of the ice can be clearly seen in both pictures.

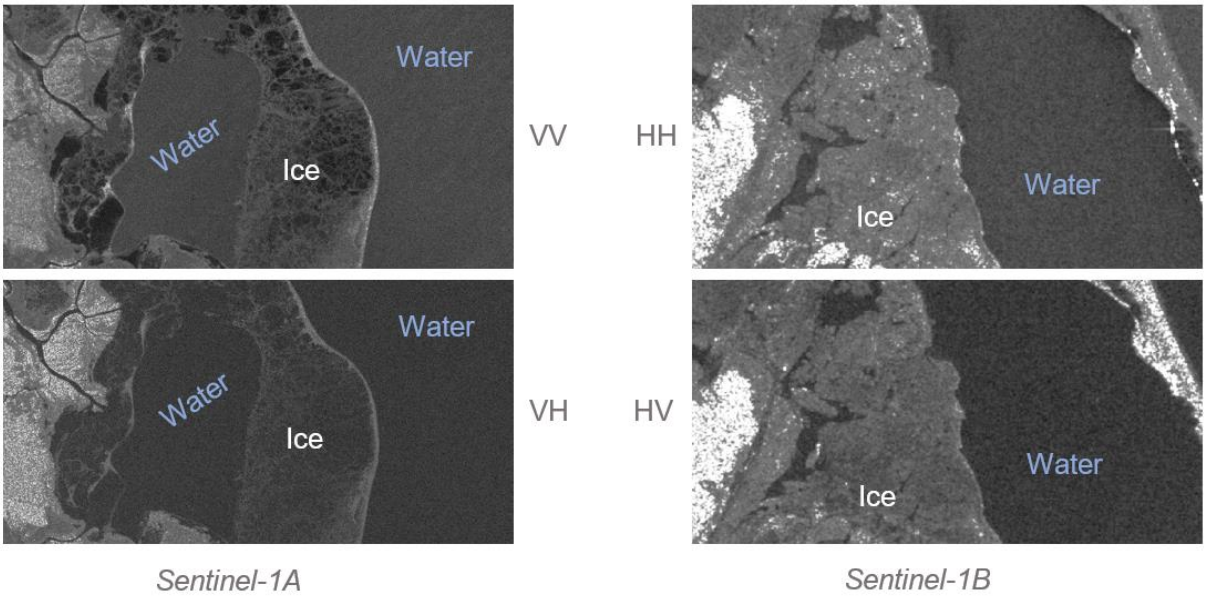

Figure V-8. *Ice in different polarizations.*

Preprocessing of SAR Images

Preprocessing of remote sensing data plays a crucial role in ice cover detection from SAR images, ensuring data quality and consistency. The main preprocessing steps for ice cover detection include orbit correction, radiometric calibration, and terrain correction.

All SAR image processing steps are thoroughly explained in Chapter 0. By following the described guidelines, you will obtain a refined final image free of geometric distortions and aligned with a standardised coordinate system. This final image will provide a clearer representation of the ice cover and its features.

This way, ice cover detection from satellite images can be conducted with improved accuracy and reliability. It sets a solid foundation for subsequent analysis, classification, and interpretation of ice cover dynamics and variations over time.

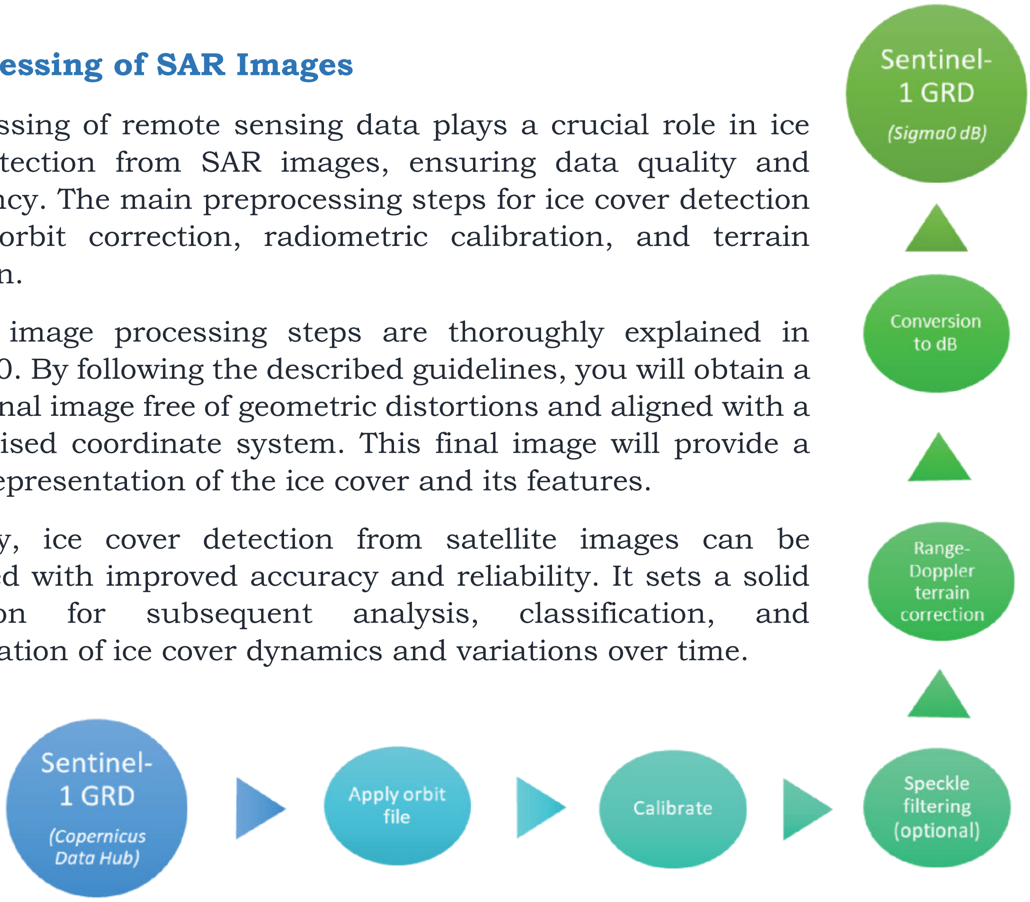

Ice cover detection

Various image interpretation techniques can be used to identify ice cover in remote sensing data. These techniques include:

Visual interpretation

The manual examination of satellite images to detect ice cover based on its visual characteristics by searching for recognizable features linked to ice, such as bright or white surfaces, which commonly signify the presence of ice. Ice patterns, such as sea ice and ice floes, can be observed to pinpoint regions with substantial ice extent.

Image classification

A computer-based technique that automatically categorises pixels or image segments into different classes, such as ice and non-ice. This process uses various algorithms to assign pixels to specific classes based on their spectral characteristics.

Change detection

Comparison of multiple satellite images acquired at different times to identify changes in ice cover extent and conditions. Pixel-based or object-based change detection methods can be used. Pixel-based methods compare individual pixels between two images to detect changes in spectral values, while object-based methods group neighbouring pixels with similar properties to detect changes in ice cover patterns, such as ice breakup or formation.

By combining various image interpretation methods, analysts and researchers can obtain a more comprehensive grasp of ice cover extent, variations, and attributes in remote sensing data.

Colour manipulation

Colour manipulation of radar images is limited compared to optical imagery. SAR images are typically grayscale, representing radar backscatter intensity values, and do not have inherent colour information like RGB (Red, Green, Blue) images. However, SNAP software provides some basic colour manipulation options (Figure V-9) that can help enhance the visualisation of SAR images for better interpretation of the observed features, e.g., distinguishing ice cover or open water areas.

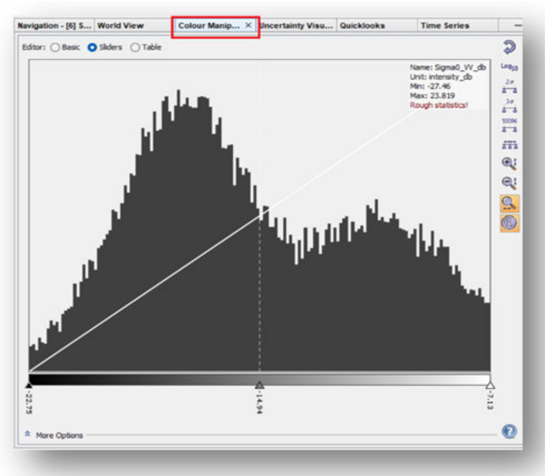

Figure V-9. *Colour manipulation in SNAP.*

After finishing the preprocessing of the SAR image, open one of the bands and in the lower left part of the SNAP window choose **Color Manipulation**. If you cannot see it, then in the upper menu bar select**: View > Tool Windows > Color Manipulation**.

By sliding the triangles below the graph, you can adjust the contrast and brightness of your opened image. Play around with it to find the best way to enhance the visibility of specific features or details in the SAR image.

TIP: try to align the middle triangle to the highest bell-shaped curve point and the other two triangles to the beginning and end of this bell.

Reset to defaults – restores the initial settings.

Expand and shrink histogram horizontally – you can see either all histogram values or shrink the visualisation only to the defined range.

The example below (Figure V-10) shows a Curonian Lagoon (triangle-shaped area, half-covered by ice) separated by a land barrier from the Baltic Sea (on the left). Underneath them, there are histograms that were applied to adjust the contrast and brightness of the image. Notice the position of the triangles at the bottom.

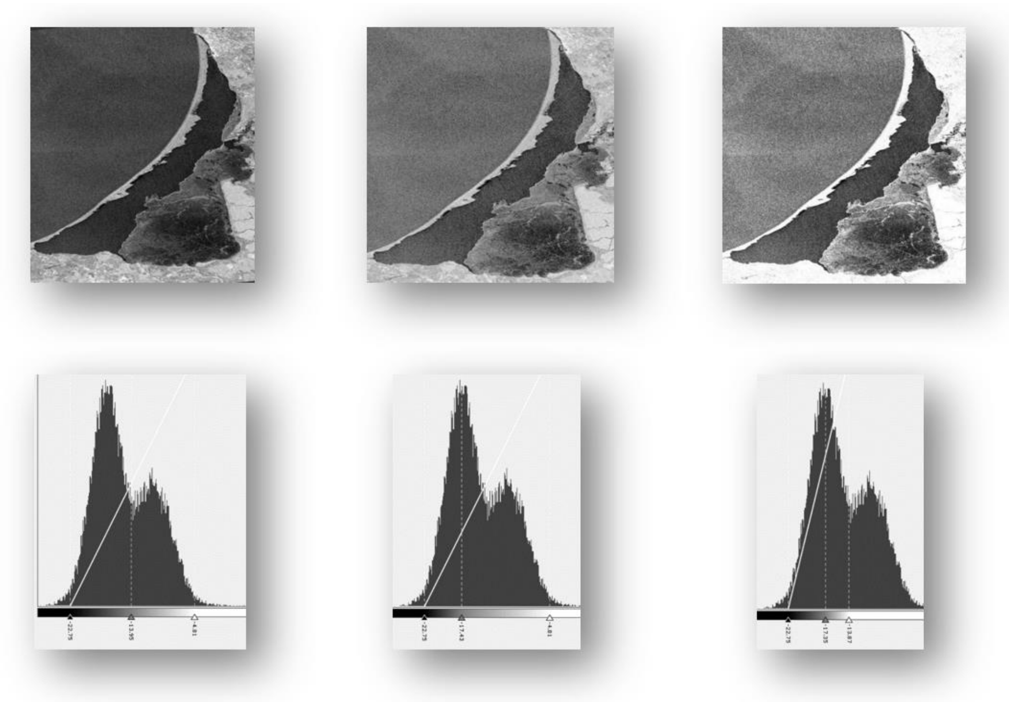

Figure V-10*. Example of colour manipulation for the Curonian Lagoon ice cover case.*

False colour composite: Utilise False Colour Composites: display SAR images in false colour composites using different polarisation combinations. This can enhance the visibility of specific features, such as open water (dark areas), ice cover (bright areas), and different ice types.

While SAR images are grayscale, you can create a false colour composite (Figure V-11) by combining different polarisation bands or images acquired at different times. A false colour composite assigns different bands to the red, green, and blue channels, creating a false-colour representation of the SAR data. This can help highlight specific features or changes in the image. Experimenting with different band combinations can help you obtain the most informative and visually appealing false colour representation of the radar data.

SNAP offers band division, multiplication, and subtraction options, enabling the creation of false colour composites for radar images (Figure V-11, Figure V-12). These operations combine bands or polarisation channels in complex ways to emphasise specific characteristics of the observed area.

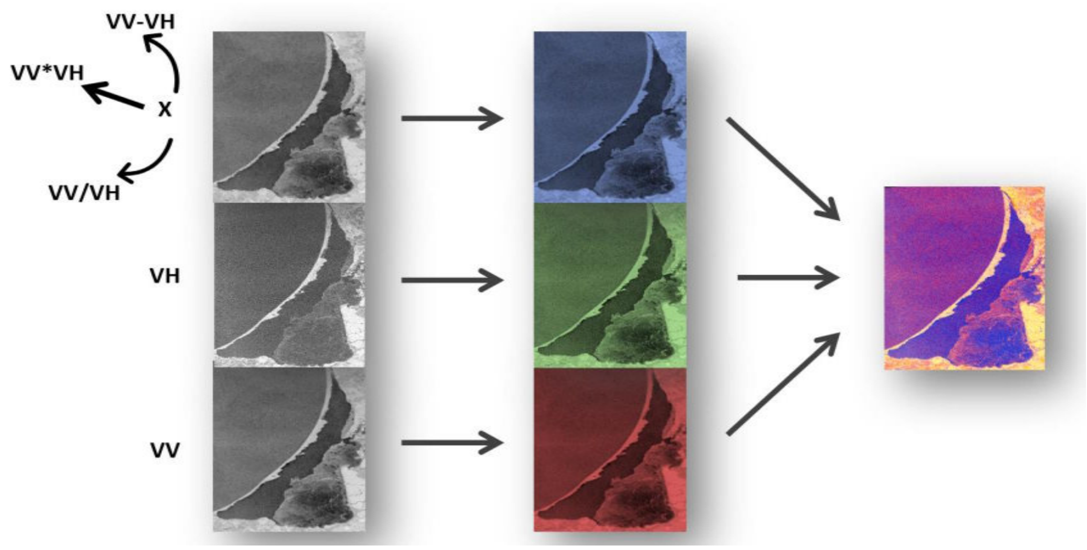

Figure V-11. *Example of false colour composite.*

To display your radar image in false colour composite using SNAP, after finishing the preprocessing steps right-click on your last layer in the **Project Explorer** window and choose **Open RGB Image Window**.

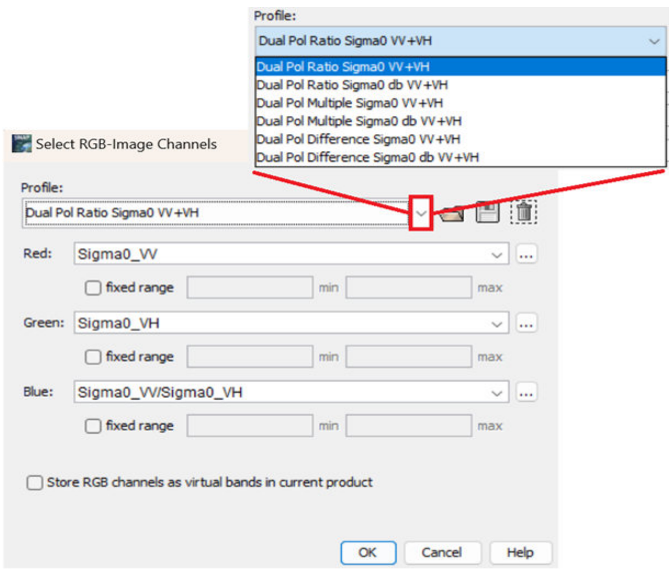

In the pop-up window, you will see that for the Red and Green colours the bands are already selected, but for the Blue one, you select a combination of bands. Press the drop-down arrow near the **Profile** section and select one of the options suggested. Preferably, select the bands converted to decibels (dB).

Play around with different combinations to determine which one visualises the ice cover features best.

Figure V-12. *Examples of these false colour combinations.*

Ice floe or open water area estimation

Computation of ice floe (Figure V-13, Figure V-14) or open water areas in the ice cover is possible using SNAP software. By drawing a polygon around your region of interest (ice or open water gap in it) you can calculate its corresponding real-world area. This feature is particularly useful for monitoring ice dynamics over time.

For computing the region of interest's (ROI) area, select the **Polygon drawing tool** and by left clicking go around the edges of ROI, and finish the polygon by double-clicking the left mouse button. After finishing drawing your polygon, in the upper menu bar select: **Raster > Mask > Mask area.** In the pop-up window see a line **Mask area**, which indicates the total area of your polygon.

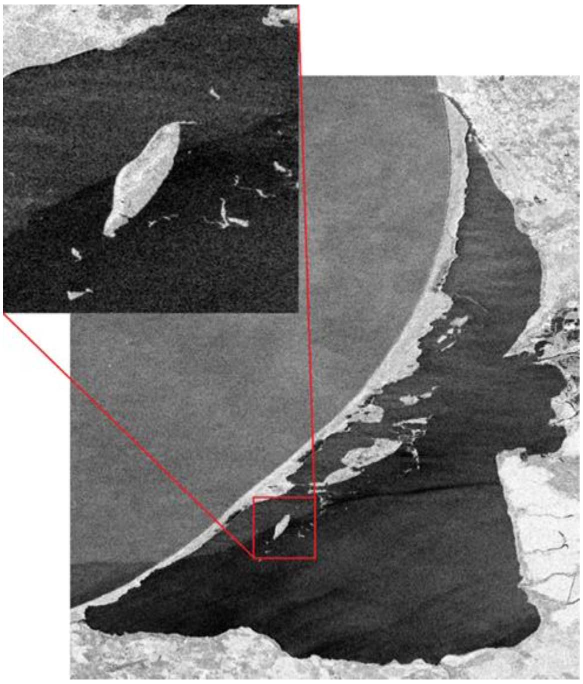

Figure V-13. *Ice floe.*

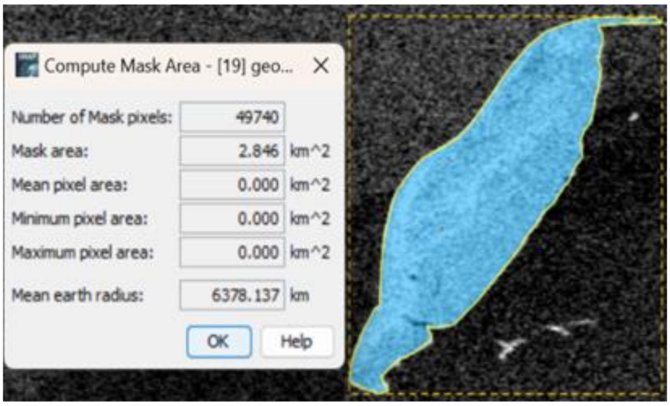

***Figure V-14**. Ice floe area estimation.*

Polygon mapping tool – can be found in the toolbar at the top of the SNAP window.

The same procedure can be applied when measuring the open water area in the ice cover (Figure V-15):

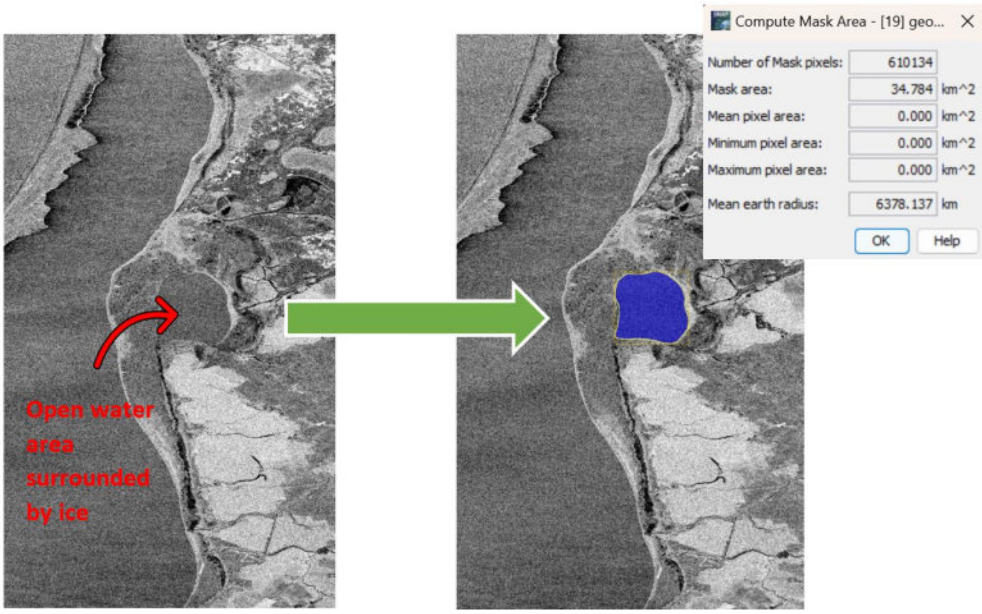

***Figure V-15**. Computation of open water area.*

Masking unwanted areas: Masking in satellite images is used to selectively filter out specific areas or features of the image, leaving only the regions of interest for further analysis or visualisation. It is a valuable technique in radar image analysis as it enables more focused and accurate interpretations of the data, contributing to improved insights of the area.

In SNAP you can automatically apply a land or sea mask, i.e., remove all the land or water parts of the image. To achieve this, select: **Raster > Mask > Land/Sea Mask.** Since we are interested in water or ice surface, in the pop-up window under the **Processing parameters** tab, select an option to mask out the land of your image and press **Run**. As you see below (Figure V-16), ice floes in the resulting image appear much brighter. This is due to the fact that we eliminated a lot of land pixels, which had high backscatter values. Now the grey colour scale represents a different range of pixel values.

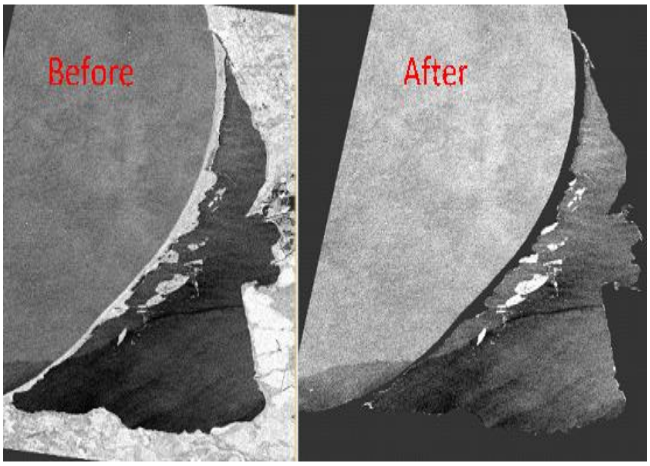

Figure V-16. *Application of masks.*

To further improve the colouring of the image, we can remove the open water area next to our study focus. On the left of this example, there is a sea (light grey colour) where ice cover usually does not form, thus it's mostly open water.

We can remove it from the image by drawing a polygon around it (using the **Polygon drawing tool**) and in the upper menu bar selecting the same **Land/Sea Mask** option as we did when masking the land area, however in the pop-up window under the **Processing parameters** tab, select the **Use Vector as Mask** option and check the box near **Invert Vector** (Figure V-17).

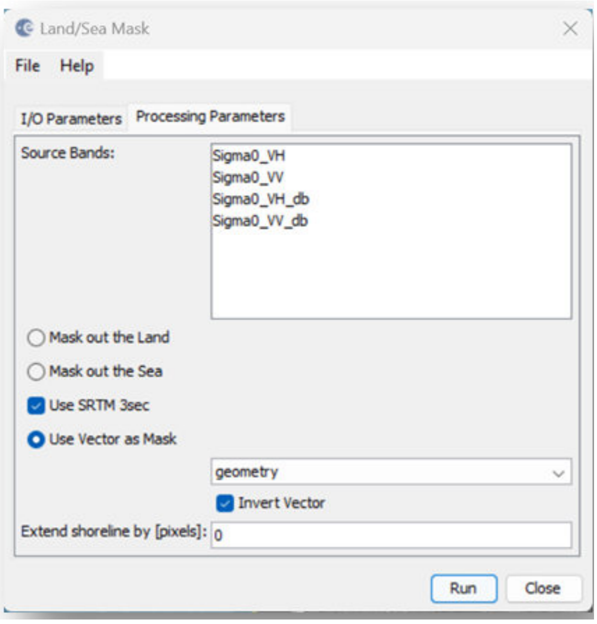

Figure V-17. *Masking land area.*

If we would not mark the inversion, then the resulting image would only show the sea area (Figure V-18).

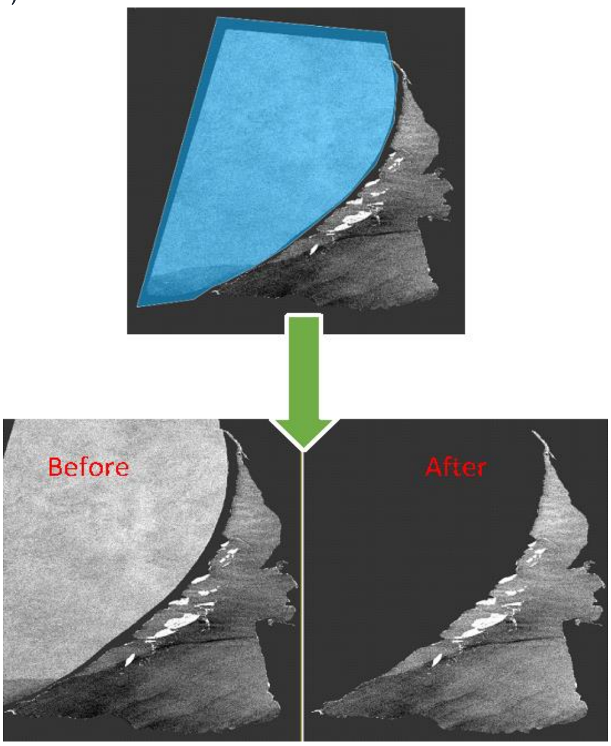

Figure V-18. Example of mask applications.

Texture Analysis: Texture analysis (Figure V-19) focuses on quantifying spatial variations in pixel intensity values within the satellite image. For ice cover identification, texture analysis can highlight different ice types and conditions based on their surface roughness and structure. Common texture analysis methods include the **Grey Level Co-occurrence Matrix**. This tool can be found in SNAP software, in the upper menu bar selecting **Raster > Image Analysis > Texture analysis > Grey Level Co-occurrence Matrix.**

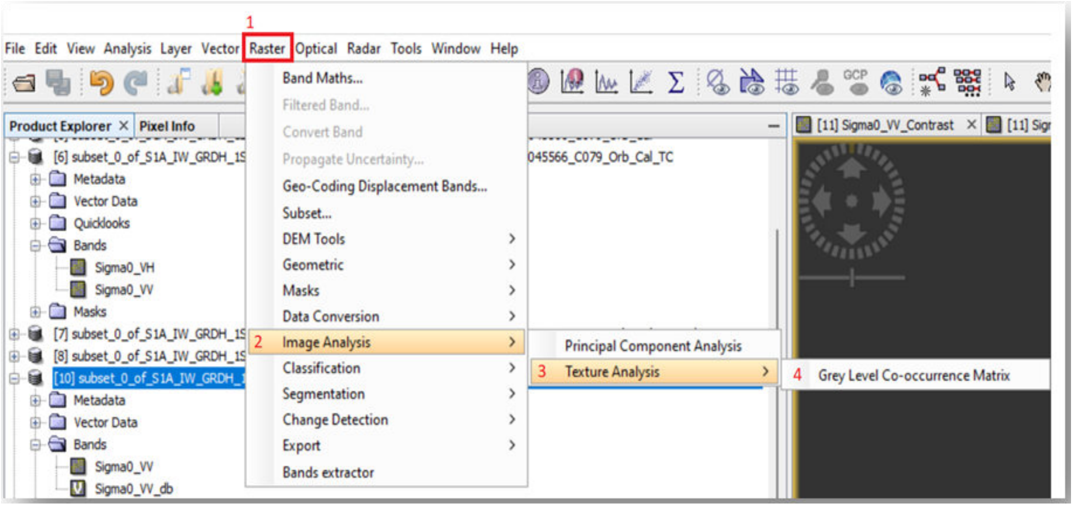

***Figure V-19**. Example of texture analysis.*

The most common texture features obtained from **Grey Level Co-occurrence Matrix** analysis (Figure V-20) include:

Contrast

Higher contrast values indicate greater variations between neighbouring pixel intensities, representing sharper texture boundaries.

Dissimilarity

Higher dissimilarity values indicate a greater dissimilarity or dissimilitude between adjacent pixel values, indicating more noticeable and pronounced differences in texture.

Homogeneity

Higher homogeneity values indicate more uniform textures.

Energy

Higher homogeneity values indicate more uniform textures.

Entropy

Higher homogeneity values indicate more uniform textures.

Correlation

Higher correlation values indicate more linearly related textures.

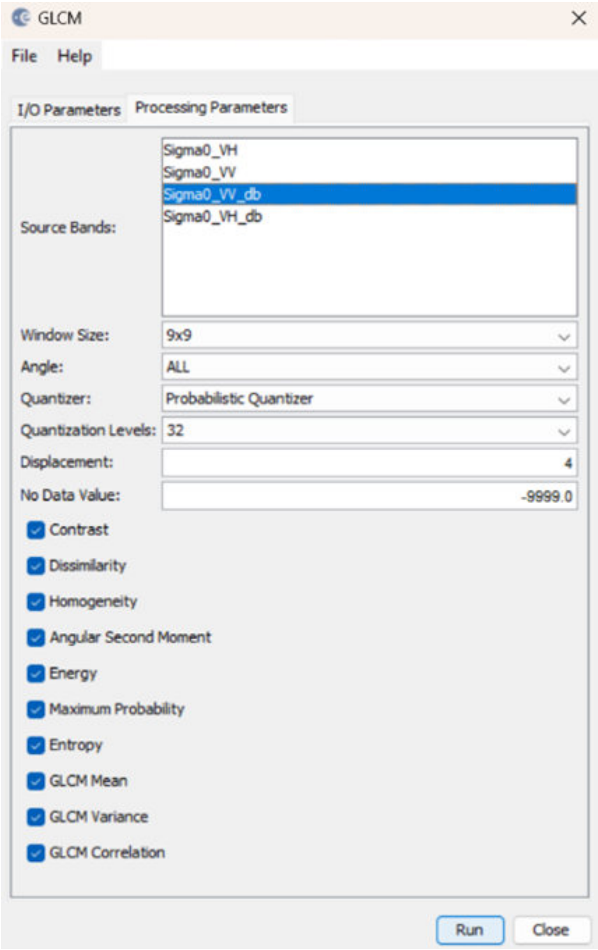

Figure V-20. *Using Grey Level Co-occurrence Matrix.*

The texture features are calculated for each pixel in the image and written into separate bands. The values in these bands represent the texture characteristics of each pixel in the original image.

By investigating the textures of each of the produced layers derived with this tool, you can distinguish different characteristics of the ice surface (Figure V-21).

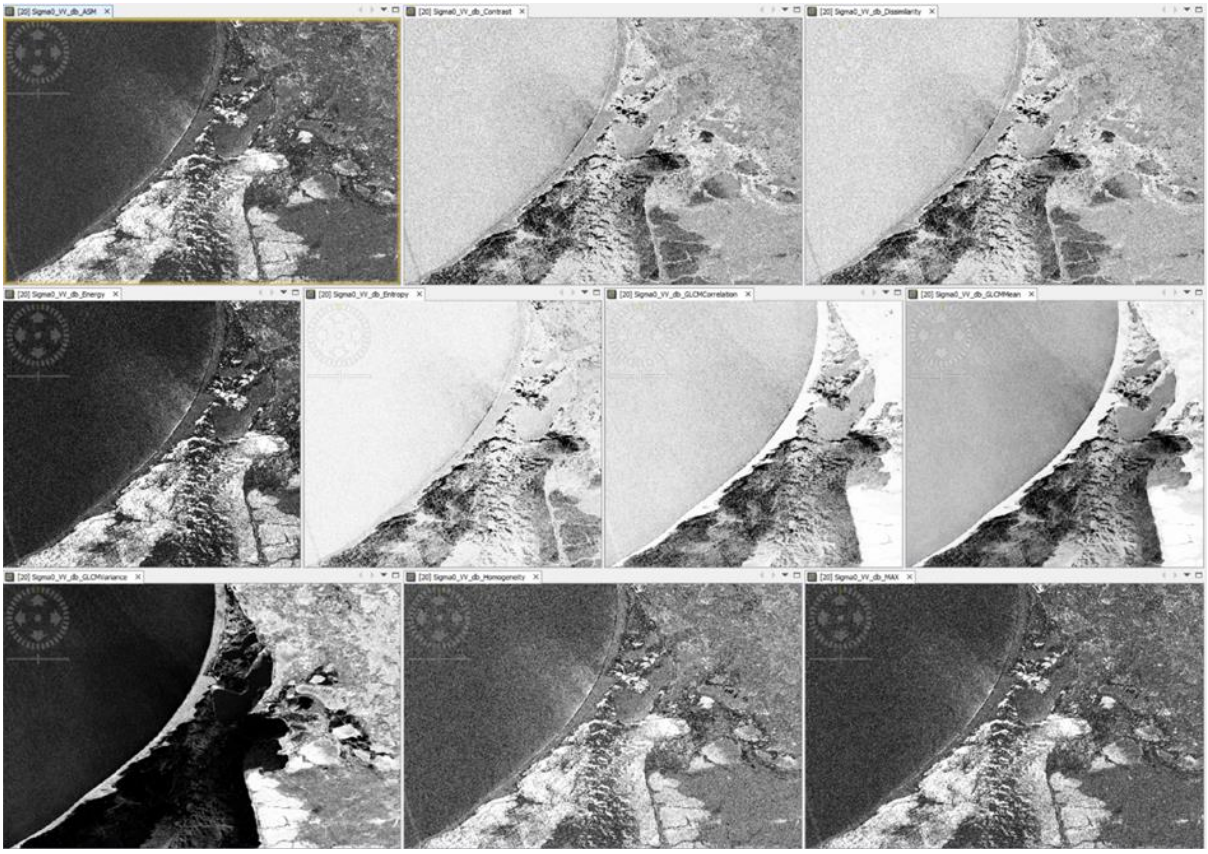

Figure V-21. *Example of different ice characteristics.*

Time series analysis: Time series data is crucial for ice observations from satellite images because it offers a continuous and dynamic record of changes in ice conditions (e.g., extent, distribution, and characteristics) over time. Satellites provide frequent and regular image captures, allowing for the creation of a sequence of images representing the evolution of ice cover over various periods, from days to years.

The high frequency of satellite images simplifies the analysis of ice temporal variability, enabling us to study ice cover dynamics, such as ice drift, fragmentation, and leads (openings in the ice), in detail. By analysing these temporal changes, we can gain valuable insights into the behaviour of ice in response to seasonal and climatic variations. For instance, we can observe the expansion and retreat of ice cover during the annual freeze-up and melt seasons.

Time series data not only allows tracking of these temporal variations (Figure V-22) but also understanding of long-term trends in ice behaviour. By examining changes in ice extent and concentration over several years or decades, we can detect patterns and anomalies that may be related to climate change. Monitoring these trends is vital for assessing the impacts of global warming and climate variability on the ice cover.

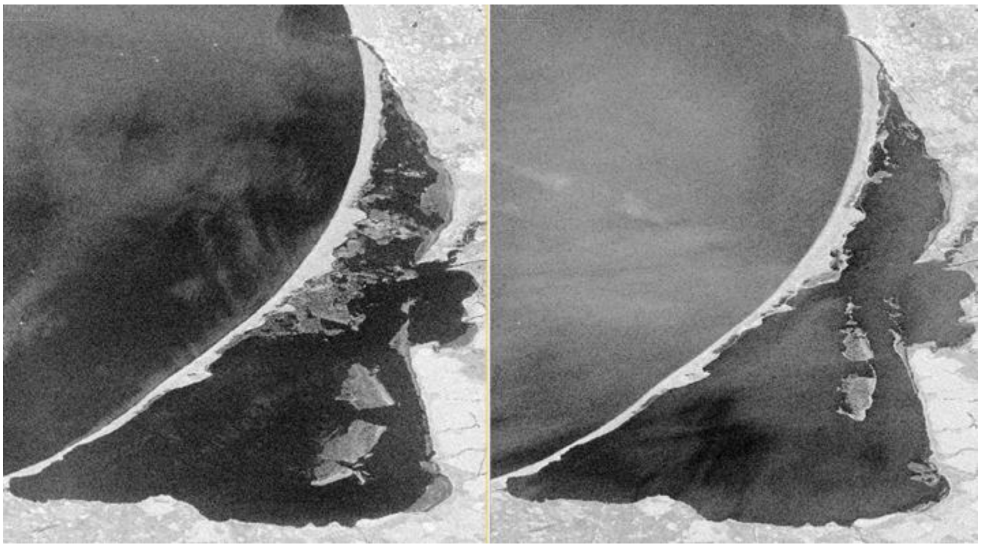

Figure V-22. *Ice floes drifting from the southern part of the lagoon towards the northern.*

Tips & Tricks

Polarization
- if available, utilize SAR images acquired in multiple polarizations. It can help discriminate between different ice types, detect leads and fractures, and provide valuable information about the ice structure and surface.

False Color Composites
- display SAR images in false color composites using different polarization combinations. This can enhance the visibility of specific features, such as open water (dark areas), thin ice (bright areas), and different ice types.

Multi-Temporal Analysis
- analyzing SAR images taken at different times can reveal changes in the ice cover, such as ice breakup, formation, and drift. Time-series analysis allows for monitoring seasonal and interannual variations..

Additional data
- combine SAR data with other remote sensing data to to enhance understanding of ice dynamics.
- look at the field observatoins or even once in a while get to your case study and have a first-hand impression on the ice conditions.
- if possible, use drone scanning of the area.

Visualization Tools
- use image processing and visualization tools to enhance and analyze the SAR images. Techniques like speckle filtering, edge detection, and histogram equalization can improve the interpretation of ice features.

Compare
- if possible, seek out a waterbody close to your study area where ice freezing is unlikely or more challenging. For example, comparing the freezing patterns of an estuary or freshwater lagoon (where ice forms rapidly) with the adjacent sea (where ice formation is more complex, resulting in more extended periods of open water during the ice season).

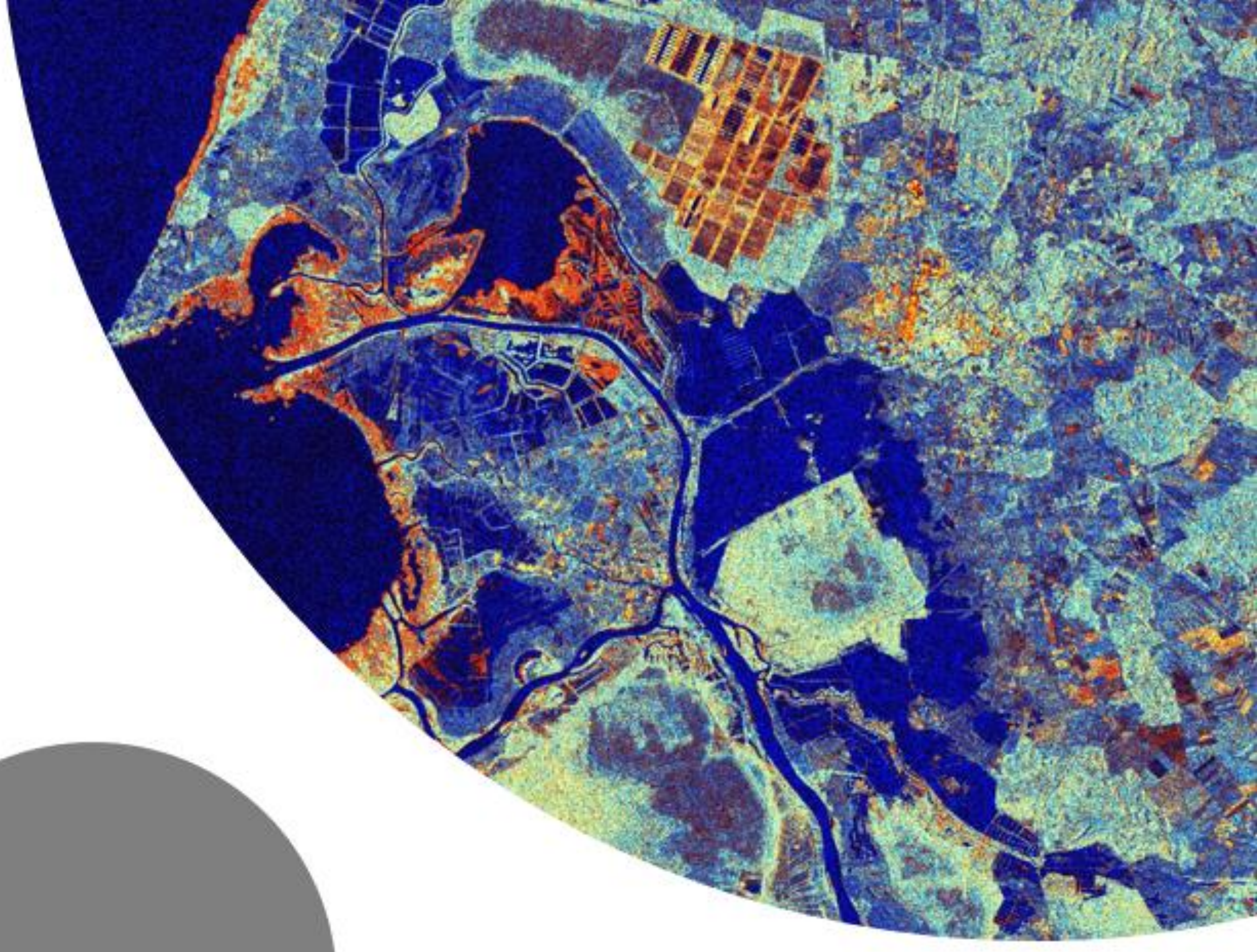

VI. Flood Detection Using Remote Sensing

Jonas Gintauskas

The main tools to detect flood extent are water level measuring stations, satellite data, radars. The floods usually cover vast areas of land and are hardly accessible, which makes monitoring of flood extent difficult or near impossible without remote sensing techniques. In this case study we propose the method to detect flood over large area using ESA's Synthetic Aperture Radar (SAR) Sentinel-1 sensor, which is used widely not only because it allows to monitor large areas but also because it is not influenced by cloud coverage as it penetrates through the atmospheric disturbances and allows to monitor evolution of the flood without disturbances.

Product type: GRDH (Ground Range Detected High Resolution)

Sensor mode: IW (Interferometric Width)

Polarisation: VV+VH

Date and time: 2022-02-27 16:20

Name: S1A_IW_GRDH_1SDV_20220227T162021_20220227T162046_042101_050412_BC83

Supplementary data entitled "mask_land.zip" can be found at: https://github.com/oxodron/Qredo/tree/main/Flood%20Detection

Using these parameters, the image has spatial resolution of 20.3x22.6 m in size and pixel size converted to 10x10 m with every pixel value representing detected magnitude of surface reflectance (Figure VI-1).

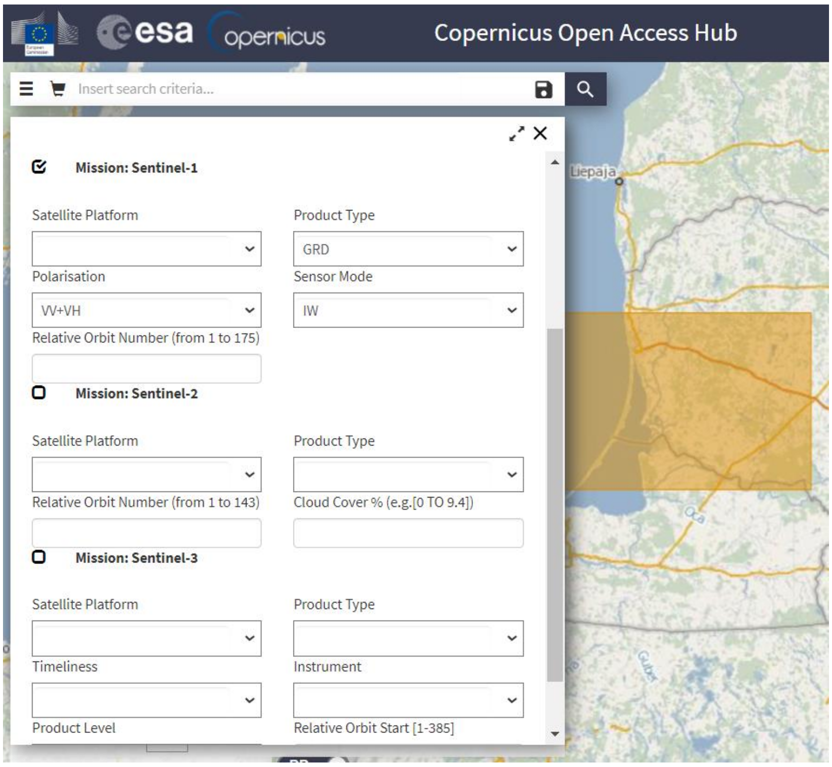

***Figure VI-1**. Parameters for Sentinel-1 download using ESA Copernicus Open Access Hub.*

After downloading SAR file, open Snap. First step is to open product (more details how to do it - in Chapter 0), navigate to the folder where the data is downloaded and open all the downloaded .zip files.

The opened file will appear in **Product Explorer** on the left of your screen if Snap is in default mode, then the file can be expanded and the file could be visualized as VV polarisation, you can find this using this path: **File you added to Product Explorer > Bands > Amplitude_VV** (Figure VI-2).

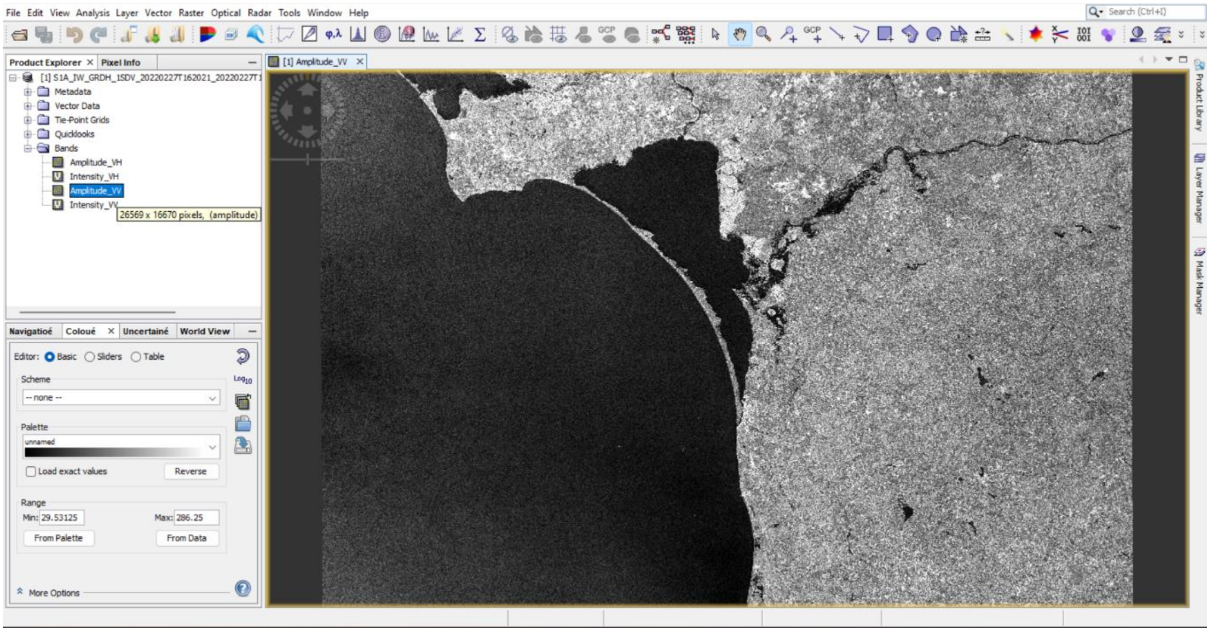

***Figure VI-2**. Example of visualization.*

In this exercise we will perform most common pre-processing steps used for SAR image preparation using **Graph Builder** .

These steps include **Read** > **Subset** > **Apply-Orbit-File** > **ThermalNoiseRemoval** > **Calibration** > **Speckle-Filter** > **Terain-Correction** > **Write.**

When **Graph Builder** is opened, it has only 2 operators: **Read** and **Write**.

The flood, in this case, is only expected in the river delta, so not all the image is needed. As we do not need whole area for analysis, we use **Subset** operator to crop image to the required extent. You have to right-click on the blank space in the **Graph Builder** (it is written: Right click here to add an operator) and go to **Add** > **Raster** > **Subset.**

The next step is to add **Apply-Orbit-File** operator to **Graph Builder**. This step is needed because orbit state vectors, provided in the SAR metadata, are not accurate and, therefore, should be updated. Once again, right-click on the blank space in the **Graph Builder** and go to **Add** > **Radar** > **Apply-Orbit-File.**

The next step is to add **ThermalNoiseRemoval** operator to **Graph Builder**. This step is needed because SAR emits Thermal Noise which hampers with SAR reflectivity estimates. Right-click on the blank space in the **Graph Builder** and go to **Add > Radar > Radiometric > ThermalNoiseRemoval.**

The next step is to add **Calibration** operator to **Graph Builder**. This step is needed because SAR does not include radiometric correction, thus this step is required for the pixel values to truly represent the radar backscatter of reflecting structure. Once again right-click on the blank space in the **Graph Builder** and go to **Add > Radar > Radiometric > Calibration.**

The next step is to add **Speckle-Filter** operator to **Graph Builder**. This step is needed because SAR images has "salt and pepper" effect, called speckles, which is caused by random constructive and destructive interference. To do this right-click on the blank space in the **Graph Builder** and go to **Add > Radar > Speckle Filtering > Speckle-Filter.**

The last operator to add to **Graph Builder** is **Terrain-Correction** operator. As you can see in main canvas, SAR image is upside down, it means that the image is still in radar geometry, and further some pixels can be distorted due to satellite tilt and topographical variations on the ground. Right-click on the blank space in the **Graph Builder** and go to **Add > Radar > Geometric > Terrain Correction > Terrain-Correction.**

This step requires to connect all the operators together if they appear in the **Graph Builder** canvas, in order as presented by the steps above. You can right-click on any of the operator and select **Connect Graph,** otherwise, this step can be done manually by dragging arrow, which appears next to operator box. Then you glide over it and drag to another operator (Figure VI-3).

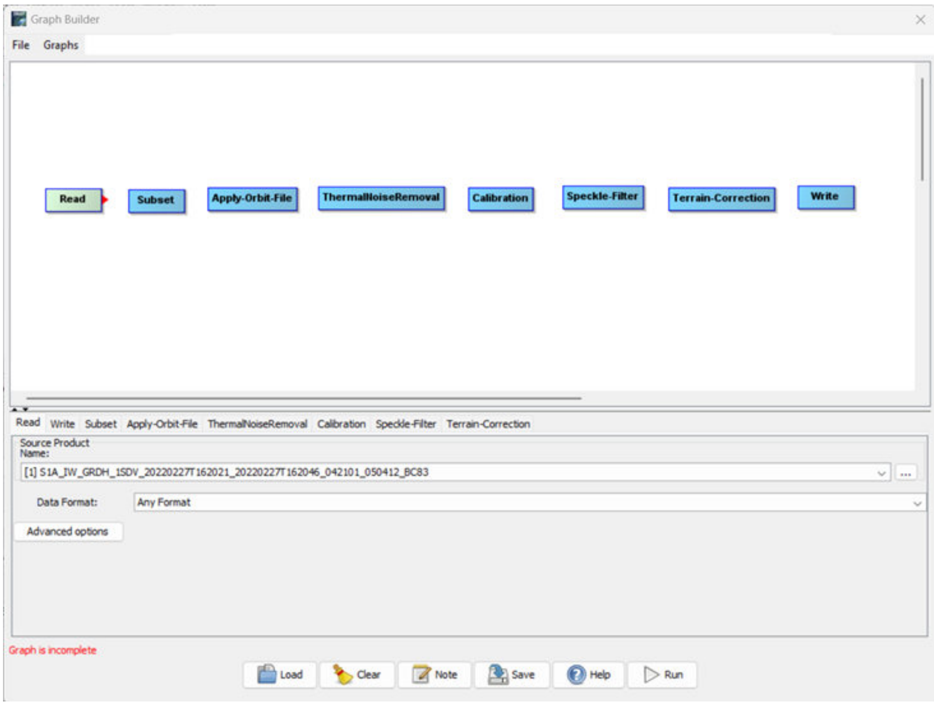

Figure VI-3. *Example of using Graph Builder.*

After we prepared Graph, we still need to set parameters for pre-processing. All of this can be done using **Graph Builder**.

NOTE: **Graph Builder** does not always work and might give the following error: Error: [NodeId: ThermalNoiseRemoval] java.lang.NullPointerException., if it is the case, then all of the steps must be produced manually and separately, one by one which can be done using all the same directories (except of **Read** and **Write**) in the **Menu Bar:**

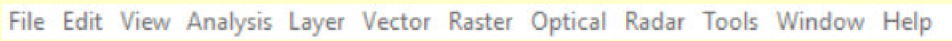

First, make sure that in **Read** operator the right Source Product is chosen. After that select **Subset** operator and tick these boxes: Copy Metadata and choose Subset image to Geographic Coordinates and you fill the box under the map with your desired coordinates and click Update (if you will use **Subset** in **Menu Bar** you have to fill following coordinates in **Geo coordinates** tab).

North latitude bound: 55.6

West longitude bound: 21.1

South latitude bound: 54.9

East longitude bound: 22.3

POLYGON ((21.1 54.9, 22.3 54.9, 22.3 55.6, 21.1 55.6, 21.1 54.9))

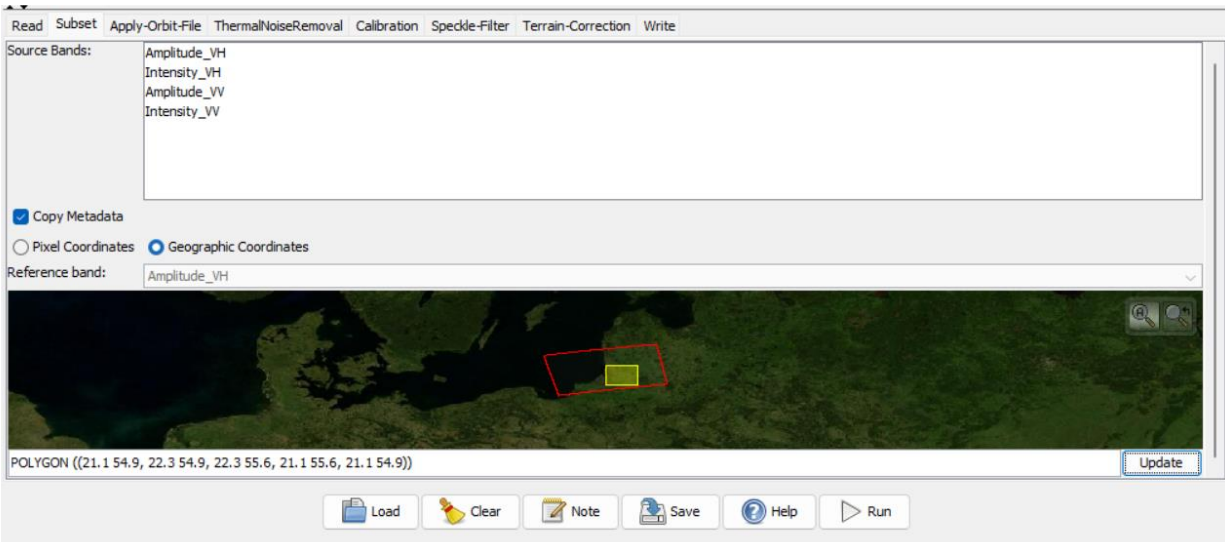

Figure VI-4. *Processing steps.*

In the **Apply-Orbit-File operator** (Figure VI-5) keep the default settings:

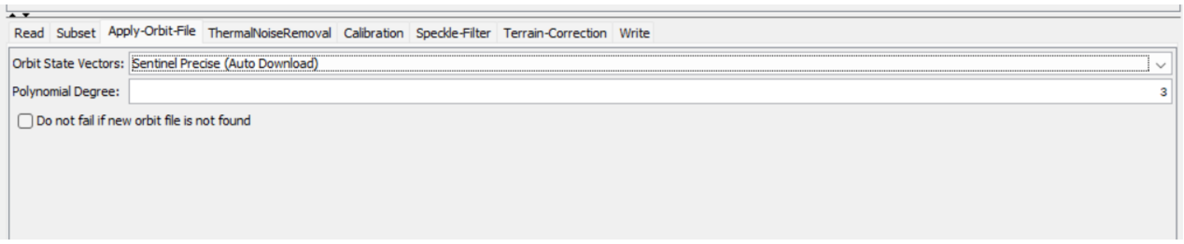

***Figure VI-5**. Processing steps.*

In **ThermalNoiseRemoval** operator we make sure that *Remove Thermal Noise* box is ticked (it should be ticked by default) (Figure VI-6):

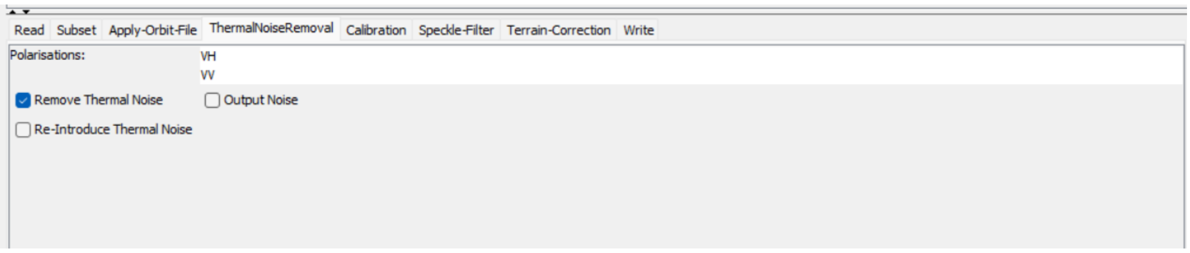

***Figure VI-6.** Processing steps.*

In the **Calibration** operator we leave default settings (Figure VI-7):

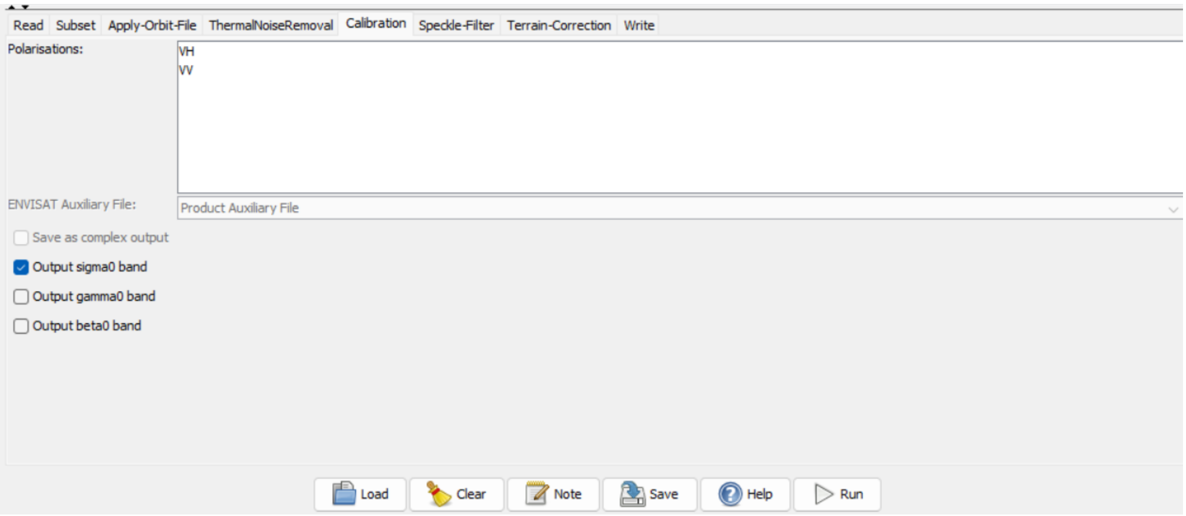

***Figure VI-7.** Processing steps.*

In the **Speckle-Filter** operator we use following parameters:

Filter: *Lee Sigma*

Window Size: *7x7*

Sigma: *0.9*

Target Window Size: *3x3*

For the Terrain-Correction operator we keep the default *Map Projection* set as WGS84(DD). We will use SRTM 3Sec **Digital Elevation Model**. In this exercise we will untick the box **Mask out areas without elevation** (note: this could be used if there are no available permanent water body mask) as we have more accurate .shp file for excluding permanent water bodies "mask_land.shp", which we will use in the GIS part of this exercise (Figure VI-8).

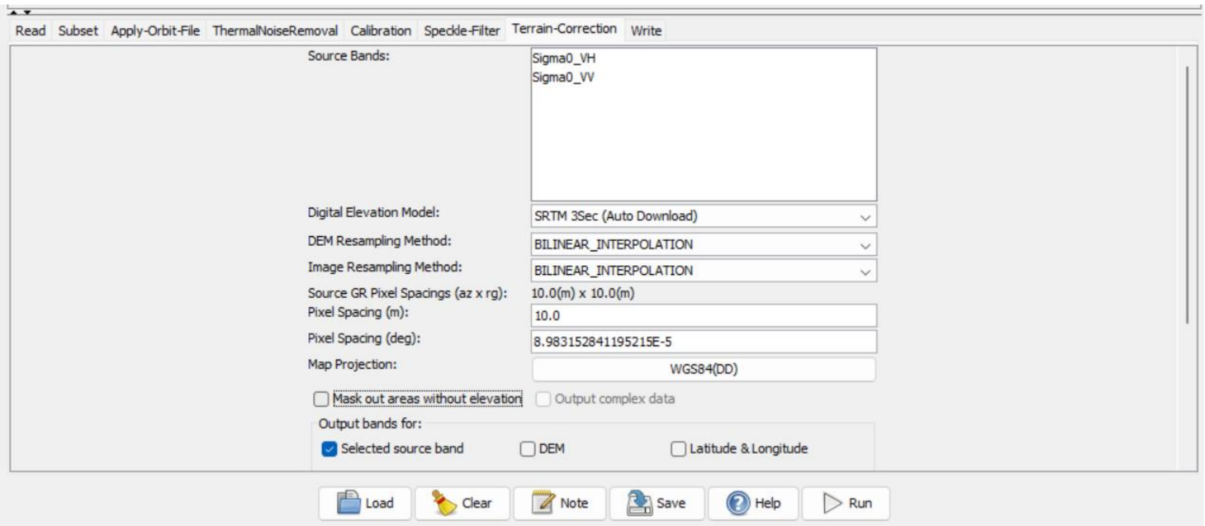

***Figure VI-8**. Processing steps.*

In the **Write** operator we choose the Name of SAR product which will be saved and **Save as**: BEAM-DIMAP and choose a Directory to Save to.

After all these parameters are ready, one can click **Run** (depending on the computer, it can take 1 to 5 minutes to process).

The pre-processed file will appear in **Product Explorer** on the left of your screen if Snap is in default mode, then the file can be expanded and visualized as VV polarisation. One can find this using this path: **"File you produced" in Product Explorer > Bands > Sigma0_VV.**

The water surface and land surface have different characteristics of surface roughness and those characteristics are quite recognisable using SAR imagery.

After preparing the image for work we will choose the best threshold for separating water from land surface. This approach to map floods is called histogram thresholding. First, we look into **Colour Manipulation** tab and **Switch** the view of image **to logarithmic display** (Figure VI-9).

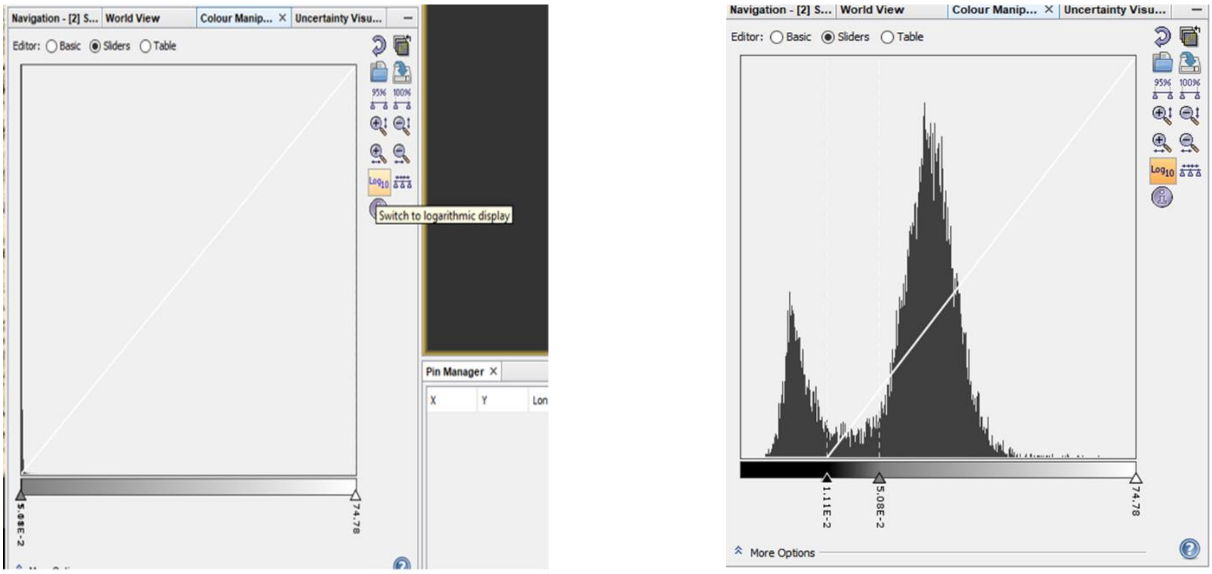

***Figure VI-9**. Colour manipulation steps.*

Water surface has a low signal return compared to land surface due to specular backscattering characteristics. Determination of the appropriate threshold will have the most influence for the end result. In the Figure VI-9 histogram (on the left bottom of the screen, if it is default view), we first switch to logarithmic display to see more comprehensible view. Two peaks can be seen: the first one is water surface (as mentioned above, water has lower signal return), the second one is land surface (which has higher signal return). In this case, the land surface seems to start from the values of 1.1E-2 which is equal to 0.01 (the value can be determined using sliders on the bottom of grayscale).

In the next step we will use the threshold established using histogram to separate water from land surfaces in SAR image. For this step once again open **Model Builder** and click on the blank space in the **Graph Builder,** then right-click to **Add** > **Raster** > **BandMaths**. We should produce a short Graph, which consists of the following operators: **Read** > **BandMaths** > **Write** (Figure VI-10).

***Figure VI-10**. Example of building a graph.*

This step requires to connect all the operators together if they appear in the **Graph Builder** canvas in order as presented by the steps above, as was explained before.

In the **Read** operator, make sure you have chosen the newly produced product. It should be marked as **[2]** product before the name. In this case, we will leave default name of *Target Band* but one can choose any other, which fits better for the research purposes (Figure VI-11). The **Band maths expression** is the following:

if Sigma0_VV < 0.01 and Sigma0_VV > 0 then 1 else 0.

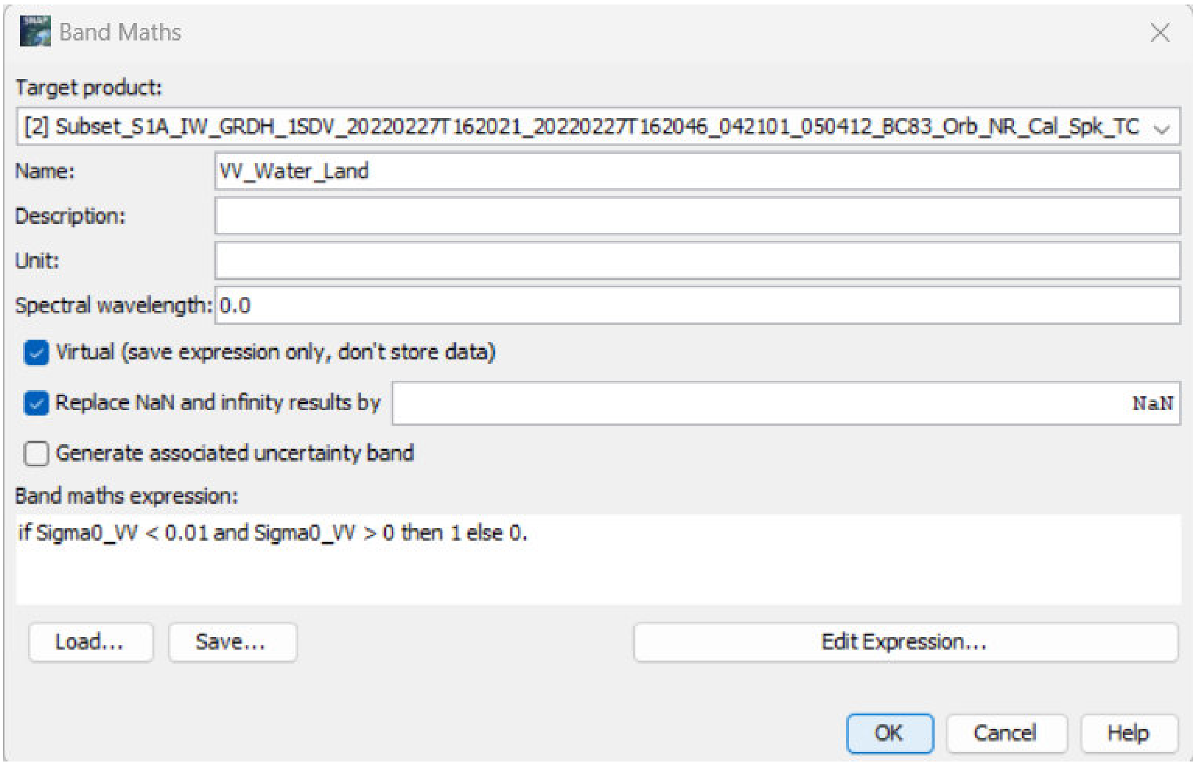

Figure VI-11. *Example of Band Maths.*

This expression will produce the binary layer where pixels with value of 1 represent water surface, and pixels with value of 0 represent land surface. This layer should appear on canvas.

Now, open **Write** operator, choose the **Name** of a file (in our case we will leave it as default, choose directory. And most importantly, **Save as: GeoTIFF** (Figure VI-12).

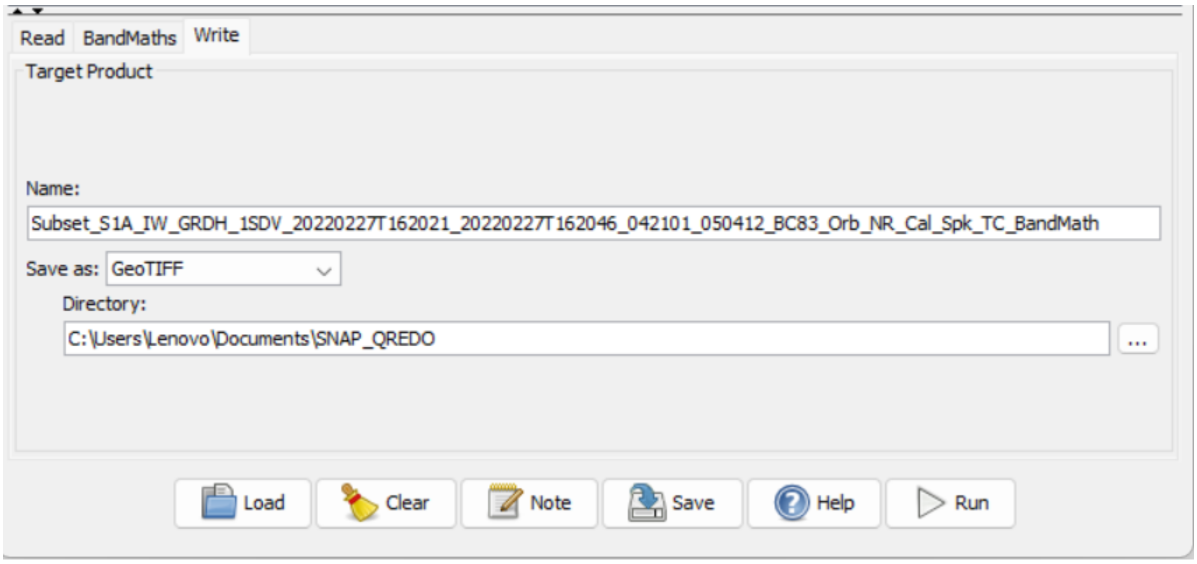

Figure VI-12*. Processing steps.*

After everything is ready, click Run and it will produce a binary GeoTIFF layer, which can be used in GIS.

Now open QGIS and open raster produced using ESA Snap using Menu bar: **Layer > Add Layer > Add Raster Layer…** and add a shapefile which is in the supplementary material **mask_land.shp** using directory **Layer > Add Layer > Add Vector Layer…**

After adding both layers to QGIS, open *Processing Toolbox* and find **Clip Raster With Polygon** tool. Use Raster produced with ESA Snap in the **Input** and mask_land in **Polygons**. Make sure that both layers are in the same projection (written in [] at the end of a layer Name, in this case it is [EPSG:4326]) (Figure VI-13).

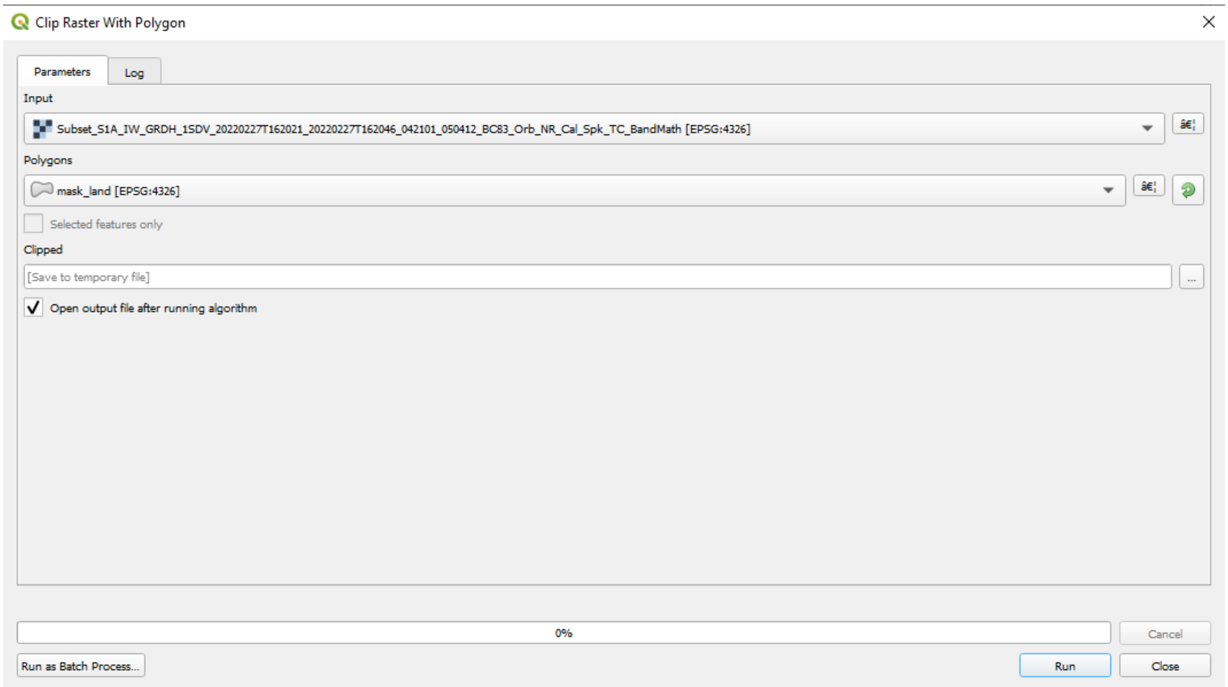

Figure VI-13. Example of clipping raster.

After performing this step, you will get black and white layer with permanent water bodies clipped. To visualize the flood better, we need to change visualization, which can be done by right-clicking on layer, produced using **Clip Raster With Polygon** and clicking on **Properties…** Then click on **Symbology** and change *Render type* to *Paletted/Unique values*, then click on **classify** (Figure VI-14).

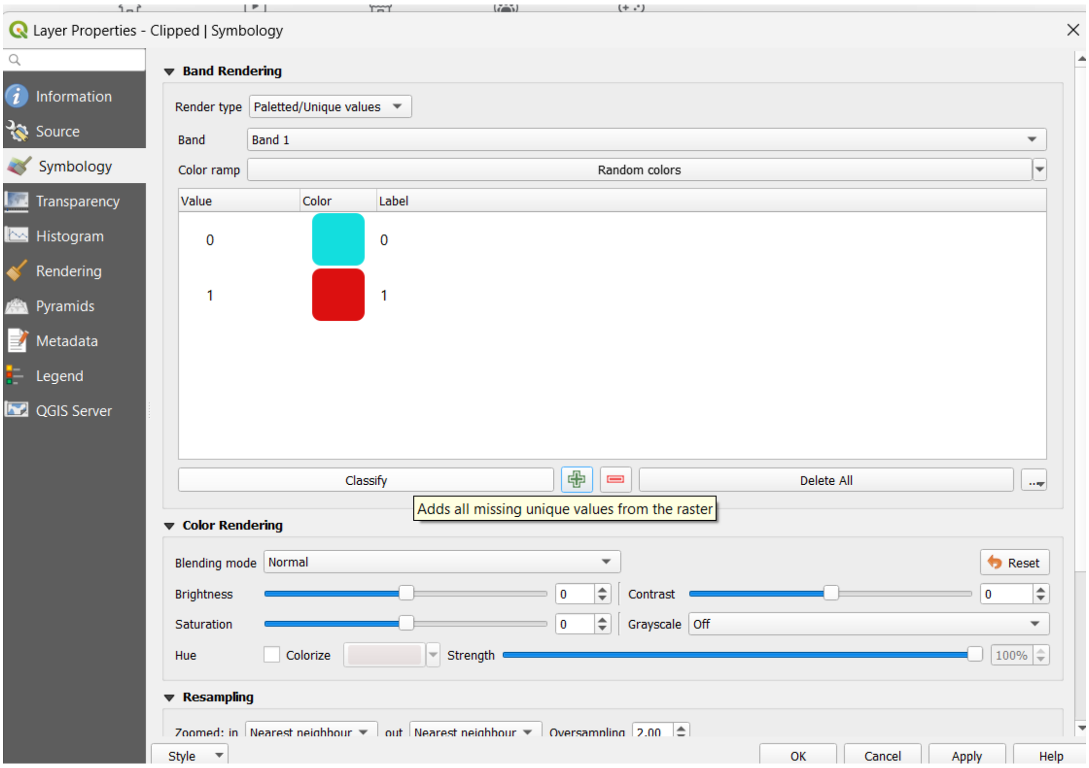

Figure VI-14. *Visualization steps.*

And, before finishing, one can choose more representative colours by clicking on the color itself. Value "0" is land, and "1" is floodwater. After choosing the colours of your liking, click OK and in the end, you will have a map looking like that in the canvas of QGIS (Figure VI-15).

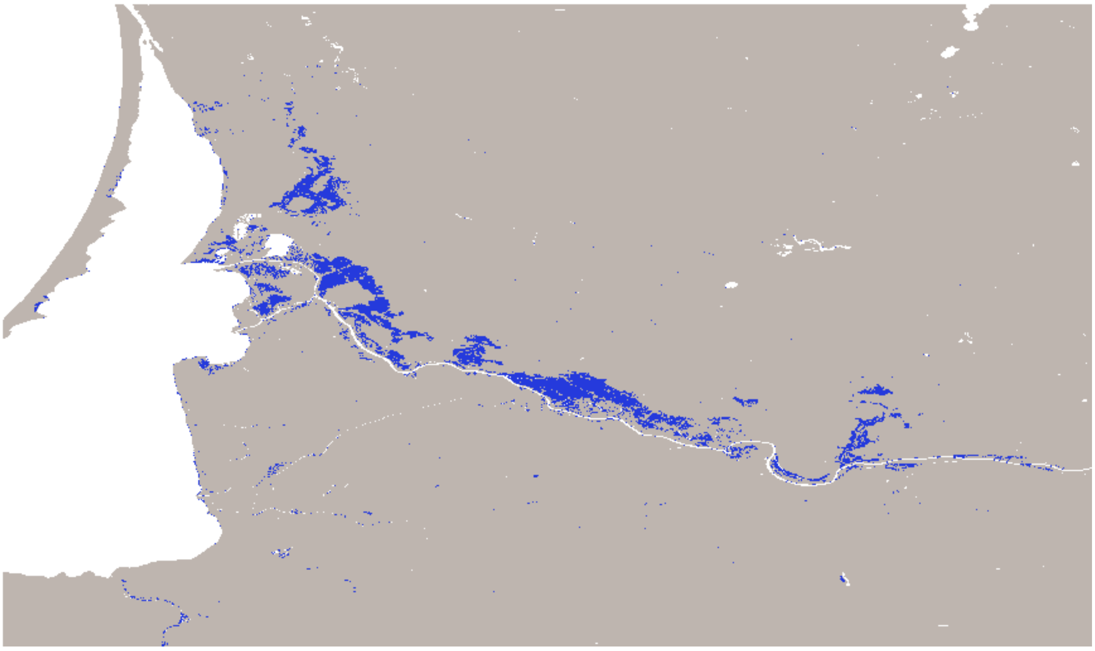

Figure VI-15. *Final flood map.*

VII. Remote Sensing of Chlorophyll-a Concentration Mapping

Diana Vaičiūtė

From satellite observations in the optical part of the spectrum the concentrations of different constituents (pure water, chlorophyll, sediments, coloured dissolved organic matter) can be estimated. Chlorophyll concentration is one of the most important variables as it is an indicator of algal blooms. Phytoplankton blooms occur naturally in areas with high nutrient concentrations (coastal areas – nutrient runoff from land). When phytoplankton cells die, they sink to the seabed where they are decomposed by bacteria requiring oxygen.

Case study: remote sensing of chlorophyll-a: The study area for this exercise will be the Curonian Lagoon (the Baltic Sea). Eutrophication, led by cyanobacteria blooms and hypoxia, have been increasingly observed in the Curonian Lagoon. Monitoring of the chlorophyll concentrations is important to investigate the spatio-temporal changes of algal blooms, determine the water quality and evaluate if the overtaken measures (improvement of wastewater treatment plants) are effective to mitigate the pollution.

Data used: one Sentinel-3A level 1 image acquired on 28 September 2020 (S3A_OL_1_EFR____20200928T094012_20200928T094312_20200929T134412_0179_063_193_1980_LN1_O_NT_002.SEN3). NOTE: the satellite image downloaded from the archive is zipped. Prior the exercise, the satellite image should be unzipped.

Software in use: SNAP and QGIS

Opening and exploring satellite data in SNAP: Open SNAP on the desktop. Click on the **Open product** icon (Figure VII-1) or go to **File > Open Product** and find the satellite image. Navigate to the folders of the extracted product, select **xfdumanifest.xml** file and **Open** to load the product to SNAP:

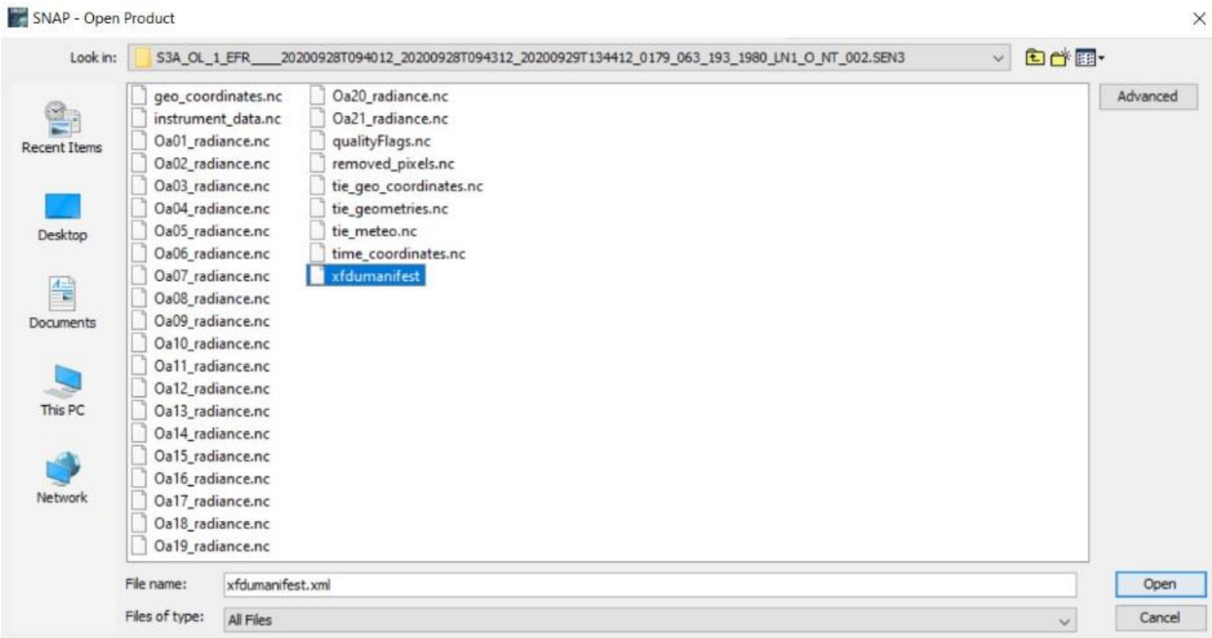

Figure VII-1. *Opening the product.*

The opened products will appear at the Product Explorer tab in the upper left part of the window (Figure VII-2).

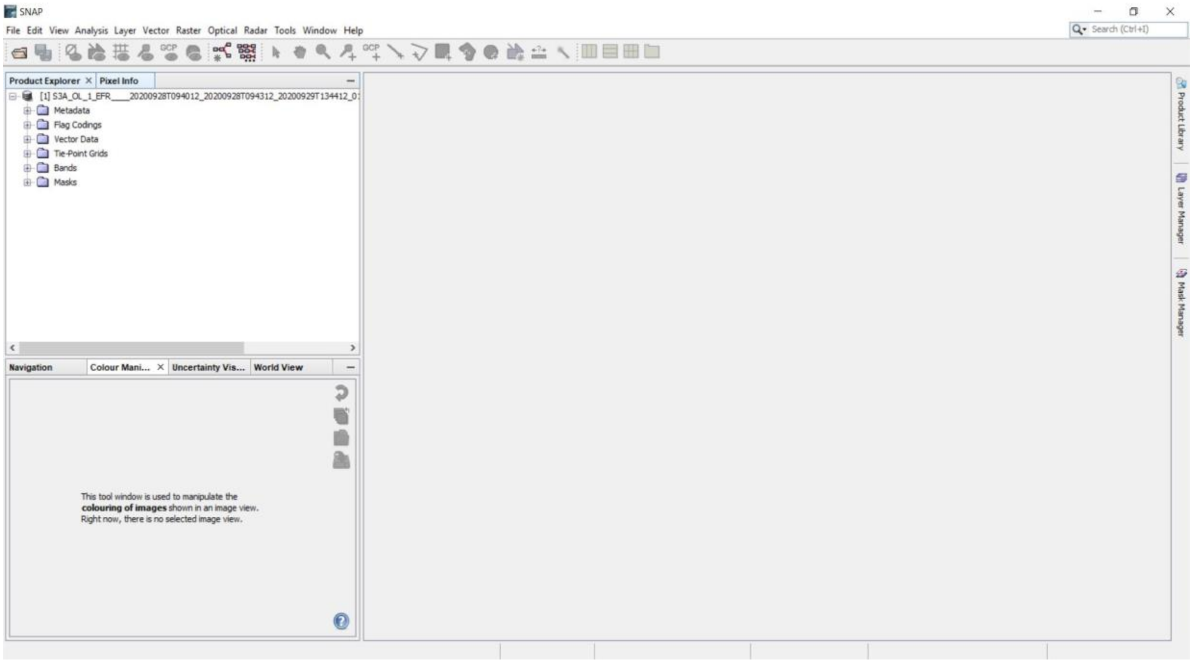

Figure VII-2. Product Explorer view in SNAP.

Right click the Level-1 product name (S3A_OL_1_EFR____20200928T094012_20200928T094312_20200929T134412_0179_063_193_1980_LN1_O_NT_002) and select **Open RGB Image Window** to create and visualize an RGB composition image. In a new window select **Profile > OLCI L1 - Tristimulus** and click **OK** (Figure VII-3).

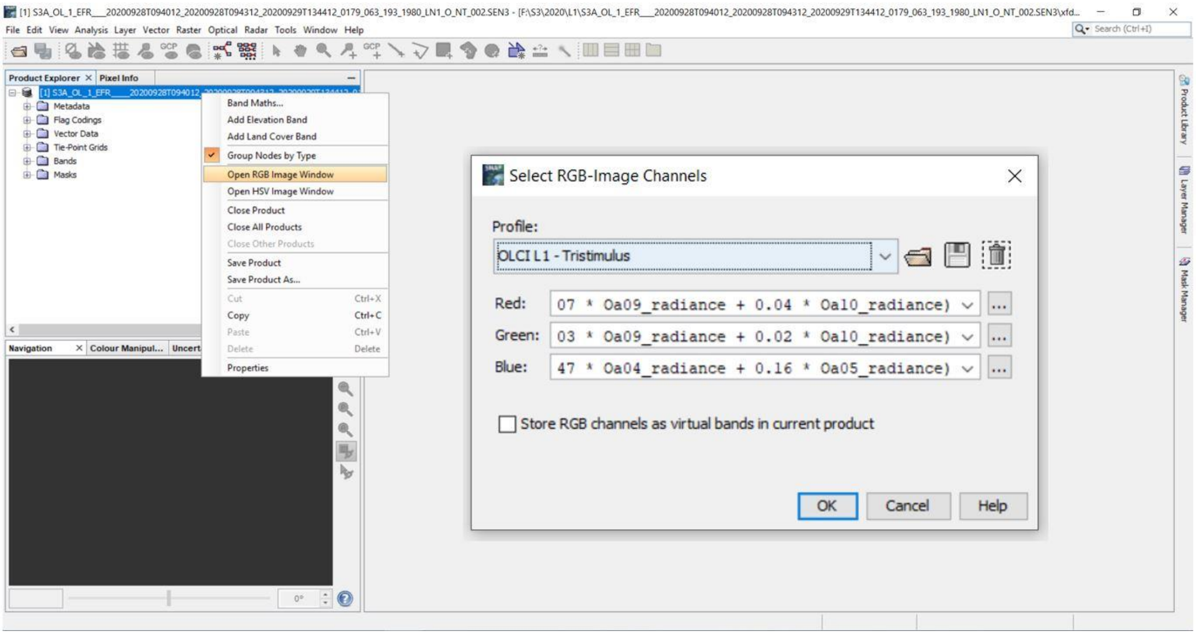

Figure VII-3. Steps of image visualization.

117

The view of the image is very dark and for that reason it should be enhanced. Go to the **Colour Manipulation** tab in the lower left corner of the SNAP window. Here the histogram stretch for each of the RGB component bands can be changed (Figure VII-4 and Figure VII-5).

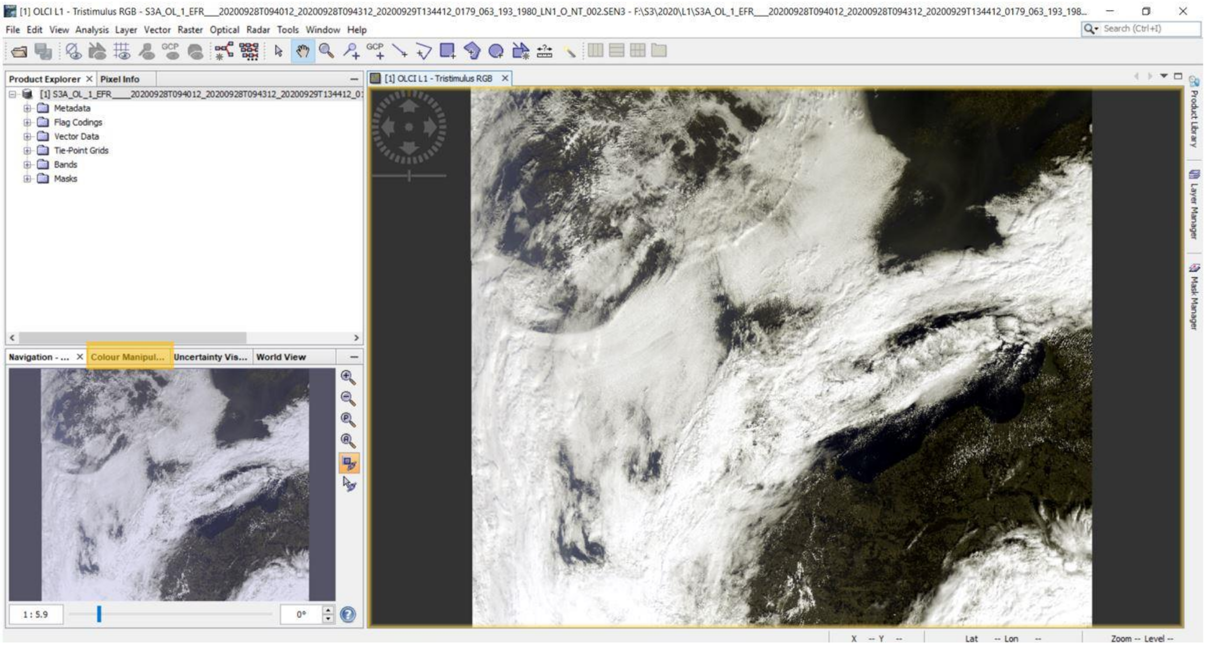

Figure VII-4. *Steps of colour manipulation.*

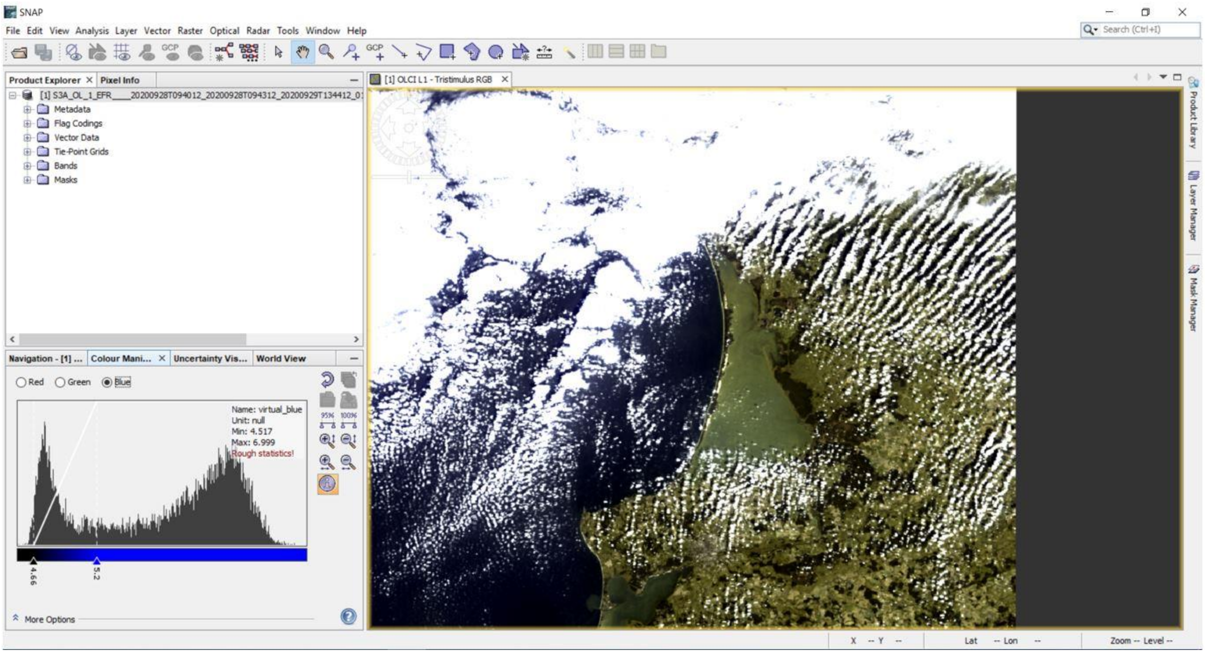

Figure VII-5. *Steps of colour manipulation.*

Satellite data pre-processing in SNAP: Satellite images cover larger areas, contain a lot of information (therefore, their volume can vary from 300 MB to 1.5 GB) than is required for analysis, therefore, before further analysis, the satellite image can be subsetted and only the area that will be needed in further steps can be left. Press the Right mouse button on the satellite image and select **Spatial Subset from View** (Figure VII-6). The subsetting can be performed by selecting the Region of interest or by selecting the Bands (Figure VII-7).

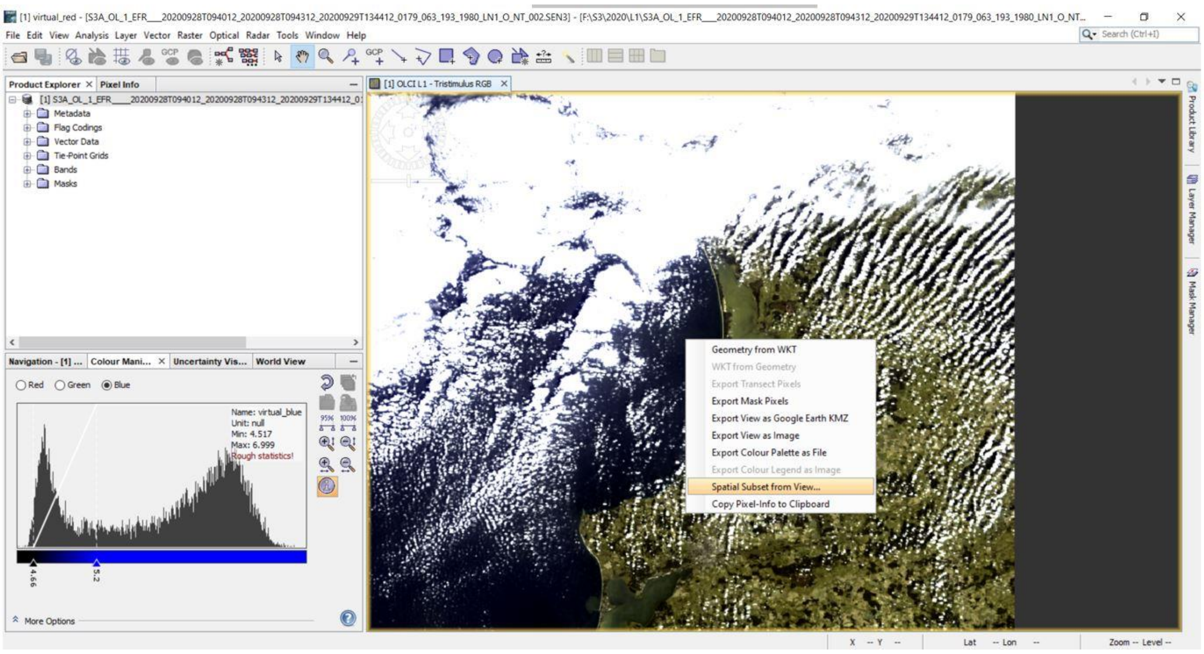

Figure VII-6. *Subsetting the image.*

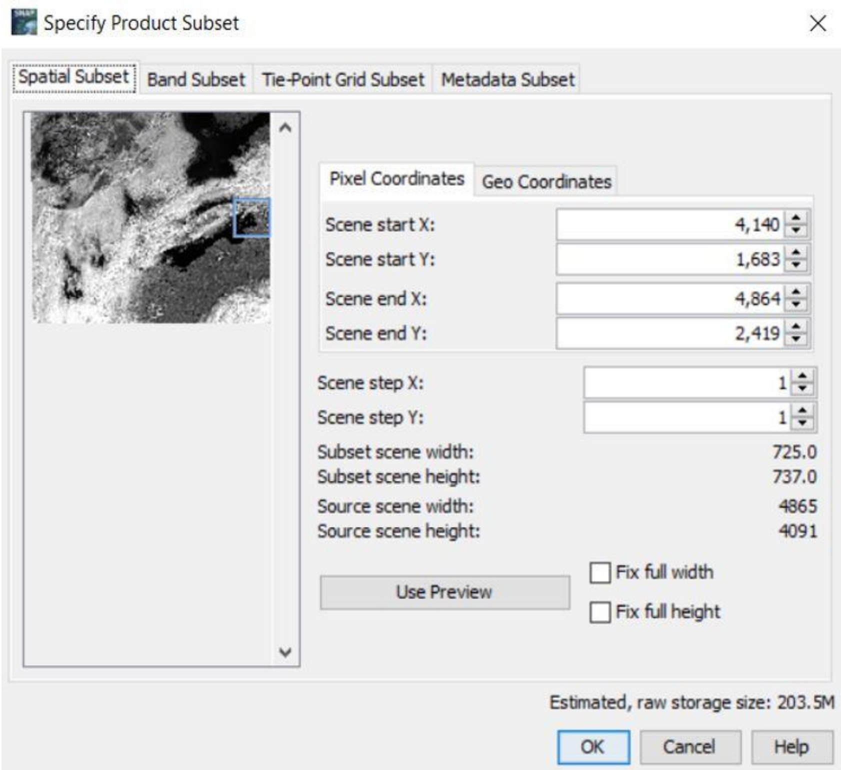

Figure VII-7*. Subsetting the image.*

In the SNAP program a new product will appear that is virtual [2]. The new product can be saved on the computer. Right mouse click on [2] satellite image name, select **Save Product > YES, shorten name to sensor, level of processing and date > Save**, e.g., 20200928T094012_S3A_OL_1_EFR_Kursiu marios.dim. Right-click on this image and select Open **RGB Image Window**. In the new window that appears, select Profile: **OLCI L1 - Tristimulus**. Press **OK**. An RGB photo composite will open in a window. The cropped satellite image according to the selected parameters will appear (Figure VII-8).

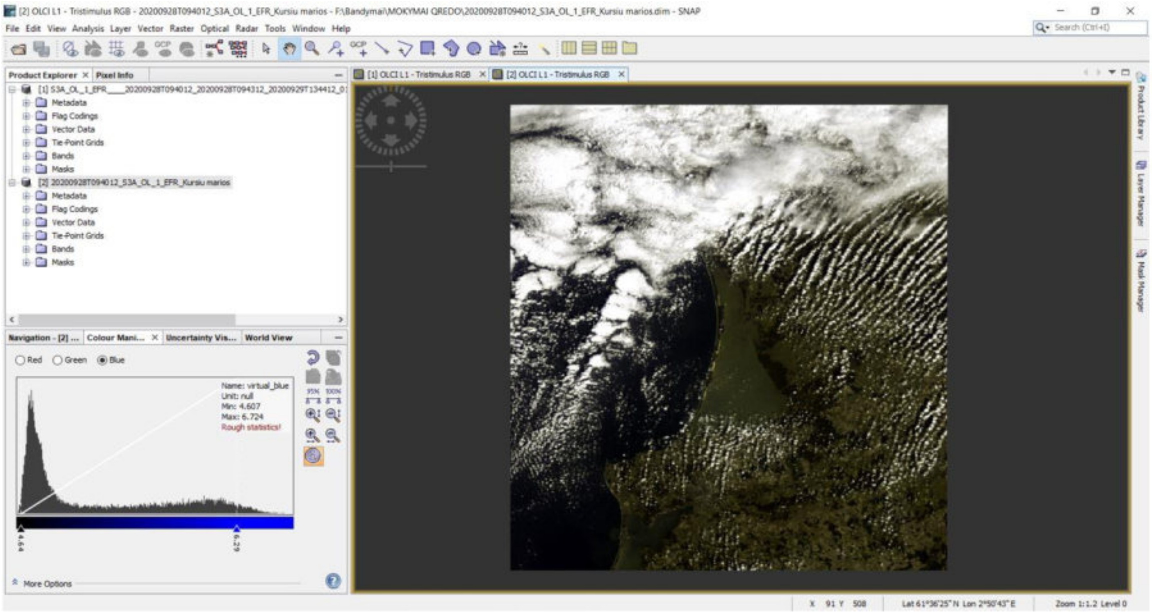

Figure VII-8. *Processing steps.*

Secondly, the projection to the satellite image will be applied, and the spatial resolution will be unified: **Select Raster > Geometric > Reprojection > specify the location on the computer where the new file will be saved > select the coordinate system (WGS 1984, Projection UTM Zone, specify the UTM zone (e.g., 34N), change the spatial resolution to 300x300 m > RUN** (Figure VII-9).

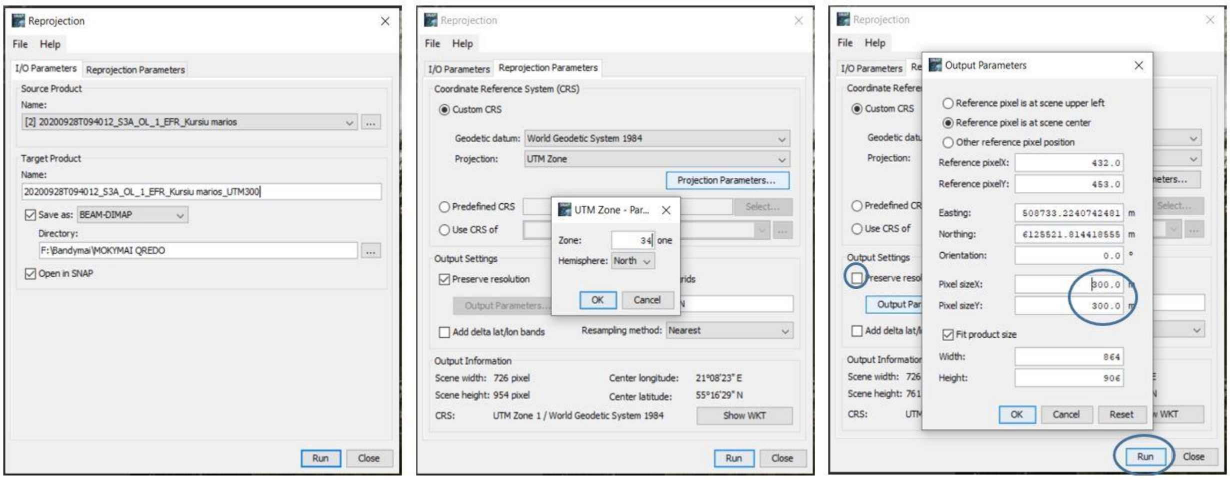

Figure VII-9. *Steps of reprojecting the image.*

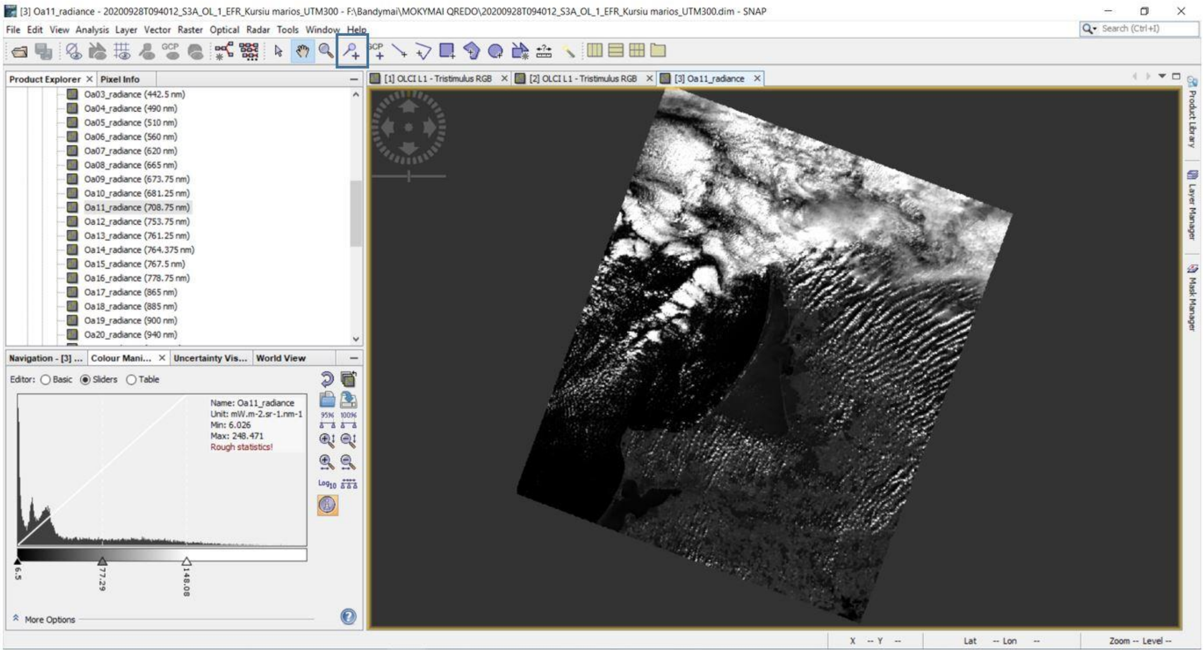

***Figure VII-10**. Example of using Pin placing tool.*

The radiation registered by the optical sensor can be investigated. Select several places in the satellite image, this can be done using the **Pin Placing tool** function (Figure VII-11 and Figure VII-11). The **Pin Manager** can be prompted in the SNAP by navigating to **View** > **Tool Windows** > selecting **Pin Manager**.

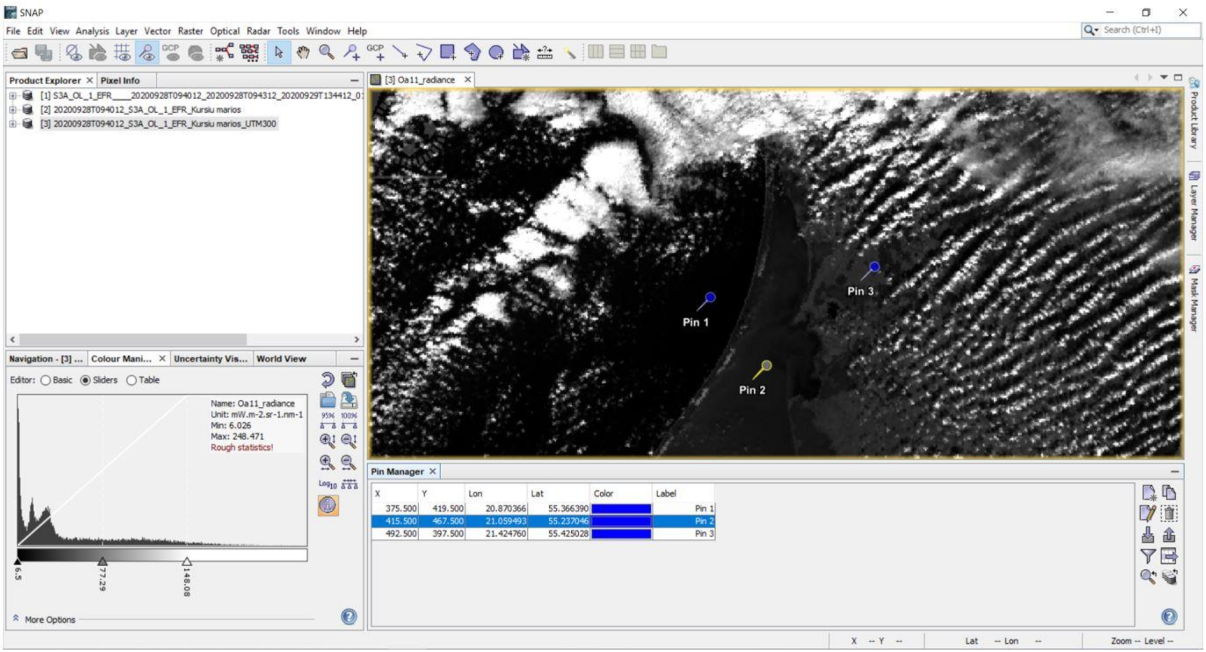

***Figure VII-11**. Example of using Pin placing tool.*

Select **Optical** > **Spectrum View**. This tool allows to visualize the signal registered by the optical sensor in different spectral bands (Figure VII-12).

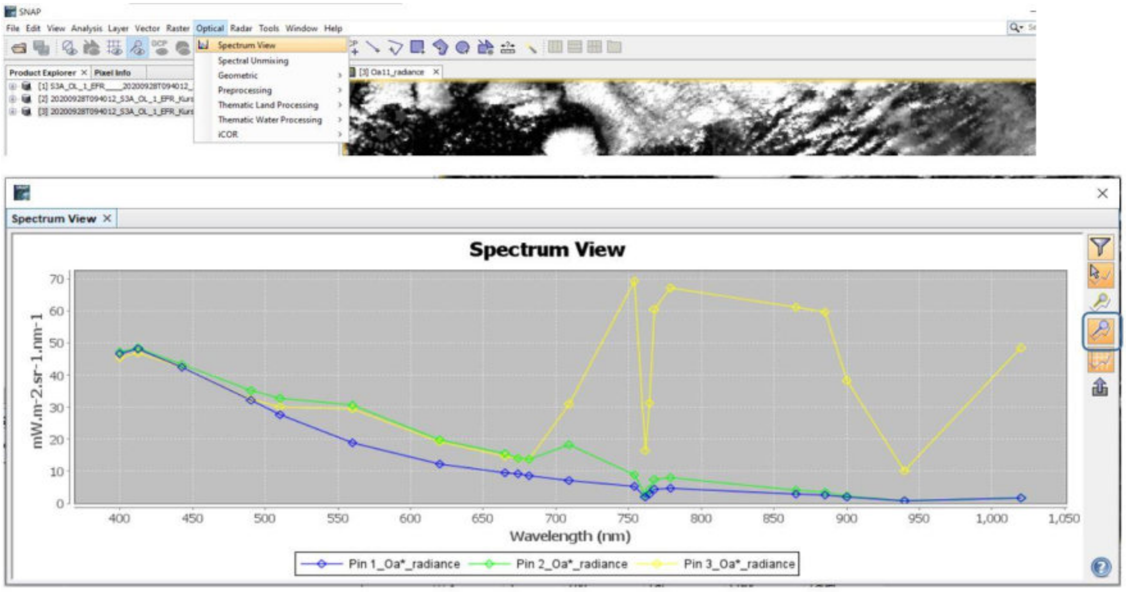

Figure VII-12. *Example of visualizing the signal.*

Satellite image processing in SNAP: The Case 2 Regional Coast Colour processor (C2RCC) had originally been developed by Doerffer and Schiller for the MERIS sensor, and then it was improved through the ESA DUE CoastColour project (Brockmann et al., 2016). It is applicable to all past and current ocean colour sensors (such as Sentinel-3) as well as Sentinel-2. It has been validated in various studies and is available through ESA's Sentinel toolbox SNAP. It is also used in the Sentinel-3 OLCI ground segment processor of ESA for the generation of the Case 2 water products. C2RCC will be used to reproduce the Level-2 Water product that contains chlorophyll-a concentration among other water quality parameters (total suspended matter, coloured dissolved organic matter, transparency etc.).

In the toolbar, select **Optical > Thematic Water Processing > C2CC Processors > OLCI** (Figure VII-13).

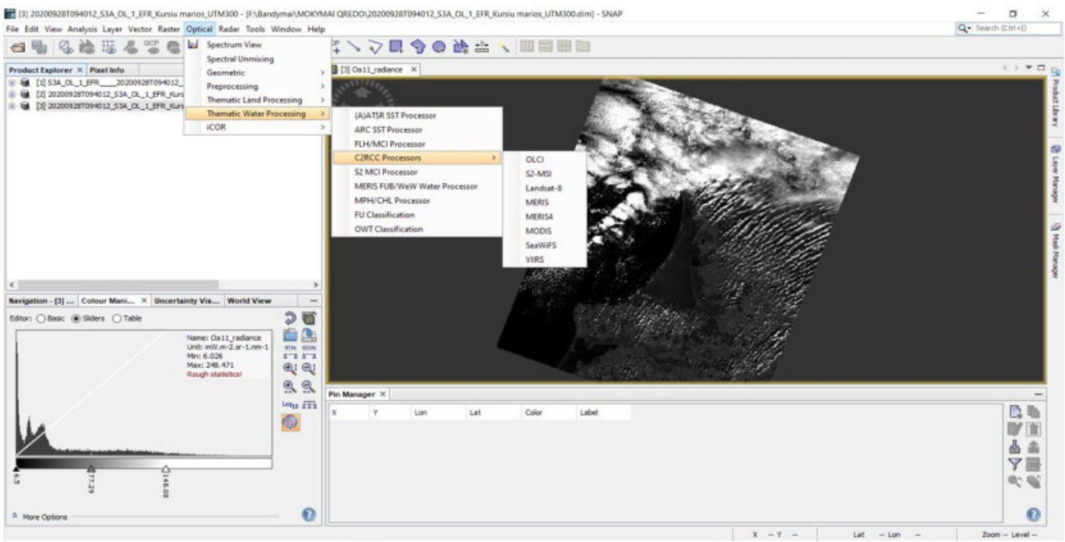

Figure VII-13. *Processing steps.*

The parameters used are listed below (Figure VII-14). For this exercise the default I/O Parameters will be left, the output product name and Folder will be indicated. Majority of Processing Parameters will be left as default. It is suggested to specify water temperature and salinity using in situ data, if exist, or can be adjusted according to common average values of the parameters. In case of the Curonian Lagoon, water salinity on the date of investigation was 2.9 PSU on average, water temperature - 17.0 °C. 'Output AC reflectances as rrs instead of rhow' was selected, as the major parameter of interest for further investigation is Remote Sensing Reflectance. After specifying the parameters, select **RUN**. the processing might take several minutes depending on the size of the satellite image. After the processing is completed, a new product [3] will be automatically opened in SNAP.

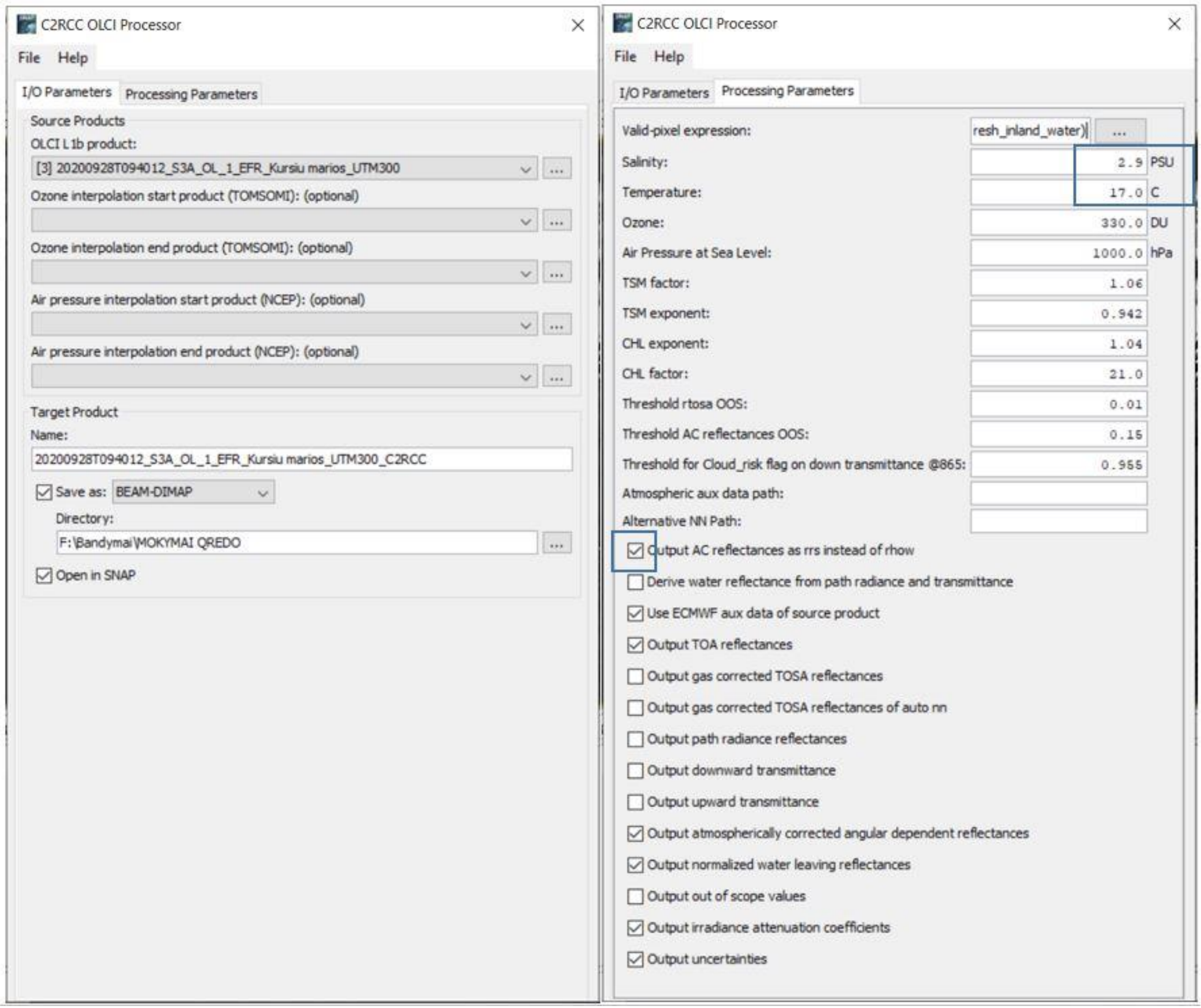

***Figure VII-14**. Processing steps.*

The layer containing chlorophyll-a concentration can be visualised:

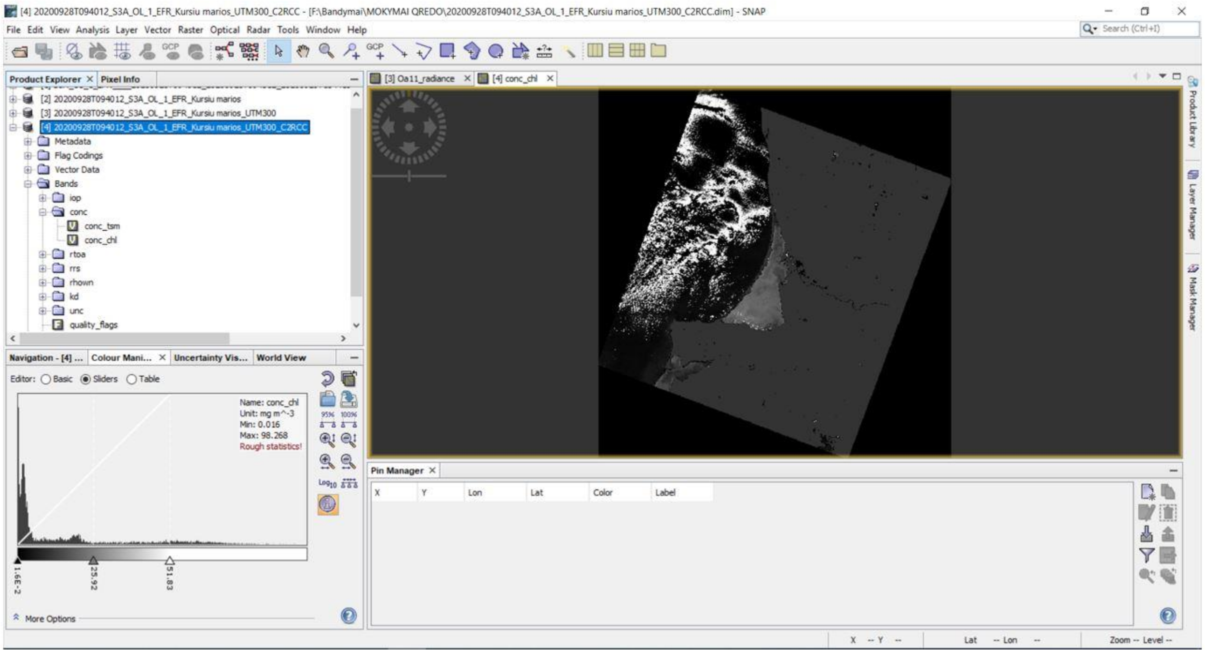

Figure VII-15*. Visualization of Chl-a layer.*

The colour palette can be applied to the visualised layer: **Colour Manipulator > Import colour palette from text file > cc_chl.cpd > NO**

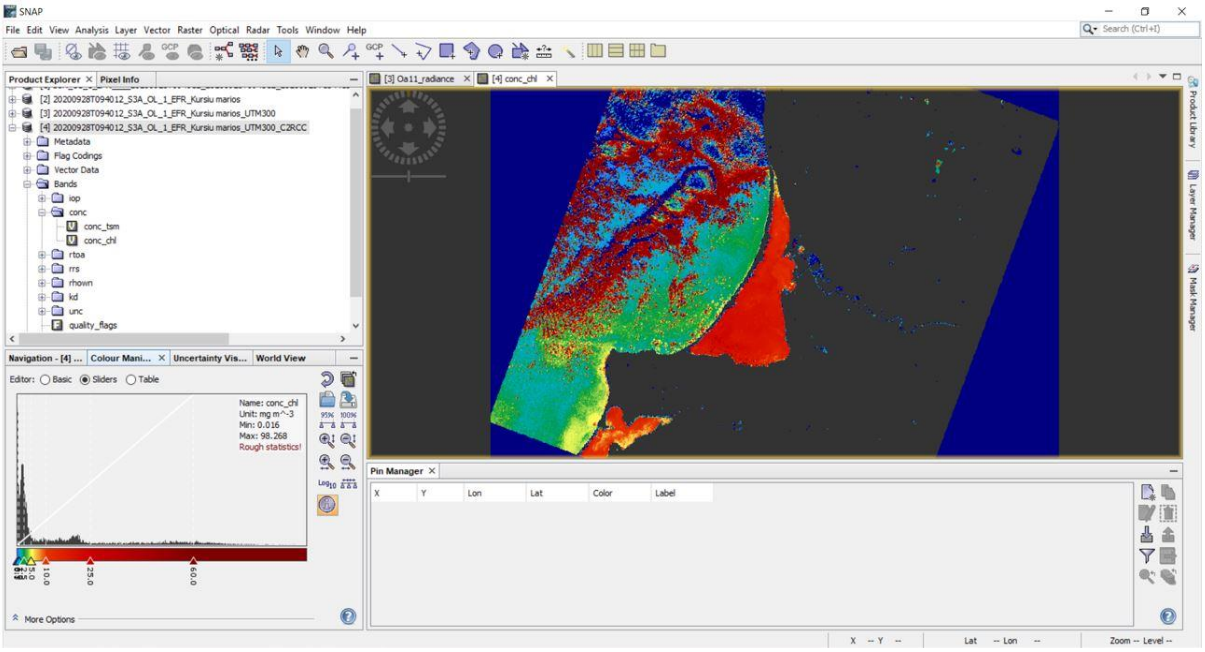

Figure VII-16*. Application of colour palette.*

The layer containing chlorophyll-a concentration (conc_chl) is virtual. It can be changed by **right mouse click on the layer > Convert band** and **right click on the name of satellite image > Save Product**.

Investigate how the atmospheric correction affected the reflected radiation recorded by the satellite sensor **Optical > Spectrum View**.

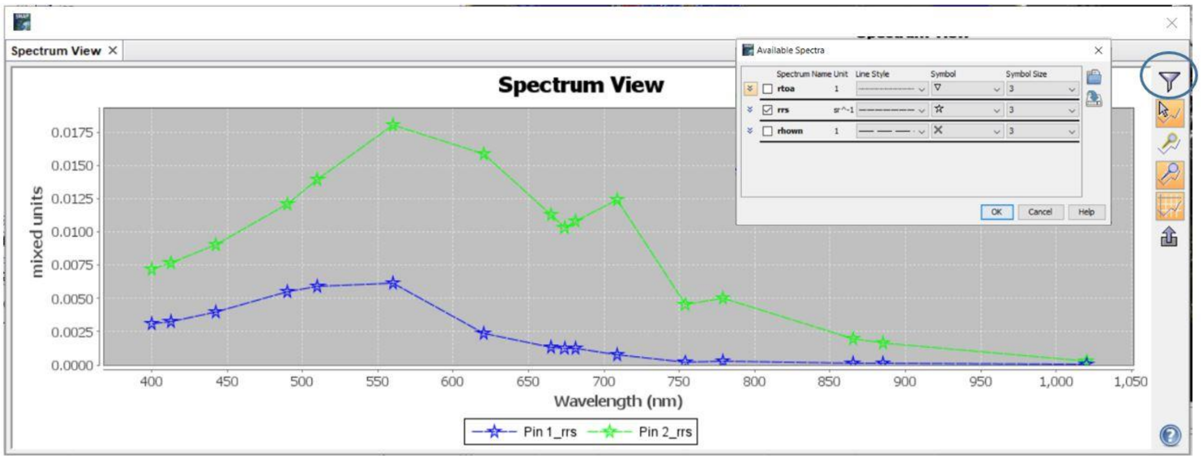

Figure VII-17. *Example of Spectrum view.*

Cloud masking in SNAP: The obtained result shows that clouds have a great impact on the quality and accuracy of satellite information, the presence of clouds results in artefacts - very high concentrations of chlorophyll-a, which are incorrect. In this case, cloud masking is an important step to leave pixels that are not affected by clouds.

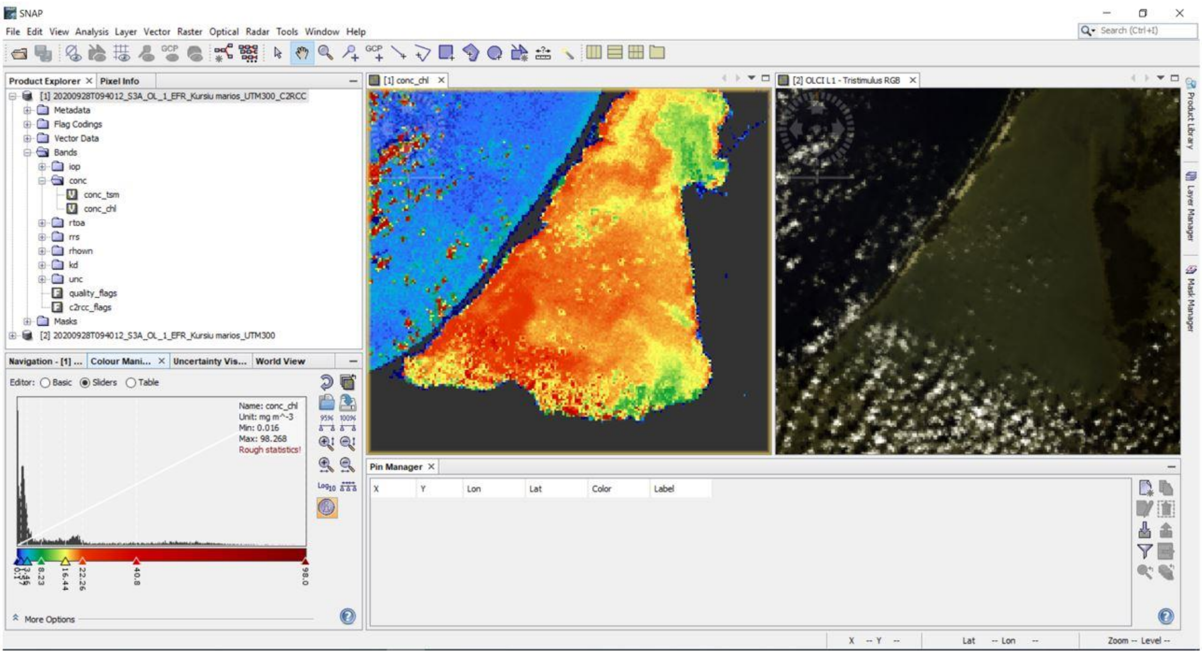

Figure VII-18. *Example of cloud masking.*

For this purpose, the C2RCC provides information layers that can be found at the Mask Manager, the Cloud_risk layer is used for cloud masking:

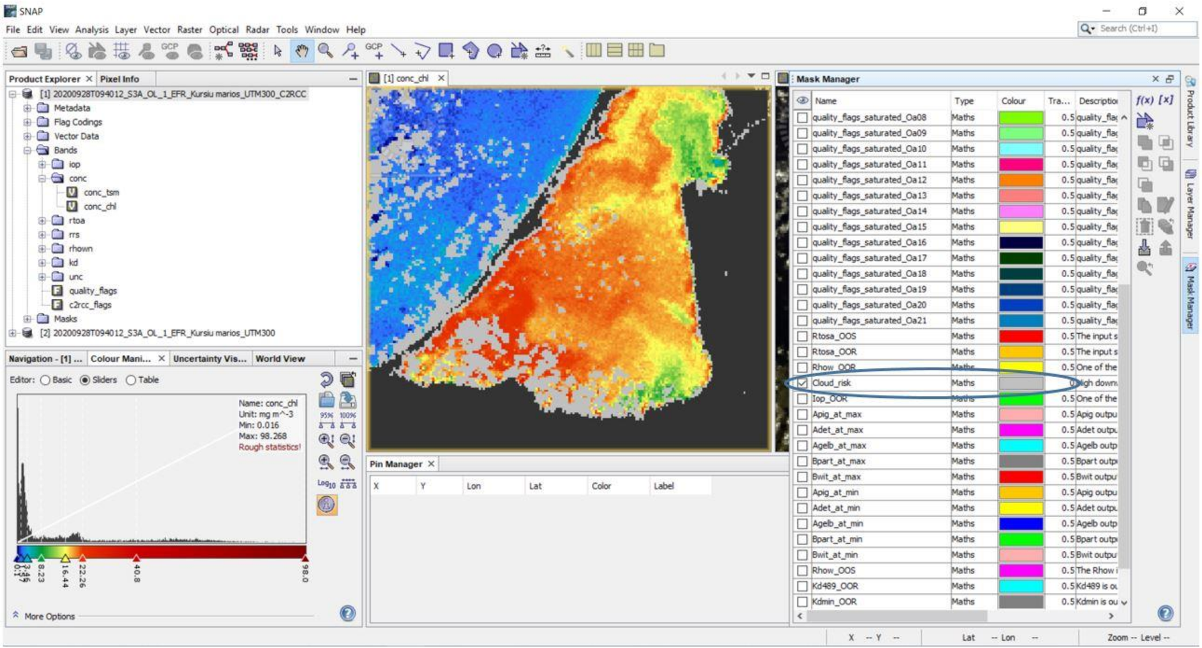

Figure VII-19. *Information in Mask Manager.*

The Cloud_risk information layer can be applied to the chlorophyll-a concentration layer, as a result of which the incorrect values will be changed to No Data. **Right click on the layer conc_chl > Properties > Valid pixel expression > c2rcc_flags.Valid_PE&&!Cloud_risk > Close**

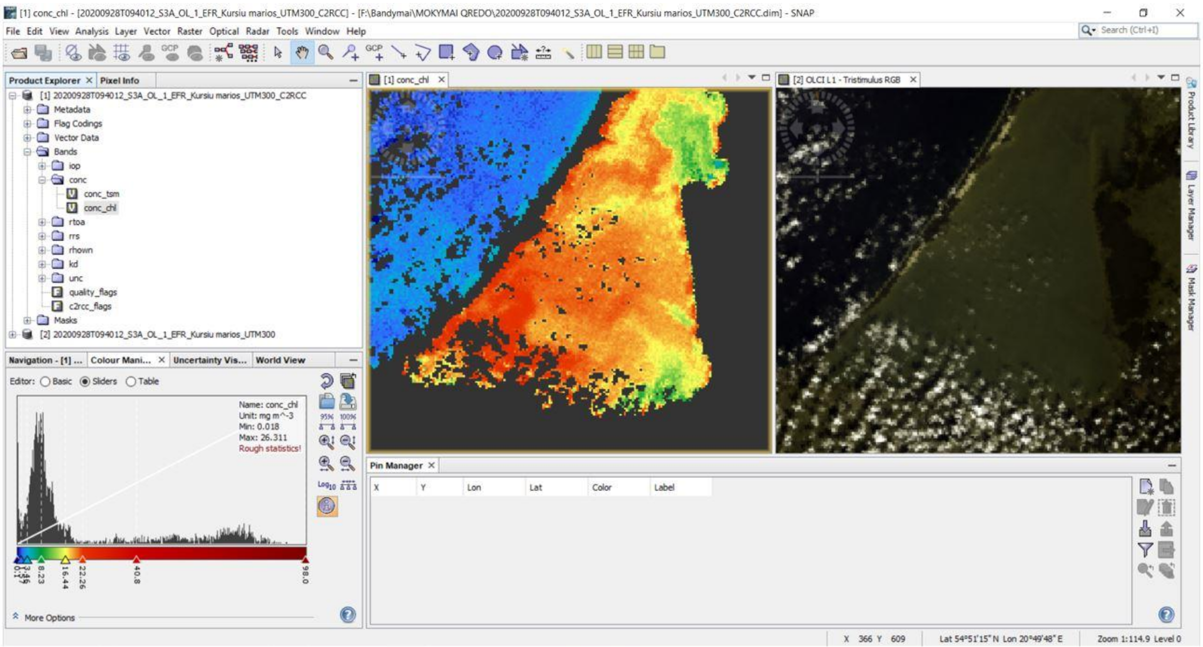

Figure VII-20. *Processing steps.*

The layer that will allow us to eliminate pixels that are significantly affected by clouds can be created: **Raster > Band math > Name: let's create a layer name "Cloud_mask" > Uncheck Virtual Band > choose Edit Expression... > in the window specify "$2.conc_chl && ! $2.Cloud_risk" > OK > OK**

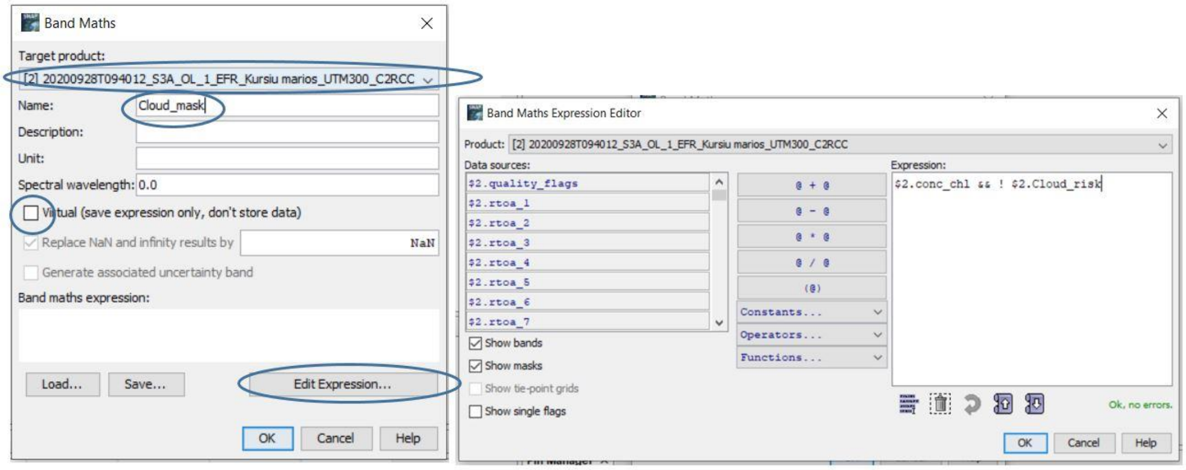

Figure VII-21. *Application of Band Maths.*

The output:

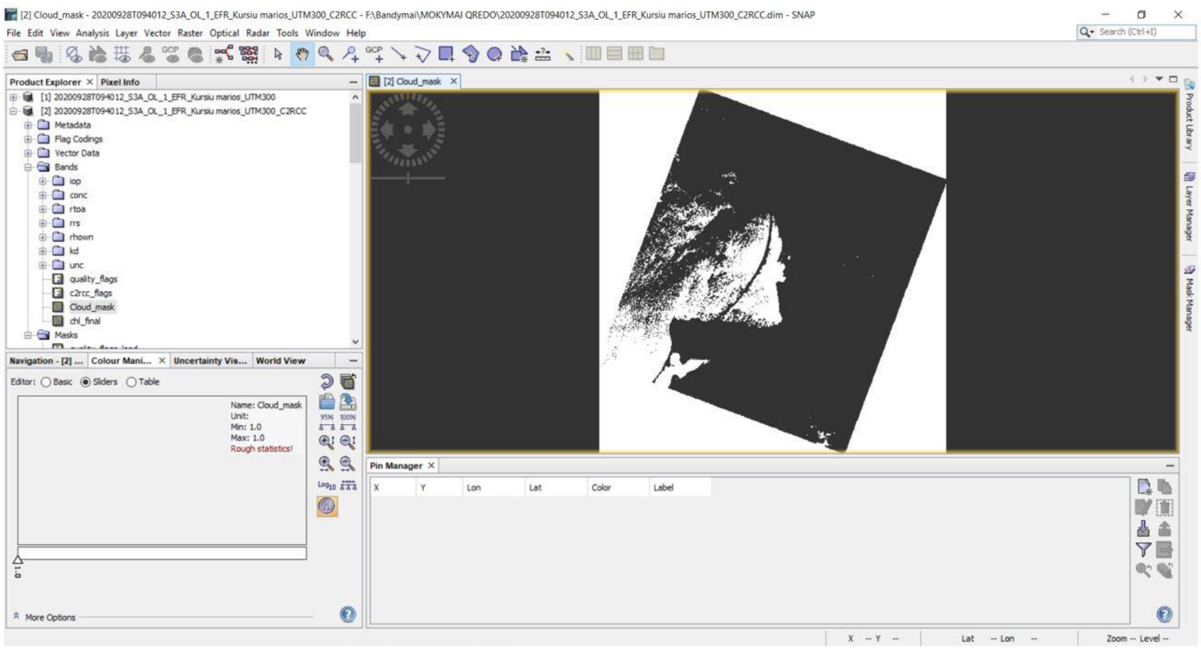

Figure VII-22. *Output result.*

The created layer can be applied to the chlorophyll-a concentration layer, so the values near the clouds will be changed to No Data: **Raster > Band math > Name: create a new layer name, e.g., Chl_final > uncheck the Virtual Band > Edit Expression... > indicate in the window $2.conc_chl * $2.Cloud_mask > OK > OK**.

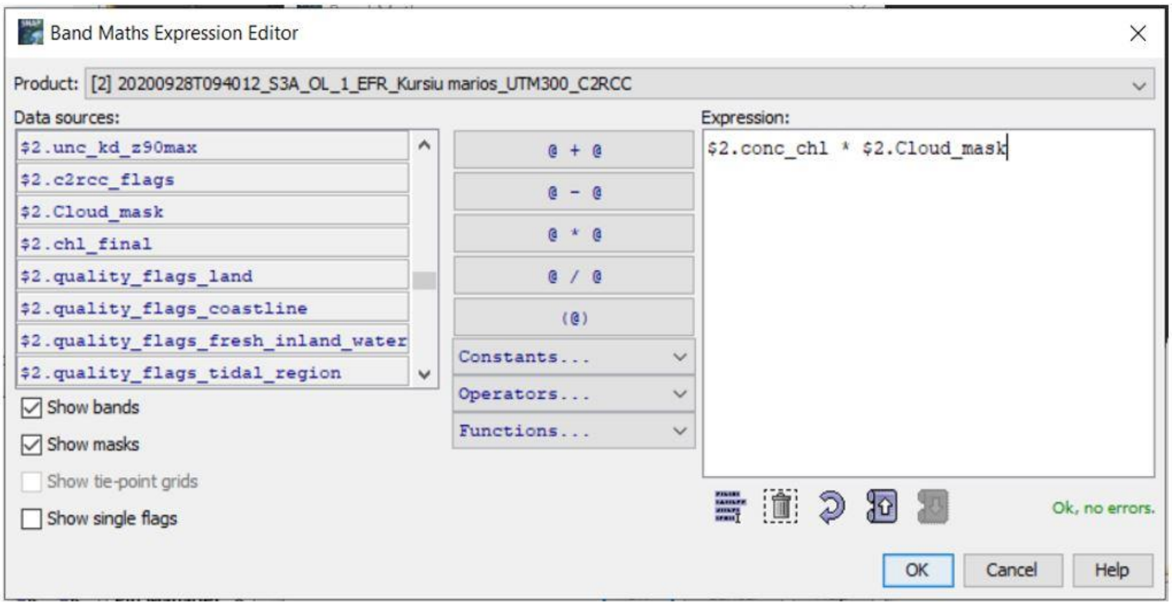

Figure VII-23. *Editing Band Maths.*

The output:

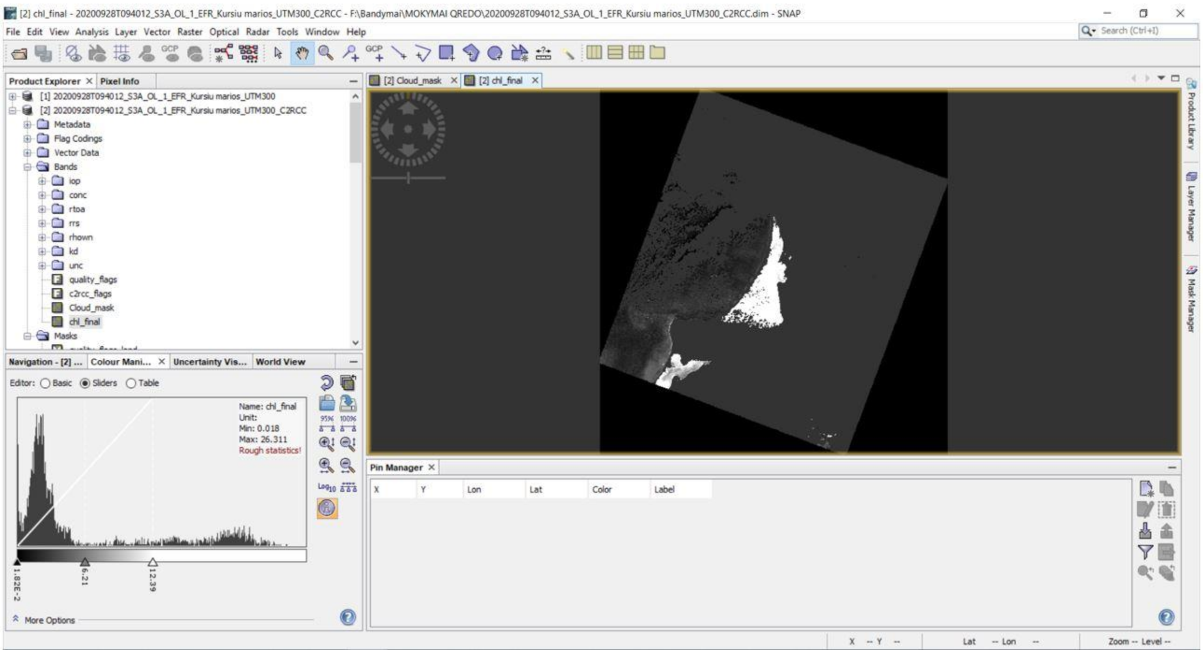

Figure VII-24. *Output result.*

Exporting the created chlorophyll-a concentration layer: File > Export > GeoTIFF > Subset... > Band subset > select only chl_final > NO (optional) > NO (optional). The name of the file can be changed.

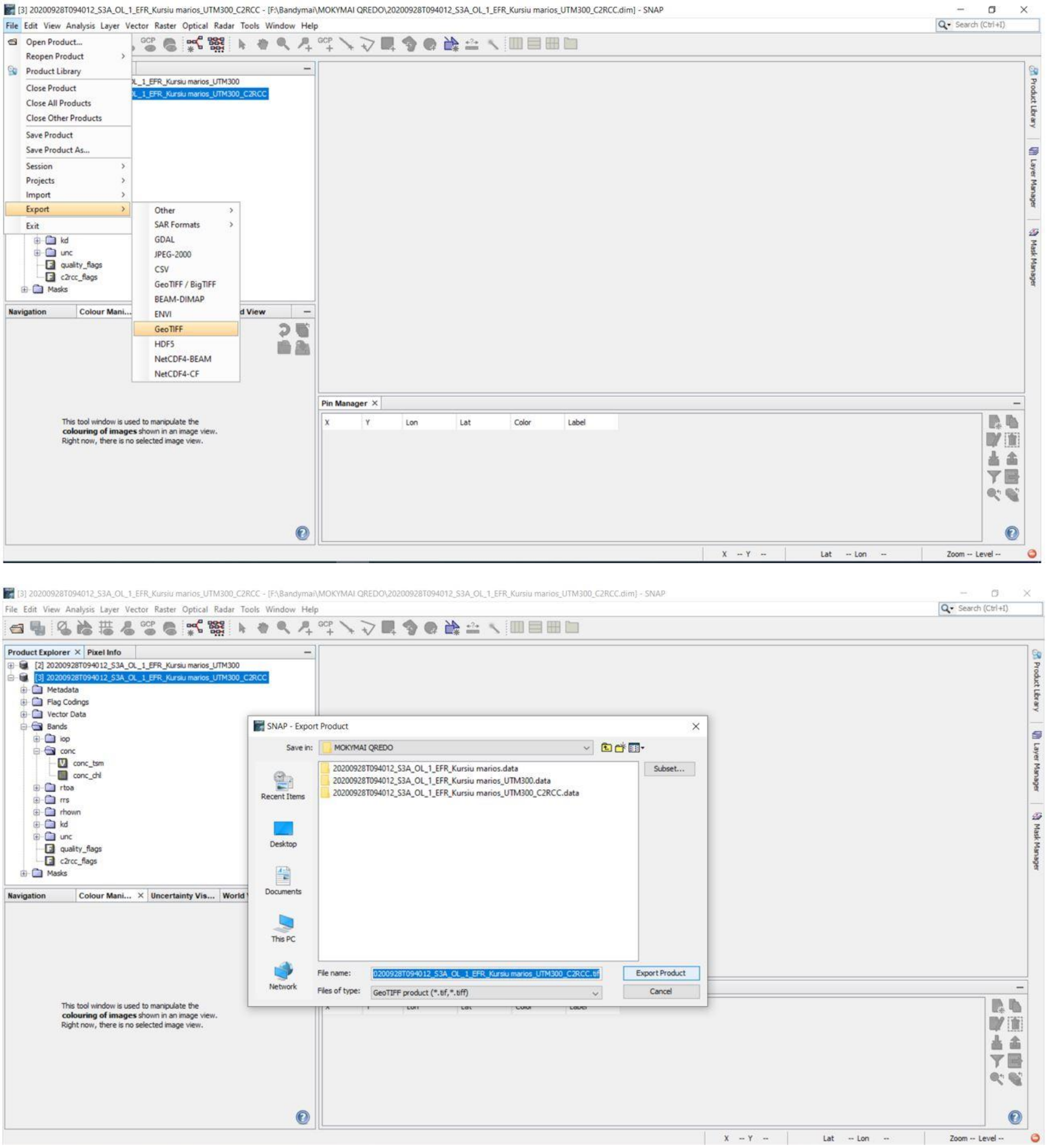

Figure VII-25. *Exporting layer.*

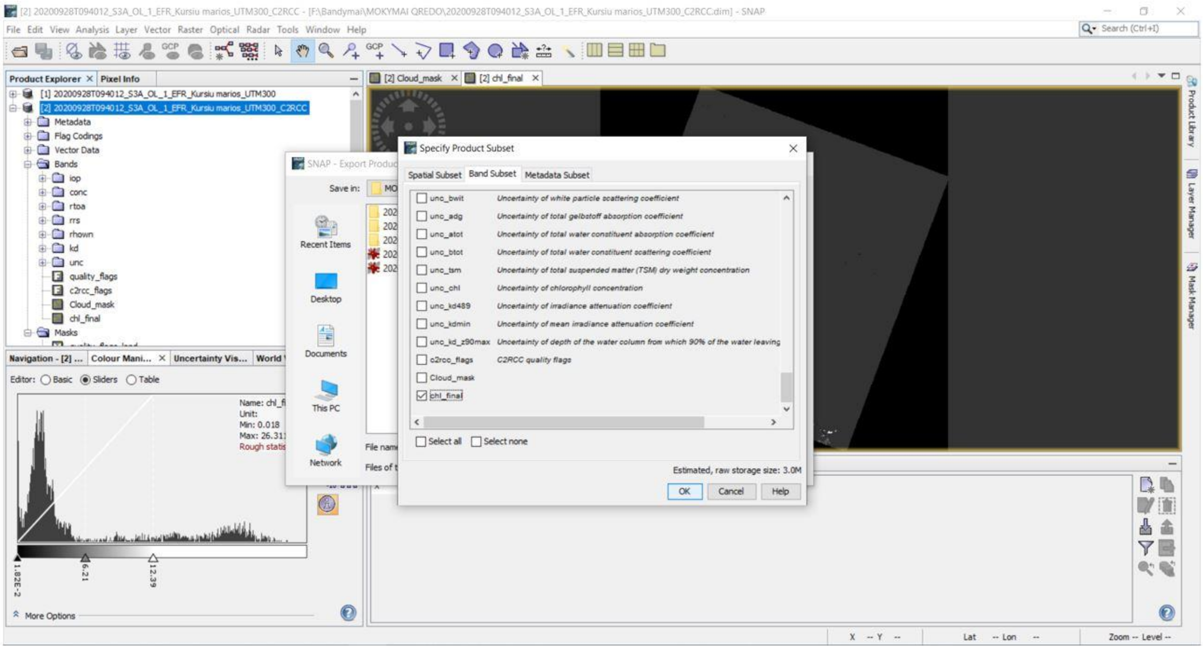

Figure VII-26. *Exporting layer.*

According to the same procedure it is recommended to export as Geotiff file the created cloud mask layer.

Data visualisation in QGIS: Open the exported GeoTIFF file in QGIS: **QGIS > Layer > Add Layer > Add Raster Layer > select the exported file > apply the color palette** (for more information on QGIS, see Chapter III)

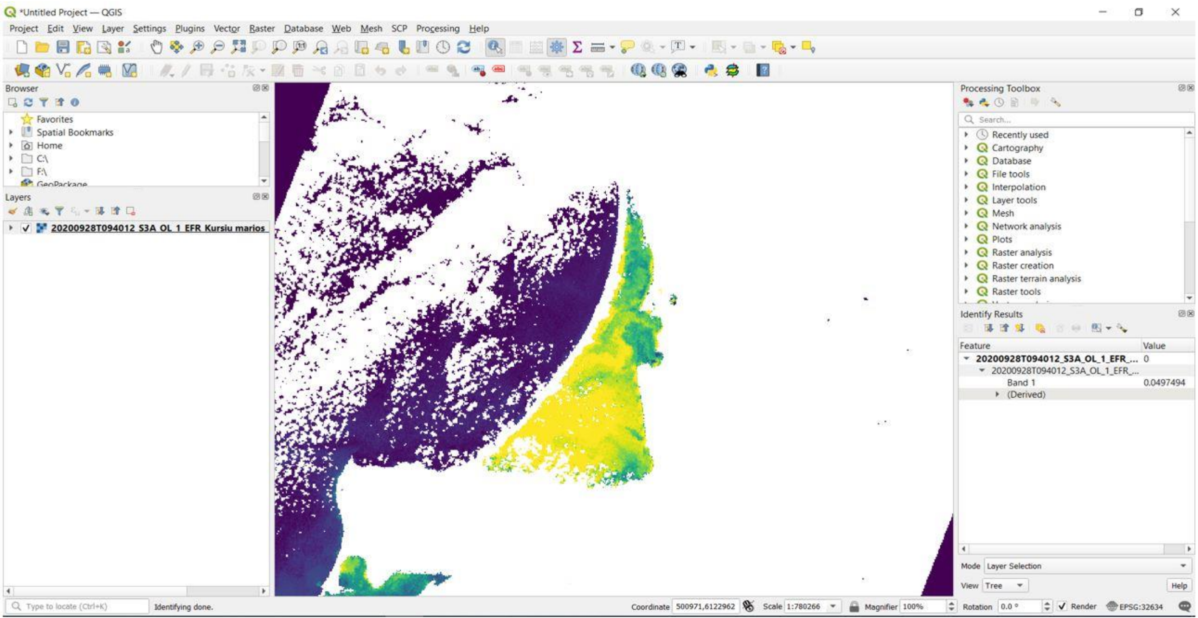

Figure VII-27. *Data visualization.*

Final notes: Atmospheric Correction is a crucial step for the chlorophyll-a concentration accuracy. Currently, there are various atmospheric correction algorithms: Acolite, iCOR, C2RCC and its variants for different optical sensors, POLYMER, MODTRAN4, 6SV etc. that can be applied prior to the retrieval of chlorophyll-a concentration. Therefore, before the further use, the chlorophyll-a concentrations obtained from satellite OLCI data after applying C2RCC processors should be validated with in situ chlorophyll-a concentration for the accuracy investigation. If the accuracy of data is nor satisfactory, other Atmospheric Correction, or chlorophyll-a concentration retrieval algorithm should be tested for the area of investigation.

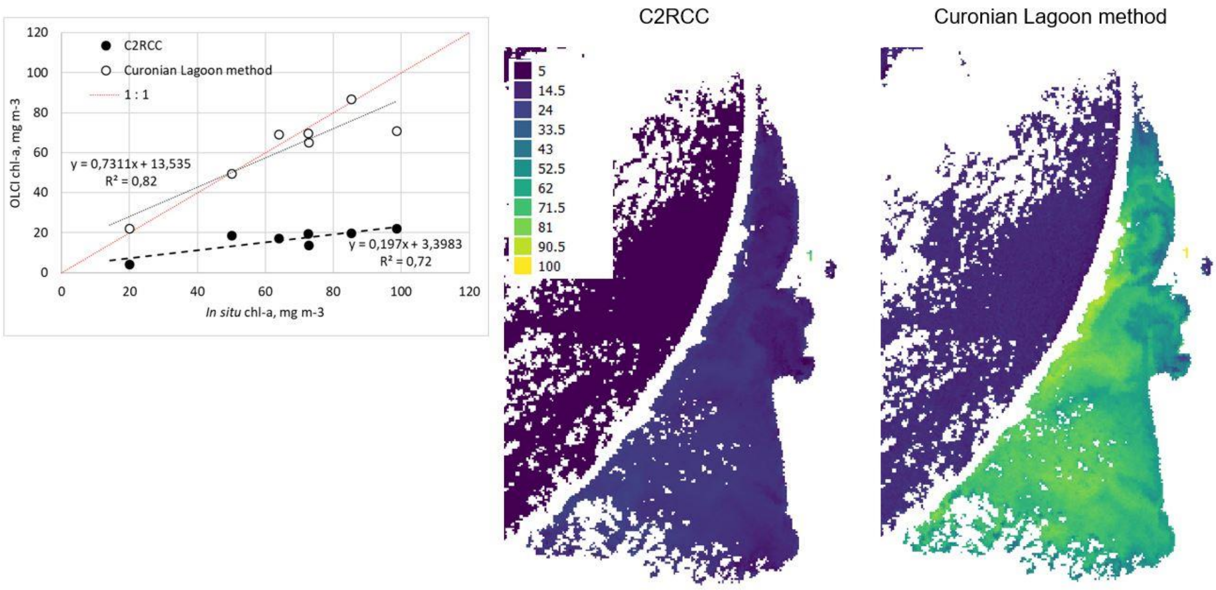

Figure VII-28. Comparison of the chlorophyll-a concentration in the Curonian Lagoon derived from OLCI data after application of C2RCC processor (C2RCC) and 6SV for Atmospheric Correction and band-ratio algorithm (Curonian Lagoon method) as described in Vaičiūtė et al., 2021.

VIII. Bathymetry and Water Transparency Mapping

Edvinas Tiškus

Bathymetry, the study of underwater depth of lake or ocean floors, is a crucial aspect of marine and limnological sciences. For many years, scientists and researchers have been leveraging modern technology to map the depths of water bodies. The advent of satellite remote sensing has revolutionized this field by providing an efficient, large-scale, and cost-effective method to acquire bathymetric data. This guidebook chapter focuses on the utilization of satellite imagery for bathymetry acquisition with the exemplar case of Plateliai Lake, Lithuania from 02.05.2022. In situ depth data for validation is provided in the **supplementary material** under "Bathymetry" and can be found via this link: https://github.com/oxodron/Qredo. 133

Case study: bathymetry acquisition: In this exercise, Sentinel-2 Level 2 data will be utilized, available for direct download from the Copernicus Hub. Level 2 data inherently contains atmospheric correction, making it a valuable resource for our study. However, in instances where only Level 1 data is accessible, supplementary instructions will be provided to elucidate the process of conducting manual atmospheric correction. This ensures the refinement of data quality and accuracy, indispensable for the success of our scientific exploration.

Data used: S2A_MSIL2A_20220502T095031_N0400_R079_T34VEH_20220502T140620.zip
Validation data and polygons: Qredo/Bathymetry at main oxodron/Qredo (github.com)
Merging images: The first step in using satellite images for bathymetry involves merging multiple images to get a comprehensive and holistic view of the area of interest, in this case, Plateliai Lake in Lithuania. Depending on the area size and satellite's orbit, a single image might not capture the entire region of interest, so it's essential to merge multiple images. SNAP provides the perfect tool for this task, you can access it via **Raster > Geometric > Multi-size mosaic**. This process ensures that the resulting image is a geometrically coherent mosaic, essential for accurate georeferencing and subsequent analysis steps.

Figure VIII-1. *The process of merging satellite images to create a comprehensive and geometrically coherent mosaic. The mosaic enables accurate georeferencing and analysis of the water body. On the left is two images before merging and on the right) after merging to one.*

Atmospheric correction.

[Important note: if LVL2 data was downloaded directly, this step can be skipped.]

Atmospheric correction is a crucial step in the process of using satellite images for bathymetry. When a satellite captures an image, the signals are susceptible to interference from the atmosphere, which can cause distortions such as scattering and absorption by atmospheric particles and gases. It's therefore vital to correct these distortions to obtain the true reflectance values of the target object on the ground — in our case, the water body.

The most commonly used algorithm for this task is Sen2Cor, a plugin available within the Sentinel Application Platform (SNAP). In the event that the Sen2Cor plugin is not pre-installed, it can be seamlessly integrated using the ESA SNAP software. To initiate this, navigate to the menu bar, select **Tools**, then **Plugins**, followed by **Available Plugins**, and finally, choose ***Sentinel-2 SEN2COR Processor***. Upon completing the installation and restarting the SNAP software, the plugin should be readily available, facilitating further progression of our scientific endeavour. SEN2COR can be accessed through the path **Optical > Thematic Land Processing > Sen2Cor**. The primary function of Sen2Cor is to provide scene classification, atmospheric correction, and cirrus correction for Sentinel-2 Level-1C products, which ultimately improves the accuracy and quality of the bathymetric data derived from these images. (Figure VIII-2).

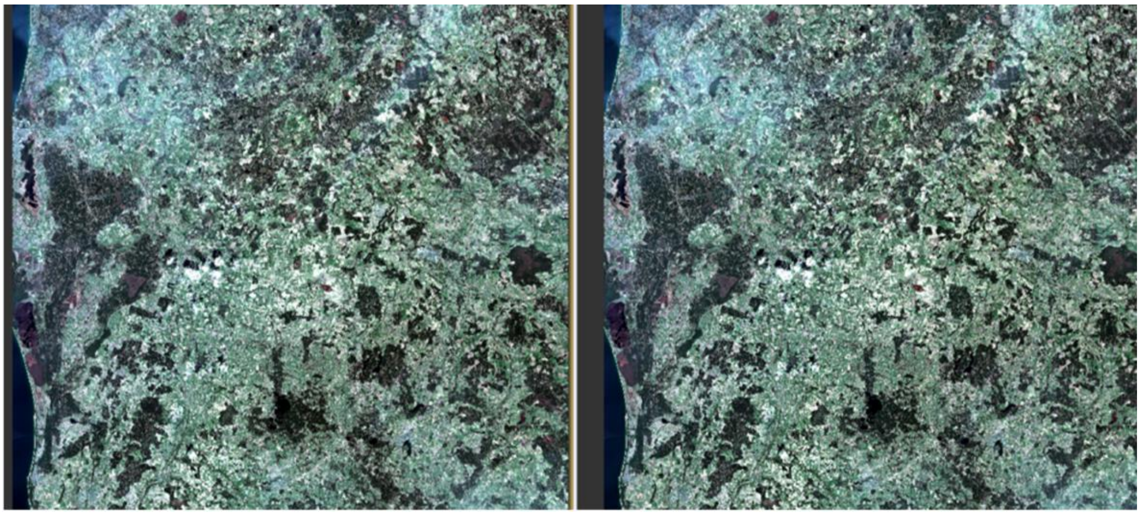

Figure VIII-2. *Atmospheric correction using the Sen2Cor algorithm. This step is essential for mitigating distortions caused by atmospheric scattering and absorption, thereby refining the true reflectance values of the required waterbody.*

Clipping and Georeferencing: After atmospheric correction, the next step involves narrowing down the satellite imagery to only the region of interest, a process known as clipping or subsetting. For our case study, the area of interest is Plateliai Lake. This clipping process reduces computational demands and focuses the subsequent analyses on the area of importance. In SNAP, the tool used for this task can be accessed via **Raster > Subset**.

Within the Subset tool, there are options for both a Spatial Subset and a Band Subset. For the Spatial Subset, you should define the area encompassing Plateliai Lake, effectively creating a square that contains the entire lake and cuts out the surrounding areas.

For the Band Subset, the selection of specific bands is critical as they relate to the light wavelengths most useful for bathymetry calculation. For Sentinel-2 images, the required bands for bathymetry include B2 (Blue), B3 (Green), B4 (Red), and B8 (Near-Infrared). Each of these bands captures a different part of the electromagnetic spectrum, providing essential information for accurate depth calculation.

Following subsetting, georeferencing is performed to ensure the spatial accuracy of the imagery. This process aligns the subset satellite images to a spatial grid, ensuring each pixel corresponds to a specific geographical location. This is an essential step to ensure that bathymetric data derived from satellite images align accurately with other geographic datasets. (Figure VIII-3).

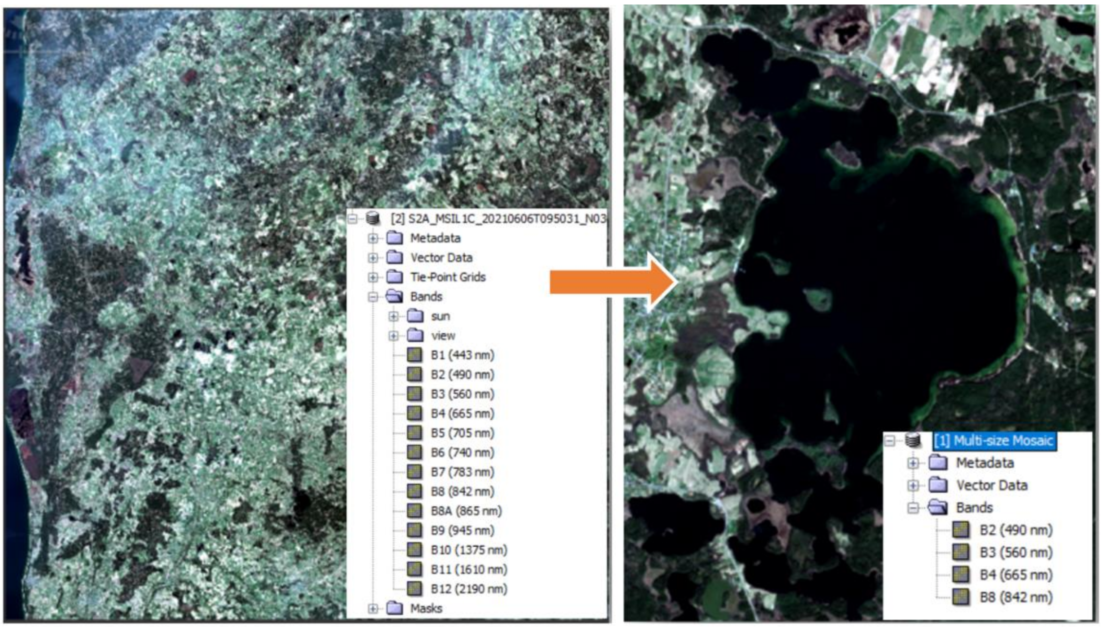

***Figure VIII-3**. Depicted is the process of clipping the satellite image, focusing solely on Plateliai Lake. This subset is further reduced in size by removing the bands that are not required for depth calculations.*

Land Masking: Land masking is the next critical step in the process of acquiring bathymetric data from satellite images. This process involves differentiating between the water body and the surrounding terrestrial areas within the satellite image. Ensuring that the subsequent bathymetric analyses are conducted only on the water body is crucial to avoiding any inaccuracies due to depth calculations made on land areas.

One common and efficient method for performing land masking utilizes the Near-Infrared (NIR) band (B8 in Sentinel-2 images). This band is particularly useful due to the spectral properties of water and land. While water bodies absorb most NIR light leading to low reflectance values, land areas reflect a higher amount of NIR light.

In this context, we employ a conditional rule for differentiating between water and land pixels (Figure VIII-4). If the NIR reflectance is greater than 0.05, it is classified as land and removed from the analysis. This is expressed through the statement "**if B8 > 0.05 then NaN else 1**". Any pixels with a B8 value exceeding 0.05 (indicative of land) are assigned a NaN (Not a Number) value, effectively masking them out, whereas water bodies (with reflectance values less or equal to 0.05) are assigned a value of 1.

Figure VIII-4. *The image demonstrates the application of land masking on Plateliai Lake using the Near-Infrared (NIR) band. The operation classifies water and land pixels based on their NIR reflectance values, effectively isolating the water body for subsequent analysis.*

This operation is performed using the **Band Maths** tool in SNAP, which can be accessed via a right-click on the image. After applying this rule, only the water body, Plateliai Lake in our case, remains active for subsequent analysis, with all terrestrial areas effectively masked out (Figure VIII-5). We name the new calculated product "Masked_land". After this step we apply "Masked_land" to each band using same Band Maths functions and name each band accordingly B2_land_masked, B3_land_masked, B4_land_masked, B8_land_masked.

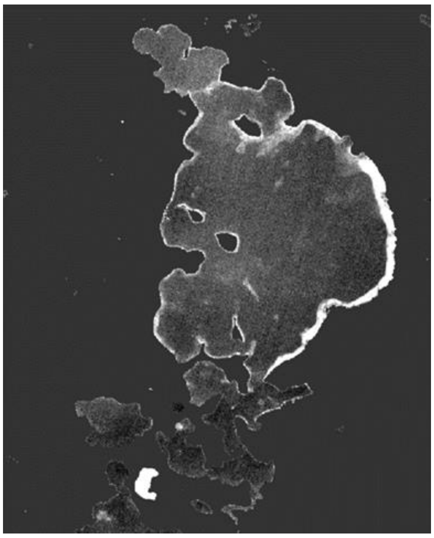

Figure VIII-5. *Displayed is the "Masked_land" product and the corresponding land-masked bands. These bands—B2_land_masked, B3_land_masked, B4_land_masked, B8_land_masked—are prepared for further processing.*

Sun Glint Correction: One of the challenges faced when using satellite images for bathymetry is the occurrence of sun glint. Sun glint is the reflection of sunlight off the water's surface, which can cause distortions in the satellite images and, in turn, affect the accuracy of water depth measurements. Therefore, an essential step in the process of bathymetric data acquisition from satellite images is sun glint correction.

The formula used for sun glint correction, as proposed by Hedley et al. (2005), is as follows: R'i = Ri – bi * (RNIR – MinNIR). In this equation, R'i is the corrected reflectance, Ri is the original reflectance of the band, bi is the correction coefficient for each band, RNIR is the reflectance of the NIR band, and MinNIR is the minimum NIR reflectance value. For instance, when applying this formula to Band 2 (Blue) of a land-masked image, the formula becomes: R'i = B2_land_mask – 0.0043 * (B8_land_mask - 0.009). Note that 0.0043 is the correction coefficient for Band 2 and 0.009 is the minimum NIR reflectance.

This sun glint correction operation is repeated for each of the subset bands: B2 (Blue), B3 (Green), and B4 (Red). Note that it isn't applied to the NIR band (B8) because it was used as a reference in the sun glint correction equation. We name each new band accordingly B2_glint_corrected, B3_glint_corrected, B4_glint_corrected. The result is an image with significantly reduced sun glint effect, making it much more suitable for subsequent bathymetric analysis (Figure VIII-6).

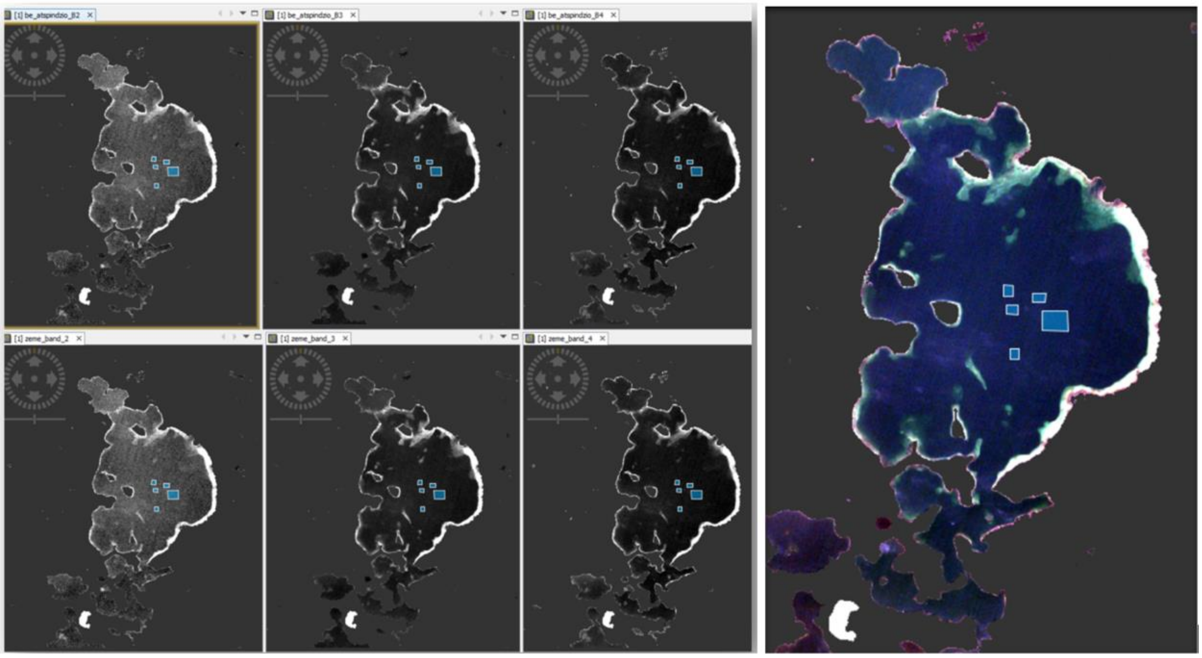

Figure VIII-6. *Sun glint correction process, employing Hedley et al.'s formula. The operation reduces the sun's reflective interference on the water surface, enhancing the accuracy of the bathymetric data. (left) each band after the sun glint correction and (right) the RGB composite from these bands. Squares in the lake represent polygons, found in course Github repository as shape file, for sampling of deep areas.*

Correction of Dark Atmospheric Objects: The next step in the process is the correction of dark atmospheric objects. Dark objects like shadows and some dark surfaces can interfere with the accuracy of water depth measurements in the satellite images. Therefore, it is crucial to correct these effects to enhance the overall quality of bathymetric data.

The procedure involves subtracting a specific value from the sun glint-corrected bands, with this value corresponding to the minimum reflectance value of a particular Region of Interest (ROI) within the image. The formula for the correction of dark objects would look like this: B2_glint_corrected - 0.005 for Band 2 (Blue) and B3_glint_corrected - 0.0095 for Band 3 (Green). The results are named accordingly: B2_dark_object_removed and B3_dark_object_removed.

The values of 0.005 and 0.0095 are determined by the minimum reflectance value within the ROI (Region of interest). This region should ideally be selected in an area that is not affected by sun glint to avoid biasing the dark object correction with values skewed by glint effects (Figure VIII-7). By doing this, you ensure that the correction value is representative of the minimum reflectance values caused by dark atmospheric objects rather than reflective interference. After this step, the satellite image is much better prepared for accurate bathymetric analysis.

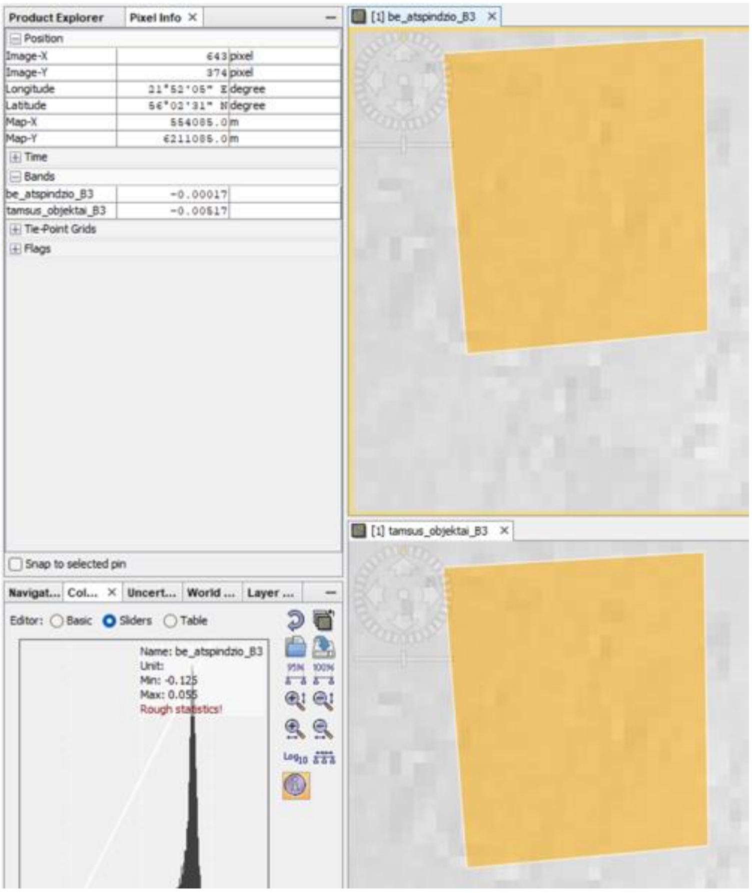

Figure VIII-7. *This image represents the correction of dark atmospheric objects within the image, removing their interference with the water depth measurements. This step increases the overall quality of the derived bathymetric data.*

Empirical Application of Bathymetry: In this step all the previous corrections and adjustments culminate in the conversion of satellite-derived data into water depth information, forming the bathymetric map.

According to the methodology proposed by Stumpf et al. in 2003, the bathymetric calculation can be achieved by correlating water depth with the ratio of green and blue wavelengths' reflectance. This method is based on the observation that different wavelengths of light penetrate water bodies to different depths. Blue light can penetrate deeper into the water than green light (Figure VIII-8).

The formula for this calculation in band maths window is: log(1000 * B3_dark_object_removed) / log(1000 * B2_dark_object_removed). The output of this calculation is a numerical representation of water depth across Plateliai Lake. It's important to note that this empirical model should ideally be calibrated with in situ measurements to validate and increase the accuracy of the depth estimations. Once the bathymetry calculation is completed, you will have a bathymetric map of the lake ready for further studies or applications.

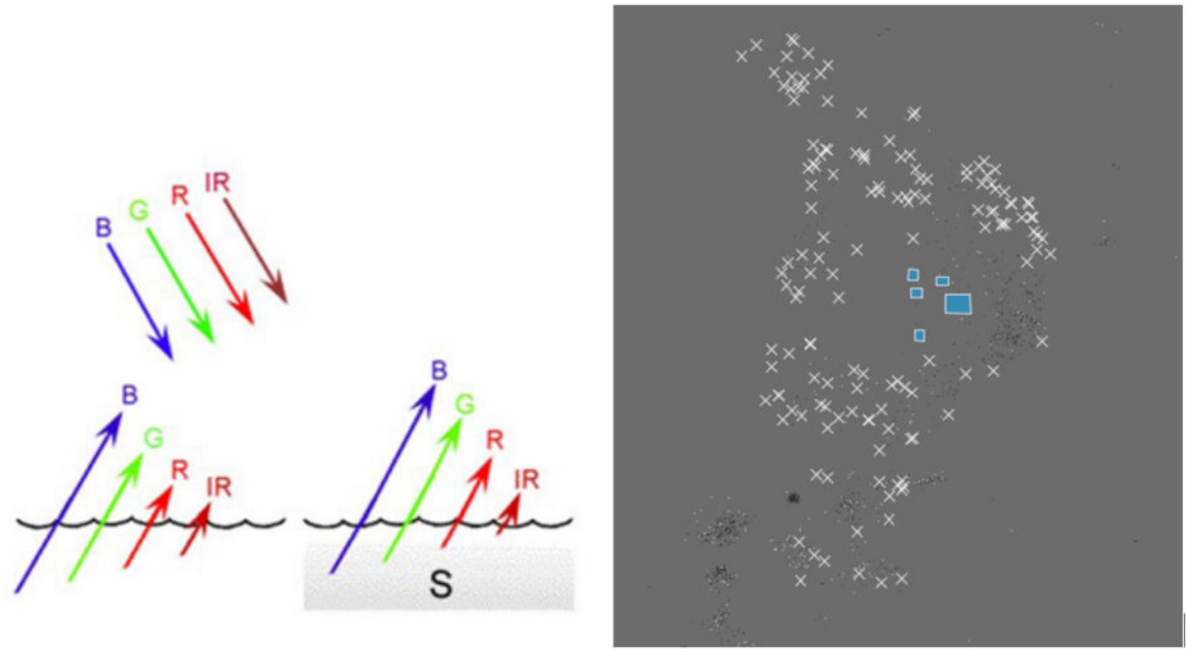

Figure VIII-8*.The final image showcases the application of empirical bathymetry, converting the corrected and adjusted satellite-derived data into a numerical representation of water depth across Plateliai Lake.*

Validation: The final stage in the process of bathymetric data acquisition involves the validation and calibration of the computed bathymetry with *in situ* measurements. This step is vital for assessing the accuracy of the bathymetric model derived from satellite images and making any necessary adjustments to improve its reliability.

To execute this, you will need to import in situ depth points, typically provided in the form of a vector file, such as an ESRI Shapefile, into SNAP. These files contain precise depth measurements at specific points in the lake, taken directly on-site.

Once the *in situ* depth points are loaded into SNAP, you can proceed to draw a correlation graph between these points and the computed bathymetry. This can be done using the Correlative Plot tool within SNAP. By comparing the two datasets, you can gauge the accuracy of your bathymetric model. Discrepancies between the model and the *in situ* data can indicate areas where the model may need to be calibrated or refined.

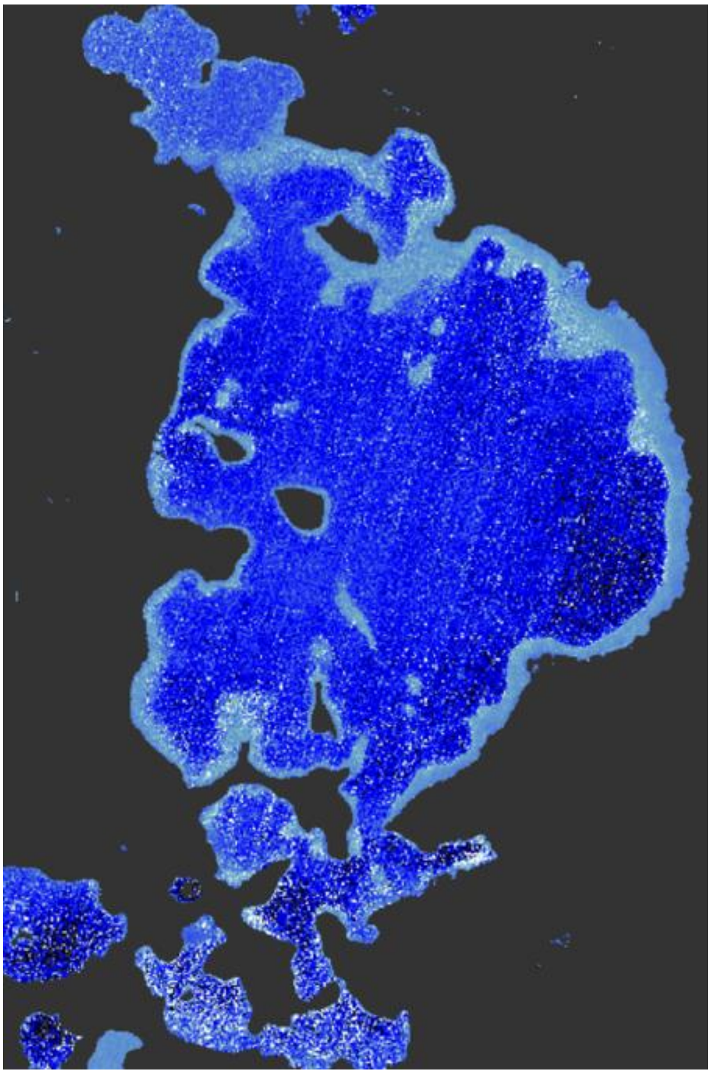

Figure VIII-9. *Bathymetric map of Plateliai Lake, derived from satellite imagery and validated against in situ measurements. This map provides a spatially accurate depiction of underwater topography, serving as a critical resource for scientific studies and applications in marine ecology and limnology.*

This iterative process of comparison and adjustment ensures the final bathymetric model is as accurate and reliable as possible, thereby enhancing the utility of the derived depth data for further studies or applications on Plateliai Lake.

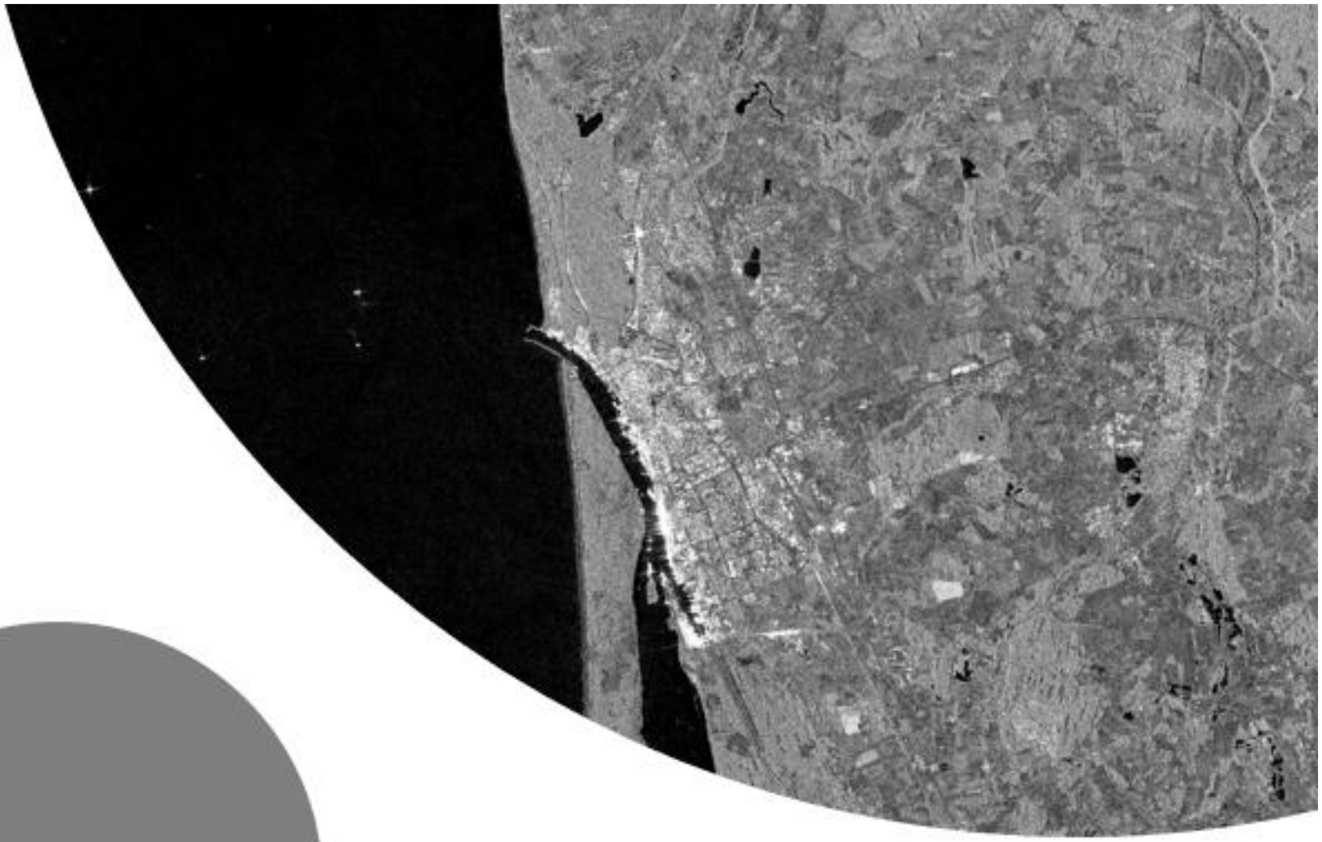

IX. Ship Detection Using Remote Sensing

Jonas Gintauskas

Marine traffic surveillance can be performed using different technologies. Usually ships identify their position using cooperatives systems, such as Automatic Identification System (AIS), Long Range Identification and Tracking (LRIT) and Vessel Monitoring System (VMS). In case ships are not identifiable using cooperative systems (e.g., due to illegal fishing) other means to control ship traffic can be used, such as remote sensing techniques as SAR. It is a quite reliable tool to monitor ships as any of the man-made structure in the water can be detect as it emits high backscatter values, meanwhile, the water surface has low backscatter values.

Case study: ship detection. In this exercise we will use Sentinel-1 Level-1 image which has the following parameters:

Product type: GRDH (Ground Range Detected High Resolution)

Sensor mode: IW (Interferometric Width)

Polarisation: VV+VH

Date and time: 2021-07-22 04:51

Name: S1B_IW_GRDH_1SDV_20210722T045103_20210722T045128_027902_035453_2D5A

Supplementary data entitled "LT_1km.zip" can be found at: https://github.com/oxodron/Qredo/tree/main/Ship%20detection

Using these parameters, the image has a spatial resolution of 20.3x22.6 m in size and pixel size converted to 10x10 m with every pixel value representing the detected magnitude of backscatter from the Earth's surface.

After downloading SAR file, open Snap. The first step is to open the product. Navigate to the folder where the data is downloaded and open all the downloaded .zip files. The opened file will appear in **Product Explorer** on the left of your screen if Snap is in default mode, then the file can be expanded and visualized as VV polarisation. One can find it using this path: "**File you added" to Product Explorer** > **Bands** > **Amplitude_VV.**

In this scenario, we are only interested in ships around the entrance of Klaipeda Seaport, so not all the image is needed. As we do not need the whole area for analysis, we use **Subset** to crop the image to the required extent. You have to click on the **Raster** menu in Menu Bar at the top and choose **Subset.**

First, choose to Subset image to the Geographic Coordinates tab (it can be found in the **Spatial Subset** tab), fill in the coordinates of the Subset and click OK (Figure IX-1). In this case, we will use the following coordinates:

North latitude bound: 55.80
West longitude bound: 21.20
South longitude bound: 55.60
East longitude bound: 20.60

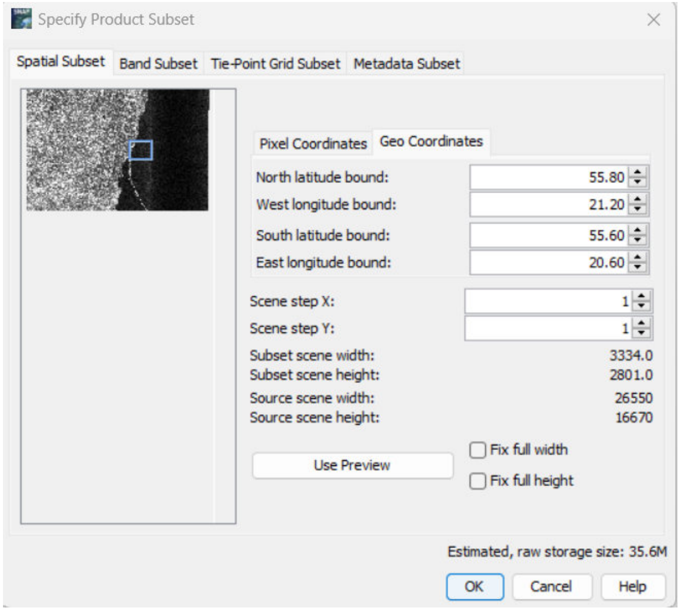

Figure IX-1. *Specifying Product Subset.*

The next step is to add **Apply-Orbit-File**. This step is needed because orbit state vectors, provided in the SAR metadata, are not accurate and should be updated. Mark the subset that was just produced, go to the menu bar and choose **Radar > Apply-Orbit-File** (Figure IX-2).

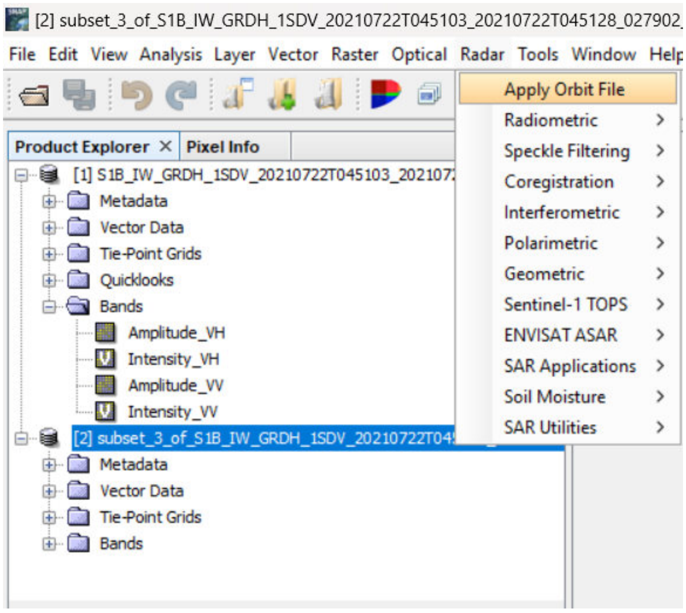

Figure IX-2. *Application of Orbit file.*

In the **Apply-Orbit-File** we keep the default settings and save as BEAM-DIMAP, then click Run. Now you can open an image which was just produced. It should be marked with a number [3] at the beginning of an image. To open an image and expand the file go to **Bands > Amplitude_VV** and double click on it. The image should be still in radar geometry.

In next part, we will eliminate artificial objects on ground and only artificial objects left should be ships, by using shapefile. There are other options how to eliminate land, such as using Land-Sea-Mask in Ocean Object Detection. If you want to do this, skip this part.

In the next step we will import a shapefile of a Lithuanian cost with 1 kilometre expanding into the sea. We will use a file named **LT_1km.shp** in the supplementary material. To import a shapefile, click on subset, which was recently produced and should be marked with a number [3]. Then go to the *Menu bar,* choose **Vector** > **Import** > **ESRI file** and locate **LT_1km.shp** file (Figure IX-3).

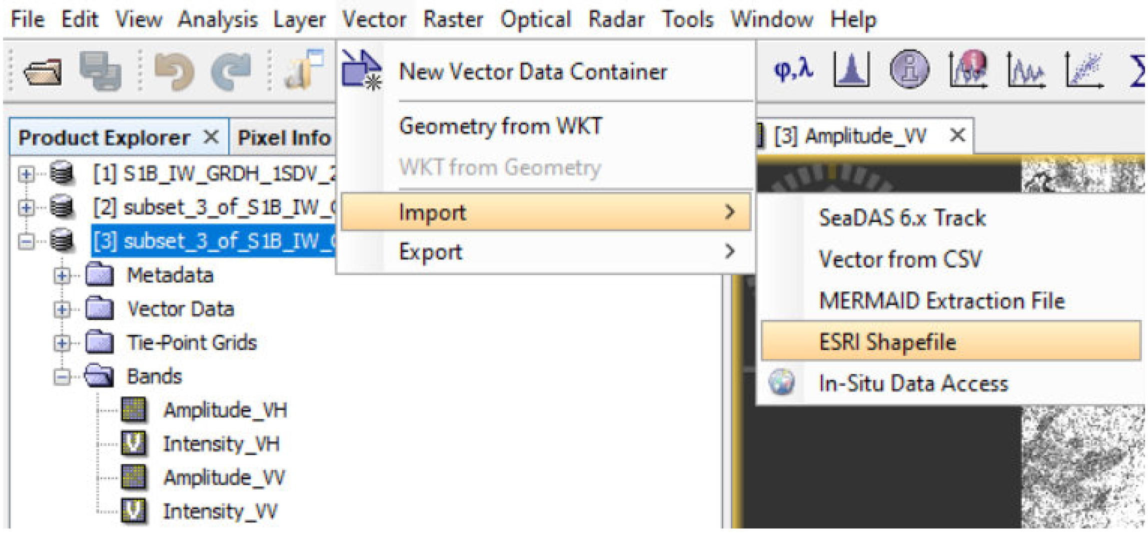

Figure IX-3. *Importing shape file.*

The shapefile should appear on canvas on SAR image as shown in Figure IX-4.

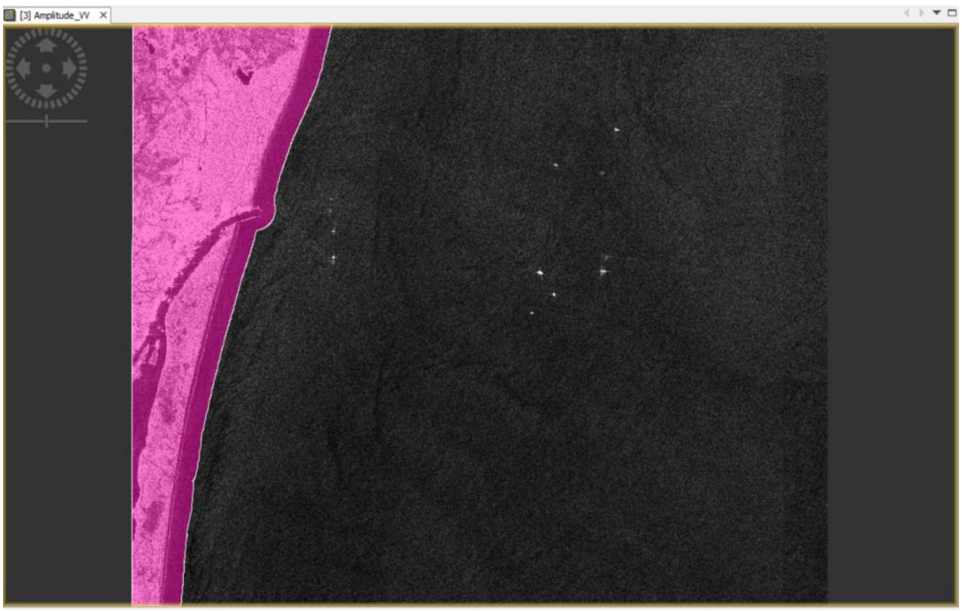

Figure IX-4. *Example of imported shape file.*

Now we will do a part, where we detect objects in the Sea, we need to locate it in menu tab **Radar > SAR Applications > Ocean Applications > Ocean Object Detection** (Figure IX-5).

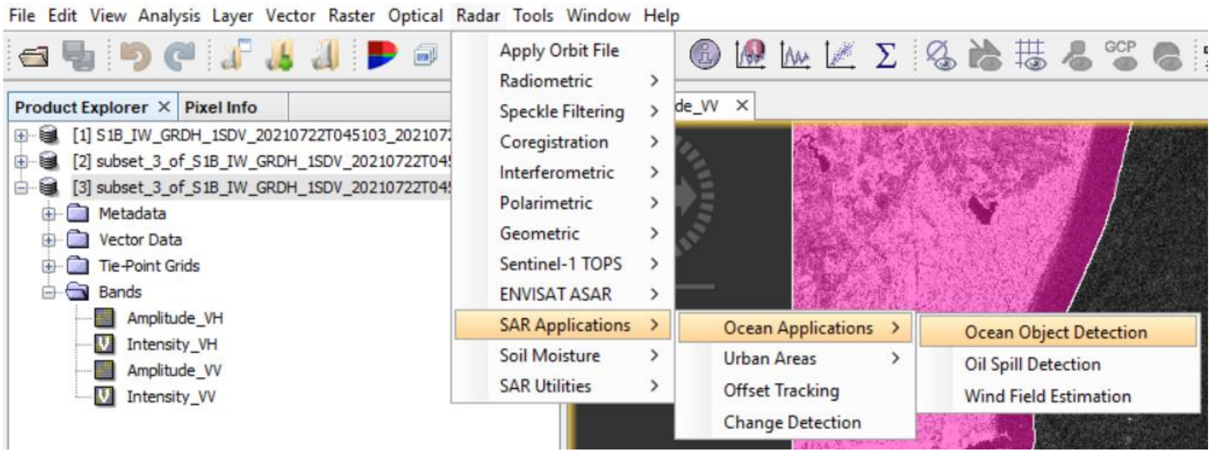

Figure IX-5. *Object detection steps.*

In the first tab called **Read** of the **Ocean Object Detection** operator, make sure, that the chosen image is the last one produced. It should be marked with **[3]** (Figure IX-6).

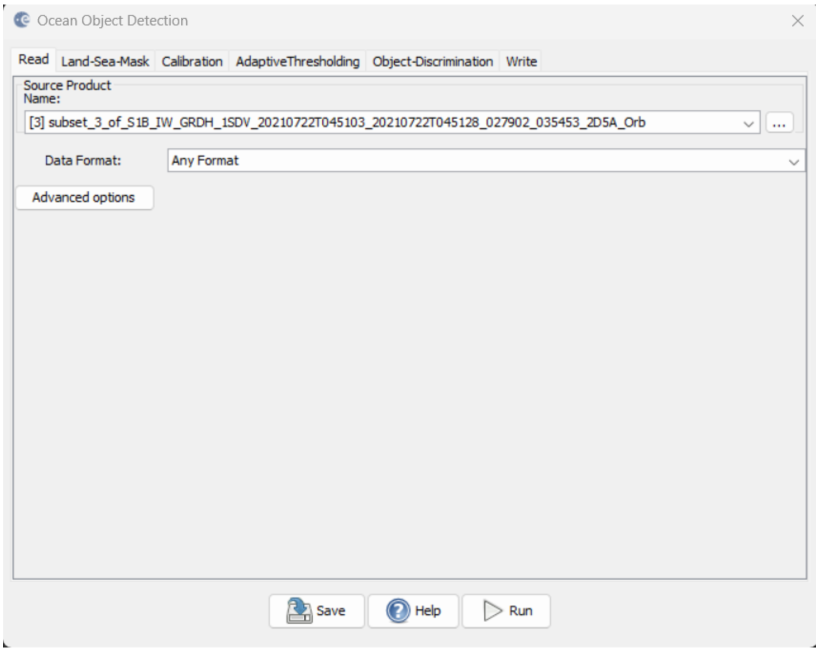

Figure IX-6. *Object detection steps.*

In the second tab called Land-Sea-Mask, we choose to **Use Vector as Mask.** The choice must be *LT_1km*, then mark **Invert Vector** and as we already have a shapefile with extended shoreline, we fill **Extend shoreline by [pixels]** to 0. Otherwise, you can choose to **Use SRTM 3sec**, choose to **Mask out the Land** and then **Extend shoreline by [pixels]**: at least 100 pixels as 1pixel size is 10 m (Figure IX-7).

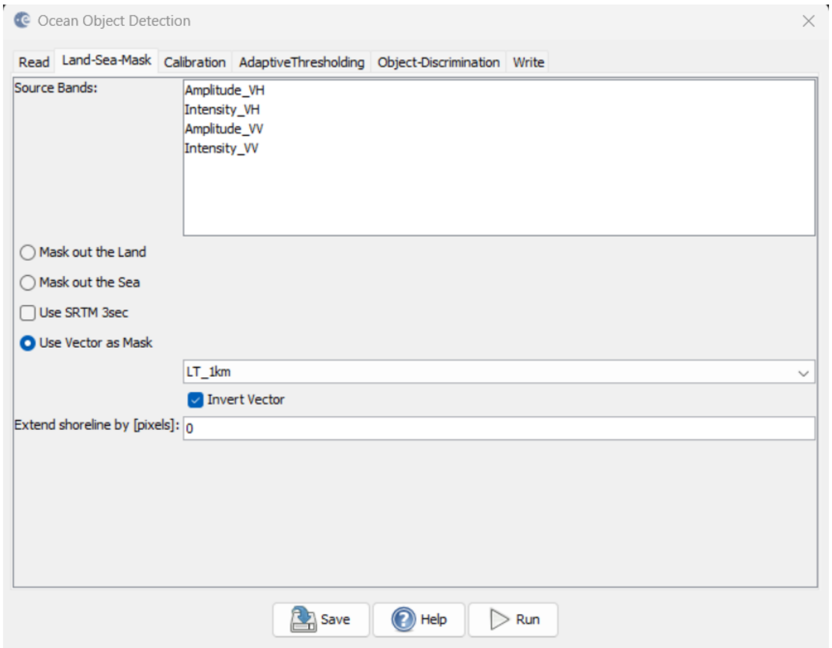

***Figure IX-7**. Object detection steps.*

Then go to **Object-Discrimination** tab where the *Minimum* and *Maximum Target Size* can be changed. It means that objects, that are smaller than *Minimum Target Size* will not be detected and larger than *Maximum Target Size* objects will not be detected (in this case we keep the default settings) (Figure IX-8).

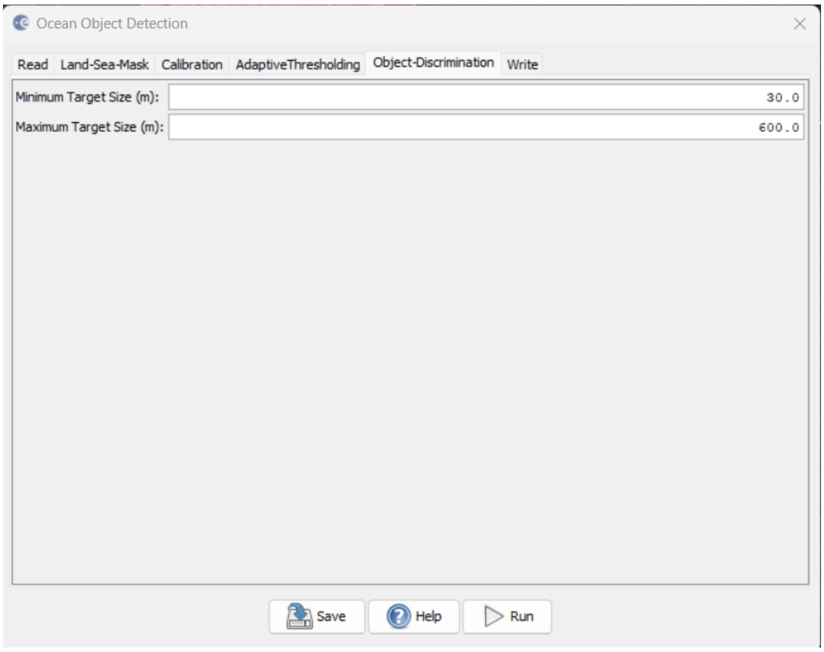

***Figure IX-8**. Object detection steps*

Lastly, go to **Write** tab and make sure it is saved as BEAM-DIMAP. After that click **Run**.

In this exercise we still need to perform one step as our image is still not *Terrain corrected* and is in radar projection. We locate *Menu* tab and go to this directory: **Radar > Geometric > Terrain Correction > Range-Doppler Terrain Correction.**

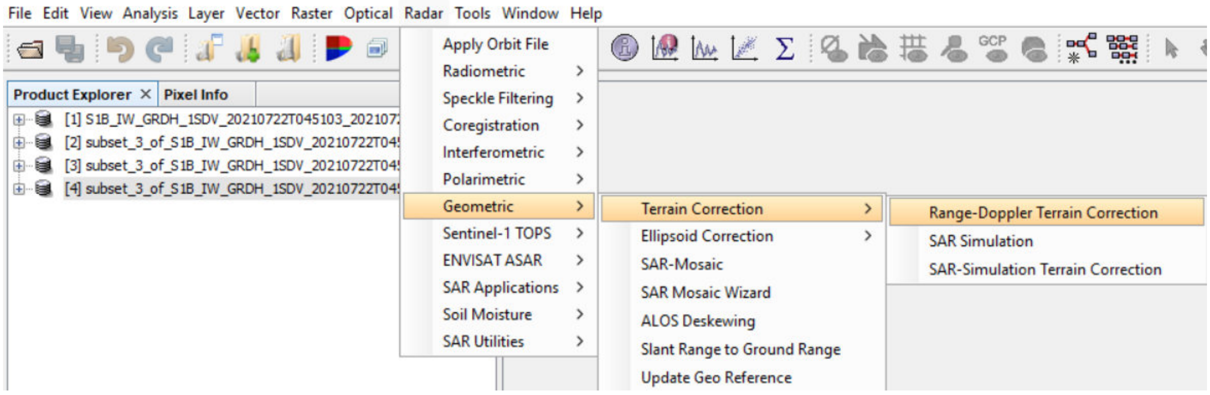

Figure IX-9. *Steps of terrain correction.*

After opening *Range Doppler Terrain Correction* operator in **I/O Parameters** tab we make sure that we chose the right Source Product (it should be the last one produced with number **[4]** at the front), we choose to **Save as: GeoTIFF** (Figure IX-10).

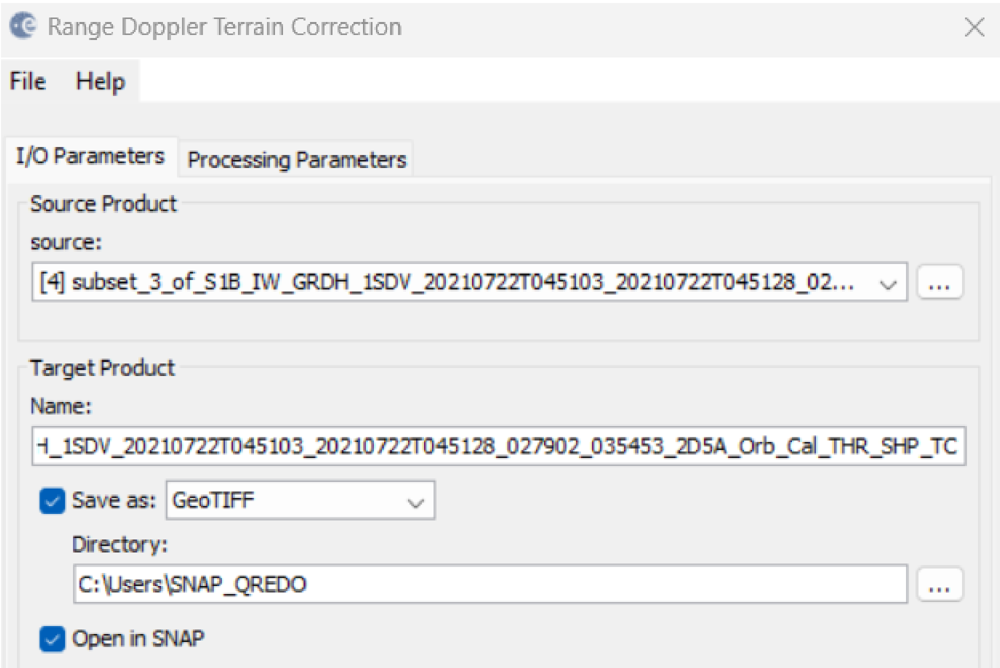

Figure IX-10. *Steps of range Doppler terrain correction*

Then click on **Processing Parameters** tab where you have to untick **Mask out areas without elevation** to not lose any information. Leave everything else in default and click **Run** (Figure IX-11).

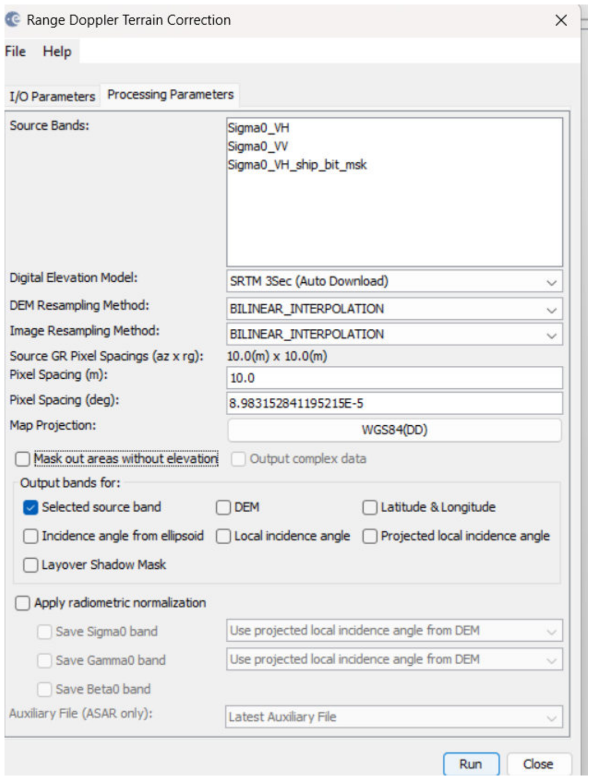

Figure IX-11. *Steps of range Doppler terrain correction*

Now we open **QGIS** and import the layer we just produced into canvas. To do so, go to **Layer > Add Layer > Add Delimited Text Layer...**(Figure IX-12).

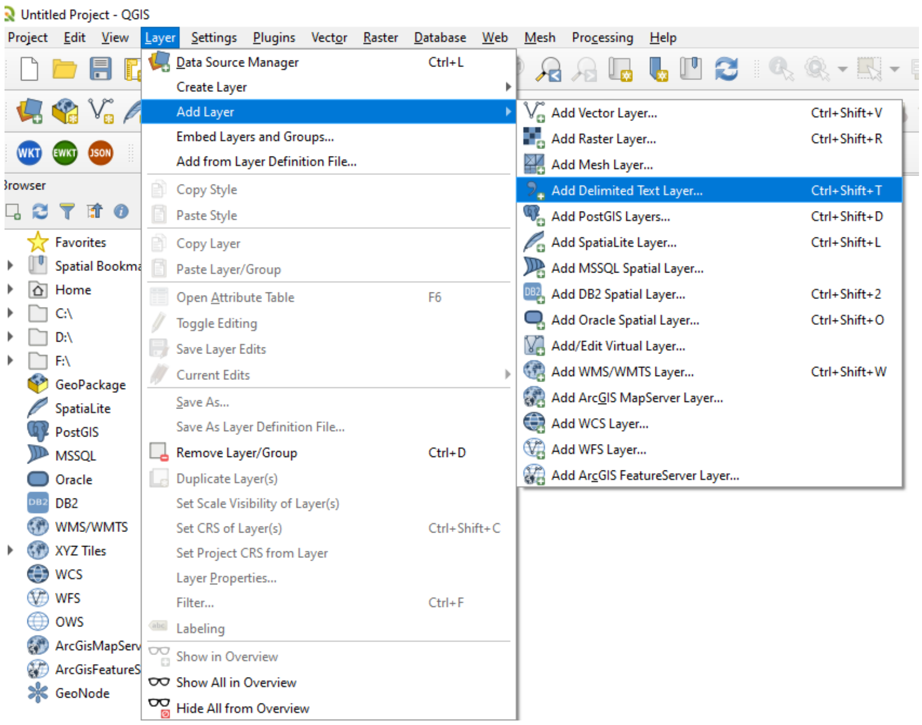

Figure IX-12. *Importing layer in QGIS.*

When opened, click on 3 dots located next to the **File name** ... and locate **ShipDetections.csv** it should be located in: *your_saving_directory*\subset_0_of_S1B_IW_GRDH_1SDV_20210722T045103_20210722T045128_027902_035453_2D5A_Orb_Cal_THR_SHP.data\vector_data\ShipDetections.csv (Figure IX-13).

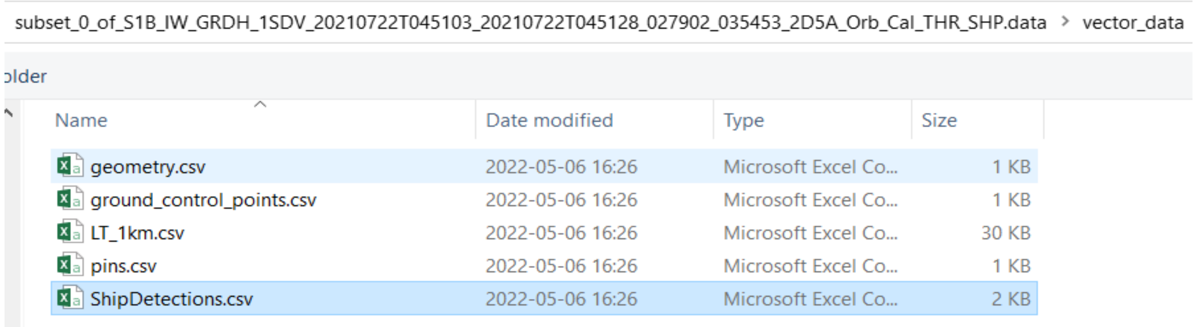

Figure IX-13. *Example of locating the file.*

After locating **ShipDetections.csv**, tick the box **Custom delimiters** in the **File Format.** After ticking the box, the additional boxes will appear. Untick other boxes and only tick **Tab** box. In *Geometry Definition* tab tick **Point coordinates** box and choose **X field** as **field_6**, **Y field** as **field_5**. Make sure that Geometry CRS is in EPSG:4326 – WGS 84. After everything is ready, click **Add** (Figure IX-14).

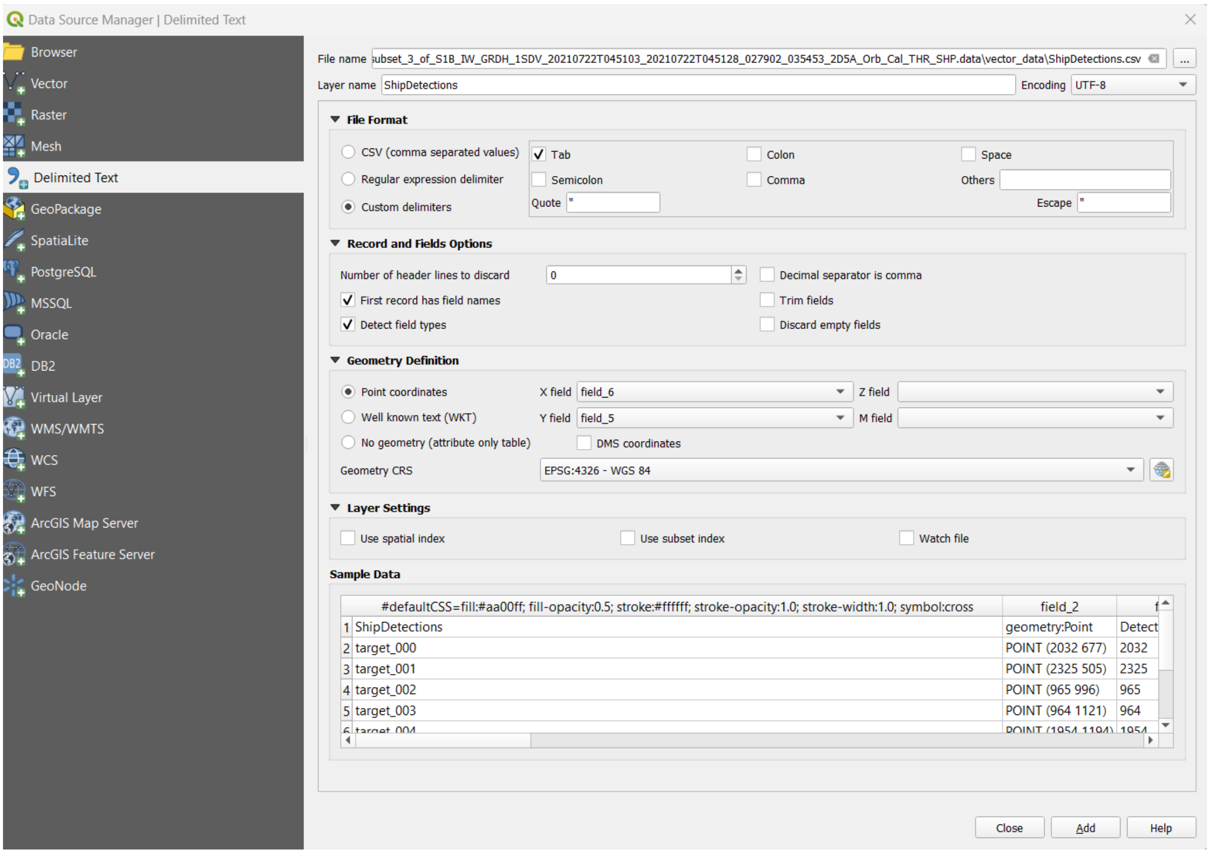

Figure IX-14*. Ship detection steps.*

Now, we can add Open Street Map in QGIS in the **Menu** go to **Web > Map Library > Map**, expand **Topography and Roads** and select **OpenStreetMap** to visualize positions of the ships. In the Figure IX-15 the map with ships detected is presented.

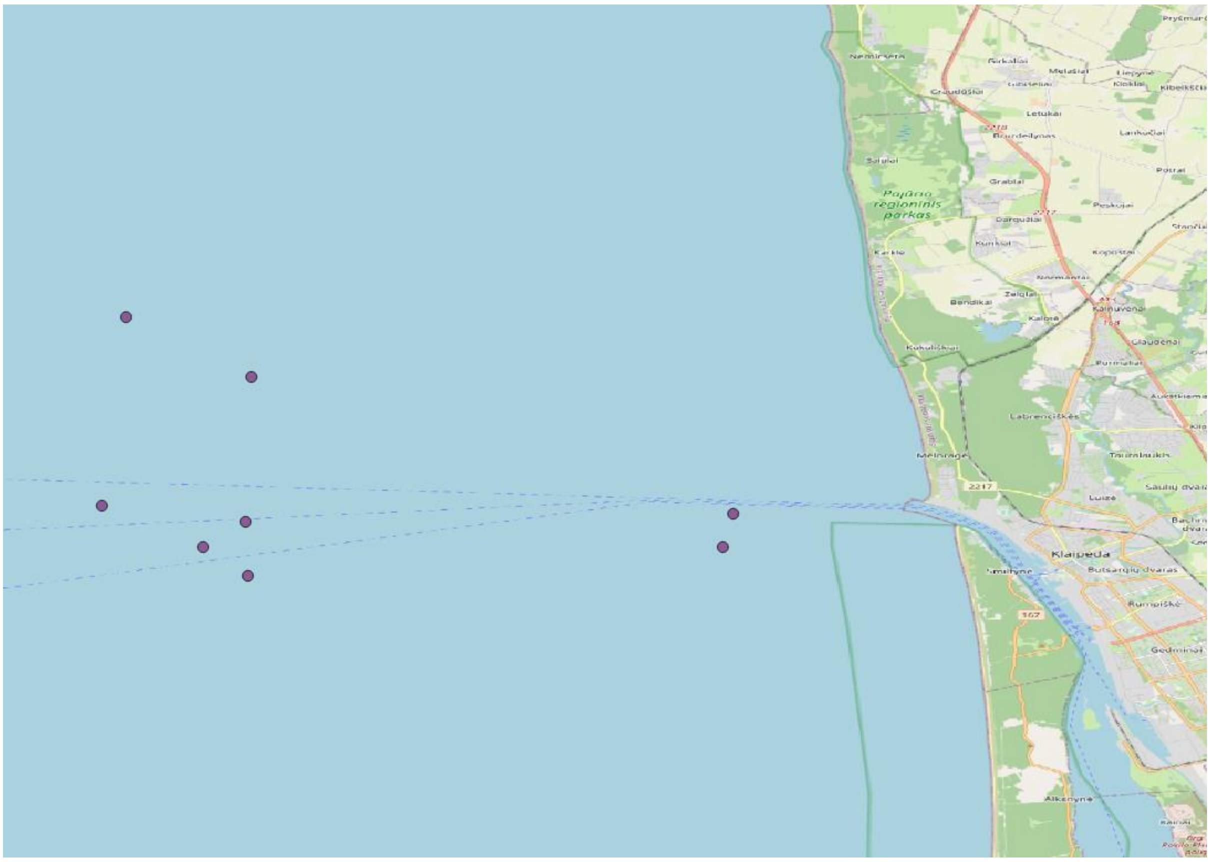

Figure IX-15. *Map with the detected ships.*

References

Biguino, B., Antunes, C., Lamas, L., Jenkins, L.J., Dias, J.M., Haigh, I.D., Brito, A.C., 2023. 40 years of changes in sea surface temperature along the Western Iberian Coast. Science of The Total Environment 888, 164193. https://doi.org/10.1016/j.scitotenv.2023.164193

Cuervo, J., 2019. Half a century of satellite remote sensing of sea-surface temperature. Remote Sensing of Environment 233, 111366. https://doi.org/10.1016/j.rse.2019.111366

Cummings, J.A., 2011. Ocean Data Quality Control, in: Schiller, A., Brassington, G.B. (Eds.), Operational Oceanography in the 21st Century. Springer Netherlands, Dordrecht, pp. 91–121. https://doi.org/10.1007/978-94-007-0332-2_4

Donlon, C.J., Minnett, P.J., Gentemann, C., Nightingale, T.J., Barton, I.J., Ward, B., Murray, M.J., 2002. Toward Improved Validation of Satellite Sea Surface Skin Temperature Measurements for Climate Research. Journal of Climate 15, 353–369. https://doi.org/10.1175/1520-0442(2002)015<0353:TIVOSS>2.0.CO;2

Fingas, M., 2019. Chapter 5 - Remote Sensing for Marine Management, in: Sheppard, C. (Ed.), World Seas: An Environmental Evaluation (Second Edition). Academic Press, pp. 103–119. https://doi.org/10.1016/B978-0-12-805052-1.00005-X

Gordon, H. R. and Morel, A., 1983. Remote Assessment of Ocean Color for Interpretation of Satellite Visible Imagery. A Review, Lecture Notes on Coastal and Estuarine Studies, R. T. Barber, N. K. Mooers, M. J. Bowman and B. Zeitzschel (eds.), Springer-Verlag, New York, 114 p.

IOCCG, 2000. Remote Sensing of Ocean Colour in Coastal, and Other Optically-Complex, Waters. Sathyendranath, S. (ed.), Reports of the International Ocean-Colour Coordinating Group, No. 3, IOCCG, Dartmouth, Canada.

Langille, A.K., Buckley, J.R., 2002. Estimation of sea surface temperature using passive microwave satellite imagery. https://doi.org/10.1109/IGARSS.2002.1026471

Mini Physics, 2016. The Electromagnetic Spectrum. https://www.miniphysics.com/electromagnetic-spectrum_25.html.

Morel, A. and Prieur, L., 1977. Analysis of variations in ocean color. Limnol. Oceanogr. 22: 709-722.

Minnett, P.J., 2001. Satellite Remote Sensing of Sea Surface Temperatures*, in: Steele, J.H. (Ed.), Encyclopedia of Ocean Sciences (Second Edition). Academic Press, Oxford, pp. 91–102. https://doi.org/10.1016/B978-012374473-9.00343-X

Minnett, P.J., Alvera-Azcárate, A., Chin, T.M., Corlett, G.K., Gentemann, C.L., Karagali, I., Li, X., Marsouin, A., Marullo, S., Maturi, E., Santoleri, R., Saux Picart, S., Steele, M., Vazquez-

NASA Science. Tour of the Electromagnetic Spectrum. https://science.nasa.gov/ems/01_intro.

Nielsen-Englyst, P., Høyer, J.L., Alerskans, E., Pedersen, L.T., Donlon, C., 2021. Impact of channel selection on SST retrievals from passive microwave observations. Remote Sensing of Environment 254, 112252. https://doi.org/10.1016/j.rse.2020.112252

O'Carroll, A.G., Armstrong, E.M., Beggs, H.M., Bouali, M., Casey, K.S., Corlett, G.K., Dash, P., Donlon, C.J., Gentemann, C.L., Høyer, J.L., Ignatov, A., Kabobah, K., Kachi, M., Kurihara, Y., Karagali, I., Maturi, E., Merchant, C.J., Marullo, S., Minnett, P.J., Pennybacker, M., Ramakrishnan, B., Ramsankaran, R., Santoleri, R., Sunder, S., Saux Picart, S., Vázquez-Cuervo, J., Wimmer, W., 2019. Observational Needs of Sea Surface Temperature. Frontiers in Marine Science 6.

Robinson, Ian S., 2010. Discovering the ocean from space: the unique applications of satellite oceanography, Berlin, Germany. Springer/Praxis Publishing, 638 pp.

Ruela, R., Sousa, M.C., deCastro, M., Dias, J.M., 2020. Global and regional evolution of sea surface temperature under climate change. Global and Planetary Change 190, 103190. https://doi.org/10.1016/j.gloplacha.2020.103190

URSA Space. https://ursaspace.com/blog/faq-what-is-remote-sensing/

Klaipėdos universiteto leidykla

Toma Dabulevičienė, Diana Vaičiūtė, Edvinas Tiškus, Jonas Gintauskas, Rasa Idzelytė, Martynas Bučas
Guide to Remote Sensing Applications for Aquatic Environment Monitoring (Elektroninis leidinys)

Klaipėda, 2024 04 24. Apimtis 19 sąl. sp. l.
Klaipėdos universiteto leidykla, Herkaus Manto g. 84, 92294 Klaipėda
Tel. (8 46) 398891, el. paštas: leidykla@ku.lt,
interneto adresas:http://www.ku/lt/leidykla/